Characterization of NiTi Shape Memory Alloy Spring Actuators and Their Application in an Elbow-Flexion Exoskeleton for Females

A THESIS

SUBMITTED TO THE FACULTY OF THE

UNIVERSITY OF MINNESOTA

BY

Sophia Victoria Vandycke

IN PARTIAL FULFILLMENT OF THE REQUIREMENTS FOR

THE DEGREE OF MASTER OF SCIENCE IN DESIGN

Dr. Lucy Dunne

December 2019

© Sophia Victoria Vandycke 2019

Acknowledgements

I would like to thank everyone who has helped me during my pursuit of my graduate degree. I would first like to thank my committee members Lucy Dunne, Peter Marchetto, Linsey Griffin and all those at the University of Minnesota who have helped me get to where I am. Peter Marchetto has been a great person to turn to for mentorship and to talk through the technical aspects of this thesis. I would also like to thank Midori Green for all her assistance and Esther Foo for her help with the biomechanical model of the arm and guidance with the methods. It takes people supporting you and guiding you to be the best you can in order to succeed. To me those people are my husband Stijn Vandycke, and my parents Dr. Tom Ward and Dr. Luisa Utset-Ward. Stijn Vandycke also helped me by being my shop buddy building the arm.

Dedication

"We keep moving forward, opening new doors, and doing new things, because we're curious and curiosity keeps leading us down new paths."
-Walt Disney

This thesis is dedicated to the most amazing man I know, my husband, Stijn Vandycke. Thank you for staying up with me all night while I write and work on this thesis. Your love, support, and encouragement got me through the rough parts of this journey; I am so lucky to have you in my life. I would also like to dedicate this thesis to my parents, Luisa Utset-Ward and Thomas Ward. Thank you for all you have done for me and all the sacrifices you have made to help me get where I am today. You have motivated me to work hard and have taught me that if I persevere, there is no obstacle large enough to prevent me from reaching my dreams.

Table of Contents

ACKNOWLEDGEMENTS ..... **I**

DEDICATION ..... **II**

TABLE OF CONTENTS ..... **III**

LIST OF TABLES ..... **VIII**

LIST OF FIGURES ..... **X**

CHAPTER 1: INTRODUCTION **1**

1.1 BACKGROUND 1

1.2 THE PROBLEM 2

1.3 OBJECTIVE OF THE STUDY 4

1.4 SIGNIFICANCE OF INVESTIGATING USING SMAS FOR ELBOW FLEXION EXOSKELETON 5

CHAPTER 2: LITERATURE REVIEW AND BACKGROUND INFORMATION **7**

2.1 ANATOMY AND KINESIOLOGY 7

2.1.1 Components of the elbow *7*

2.1.2 Difference in female and male arm anthropometrics *10*

2.2 BIOMECHANICS OF THE ELBOW 15

2.3 SYSTEM REQUIREMENTS FOR ELBOW FLEXION EXOSKELETON 17

2.3.1 The force needed to achieve elbow flexion *17*

2.3.2 Power to achieve elbow flexion *18*

2.3.3 Efficiency *19*

2.3.4 Speed *19*

2.3.5 Range of motion *20*

2.3.6 Repeatability *20*

2.4 EXISTING EXOSKELETONS 21

2.4.1 Passive exoskeletons *21*

2.4.2 Electric motor exoskeletons *22*

2.4.3 Soft exoskeletons *25*

2.4.4 Shape memory exoskeletons *26*

2.5 SHAPE MEMORY ALLOYS 27

2.5.1 Joule heating *31*

2.5.2 Benefits and limitations of SMA actuators *32*

2.5.3 SMA spring actuators *37*

2.5.3.1 Spring index 37

2.5.3.2 Extensional strain 38

2.5.3.3 Theoretical force of SMA springs 40

2.5.3.4 Flexinol actuator technical and design data 41

2.6 CONCLUSION 44

CHAPTER 3: CHARACTERIZATION TESTING 46

3.1 METHODS 46

3.1.1 Making of actuators *46*

3.1.1.1 Coiling process 47

3.1.1.2 Heat treating/Annealing process 48

3.1.2 Characterization testing *49*

3.1.2.1 Parameter determination 49

3.1.3 Data collection *51*

3.1.3.1 Testing setup 52

3.1.3.2 Procedures 55

3.1.4 Data analysis *57*

3.2 RESULTS 58

3.2.1 Maximum force and time to maximum force *58*

3.2.2 Time to reach maximum force *60*

3.2.3 Force vs. current vs. extensional strain *67*

3.2.4 Power and Resistance vs. Time *69*

3.2.5 Potential for spring fatigue and degradation *74*

3.3 DISCUSSION 75

3.3.1 Maximum force and time to maximum force *75*

3.3.3 Power and resistance vs. time *77*

3.3.4 Potential for spring fatigue and degradation *77*

3.3.4.1 Memory loss 78

3.3.4.2 Two-way SMA actuation 78

3.3.5 Temperature *81*

3.3.3.6 Actuator choice conclusion *82*

3.4 LIMITATIONS OF CHARACTERIZATION STUDIES 83

3.5 CONCLUSIONS OF CHARACTERIZATION STUDIES 84

CHAPTER 4: PRACTICAL DESIGN TESTING 86

4.1 METHODS 86

4.1.1 Set up of the SMA testing rigs *86*

4.1.1.1 Lever arm set up 87

4.1.2 Servo motor rig setup 90

4.1.3 Test methods and data collection *92*

4.1.3.1 Benchmark test: Setting parameters for maximum weight, actuation and cooling time, and current 93

4.1.3.2 Repeatability testing for determining potential drift in 0.381 mm diameter wire spring 98

4.1.3.3 Load cell testing 110

4.3 RESULTS 118

4.3.1 Benchmark test results: Setting parameters for maximum weight, actuation and cooling time, and current *118*

4.3.1.1 Efficiency of the two SMA rigs and the servo motor rig 120

4.3.2 Repeatability testing for determining potential drift in 0.381 mm diameter wire spring *121*

4.3.3 Load testing..... 126

4.4 DISCUSSION..... 127

4.4.1 Benchmark test: Setting parameters for maximum weight, actuation and cooling time, and current..... 127

4.4.1.1 Efficiency of the two SMA rigs and the servo motor rig..... 130

4.4.2 Repeatability testing for determining potential drift in 0.381 mm diameter wire spring 131

4.4.3 Load testing..... 132

4.4.4 Space needed to fit the actuators..... 135

4.5 LIMITATIONS..... 137

4.6 CONCLUSION OF PRACTICAL DESIGN TESTING..... 139

CHAPTER 5: CONCLUSION AND FUTURE WORK..... 141

5.1 OVERVIEW..... 141

5.1.1 Characterization test..... 141

5.1.2 Practical design test..... 142

5.2 FUTURE WORK..... 142

5.2.1 Spring actuator considerations..... 142

5.2.1.1 Types of SMAs..... 142

5.2.1.2 Behavior..... 143

5.2.2 Elbow-flexion exoskeleton considerations..... 144

5.3 CONCLUSION..... 144

BIBLIOGRAPHY..... 146

APPENDIX A..... 155

Force vs time for Extensional strain of 0..... 155

Diameter 1..... 155

Diameter 2..... 158

Force vs time for extensional strain of .5..... 162

Diameter 1 162

Diameter 2 162

Force vs. time for extensional strain of 1 ..... *167*

Diameter 1 167

Diameter 2 167

Force vs. time for extensional strain of 1.5 ..... *171*

Diameter 1 171

Diameter 2 171

Force vs. time extensional strain of 2 ..... *176*

Diameter 1 176

Diameter2 176

Resistance vs. time for extensional strain of 0 ..... *180*

Diameter 2 185

Resistance vs. time for extensional strain of 0.5 ..... *189*

Diameter 1 189

Diameter 2 190

Resistance vs. time for extensional strain of 1 ..... *194*

Diameter 1 194

Resistance vs. time for extensional strain of 1.5 ..... *199*

Diameter1 199

Diameter 2 203

Resistance vs Time for Extensional strain of 2 ..... *207*

Diameter 1 207

Diameter 2 211

RESULTS OF DIAMETER 1 (0.31 MM) SAMPLES 1 AND 2 INCLUDED 215

FORCE, RESISTANCE, POWER TABLES DIAMETER 1 239

FORCE, RESISTANCE, AND POWER DIAMETER 2 249

AVERAGE MAX FORCE, TIME TO MAX FORCE, AND RESISTANCE FOR DIAMETER 1 (0.31 MM)
SAMPLES 1 AND 2 275
APPENDIX B. 277
ARDUINO CODE 281
Encoder and load cell code *281*
Relay code *283*

List of tables

Table 1: Anthropometric data for upper body of males and females 10
Table 2: Approximate bicep widths and heights for males and females 14
Table 3: Comparison of different actuator systems.....18
.....42
Table 5: Flexinol wire specifications for different diameter spring 43
Table 6:Benchtop results for determining testing current parameters.....49
Table 7: Summary of total average time to the maximum force.....61
Table 8: Max force and actuation time for D2 E3 for all trials. 62
Table 9:Minimum and maximum resistance for D2E2. 70
Table 10: Summary comparison of average maximum power. 73
Table 11: Benchmark parameters.....95
Table 12: Efficiency test parameters to finish the efficiency calculation. 96
Table 13: Parameters of one cycle of the repeatability test, one cycle. 105
Table 14:Parameters for repeatability test. 106
Table 15: Load cell test parameters. 113

Table 16: Load cell raw data to load (kg). 117

Table 17: Rig actuation testing for extensional strain of 1.5 and 3. 118

Table 18: Data collected during efficiency testing. 120

Table 19: Efficiency comparison of tested actuators.....120

Table 20: Start and end conditions of actuator systems. 125

List of figures

Figure 1: Joints of the elbow (from Thieme Atlas of Anatomy [15]) 8

Figure 2: Muscles involved in elbow bend. [74].....9

Figure 3:Comparison of arm dimensions for the 50th and 95th percentile males and females. The measurements are in cm. 11

Figure 4: Force exerted by bicep of a female arm modified from OpenStax [25]. 16

Figure 5: WREX passive exoskeleton [32].....22

Figure 6: Wearable cable driven exoskeleton by Cappello et al. [33].....25

Figure 7: Bowden cable SMA elbow bend exoskeleton by Copaci et. al.....26

Figure 8: SMA transition phases and temperatures [75] 28

Figure 9: Stress-strain and temperature for SMA [42] 29

Figure 10: Yield stress and Martensite start temperatures for different annealing temperatures.[38].....30

Figure 11: Equations for Joule heating to find wire temperature [76] 31

Figure 12: Cross section of a spring[47] 33

Figure 13: Modes of induced stress [48]. 33

Figure 14: Stretched vs. compressed spring [49] 34

Figure 15: Axial vs torsional loading [50].....35

Figure 16: Spring parameters [45].....37

Figure 17: Maximum pitch angle and extensional strain of SMA springs [57].....39

Figure 18: Actuator spring maker. 47

Figure 19: Sample setup in Instron.....53

Figure 20: The Keysight E631A power supply with constant current capabilities is on the bottom with a Fluke 8846A digital multimeter (DMM) on top. 54
Figure 21: Graphs of the force vs time for D1 & D2 59
Figure 22:Graph of force vs. time from diameter1 at extensional strain of 0 depicting spring elongation.....60
Figure 23: Box and whisker graph depicting range and average max force for all extensional strains and currents tested for diameter 1 (0.31mm) 63
Figure 24:Box and whisker graph depicting range and average max force for all extensional strains and currents tested for diameter 2 (0.38mm) 64
Figure 25:Box and whisker graph depicting range and average time to reach max force for all extensional strains and currents tested for diameter 1 (0.31mm) 65
Figure 26:Box and whisker graph depicting range and average time to reach max force for all extensional strains and currents tested for diameter 2 (0.38mm) 66
Figure 27: Graph depicting force vs current vs extensional strain for D1. Graph actually goes to extensional strain of 2. 67
Figure 28: Graph depicting force vs current vs extensional strain for D2.....68
Figure 29: Resistance vs. time for diameter 1 extensional strain of 1.5 at .8 A.....69
Figure 30: Box and whisker graph depicting range and average change in resistance for all extensional strains and currents tested for diameter 1 (0.31mm).....71
Figure 31: Box and whisker graph depicting range and average change in resistance for all extensional strains and currents tested for diameter 2 (0.381mm).....72
Figure 32: The final compressed length after completed testing. 74

Figure 33: Lever arm showing 4 cm from elbow surface is approximately 8 cm from elbow joint [25].....87
Figure 34: Left, Actuator series connection; right, actuator parallel connection.....88
Figure 35: Two actuator lengths. Left extensional strain of 1.5 (6.66 cm compressed). Right original extensional strain of 3 (3.33 cm compressed), 40 cm during testing when image was taken.....90
Figure 36:Right image depicts the loads of the SMA actuators with extensional strain of 1.5. Left image depicts components and loads of the servo system.....91
Figure 37: Static model and equation to determine potential energy.....98
Figure 38: Right rig of SMA system extensional strain of 1.5, middle SMA system extensional strain of 3, and left servo motor system. Pictures show data logger, linear encoder, and computer fan.....100
Figure 39: Linear encoder on SMA system of extensional strain of 1.5. 101
Figure 40: Load cell on the SMA system and cooling fan. Two Arduinos and data loggers were used. One was connected to the load cell and the other to the encoder. 101
Figure 41: Arm rig with extensional strain of 1.5 with a 1 kg weight. 102
Figure 42: Up and down switch for servo motor with meter testing ports. 102
Figure 43:Stopper.....103
Figure 44: Force required to lift load at center of mass at 120 degree angle.....114
Figure 45:Force required to lift load at center of mass at a 30 degree angle.....115
Figure 46:Force required to lift load at center of mass at a 90 degree angle.....116
Figure 47: Load cell calibration curve and calibration factor.....117

Figure 48: Graph of the path of actuation over time for extensional strain of 1.5 lifting 1kg at 0.8A.....121
Figure 49:Graph depicting total actuation per cycle with a stopper for extensional strain of 1.5. 122
Figure 50: Graph depicting total actuation per cycle without a stopper for extensional strain of 1.5. 123
Figure 51: Graph of total actuation per cycle for 1.5 extensional strain system with and without a stopper. 124
Figure 52: Total actuation per cycle of extensional strain of 3 with and without a stopper. 125
Figure 53: Graph depicting force vs vertical location of the bottom end of the actuators, with and without a stopper for extensional strain of 1.5.....126
Figure 54: Graph depicting force vs vertical location of the bottom end of the SMA actuators for extensional strain of 3*.....127

Chapter 1: Introduction

1.1 Background

An exoskeleton is a type of orthosis that is external to the body and assists in applying and distributing forces to improve the wearer's strength, endurance, and motion. Exoskeletons differ from prosthetics and orthoses; where prosthetics aim to replace a part of the body and orthoses support the body part, exoskeletons are designed to enhance the body [1].

Advances in technology have allowed for the integration of human and machine to become more prevalent. Exoskeletons are a significant area of focus for the military, industry, and medical fields. The military and industrial sectors have turned to exoskeletons as a method of solving ergonomics issues. Workers who perform many repetitive tasks involving lifting and holding heavy objects and tools experience external stresses on the body that can lead to injury. According to the Occupational Health and Safety Administration (OSHA), Muscular Skeletal Disorders (MSD) caused by poor ergonomic conditions are a leading type of workplace injury. The types of exoskeletons developed for the military to improve ergonomics focus on improving endurance by lightening the loads of soldiers. Industry has improved ergonomics by adopting exoskeletons that work as zero-gravity arms, so the worker is not bearing the weight of the tool.

The medical industry has numerous other uses for this technology. One use is as an interface between doctors and surgical robots [2] but, the most common application is as a method to enhance the body and assist in the motion of those undergoing rehabilitation and those with muscular-skeletal disorders [3]. For those with muscular- skeletal disorders, the

external structures allow one to perform actions and tasks previously unachievable. These include walking, gripping, and lifting arms.

1.2 The Problem

For adults, the amount of upper body dexterity and control, including the ability to raise and move their arms, can be the difference between independent and dependent living. According to the US Department of Health and Human Services [4], there is a set of necessary activities of daily living (ADLs) that are defined as the vital activities one must be able to perform to live independently. The key ADLs include getting dressed, personal care, eating, moving to and from a bed [5][6].

Studies have found that immediately starting rehabilitation therapy after a stroke increases the chances of recovery, as directly after a stroke there is some neural plasticity that eases the ability to relearn movements [7]. For the purpose of rehabilitation, the combination of physical therapy with a therapist and an exoskeleton increased the speed of recovery and the patient's ability to perform vital tasks [8] [9]. In both the rehabilitative and every day assistive capabilities, upper body exoskeletons improve a wearer’s ability to complete necessary ADLs.

There is a higher rate of incidence of stroke in females than in males. Strokes are a leading cause of impairments in ADLs [6][10]. A study from the national heart, lung, and blood institute in cooperation with Boston University found that not only were strokes more prevalent in females but of stroke survivors, women were 20% more likely to experience total loss or impairment in the ability to perform ADLs. Reading through articles on existing exoskeletons and those being developed, most of the exoskeleton design caters specifically to the average male. Additionally, many of the of the exoskeletons that exist

for rehabilitation are either large, bulky, and heavy (requiring an external mounting area for support) or are completely passive.

Elbow flexion is important for ADLs such as getting dressed and eating. As such, it is often the focus of occupational therapy and rehabilitation for stroke patients who have lost use of one or both arms. The elbow is also an ideal starting point for therapists because it has fewer degrees of freedom and is responsible for just lifting the forearm. Therefore, the long axis of the exoskeleton and the elbow can easily be kept in alignment during movement. Whereas the shoulder, for example, must support the weight of the entire arm including the hand in multiple planes in space.

As with other medical devices worn by users, a rehabilitation elbow-flexion exoskeleton should be both effective and wearable. At a minimum, such an exoskeleton should have the requisite force necessary to help the patient bend the elbow. It should also be portable, safe, easy to control, and tailored for different types of disabilities and users [11]. A wearable medical device should also "fit within the user's lifestyle without adding additional stress, unwanted negative social attention, or interrupting the user's daily life [12]." My main research question is to determine if a certain diameter SMA spring in an exoskeleton can produce sufficient force to flex a female's arm and if it is possible to design an effective and wearable rehabilitation elbow-flexion exoskeleton tailored for the specific needs of females? That is, one that is more compact, lightweight, and discrete so that it will help promote comfort and social acceptance.

To further answer the question on whether it is possible to create an elbow-flexion exoskeleton using SMA springs, other questions on the designs of elbow-flexion exoskeletons must first be addressed. First, are the larger diameter SMA actuators with a

larger diameter and extensional strain the best actuator suited for powering such an exoskeleton? Second, how does efficiency compare to existing actuation method? Third, after how many cycles do the actuators begin to decay? Is there a point in which the amount of decay begins to stabilize? Finally, how do the theoretical forces generated by the SMA actuator systems compare to the actual, measured forces produced? It is important to answer all these questions before proceeding to design an actual effective and wearable elbow-flexion exoskeleton for female rehabilitation patients. Finally, while this study focuses on an SMA elbow-flexion exoskeleton for an adult female patient, some of the findings regarding maximum forces and actuation time will generalize to adult males and children of both sexes. The specifics of such generalizations are beyond the scope of this study.

To test these questions, two tests ere conducted. First the actuators where characterized using an Instron to measure the forces generated ty SMA spring actuators. Second a rig was built which incorporated the results of the first test in a wig with 6 SMA spring actuators.

1.3 Objective of the Study

The thesis has three goals, the first goal is to determine which are the system requirements that an elbow-flexion exoskeleton using SMA actuators would need to meet. To address this goal, chapter 2 begins with a literature review of the anatomy, kinesiology, and biomechanics of the human elbow, including a review of the differences between the female and male elbow. The second chapter then provides a literature review of the system

requirements for elbow-flexion exoskeletons and of existing exoskeleton designs. The last part of the second chapter is a literature review of SMA spring actuators.

The second goal of the thesis is to explore possible configurations of SMA springs that can be used for creating an elbow-flexion exoskeleton that could meet the requirements described in the literature review. Chapter 3 reports the results of the SMA spring characterization study. Different diameter actuators were characterized to determine their actuation behavior and force output; their maximum force; the time needed to actuate to that maximum force; the power needed to reach maximum force, and the potential for spring fatigue and degradation. Chapter three also addressses various limitations with the characterization study.

Chapter 4 addresses the third goal of the thesis, which is to begin the process of designing an SMA spring-powered elbow-flexion exoskeleton. The goal, however, was not to design and build a fully functional exoskeleton. The goal instead is to use the more promising SMA spring configuration identified in the characterization study to build and test a simple elbow-flexion rig. The main purpose of the rig is to test whether the chosen SMA spring configuration has sufficient force to lift and hold an average female's forearm, given power limitations and various other factors. A second purpose of the rig study is to identify potential degradation in the maximum force of the SMA spring actuators after repeated use in an elbow flexion exoskeleton rig. Chapter four reports the results of the rig study and discusses certain limitations.

1.4 Significance of investigating using SMAs for elbow flexion exoskeleton

Female adults are more likely than male counterparts to experience a decreased ability in performing ADLs. An exoskeleton that can cater to the female wearer would

impact the rate of occupational adaptation and recovery of female who have residual muscle weakness post cerebral accident. Since females are smaller and lighter than males, it is important to have an exoskeleton that is designed to properly fit and exert the forces necessary to bend the elbow of a female. Additionally, a new wearable interface between the exoskeleton and the user could have multiple implications for the future of exoskeleton design. Since SMA spring actuators are small and compact, they may be a good choice of actuator for the purpose of an elbow flexion exoskeleton. Studies have been done using straight wire SMA actuation for upper body exoskeletons, but further investigation into spring actuators can determine their use for this application.

Chapter 2: Literature review and background information

This chapter provides a literature review and background information regarding the requirements that and elbow flexion exoskeleton using SMA actuators would need to meet. The first section focuses on the anatomy and kinesiology of the male and female elbow, and the biomechanics of the elbow. The second section of this chapter is a literature review of the system requirements for elbow-flexion exoskeletons. The third section describes various existing upper limb exoskeletons. The fourth section of this chapter provides a literature review and background information of SMAs

2.1 Anatomy and Kinesiology

The goal of the exoskeleton is to enhance users' arm movements by simulating the natural movements and musculature propulsion of the arm. This section describes the anatomy and kinesiology of the human elbow, including highlighting some of the principal differences between the female and male upper arm anthropometrics. Taking into account anatomy and kinesiology is important when designing an elbow-flexion exoskeleton and determining how many SMA spring actuators to include and the spacing between them.

2.1.1 Components of the elbow

The human arm excluding the hand can naturally articulate in seven directions and thus has seven degrees of freedom (DOF). They are First Degree: Shoulder Pitch, Second Degree: Arm Yaw, Third Degree: Shoulder Roll, Fourth Degree: Elbow Pitch, Fifth Degree: Wrist Pitch, Sixth Degree: Wrist Yaw**,** and Seventh Degree: Wrist Roll. The axis of the movements are at the wrist, elbow, and shoulder [13]. Complex muscular and skeletal systems facilitate movement about the joints. The muscles provide the force necessary for displacement and for stabilizing the arm.

The elbow is where the humerus meets with the radius and ulna. The elbow provides two of the degrees of freedom for the upper limb, flexion/extension (elbow bend) and pronation/supination (forearm rotation). The joints at the elbow, which provide the bending motion are the humeroradial joint, between the humerus and radius, and the humeroulnar joint, between the humerus and ulna [14]. Two additional joints, the superior radioulnar joint, just below the elbow, and the inferior radioulnar joint, above the wrist, serve as pivot points of the radius and ulna during forearm rotation.

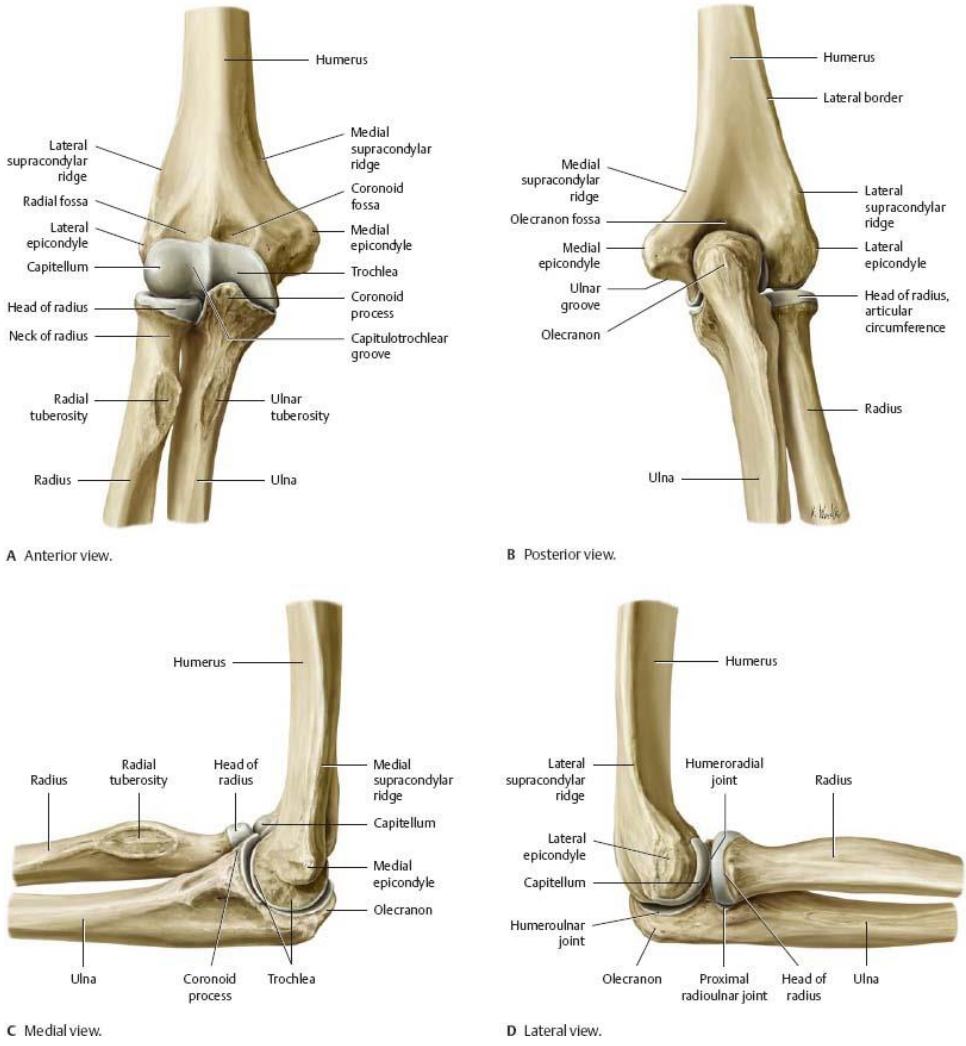

Figure 1: Joints of the elbow (from Thieme Atlas of Anatomy [15]*)*

For adults, the average ranges of motion of an elbow are 31.0 - 41.0 degrees for flexion (forearm overlapping upper arm is 0) , 180.7 – 184.9 degrees for extension (forearm overlapping upper arm is 0), 68.0-87.8 degrees for pronation, and 65.0-88.3 degrees for supination [14]. For the frame of this project the range of motion is measured from complete flexion (forearm overlapping upper arm is 0) with flexion being between 31-41 degrees. An elbow bend involves the activation of the brachialis, biceps brachii, brachioradialis, flexor carpi radialis, and pronator teres for flexion and the tricep muscle for extension (Figure 2) [16]. Activation of the pronator teres and pronator quadratus provide pronation; activation of the supinator, biceps brachii, and brachioradialis provide supination.

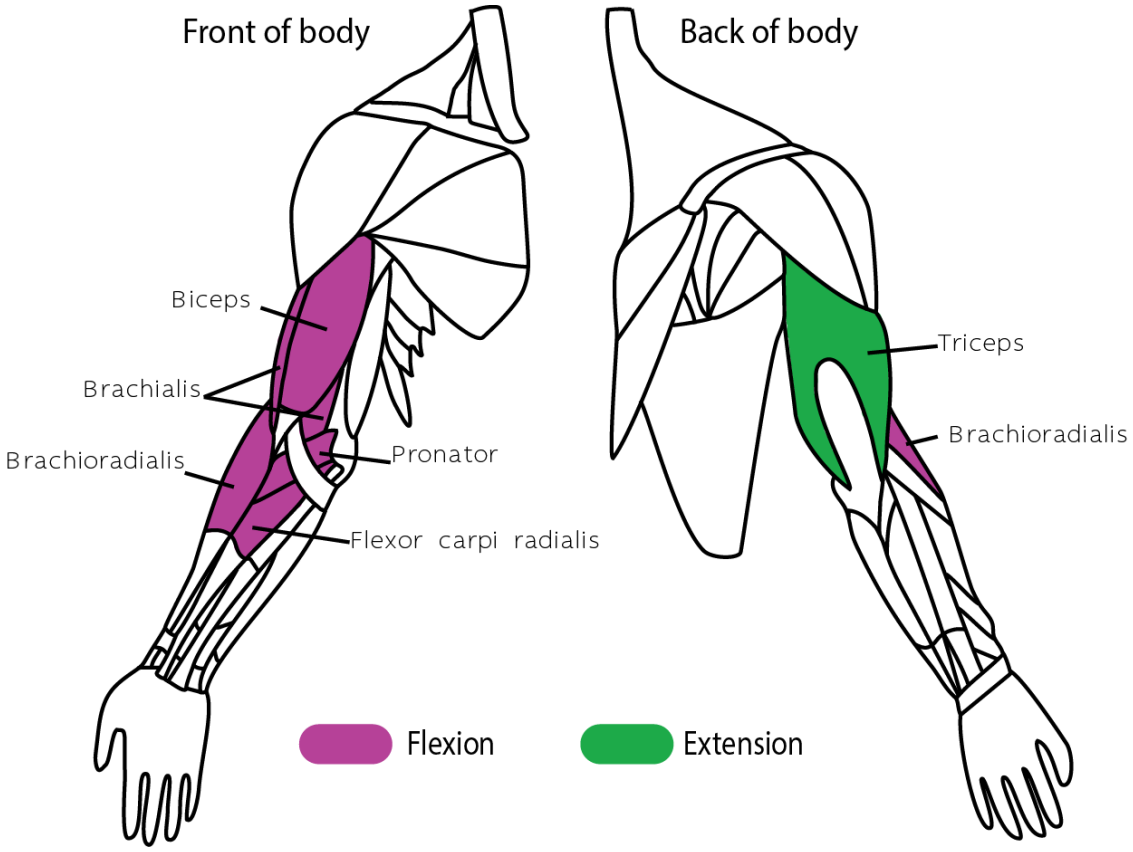

Figure 2: Muscles involved in elbow bend. [74]

2.1.2 Difference in female and male arm anthropometrics

The important anthropometrics for upper body exoskeleton design are upper arm length, forearm length, forearm mass, bicep circumference, and forearm circumference. These differences impact the design of the exoskeleton as the limitation on system size and force requirements differ between the two genders.

The majority of those who suffer cerebral accidents are above the age of 55 [6]; nonetheless, individuals of all ages may suffer from cerebral accidents that may require use of an exoskeleton. The anthropometric data used in this study are compiled from databases that used the total adult population of males and females in their reports. With the exception of the mass data which comes from Huston's *Principles of Biomechanics* [17], the information in the table below comes from the 2012 Anthropometric Survey of U.S. Army Personnel [18]. The data in Table 1 shows the 5^{th} to 95^{th} percentile.

Table 1: Anthropometric data for upper body of males and females

Dimension	Male 5%	Male 50%	Male 95%	Female 5%	Female 50%	Female 95%
Upper arm length (cm)	33.4	36.3	39.4	30.70	33.4	36.3
Lower arm + hand length (cm)	44.40	48.0	52.0	40.40	43.8	48.0
Lower arm (elbow to wrist) (cm)	24.4	26.7	29.5	21.80	24.00	26.80
Upper arm mass (kg)	1.84	2.23	2.67	1.41	1.71	2.07
Lower arm + hand mass (kg)	1.57	1.91	2.29	1.18	1.44	1.74
Bicep circumference flexed (cm)	30.30	35.7	41.8	25.90	30.40	36.00
Forearm circumference flexed (cm)	27.50	31.0	34.8	23.50	26.3	29.6

The average male arm is longer, has a larger circumference, and is heavier than that of an average female (**Error! Reference source not found.**). Creating a wearable exoskeleton requires that the system fit within the parameters of the wearer's anthropometric data. Since the average female arm is smaller than the average male arm, the resulting system should suited for a smaller size range. This does acknowledge that there is an overlap between the male and female arm size ranges. For the design of the exoskeleton in this project, this translates into smaller proximal and distal lengths of the actuator from the elbow. The decrease in circumference also impacts the design as there is a smaller surface area to attach the actuators to; there might be limitations to the number of parallel actuators that can fit on a thinner arm. For an SMA spring system to function efficiently, the actuators must be in line with the desired motion, so the maximum space that could be occupied by the actuators is dictated by the width of the front of the bicep.

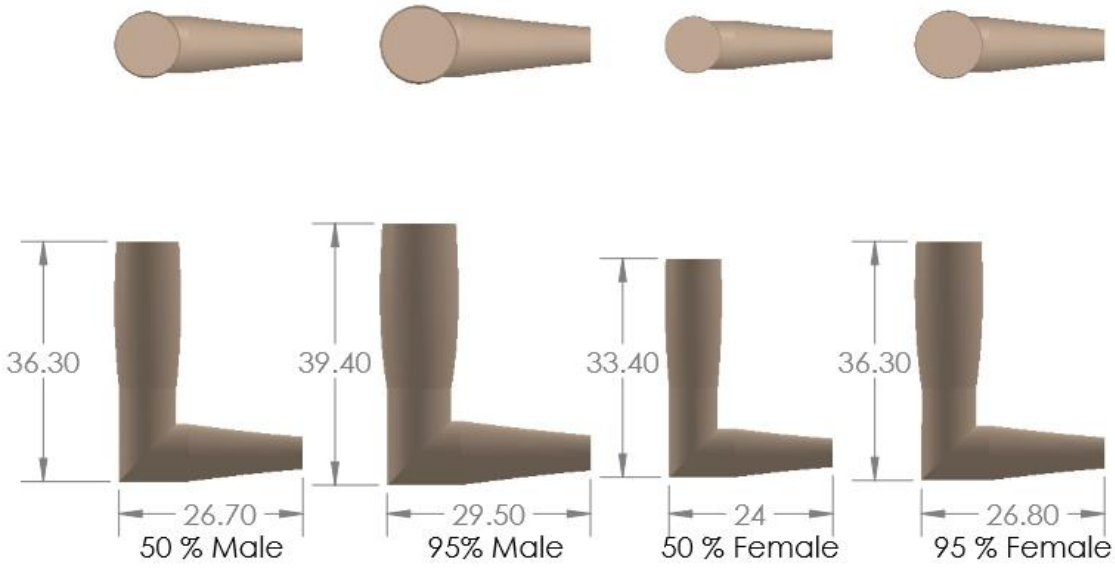

Figure 3:Comparison of arm dimensions for the 50th and 95th percentile males and females. The measurements are in cm.

Deviations from this area of placement (such as wrapping the actuators along the arm) will introduce torque into the system.

Designing an elbow-flexion exoskeleton relies on multiple (multivariant) parameters, such as those listed in Table 1, to determine the design parameters and fitting criteria. Multivariant procedures are complex as each parameter is not directly tied to the other [19]. For example, the 95th% in mass does not correspond to the 95th % in height. To properly design an elbow flexion exoskeleton for females, or any body-worn system, a method of relating the different anthropometric data must be established. In the case of fit criteria, one method currently being studied is the use of Principal Component Analysis to analyze the different anthropometric data. For the design parameters, more methods of varying complexity exist, all with the goal of trying to accommodate the largest population range. The simplest and most commonly used method is the univariant or 1D approach. This approach uses the 5th% to 95th% to anthropometric data of the different parameters to directly inform the design. Other methods rely on feedback, prototypes, and digital modeling [19] .

As the design of the actual exoskeleton is beyond the scope of this project, a simplified univariant approach was used to establish the testing weight and the location of the center of mass of the arm. Although the 5th% to 95th% are depicted in Table 1, this study focused only the 50th to 95th percentile mass, as the mass of the arm is a main consideration of the characterization of the SMA's for their application and use in the elbow-flexion exoskeleton. It is important to note that the focus is on characterizing the springs for their application and use. The design of the exoskeleton itself and its interface

for the smaller arm range is outside of the scope of this project. Therefore, instead of characterizing the load for the smaller portion of the female population, the springs were characterized for the higher loading conditions, long arm segments and large segment masses. The 50^{th} to 95^{th} percentile will be the higher load case and the springs would need to produce more force. For smaller segment lengths, the 5^{th} percentile, the center of mass would be closest to the elbow which would lead to a mechanical advantage. I have designed for the average female population. Although the 5^{th} percentile might not fit the solution designed, the system for the average would probably still be able to work for the 5^{th} percentile due to the smaller load. Results from this study can then be used as reference to design for the smaller arm sizes and ensure that it meets the requirements discussed in the introduction.

In future studies, the methods described by Iman et al. [19] could be used to determine and test the design of a full elbow-flexion exoskeleton to ensure that it fits and conforms to the requirements necessary for the 5^{th} to 95^{th} percentile female length and 5^{th} to 95^{th} percentile female weight.

Using the data in Table 1, the diameter of the 50th percentile female bicep is 9.68 cm (3.81 in). The human arm, however, is not perfectly round. None of the anthropometric databases have information on the height and width of the bicep. Grosso et. al from the University of Pennsylvania created a method for approximating the short and long axis of the bicep based off of the circumfrance using an approximate ratio of the axis. This method was developed for the creation of human-like avatars but takes into consideration real anthropometric data and measurements. According to Grosso et. al, the following equations can be used for determining the hight and width of the bicep [20]:

$$C = Circumfrance$$

$$A = Minor\ axis\ (width)$$

$$B = Major\ axis\ (height)$$

$$K = Axis\ ratio = \frac{A}{B} \approx \frac{17}{20}$$

$$C = 2\pi\sqrt{\frac{A^2 + B^2}{2}} \quad (1)$$

$$A \approx \frac{CK\sqrt{\frac{2}{K^2 + 1}}}{2\pi} \quad (2)$$

$$B \approx \frac{A}{K} \quad (3)$$

Using the equations above, a new table, Table 2 , is created to show the aproximate major and minor axis for 50 and 95th percentile males and females.

Table 2: Approximate bicep widths and heights for males and females

Dimension (cm)	Male 5%	Male 50%	Male 95%	Female 5%	Female 50%	Female 95%
Cirmumfrance (C)	30.30	35.70	41.80	25.90	30.40	36.00
Width (A)	4.41	5.20	6.09	3.78	4.43	5.25
Height (B)	5.20	6.12	7.168	4.44	5.21	6.17

Using the values in Table 2, the available space to mount actuators in a female upper arm is approximately 4.43 – 5.25 cm (2.5 in) in females. Thus, the space available in the female upper arm is approximately 0.77 to 1.66 cm less than the space available in the male upper arm.

2.2 Biomechanics of the elbow

In designing an elbow flexion exoskeleton, it is also important to understand the biomechanics of the human elbow. Biomechanics is the study of the internal and external forces on the body [14]. Part of biomechanics is the kinetic study of motion which looks at the forces that cause and impact motion. Breaking down the muscles, bones, ligaments, and tendons and turning them into mechanical components such as pulleys and levers, an approximate analysis can be made to determine the forces required for a movement or task to occur. Given the complex musculature, the number of bones and joints in the body, as well as variation in subjects, the mechanical analysis of a movement is complicated. The result is a model of body movement and associated values that are approximations of actual values. Additionally, exoskeleton designers need to take into account the difference between human and exoskeleton kinematics [21].

Notwithstanding this complexity, the majority of researchers have found it sufficient to rely on approximations of torque experienced at each joint and keep an armed lifted [22], [23].

In these models, the lever arm most commonly used is 4 cm. As for the center of mass, according to Zatsiorsky et al. as modified by de Leva, the center of mass for the female forearm is located at 49.59% of the total length for the forearm as measured from the from the proximal end (the elbow) [24]. For the purpose of the calculations and study, I used a length of arm between the 50th and 95th percentile forearm length of the female population, which is 25.4 cm. The resultant center of mass for this length is 11.5 cm from the elbow with an arm mass of 1.59 kg. Using this information, Figure 4 and Equation 4 show that the approximate force required by the bicep to maintain a female arm at a 90-degree angle is 44.25 N.

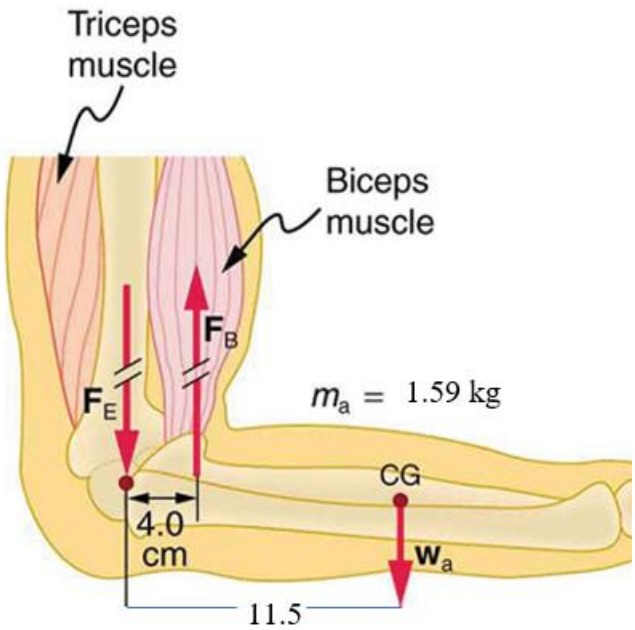

Figure 4: Force exerted by bicep of a female arm modified from OpenStax [25].

$$F_B * .040m - W_a * .115m = 0$$

$$W_a = 1.59kg * 9.81\frac{m}{s^2} = 15.60N$$

$$F_B = 44.85N \text{ or } 4.57kg$$

Equation 4: Equation for determining force excreted by bicep

2.3 System requirements for elbow flexion exoskeleton

Exoskeleton requirements can be divided into system requirements, which pertain to the system's performance, and user requirements, which pertain to wearability. This section discusses system requirements. User requirements are beyond the scope of this study. The elbow flexion system requirements relevant to this study are the following: the force needed to achieve elbow flexion; the power required to lift the exoskeleton; efficiency; speed; range of motion; reliability and repeatability

Other system requirements that are referred to in the literature but are beyond the scope of this study include: size and weight of the exoskeleton; compliance (which is relevant to the interface between the human body and the exoskeleton); system control; and natural motion [11][26].

2.3.1 The force needed to achieve elbow flexion

As discussed in the previous section, the exoskeleton would need to provide a minimum force of 44.85 N or 4.57 kg. Generally, the mechanical capability of an elbow flexion exoskeleton can either be measured as force or torque at the elbow. The examples that I use in section 2.4 of this paper on existing exoskeletons did not provide enough information do determine maximum loads or torques as well as sufficient information to be able to calculate them. The articles also did not include power and speed. Some sources did list a minimum torque that they used to ensure that the system could lift an arm, but did not list all of the requirements or if the system could lift more than just the arm.

Table 3, modified from Ninhuijs et al. [26], set forth the force and elbow torqure requirements for the elbow bend for electric motor, pneumatic, and hydraulic systems. The table also includes efficiency based on the values from Veale's paper [11]. The table also includes speed and power. It should be noted that the power measurements are for a full

upper body system, not just the elbow. Moreover, the measurements in the table are meant only to provide general metrics and capabilities for an elbow flexion exoskeleton. More precision is difficult given that some sources provide torques (Nm) and others forces (N). Similarly, some sources are listed as degrees per second and others as meters per second. Finally, the location of the actuators also varies.

Table 3: Comparison of different actuator systems

Actuation technology	Actuator Configuration	Elbow Torque max (Nm)	Force (N)	Speed	Power (W)	Efficiency (%)
Electromagnetic actuators (motors)	Directly on the joint	23	-	48°/s	19	40-80%
		7.2	-	75°/s	19.6	40-80%
	External position	28.4	-	95°/s	185	40-80%
	Gravity compensation	-	50	0	0	-
Pneumatic	Directly on the joint	-	220	1.1 m/s	242	< 30
Hydraulic	Directly on the joint	89	-	-	-	7-40%

2.3.2 Power to achieve elbow flexion

The goal for most systems is to generate sufficient force while reducing power consumption, thereby maximizing efficiency and portability. The issues of weight and size are important in that a low-profile design is also desirable to make the system non-invasive.

This project is an investigation into the application of SMA springs for an elbow flexion exoskeleton, and not on the design and evaluation of a complete system. The focus will be on power, force, range of motion, reliability, and speed of motion. These are the minimum requirements that must be considered when evaluating the feasibility of an actuator.

Like with many of the other requirements there is no set parameter for power, but the aim is to keep power low and within a reasonable range for available batteries. A reasonable range is defined here as using a maximum of a 25V battery and operating for a full day, 8 hours. Depending on the Voltage and the Amp-hour (Ah) of the selected battery, the maximum allowable power consumption will vary. Looking at the available batteries on amazon, for an average large battery of 25V, the current rating is 2.1 Ah. With this value of 2.1 Ah in mind, the maximum current that the system can draw to remain powered for 8 hours is .26 A. Since the actuation is likely to not be constant for all 8 hours [11], the amount of maximum on time can be approximated to 2-4 hours. There is no information available on how long an elbow is bent during the day and this estimate is just an approximation. This range brings the system max current to 0.52-1.05 A.

2.3.3 Efficiency

Efficiency (η) is the percentage of work or energy output by a system compared to work or energy put in. Efficiency is given as a percentage. The efficiency of an elbow flexion exoskeleton is important as in a full system it is related to power and weight of the system; a more efficient system uses less power to perform an action, and with less required power, there is less total weight. The goal of many exoskeleton research projects, is to increase efficiency and optimize systems [27].

2.3.4 Speed

Speed and the ability to control that speed are both important for an elbow flexion exoskeleton. Although the exoskeleton is a robotic device, it is being used as an assistive device on a human and should be compatible with human motion. Depending on the requirements for the use of the exoskeleton the speed requirement will vary. However, for

safety reasons, the maximum speed should be between 1-2 seconds for complete elbow flexion, approximately 100 degrees of rotation [28].

2.3.5 Range of motion

To achieve the required range of motion to complete activities of daily living, the exoskeleton must be able to complete the full range of motion which is from 130 degrees (arm extended) and 30 degrees (arm flexion) assuming that 0 degrees is with forearm overlapping the humerus[29].

The SMA spring actuators should be able to hold the arm in the required position to complete the desired task. To my knowledge and to the extent of my search, data regarding the amount of time a position is held when performing ADLs is not available. Since the activity of brushing teeth is a task that has a recommended time, it could be assumed that an exoskeleton must be able to maintain the bent position in the elbow for two minutes, the time recommended by the ADA (American Dental Association) for brushing teeth [30].

2.3.6 Repeatability

As was previously stated for durability, given the life challenges that the devices intended users may be faced with the device must be reliable and operate as intended each time the device is initiated by the user [31]. Another way to view reliability is accuracy; the system must reach the desired position and behave as desired. The system should not only be reliable to work, but also repeatable in its actions. Repeatability is related to precision, in terms of the exoskeleton, the system should reach the same position each time it is actuated. Although accuracy is independent from precision, an elbow bend exoskeleton should meet both requirements.

2.4 Existing exoskeletons

There are numerous types of upper limb exoskeletons. The upper limb exoskeleton is not only defined by the application, but the method and amount of assistance provided. The simplest type of exoskeleton is usually used for orthosis and is meant to provide limited extra support. It is completely passive and tends to have only one degree of freedom. For rehabilitation, many exoskeletons are passive and or only negate the forces due to gravity. An overview of the different system and applications will be addressed, but the focus will be on systems that aim to assist with activities of daily living.

2.4.1 Passive exoskeletons

Passive exoskeletons do not rely on motors or other active types of actuation. Using springs and counterbalances, passive exoskeletons are able to compensate for gravity. An example of a passive exoskeleton is the WREX exoskeleton. The WREX is one of the leading and most used exoskeletons and relies on a series of rubber bands to negate the weight of the wearer's arm. The benefit of the passive system is that it is simple and does not have the added weight of actuators. The major limitation of the passive system is the size as well as limited force. The passive systems like the WREX can only offer partial assistance and are unable to bend the elbow on its own [32].

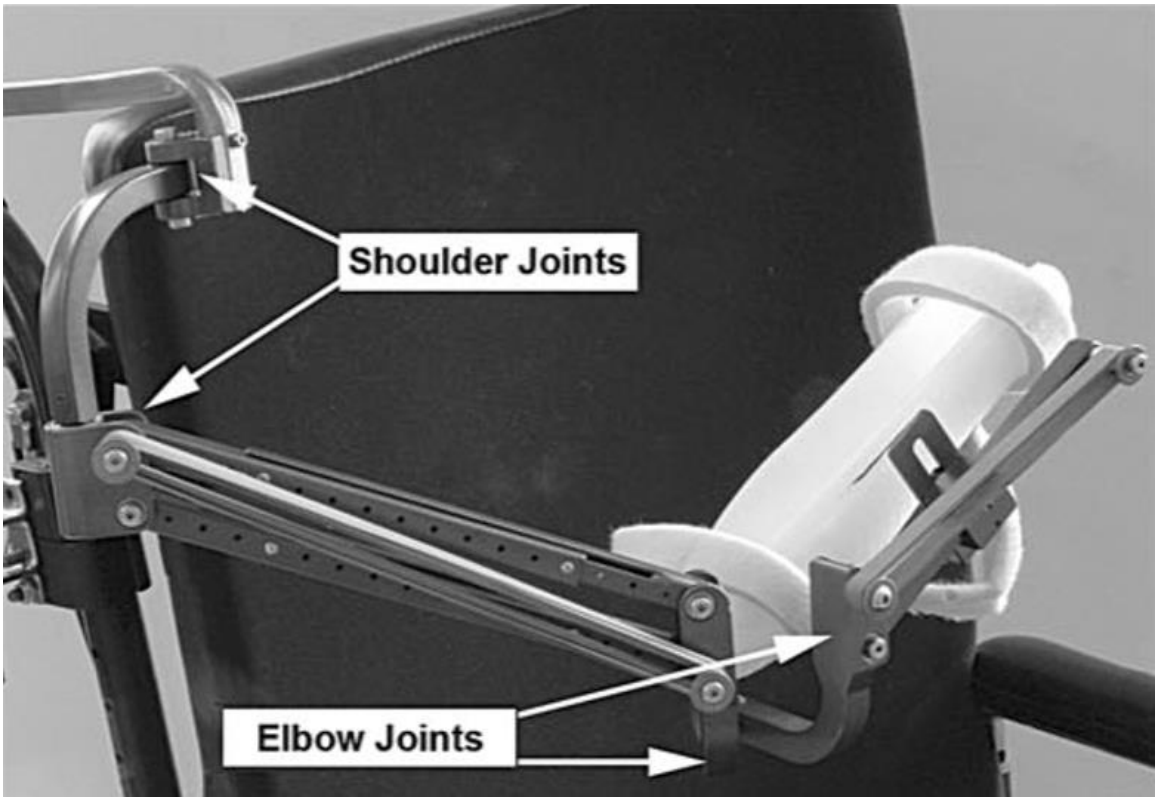

Figure 5: WREX passive exoskeleton [32].

2.4.2 Electric motor exoskeletons

Most recent studies are focused on the electric motor type exoskeleton. The goal of many of the electric exoskeletons is to provide further support and assist with the movements. Electric exoskeletons have a vast range of uses and are highly sought after for military and labor applications as well as everyday wearable orthosis.

Electric motors have the benefit of having a high torque to volume ratio as well as being high-speed. Another benefit of electric motors is their ease of control and ability to maintain a load. Control of motors takes form in both position control, and torque control. Different gearing can be used to achieve the desired torque while also reducing the speed of the resulting motion. For the application of the elbow exoskeleton, these qualities are key to successful actuation [26]. The limitations of electric motors in their use for

exoskeletons is that they are noisy and can be expensive. Additionally, the gearing reduces the efficiency of the system and influences the compliance of the exoskeleton by decreasing backdrivability [11], [26]. Back drivability is important and pertains to a motor's ability to be moved when not powered. It would be a safety hazard if an exoskeleton lost power and the user's arm was forcibly locked in a position.

Literature also cites power, size, and weight as a limitation, but the investigation into existing motors and their technology shows that this is only a limitation depending on the chosen motor and its application. Many small, lightweight, efficient, motors are available on the market but tend to come at a higher price. With regards to power most DC motors can be powered with a battery, but depending on the efficiency of the motor, the usable operation time of the motor might be limited [11].

As a main actuation method for upper body exoskeletons, many rehabilitative exoskeletons, both wearable and stationary, exist or are in development. Since the aim of this study is to look at wearable systems, a design by Cappello et al. is reviewed in terms of mechanical design and requirements. Of the motor driven exoskeleton systems, I encountered in my research, the design by Cappello et al. was the most wearable. The soft wearable exoskeleton developed by Capello et al. takes advantage of a motor and cable system, integrating a cable into a textile-based soft frame. The system was designed to meet a certain set of requirements established by the team through research and literature review with the aim of minimizing user discomfort. For an exoskeleton to be wearable, it must: be compliant, lightweight, have limited moving parts, mimic natural motion, not constrain movement, have the majority of the system located in a comfortable location, be comfortable to wear, be safe, have force and position control, and be efficient [33].

The main subsystems to point out for meeting these requirements are the motor assembly, the soft frame, and the series elastic element. The motor assembly comprises of a brushless DC motor and coil spool and aims at generating sufficient torque to lift an arm while also providing position control. The soft frame is the base of the exoskeleton and is used to transmit the force. Although the anchoring methods are not explored in this thesis, the soft frame merits elaboration as it is a novel anchoring method for exoskeletons. The soft frame takes advantage of different stiffness fabrics and nylon webbing. The placement of the different fabrics is strategic; stretchy fabric is placed in areas where flexibility is required and facilitates compliance for the more rigid nylon structures. The nylon is placed in regions were stability is necessary to distribute the experienced loads. The last subsystem, the series elastic element is the system compliance portion of the proposed exoskeleton. The elastic elements are springs which are placed in parallel with the cables to absorb any shock in the system and prevent injury to the user.

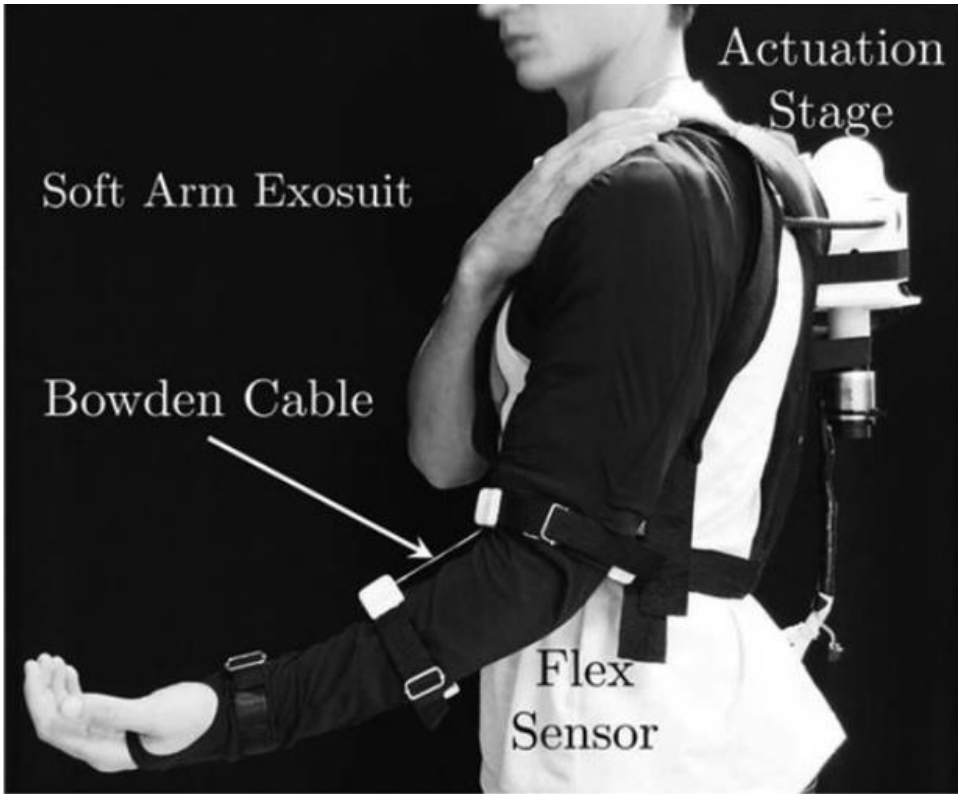

Figure 6: Wearable cable driven exoskeleton by Cappello et al. [33]

2.4.3 Soft exoskeletons

Soft robotics orthotics are a type of exoskeleton where the components are soft and flexible. A soft robotics device uses a combination of different elastomers and other soft materials to provide actuation and sensing. Often referred to as soft muscles, the elastic actuators tend to be composed of an elastic chamber and a flexible yet structured material (fabric or meshing). The soft muscles tend to be either pneumatic or hydraulic, and actuation is the result of air or liquid entering the elastic chamber. As the bladder expands, it pushes against the supporting material. The benefit of this type of actuation is that the actuators can be thin, lightweight, and easily integrated into clothing. Additionally, they provide multiple types of actuation paths. Most actuators provide linear or rotary actuation.

By altering the rigidity and placement of the soft robot, an actuator can provide shaped actuation [34]. The setbacks to the technology are that they require pumps and large battery packs to run them.

2.4.4 Shape memory exoskeletons

In exoskeleton design, a Bowden cable system provides a method of maximizing the mechanical transmission of a straight SMA wire. The Bowden cable uses the inherent change in dimension of the heated shape memory wire when heated. Since the wire inside the sheath is a straight wire actuator, with 4% compression, long lengths of material are required for very small actuation. A spring system provides a greater stroke length compared to overall length than the Bowden cable, but the Bowden cable provides greater force [35].

An SMA elbow exoskeleton was developed by Dorin Copaci at Carlos III University of Madrid that uses a Bowden cable system for actuation. The Bowden cable is comprised of a straight NiTi SMA core, a Teflon lining, and a nylon sheath. The part of the actuator directly over the joint is left uncovered for the desired length to allow for compression. As the SMA compresses, it slides along the outer layers. Since the total length of wire inside the sheaths must remain the same, the compression is observed at the

Figure 7: Bowden cable SMA elbow bend exoskeleton by Copaci et. al.

exposed section of the actuator, bringing the two sections together and causing the elbow to bend [35] Two Bowden cable methods exist and are dependent on the total length required for actuation and the available space. If the required length is less than the available space, the cables can be routed through individual pulleys. Otherwise, the cables are crimped, and the actuator runs the total desired length.

Copaci and his team also developed a flexible Bowden cable actuator system for actuating fingers. In this system, the outer sheath is a stainless-steel coil, which allows the fingers to bend. The coil has the additional benefit of acting as a heat sink, shortening the cooling time of the system [36]. A system using an SMA spring geometry of actuator has not been tested for the application of an elbow-bend exoskeleton.

2.5 Shape Memory Alloys

Shape memory alloys are a smart material that have the ability to be deformed and return to a set shape. This behavior is attributed to the underlying material properties of the alloys whose crystalline structure changes as the result of various phase transformations at different temperatures. The high stress to high actuation ration of SMAs lead to a high work output for unit volume. This specific advantage of SMAs is why the material is so often studied to use in the system. Although there is a high work per volume ratio, this does not translate into efficiency as SMAs have a low force per power ratio.

Multiple memory alloys exist, most comprising of a combination of Nickel and another metal. In this study, the focus is on the specific NiTi alloy which is 50% Nickel and 50% Titanium. NiTi SMA is most often used in the biomedical industry and has high success in integration in splints. As SMAs are not efficient, the best applications are for systems where large displacements are necessary but with little force.

The principles of SMA's memory is the phase transformation undergone by the material. The material exists in two phases with three different crystalline structures, Austenite, twinned martensite, and detwinned martensite. The resting phase of the SMA is called the twinned martensite phase. When the material is deformed, lattice distortion occurs, and stress is introduced into the material, turning the twinned martensite structure into detwinned martensite. When the SMA is heated to its starting transformation temperature, defined as Austenite starting (A_s), the material begins to change its structure and returns to its memory state (8).

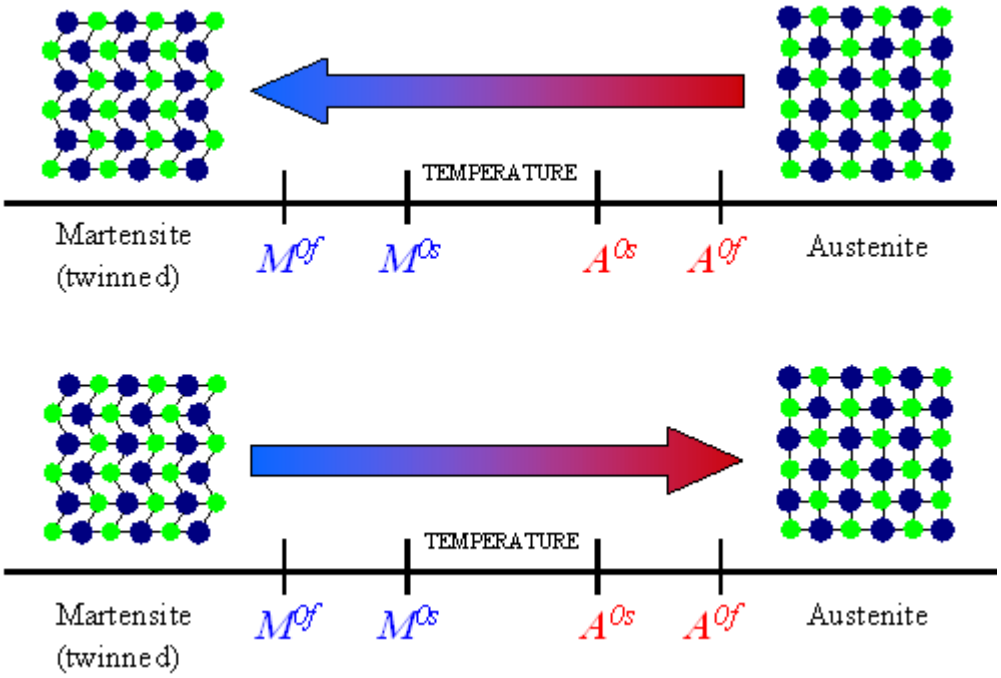

Figure 8: SMA transition phases and temperatures [75]

Forces are generated during the process of heating, and the transformation in the material structure as the strain in the material is released. The stress and strain are introduced into the material when the material is deformed. Heating the material leads to the release of energy and the reduction in strain [37] as depicted in Figure 9.

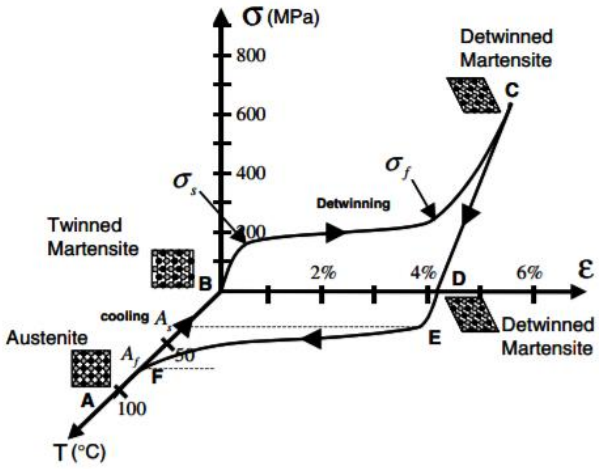

Figure 9: Stress-strain and temperature for SMA [42]

The annealing temperature, time, and alloy composition influence the yield stress and activation temperature (Austenite start and final). As far as yield stress and strain, the raw unannealed wire has a higher yield stress but less recoverable strain. Increasing the annealing temperature decreases the yield stress but increases the amount of recoverable strain, meaning an increase in actuation stroke [38], [39].

The Austenite start temperature of the wire, which is the temperature at which the SMA starts to actuate, and Martensite start temperature, which is the temperature at which the SMA can be deformed, can be modified by changing the annealing temperature. The raw SMA wire has a different behavioral pattern than the annealed wires as the microstructure of the SMA changes during the annealing process. The raw wire has a higher Austenite temperature than a wire annealed at 350, but the Martensite temperature is lower. During annealing, the structure of the alloy changes and the concentration of

Titanium increases, which is an explanation for the difference in behavior. For the other annealing temperatures, Austenite and Martensite increase with a rise in temperature. There is a large increase in Martensite temperature from 350 C to 500 C annealing, Figure 10 [38]. For this study, the actuators were annealed at 450 C for 10 minutes using the 70 C NiTi wire.

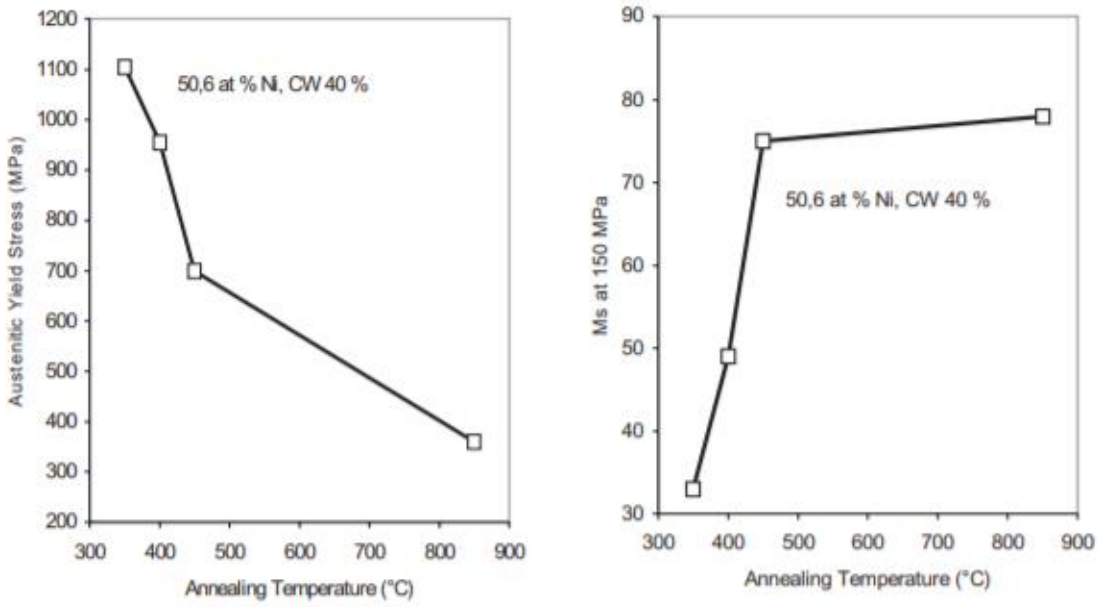

Figure 10: Yield stress and Martensite start temperatures for different annealing temperatures.[38]

Certain criteria for SMAs such as martensite temperature, hysteresis, Austenite temperature, yield, and stress, can be modified by changing the alloy and composition of NiTi. An example is NiTiFe, which adds iron for increase in strength. For decades SMAs that actuate at body temperature have been used in the biomedical industry. Example of fields and products that use SMAs are: orthodontics, braces; orthopedics, staples and plates; vascular, catheters and splints. All these devices are designed to actuate in one direction at body temperature (37 °C) with the exception of the braces which actuate with

hot food (approximately 65.5 °C) [40]. Additionally, SMAs are used in research on compression garments that can activate at body temperature [41]. Current research is being conducted on new alloys and methods of optimizing shape memory alloys for other applications beyond medical uses.

2.5.1 Joule heating

A common method of heating SMA actuators is via applied current in a method called Joule heating. Joule heating relates the applied current, the resistance of the material, and the material cross-section to a resultant temperature. As NiTi is a metal, just like other metals it compresses when heated. This means that the cross section and therefore the resistance of the material changes as it is heated.

$$CV\rho\frac{dT}{dt} = P(t) - hA(\Delta T(t))$$

$$P(t) = V_s(t)^2 R(t)$$

where

ρ	=	material density = 6.45×10^{3} kg/m^3[6]
C	=	specific heat = 465.2 J/(kg °C) [6]
V	=	wire volume = 1.434×10^{-8} m^3
h	=	convection heat transfer coefficient = 131W/(m^2 °C)
A	=	wire surface area = 2.258×10^{-4} m^2
$P(t)$	=	power consumed by SMA (W)
$\Delta T(t)$	=	Wire temperature above ambient (°C)
$V_s(t)$	=	source voltage (V)
$R(t)$	=	measured wire resistance(Ω)

Figure 11: Equations for Joule heating to find wire temperature [76]

2.5.2 Benefits and limitations of SMA actuators

In *Design Optimization of Shape Memory Alloy Linear Actuator Applications*, and *A review of shape memory alloy research, applications and opportunities*, Mohd Jani explored the benefits and limitations of SMA. He also discussed some methods to explore to attempt to compensate for some of these limitations. Benefits of SMA are their small size and high-power density for a given actuator size.

More specifically, depending on the diameter of the wire, the straight wire configuration of an SMA is able to sustain a significantly high load. The straight wire actuator achieves actuation through the inherent compression of the wire as it is heated. Since the actuation is based on the material deformation, a maximum compression of 5% of the actuator length can be achieved. However, contracting and deforming the actuator the full 5% introduces excessive strain on the material and it is therefore recommended that the straight wire only be actuated to 4% of total length [42]. To try and compensate for this, pulley systems are developed to attempt to maximize actuation.

The other configuration of the SMA actuators is the spring. The spring is unable to sustain as high loads but is able to produce maximum displacement [43], [44]. Springs have an advantage in that they provide greater displacement than the straight wire. The spring actuators can undergo displacement of up to 200% of the free spring length before the deformation becomes irreversible [45]. The drawback to the springs is that the provided activation force is greatly reduced since the internal stress is torsional in springs rather than axial in a straight wire [46].

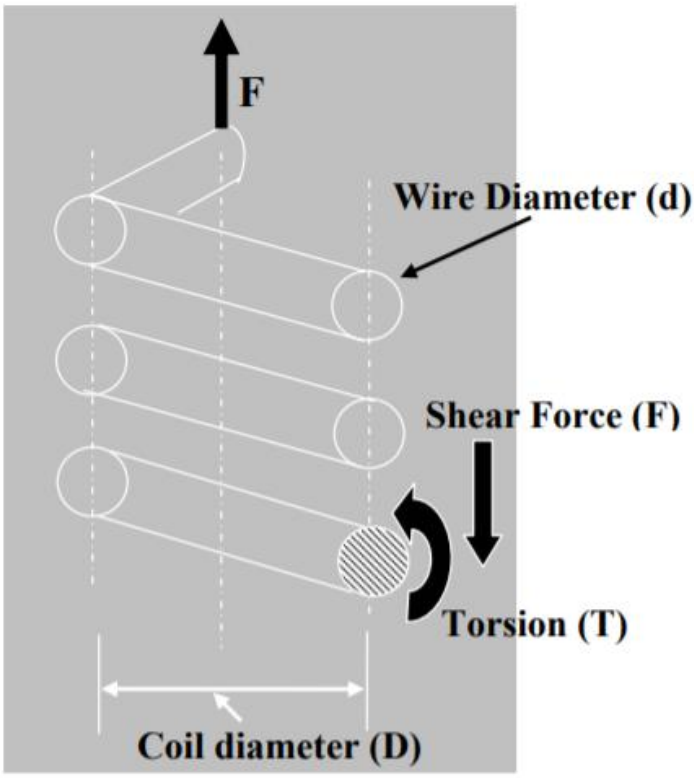

Figure 12: Cross section of a spring[47] .

The reasoning behind why linear force of a straight wire is greater than torsional force of a spring can be explained by a series of figures. Figure 12 shows the cross section of a spring. The force F (going up) is perpendicular to the wire of the coil (laying horizontal). This means that the wire will experience a shear stress as shown in Figure 13.

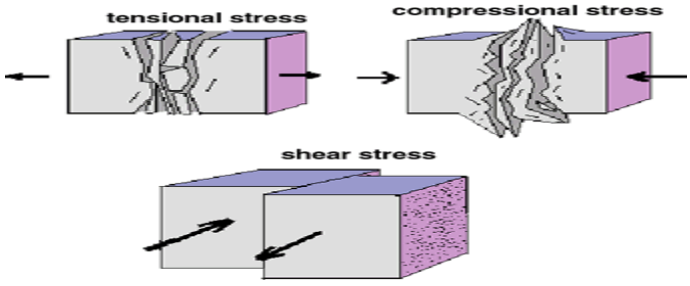

Figure 13: Modes of induced stress [48].

In addition to the shear stress, a spring has a torsional strain. In a stretched spring, the distance between the coils is greater than in the compressed spring (Figure 14). This means that angle α increased. This increase in angle causes a rotation in A which then causes torsional stress.

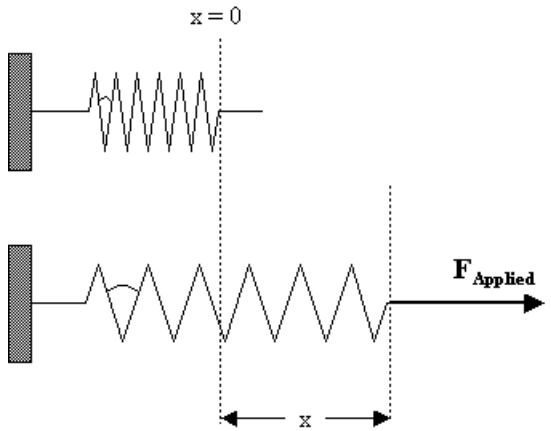

Figure 14: Stretched vs. compressed spring [49]

In the actuation of a spring, the internal stress is caused via torsional loading rather than axial loading (Figure 15). As a result, the stress is concentrated at the wire's perimeter, rather than being evenly distributed along the wire's cross-section. The recovery force decreases as a result because the inner strength of the material is not fully utilized in the spring geometry and the material on the inside of the wire does not have as much leverage creating an opposite torque from the material on the outside.

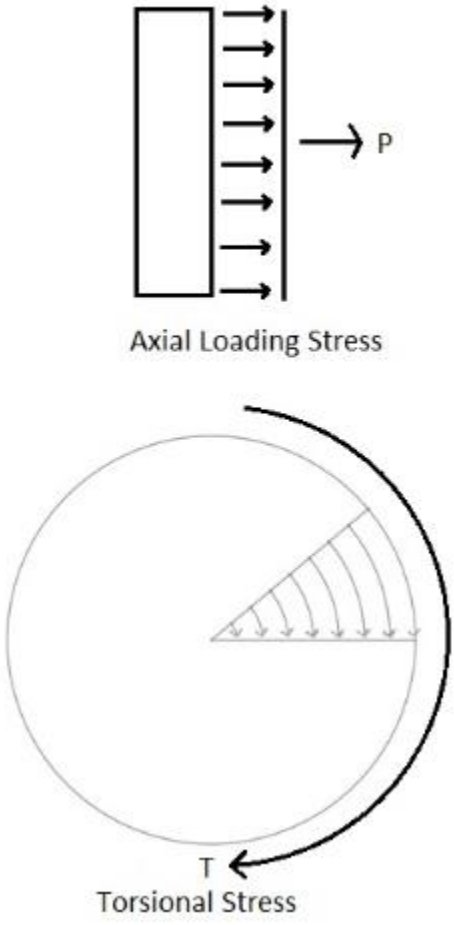

Figure 15: Axial vs torsional loading [50].

In case of axial stress, every part of the cross section (SMA) will experience an even load (Figure 15). This means that when the wire is trying to recover to its original state, every part of the wire contributes the same amount to the recovery force.

Given the stress distribution under a torsion stress (high on the outside, 0 on the inside), it's also easier to overstretch a spring than to overstretch a straight wire. When applying the same force under an axial load, the stress throughout the wire is evenly distributed. However, in case of the spring, the stress will be much higher on the outside. Since the stress is higher there, the maximum shear strain for a spring, of 6%, is reached

faster which means the spring SMA will have permanent plastic deformation much more easily.

Furthermore, the dynamic response and energy efficiency is decreased, mainly due to the power exploitation, under torsional loading, of the material in the center of the solid section, which adds to the cooling time and to the power consumption without contributing to the strength. Despite their drawbacks, helical SMA actuators have been shown to be reliable mechanical actuators, provided that the load is not substantial [43].

Besides wire geometry, wire diameter has a large impact on force, performance, and heating. As noted in the section above, as the actuators are heated via Joule heating which is a function of the diameter of the wire, smaller diameters heat and cool faster due to a high surface to volume ratio. However, the small diameter wires are not able to produce as high forces. As the diameter of the wire increases so does the force. The larger diameter wire has a greater volume of material per surface area, which means that temperature changes in both heating and cooling take longer, and are thus harder to control.

While SMAs have been used effectively in many applications, they are still the subject of active studies, in order to better understand the effect of non-linear behavior [51]–[53], variability of SMAs due to manufacturing imperfection [54], thermodynamic fatigue [55], and fatigue due to loading conditions [56]. One way of addressing the potential sources of SMA variability is to perform a characterization study as the first step when designing applications using actuators. This is a common approach in the literature. It is the approach used in this thesis.

2.5.3 SMA spring actuators

2.5.3.1 Spring index

The spring index (C), influences the resulting force and internal stresses in the spring. The spring index is the ratio of spring diameter, D (D = D_i (inner diameter) +2d), to wire diameter (d) (Figure 16). The ideal spring index is 3, this value is achieved by balancing the ratio of the wire diameter to the overall spring diameter. Higher forces are attainable at higher spring indexes, however winding the material to a smaller spring diameter requires excess stress to be applied to the material, resulting in fractures [45].

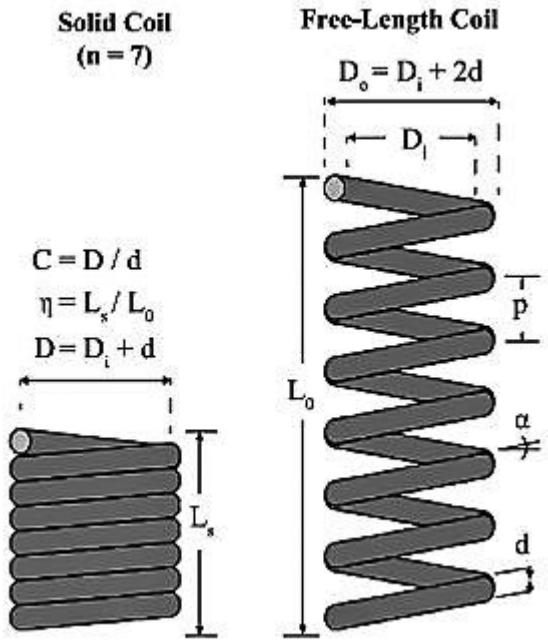

Figure 16: Spring parameters [45]

To accomplish the spring index of 3, the core wire diameter must be double the NiTi wire diameter. This is given by modifying the spring index equation to use Di.

$$C = (D_i + d)/d \quad (5)$$

$$3 = (D_i + d)/d$$

(6)

$$D_i = 2d$$

(7)

2.5.3.2 Extensional strain

Extensional strain is the ratio of displacement of the spring to the free length.

$$\varepsilon = \frac{\Delta L}{L_0}$$

(8)

Free length is the zero- load length of the spring. This differs from the starting length which is a fully compressed spring with a pitch angle of 0. For the simplicity of the problem, the free length is approximated to be the same as the starting length. This is not the case as the free length changes during actuation due to fatigue [45].

The maximum extensional strain according to *Engineering design framework for a shape memory alloy coil spring actuator using a static two-state model* by Shung-ming et al. is less than 2 for a spring index of 3. This is because the maximum shear strain for a SMA spring before it undergoes permanent plastic deformation is 6% and as shown in Figure *17*, this point occurs at an extensional strain of approximately 1.77[57]. Relating the y axis of (b) in the figure below to extensional strain, stroke length is ΔL which is the change in length from the initial length and initial length is L_0.

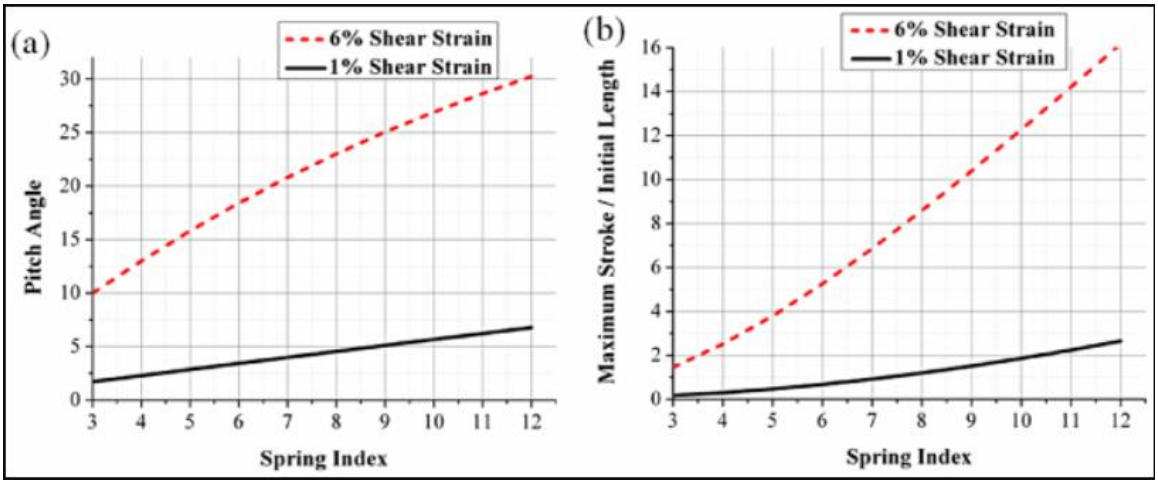

Figure 17*: Maximum pitch angle and extensional strain of SMA springs* [57].

The reason that maximum extension strain decreases with decreasing spring index is due to the increase in shear stress. As described in 2.5.2, the helical shape of a spring induces a torsional shear stress, the tighter the coil (i.e. lower spring index), the greater the stress. This relationship is visible through the equation for shear stress in a spring, τ. As shown in (9, there is a constant K (10) that relates to the spring index, C. In this equation, a decrease in C increases K, resulting in an increase in shear stress [58]. In spring design, the life (number of cycles) of a spring is improved by increasing the spring index [47].

$$\tau = K * \frac{8FD}{\pi d^3} \tag{9}$$

$$K = \frac{4C + 2}{4C - 3} \tag{10}$$

The values in SMA theoretical models do not always match actual findings in studies. For example, Holschuh and Newman found a maximum strain of 2.98 for a spring index = 3. The results of the study in this thesis also found a maximum achievable strain greater than the 1.77 predicted by the theoretical model described above in chapter 3.

These results are shown in chapter 4 where I was able to meet a maximum achievable extensional strain of 2.36. However, it should be noted that this extensional strain comes with limitations.

2.5.3.3 Theoretical force of SMA springs

Hooke's law relates stress to strain in a spring by stating that deformation of a spring (x) is linearly related (in the elastic region of the material) to the force/stress (F) applied by a spring constant (k) that is specific to the spring. An important note is that Hooke's law is only true while in the plastic, linear, region of a stress-strain curve. In a simplified form, Hooke's law is defined as shown in Equation (11 [58], [59]:

$$F = kx \tag{11}$$

Modifying Hooke's Law, a theoretical approximation of the maximum force produced by an SMA spring can be calculated following the methods by An et al. and Holschuh et al [45], [57].

$$F = \frac{Gd^2\varepsilon}{8C^3\eta} \tag{12}$$

$$G = Shear\ Modulus$$

$$d = Wire\ diameter$$

$$C = Spring\ index$$

$$\eta = Packing\ density$$

$$\varepsilon = Extensional\ strain$$

2.5.3.4 Flexinol actuator technical and design data

Wire diameter influences many of the properties of the SMA actuators including pulling force and current requirements; as diameter increases so do the pulling force and required current. To choose the desired diameter, efficiency and design must be considered. Using information from Dynalloy on the properties of straight wire actuation (Table 4) the 0.51mm wire has the highest ratio of grams to wire diameter. With respect to the amount of material used, the 0.51 mm wire is the most efficient in providing the greatest force. However, when looking at power consumption, the 0.38 mm wire produces the most force per mA and is thus the most power efficient [42]. The 0.31 mm diameter wire has a higher resistance and requires less current to actuate, but with the higher resistance, it overheats easily and consumes more power for an applied current. These three diameter wires were chosen to be used for testing.

For the purpose of this study and for comparison, it is important to include the Dynalloy Inc. information about their Flexinol actuator wire:

> *"The following chart gives rough guidelines for how much electrical current and force to expect with various wire sizes. If Flexinol® actuator wire is used within the guidelines then obtaining repeatable motion (typically 2% to 5% of working wire length) from the wire for tens of millions of cycles is reasonable. If higher stresses or strains are imposed, then the memory strain is likely to slowly decrease and good motion may be obtained for only hundreds or a few thousand of cycles. The permanent deformation, which occurs in the wire during cycling, is heavily a function of the stress imposed and the temperature under which the actuator wire is operating.*

Flexinol® wire has been specially processed to minimize this effect, but if the stress is too great or the temperature too high some permanent strain will occur. Since temperature is directly related to current density passing through the wire, care should be taken to heat, but not overheat, the actuator wire."

*Table 4: Flexinol wire specifications for different diameter straight wire. * The Heating pull force is based on 25,000 psi (172 MPa), which for many applications is the maximum safe stress for the wire. However, many applications use higher and lower stress levels. This depends on the specific conditions of a given design. The cooling deformation force is based on 10,000 psi (70 MPa), which is a good starting point in a design. However, this value can also vary depending on how the material is used. ** The contraction time is directly related to current input. The figures used here are only approximate since room temperatures, air currents, and heat sinking of specific devices vary. On small diameter wires (diameters less than or equal to 0.006" (0.15mm) diameter) currents which heat the wire in 1 second can typically be left on without over-heating it. Both heating and cooling can be dramatically changed (see section 3 of the technical characteristics at http://www.dynalloy.com//pdfs/TCF1140.pdf for more information.) *** Approximate cooling time, at room temperature in static air, using a vertical wire. The last 0.5% of deformation is not used in these approximations. LT = Low Temperature and HT = High Temperature Flexinol® Actuator wire.* [42]

Diameter Size inches (mm)	Resistance ohms/inch (ohms/meter)	Pull Force* pounds (grams)	Cooling Deformation Force* pounds (grams)	Approximate** Current for 1 Second Contraction (mA)	Cooling Time 158°F, 70°C "LT" Wire *** (seconds)	Cooling Time 194°F, 90°C "HT" Wire *** (seconds)
0.001 (0.025)	36.2 (1425)	0.02 (8.9)	0.008 (3.6)	45	0.18	0.15
0.0015 (0.038)	22.6 (890)	0.04 (20)	0.016 (8)	55	0.24	0.20
0.002 (0.050)	12.7 (500)	0.08 (36)	0.032 (14)	85	0.4	0.3
0.003 (0.076)	5.9 (232)	0.18 (80)	0.07 (32)	150	0.8	0.7
0.004 (0.10)	3.2 (126)	0.31 (143)	0.12 (57)	200	1.1	0.9
0.005, (0.13)	1.9 (75)	0.49 (223)	0.20 (89)	320	1.6	1.4
0.006 (0.15)	1.4 (55)	0.71 (321)	0.28 (128)	410	2.0	1.7
0.008 (0.20)	0.74 (29)	1.26 (570)	0.50 (228)	660	3.2	2.7
0.010 (0.25)	0.47 (18.5)	1.96 (891)	0.78 (356)	1050	5.4	4.5
0.012 (0.31)	0.31 (12.2)	2.83 (1280)	1.13 (512)	1500	8.1	6.8
0.015 (0.38)	0.21 (8.3)	4.42 (2004)	1.77 (802)	2250	10.5	8.8
0.020 (0.51)	0.11 (4.3)	7.85 (3560)	3.14 (1424)	4000	16.8	14.0

Dynalloy also includes information on a limited number of springs:

> *"While these values will vary depending on how the springs are used, are still a reasonable starting point for a design…The following chart gives rough guidelines as to how much current and force to expect with various Flexinol® actuator spring"*

*Table 5: Flexinol wire specifications for different diameter spring. *The Stretch Ratio "SR" and Displacement values are typically accurate, but remain approximate values. ** The Heating pull force is based on ~ 25,000 psi (172 MPa), which for many applications is the maximum safe stress for the wire. However, many applications use higher and lower stress levels. This depends on the specific conditions of a given design. The cooling deformation force is based on ~10,000 psi (70 MPa), which is a good starting point in a design. However, this value can also vary depending on how the material is used. *** The contraction time is directly related to current input. The figures used here are only approximate since room temperatures, air currents, and heat sinking of specific devices vary. Both heating and cooling can be dramatically changed (see section 3 of the technical characteristics at http://www.dynalloy.com/TCF1140.pdf for more information.)*
**** Approximate cooling time, at room temperature in static air, using a vertical spring. The last 0.5% of deformation is not used in these approximations. HT = High Temperature Flexinol® Actuator Spring.* [42]

Spring Wire Diameter in(mm), Outer Diameter in(mm)	SR Cold, SR Hot*	Displacement / Coil in(mm)*	Resistance on Straight Wire ohms/inch (ohms/meter)	Heating Pull Force** pounds (grams)	Cooling Deformation Force** pounds (grams)	Approximate*** Current for 2 Seconds Contraction (A)	Cooling Time 194°F, 90°C "HT" Wire**** (seconds)
0.020 (0.51), 0.136 (3.45)	6.5, 3.5	0.06 (1.5)	0.11 (4.33)	0.536 (243.3)	0.215 (97.32)	3.4	15.0
0.015 (0.381), 0.10 (2.54)	6.5, 3.5	0.04 (1.1)	0.21 (8.27)	0.307 (139.3)	0.122 (55.72)	1.9	9.0
0.008 (0.203), 0.054 (1.37)	6.5, 3.5	0.02 (0.6)	0.74 (29.13)	0.089 (39.3)	0.035 (15.94)	0.7	3.0

It is important to note for comparison of this table to the properties studied in this study, that SR (Spring ratio) is not the same as extensional strain. SR as defined by Dynalloy is L/Ls, which is what is defined in this thesis as packing density, η. For example, Dynalloy states that a SR of 4 for a 10 mm spring would result in a 40 mm spring. The spring ratio can be re-defined as extensional strain by modifying the ratio to a difference

of lengths. Using the cold SR for the 0.381 mm wire spring, the extensional strain can be found:

$$SR = \frac{L}{L_s}$$

$$\Delta L = L - L_s = L_s(SR - 1)$$

$$\varepsilon = \frac{\Delta L}{L_s} = SR - 1 = 6.5 - 1 = 5.5$$

As a result, since the values can be related to each other, the absolute length tested for the springs are not required.

Additionally, in Table 5, the spring index is not the same as used in this thesis. For the 0.381 mm wire spring, the final outer diameter of the spring is 2.54 mm. Using the equation for spring index, it is determined to be 5.667. This distinction is important as it relates to the higher maximum extensional strain. As stated by An et. al [57], maximum extensional strain increases with spring index. Looking up the spring index of the Dynalloy spring in Figure 17, the resulting maximum extensional strain is approximately 5.5, confirming the results from Dynalloy.

2.6 Conclusion

This literature review and background highlights the issues of current elbow flexion exoskeletons and the potential benefits of using SMAs and SMA springs. In particular, this chapter concludes that the average range of motion for ADLs is between 31-41 degrees of flexion and 180-184 degrees of extension. It also concludes that the anthropometrics of the female sex is different than that of the male sex and that the maximum number of actuators that can theoretically fit on a female's arm is 22, assuming no space between the actuators.

This chapter sets forth the principal factors for setting up the actuators on the arm and determining the space between them, including the constraints provided by the limitations of power, the potential of overheating, and the potential for shorting the system. This chapter also provided information on the maximum power (25 V and 1.05 A) and the importance of optimizing efficiency. Also included is information for understanding the behavior and benefits of NiTi SMAs and NiTi SMA springs that is necessary for the experiment and the rest of this thesis.

Chapter 3: Characterization testing

This study was conducted in two parts: a preliminary material characterization test and a practical design test using a simple elbow-flexion rig. The chapters for the two parts are separated as the results from the characterization testing influence the decisions for the practical design test. The purpose of the characterization test was to compare actuator springs of varying parameters to measure the force output and actuation time, so as to determine which actuator would be best suited for integration into the exoskeleton rig.

The first section of this chapter outlines the methods used for investigating the different design considerations for SMA actuators. The second section sets forth the results from the characterization testing. The third section of this chapter provides a discussion of these results. The last section discusses various limitations.

3.1 Methods

This section begins by setting forward the procedure required for making the actuators. It then describes the characterization testing: in particular, it discusses the selection of the parameters to be tested. Section 3.1.3 describes the testing set up and testing procedures. The last section sets forth the methods used for data analysis or the results.

3.1.1 Making of actuators

Coiled SMA actuators were made using NiTi Flexinol wire from Dynalloy of three varying diameters: 0.31mm (D1); 0.38 mm (D2); and 0.51 mm (D3). The 0.31 mm and 0.38 mm diameters have an austenite starting temperature of 70 ℃, and the 0.51 mm has an austenite starting temperature of 90 ℃. The Flexinol wire was chosen as it is the

standard use at the University of Minnesota Wearable technology lab and the company provides detailed specifications on the material.

3.1.1.1 Coiling process

The spring actuators are made on a specific SMA coil maker at the University of Minnesota Wearable Technology Lab which is an adaptation of the method described by Holschuh et al. [45]. The actuator maker consists of a motor at the bottom of an aluminum extrusion, a weight, a coiling tube, and a turnbuckle with a bearing, Figure 18.

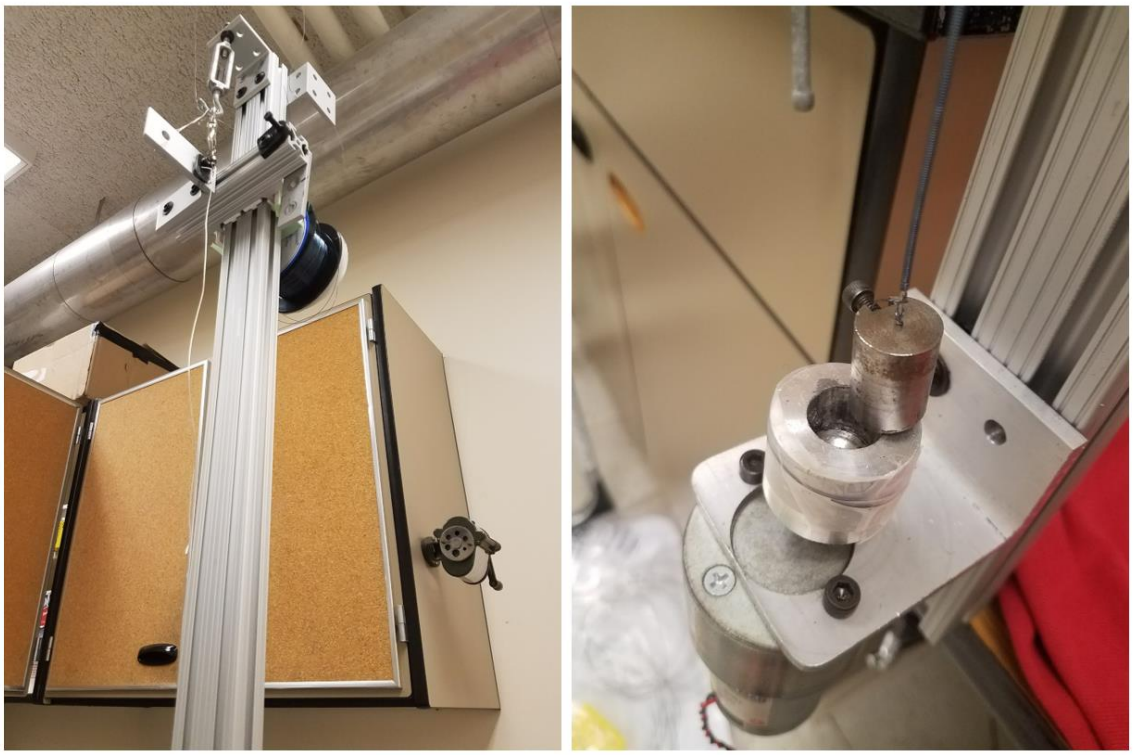

Figure 18: Actuator spring maker.

In order to make the actuator, a stainless-steel core wire is attached to the motor and the upper bearing. Before the core is secured to both ends, the coiling tube is slid over the core. The SMA is then fed through a slot in the tube and secured to the motor hub.

When everything is in place, the weight is secured to the coil tube, and the motor is powered.

The motor is kept at a constant rotation rate. As the motor turns, the SMA coils around the core. The tube constrains the outer diameter of the forming coil, the weight keeps a constant load on the tube and coil, and a wire guide between the SMA spool and the coil tube keeps tension on the wire. The combination of all these features prevents the coil from unwinding and ensures a consistent packing density and spring pitch.

The core wire and wire guide were selected for each diameter of actuator wire based on the spring index (C). The springs of each diameter wire were created to achieve the spring index of 3, mentioned in 2.5.3.1. To accomplish the spring index of 3, the core wire diameter must be double the NiTi wire diameter. This is given by (7, resulting in the following coil diameters:

$$D_{i\ diameter\ 1\ (.31mm)} = 2 * .31\ mm = 0.62mm$$

$$D_{i\ diameter\ 2\ (.38mm)} = 2 * .38\ mm = 0.76mm$$

With the inner diameter and wire diameter known, the outer diameter can be determined.

3.1.1.2 Heat treating/Annealing process

Heat treating/annealing the coil sets the memory state of the spring by setting the austenite state. The annealing process was adapted from Holschuh et al. and used an annealing temperature of 450 ℃ with 10-minutes annealing time. After the 10 minutes in the furnace, the springs are quickly removed and quenched in a bucket of cold water [45].

To minimize variability in the heat treating/annealing process, all actuators used for testing on the exoskeleton were annealed in the same batch. Heat treating/annealing all the actuators at once ensured equal heating and quenching time.

3.1.2 Characterization testing

3.1.2.1 Parameter determination

In order to perform the spring characterization and determine requirements for the exoskeleton prototype, the testing parameters must be established. The necessary parameters that must be determined are required wire diameter, test current, spring index and diameter, and spring length.

Although the 0.31, 0.38, and the 0.51 mm diameter wires were initially considered for testing, results from initial bench testing eliminated the 0.51 mm diameter from being used in the characterization testing as the temperatures required for actuation were high enough to cause the springs to lose their memory.

3.1.2.1.1 Test current

Before running the characterization tests, simple benchtop test was done to establish testing current inputs. A 5 cm sample of each of the three diameter springs was stretched to an extensional strain of 2. Lead cables from the power supply were then connected to each end of the spring and secured in place with tape. Voltage was increased until the actuators began to actuate. Voltage was increased until full compression occurred in approximately 1 second. The benchtop test was repeated 5 times for 3 different samples. Results from the benchtop testing are shown below (Table 6). The results below are the average of the different samples and trials. They were all approximately the same.

Table 6:Benchtop results for determining testing current parameters.

Diameter	First visible actuation	Actuation ≈ 2 seconds	Actuation ≈ 1 second
D1 (0.31mm)	2.5V, 0.29 Amps	4V, 0.5 Amps	5.5V, 0.68 Amps
D2 (0.38mm)	2.5V, 0.4 Amps	4V, 0.8 Amps	5.5V, 1.0 Amps
D3 (0.51mm)	2.5V, 0.87 Amps	4.5V, 1.5 Amps	5.5V, 1.95 Amps

For an even comparison, all samples were tested at the same applied currents. Results from this initial test eliminated the D3 wire as the current required for actuation was higher than the maximum suggested current for the 0.31 diameter wire. Additionally, the 0.51 mm diameter wire would heat to the point of permanent deformation after 2 to 3 cycles. Lower extensional strains still exhibited the same permanent memory loss.

Comparing the results in Table 6**Error! Reference source not found.** to the specs from Dynalloy reveals that the required current for 1 second actuator was much less than specified. Dynalloy states that the currents for 1 second actuation of the 0.31mm, 0.38 mm, and 0.51mm diameter wires straight wires are 1.5A, 2.25A, and 4.0A respectively as shown in Table 4. For the provided spring diameters in Table 5, the current for the 0.381 mm and 0.51 mm diameter wire springs for 2 second actuation are 1.9 A and 3.4 A respectively. The results from the benchtop testing showed that it only took 0.68A, 1.0A, and 1.95A for 1 second actuation and 0.5A, 0.8A, and 1.5A for 2 second actuation. I was unable to find literature to support the discrepancy and Dynalloy does not provide all information about testing conditions. Reaching out to representatives of Dynalloy, they stated that the length of the sample is not relevant or responsible for the discrepancy. Possibilities in the discrepancies could be due to sample size and geometry, although Dynalloy says that the length does not matter, there might be other factors, such as annealing temperature that might influence the results.

The chosen maximum current for testing was 1 Amp, but this was further reduced twice for the 0.31 mm diameter wire during characterization testing. During testing, a test sample was discarded and excluded from testing for the 0.31 mm diameter wire during the first test condition, as when the sample got to 0.9 Amps, it began to burn and smoke. During

subsequent tests, when the first two samples of D1 were tested, permanent deformation and change in behavior led to testing a third sample at only 0.5 Amps maximum. Although the bench top testing was consistent, the currents were only sustained for sufficient time to actuate the springs. Sustaining the current for the time required for testing and for the output force to stabilize, overheated the springs at the higher currents.

3.1.2.1.3 Actuator length

Varying the distance of the applied force from the joint as well as the length of the actuator both demonstrated effects to the resulting force. For the straight wire actuator, the actuator length can be determined by finding the required compression (C). Since a straight wire can only compress up to 4%, the required length (L) would be L=C/.04.

For the SMA spring, the length of the actuator is dependent on many factors including extensional strain. Calculating the required length first requires optimizing the system to determine the desired force and wire diameter. The relationship of $\varepsilon = \delta / L_0$ can be used to back-calculate the desired initial length for a given extensional strain.

For the spring characterization, only one compressed length was tested. The length of 5 cm was used for testing based on initial exoskeleton design where the compression region was 8 cm centered over the elbow, using data from Copaci et al. [35]. In this design, when the elbow is bent to 30 degrees, the distance between the forearm and upper arm at approximately 2 cm from where they stop touching is 5 cm. Therefore 5 cm is the minimum compressed length of an actuator for this application.

3.1.3 Data collection

Spring characterization testing was adapted from methods established by Holschuh et al. for characterization of NiTi coil actuators in active compression garments [45]. For a

wide representation of the force profile, each wire was tested at five different extensional strains ranging from 0-2 at 0.5 extensional strain intervals. Extensional strain is defined as the ratio of the change in length to the original compressed length. Since the heating of the actuators is related to current and Joule heating, the current was controlled. A total of 9 current steps were tested ranging from 0 to 0.8 Amps incrementing by 0.1 Amps. In order to constrain other parameters that affect the force of the actuator, all actuators are made using the same method, have the same packing density, and have the same spring index. Packing density refers to the number of coils per inch. To reduce the effects of environmental factors between tests, all tests were conducted in a humidity and temperature-controlled chamber.

3.1.3.1 Testing setup

An Instron 5542 tensile tester was used to collect the force data for the different tests. The Instron has two clamps to hold samples, one stationary and one dynamic. For this study they were both held static for each test, and a force was applied by the actuators on the integrated load cell.

The two clamps of the Instron were set 5 cm apart. Two samples each of D1 and D2 were cut at 7cm lengths, allowing for 1 cm of excess at each end of the actuators for clamping. The 1cm excess was stretched before clamping to reduce slipping in the clamps. Alligator clips were then attached to the top and bottom of the spring. The cable of the top alligator clip was wrapped around the Instron to prevent any tug on the spring due to the clip and cable. Once the sample was set up, the sample was stretched to the desired extensional strain. The setup is shown in Figure 19.

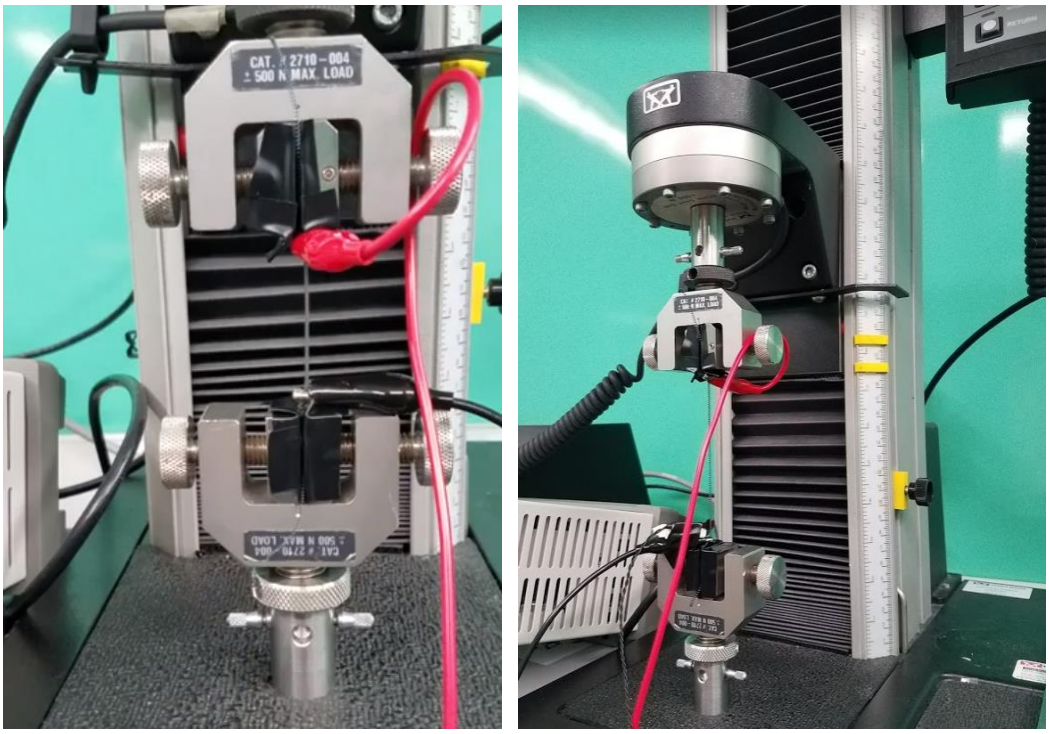

Figure 19: Sample setup in Instron. The left image is the set up with extension strain of 0 and the right image is of extension strain of 1.

A Keysight E631A power supply with constant current capabilities was used to power the actuators. It provides either 0 to 25 V and 0 to 1 Amp or 0 to 6 V and 0 to 5 A. The Keyseight E631A was chosen not only for the constant current option but because of the pre-programmable settings. These settings let me set the desired currents before testing and associate them with a button on the power supply. The set currents allowed for instantaneous application of the desired current at the beginning of the test without having to turn a nob to reach the desired current. This is important because dialing into a current would have influenced results, both for force, and time to reach maximum force as the first few seconds would have been at lower and varying currents.

A Fluke 8846A digital multimeter (DMM) was used to record the voltage (Figure 20). Recording the voltage over time on a DMM is necessary for power calculations. Since

the resistance of NiTi changes with temperature, keeping constant current results in a voltage change. In order to complete the circuit and measure the voltage, the DMM was connected to the power supply input and output. The voltage was recorded every 0.036 seconds.

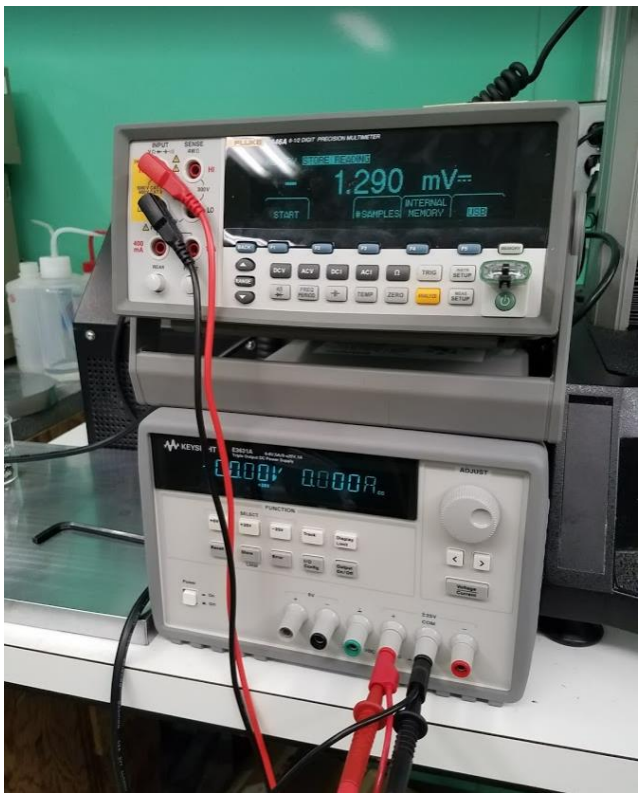

Figure 20: The Keysight E631A power supply with constant current capabilities is on the bottom with a Fluke 8846A digital multimeter (DMM) on top.

A thermistor was initially used to measure temperature through an Arduino microcontroller with a data logger. This was placed at the base of the actuators to collect thermal data. Other temperature measuring methods were attempted but not pursued. The reasoning as to why these were not viable methods for temperature collection is elaborated in the discussion section.

3.1.3.2 Procedures

As stated in chapter 2.5.3.2, the stiffness to the spring is known to decrease after multiple heating cycles [45]. The change in stiffness is greater in the first few cycles [39]. As a result, before initial testing of the samples, each sample was actuated and stretched five times to an extensional strain of 2. This was done as right after annealing, the actuators must undergo a few cycles of actuation to reach thermal and mechanical stability [39]. This pre-stretching was done using a heat gun instead of a power supply to avoid the potential of overheating.

Each sample was fully compressed before being secured. The samples were stretched while in the Instron, allowing for repeatable stretching to the desired length. The force output of the actuator was recorded for one minute for each sample at each strain and each current setting. Between each test, the clamps were returned to 5 cm of separation and the actuators were fully compressed to reset the actuators and maintain consistent extensional strain. The samples were given two minutes to cool between cycles. During testing, the samples clamped into the Instron were kept at the same spot to ensure that the total, uncoiled, wire length between the positive and negative terminals going to the power supply was constant. Keeping the coils in place also allowed for consistent extension. The samples were tested by holding the extensional strain and testing each current.

Since the samples are undergoing linear current increments in ascending order, to ensure that the results were not affected by the order of the test, the tests were conducted in an alternating manner. A test matrix is included in the appendix. The order of the tests for sample 1 of each diameter wire were:

- 0-0.8 amps and 0-2 extensional strain (45 cycles)
- 0.8-0 amps and 2-0 extensional strain (45 cycles)

- 0.8-0 amps, and 0-2 extensional strain (45 cycles)
- 0-0.8 amps and 2-0 extensional strain (45 cycles)

For sample 2 of each diameter wire were:

- 0-0.8 amps and 2-0 extensional strain (45 cycles)
- 0.8-0 amps and 0-2 extensional strain (45 cycles)
- 0.8-0 amps, and 2-0 extensional strain (45 cycles)
- 0-0.8 amps and 0-2 extensional strain (45 cycles)

Sample 1 and sample 2 of the 0.381 mm diameter wire springs ended up being actuated 180 times each. As testing for sample 1 and 2 of the 0.31mm diameter wire was not completed, they were only actuated approximately 90 times.

As mentioned in chapter 2.5.3, as the actuators are actuated the packing density decreases, resulting in an increase in final compressed length and free spring length ($L_{0)}$. As mentioned in the results below, the final compressed length of sample 1 of D1 (0.31 mm) increased by 4 cm, sample 2 of D1 (0.31 mm) increased by 3.6 cm, sample 1 of D2 (0.38 mm) increased by 0.5 cm, and sample 2 of D2 (0.38 mm) increased by 0.7 cm. The large increase in the compressed length in the D1 (0.31 mm) springs meant that the springs stopped fully compressing, such that when the Instron was brought back down to the set compressed length, there was slack formed by excess spring between the clamps. As a result, I chose to loosen the clamps and reposition the spring so the total amount of spring between the clamps was 5cm such that the stretched length for a given extensional strain would remain constant at extensional strain of 2 and keep the same set up. As the memory of the springs kept changing, they kept being readjusted. Shifting the spring meant that the total uncoiled length between the terminals changed, and so did the resistance. There were

two effects of the loose springs that led to the decision to reposition the 0.31mm diameter springs. First, at lower extensional strain settings, the springs were not being stretched as the new compressed length was longer than the desired stretched length. Being too loose, the forces were essentially the same at the lower strains as the uncompressed. Readjusting the springs of 0.31mm samples 1 and 2 influenced the results of the tests. As a result, a third sample was tested for the 0.031mm diameter wire at lower maximum extensional strains and currents. The order of the tests for sample 3 of 0.31 mm diameter wire were:

- 0-0.5 amps and 0-1.5 extensional strain
- 0.5-0 amps and 1.5-0 extensional strain
- 0.5-0 amps and 0-1.5 extensional strain
- 0-0.5 amps and 1.5-0 extensional strain.

3.1.4 Data analysis

In evaluating the actuators four factors were taken into account: maximum force; the time needed to reach maximum force, the power needed to reach maximum force, and the potential for spring fatigue and degredation. The data for the maximum force was determined by data provided by the Instron. The time needed to reach maximum force has two components. First the greatest rate of change and the time to reach the absolute max. The maximum power is found by muliplying the maximum voltage by the current. The contribution of extentional strain and current to achieving maximum force help can be summarized by the force vs. extensional strain vs. current graph. For this last metric, current was chosen instead of power since power varies greatly even within a sample, and current is held constant with the power supply. The fatigue was observed by measuring the change in compressed length.

Each sample experiences a different number of actuation cycles before reaching the same test condition. In order to deal with potential hysteresis of the spring and get comparable results, only the results in the last test were averaged and used for the force vs. extensional strain vs. current graph since by the end of testing the samples had been through approximately the same number of cycles. In the case of the D1 (0.31 mm diameter) actuators, since the first two samples were eliminated from analysis because of permanent deformation in early testing, the three-axis graph for D1 only depicts the third tested sample.

To illustrate the variability in the actuators, the range and average maximum force for each test of each sample was recorded to demonstrate just how much the actuators vary within and between samples. The variability is important as it is linked to the performance of the actuators. The range and average time to reach maximum actuation and resistance during actuation was also calculated to show the variability.

In addition to looking at the change in the resistance over time, to compare the resistance of the samples, the maximum and minimum resistance was calculated for each test along with the difference between them. The average, range, and standard deviation for the difference in resistance was calculated for each diameter at a given extensional strain and current setting. The resistance was found by dividing the measured voltages by the set current for each test.

3.2 Results

This section goes over the results of the characterization test.

3.2.1 Maximum force and time to maximum force

First, force vs. time was measured to determine the maximum force and time to achieve maximum force. The force vs. time graphs that are shown depict the highest and

lowest resultant forces for a given diameter, extensional strain, and power setting. The graphs chosen to depict the force vs. time for extensional strains of 2 and 1.5 for the two diameter wires. Looking at the graphs of force vs. time the time it takes for the actuators to heat up and produce the maximum force is visible. The remainder of the force vs. time graphs can be found in Appendix A.

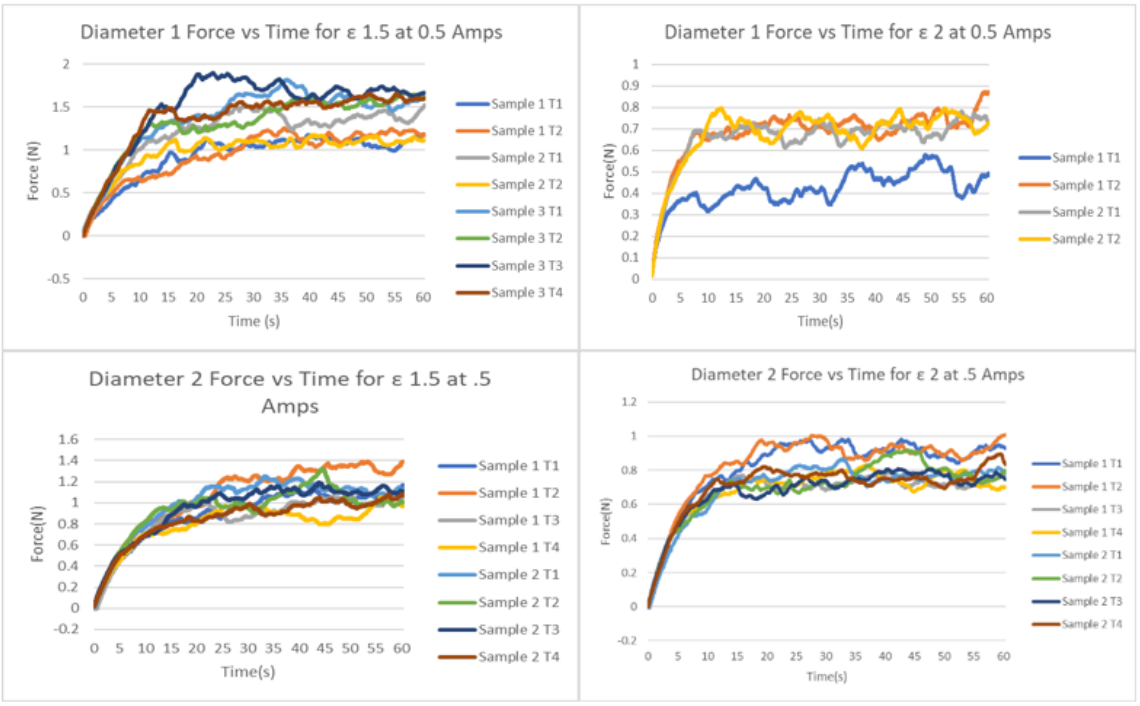

Figure 21: Graphs of the force vs time for D1 & D2

For the smaller diameter wires after multiple actuation cycles, the actuators began to exhibit behavior consistent with a Two-Way-Memory effect, instead of compressing, as further described in the discussion. The negative forces as depicted in Figure 22 are due to this Two-Way-Memory-Effect, coupled with the way that the Instron measures forces. The behavior was most notable for extensional strain of 0. At extensional strain of 0 as the actuator was heated it began to expand between the grips of the Instron, instead of compress. The way the forces are measured on the Instron is by looking at the force acting

on the grips. As the spring extended, it was no longer in tension as the excess spring began to buckle, leading to negative forces. The negative forces recorded show this behavior, however, the magnitude of the negative forces is less than the actual negative forces produced by the expanding spring. As a spring expands, the force is going in opposing directions. Instead of translating the force to both grippers, the reacting force on the two stationary grippers causes the spring to buckle, due in part to the flexibility, helical geometry, and lack of stiffness in the coils.

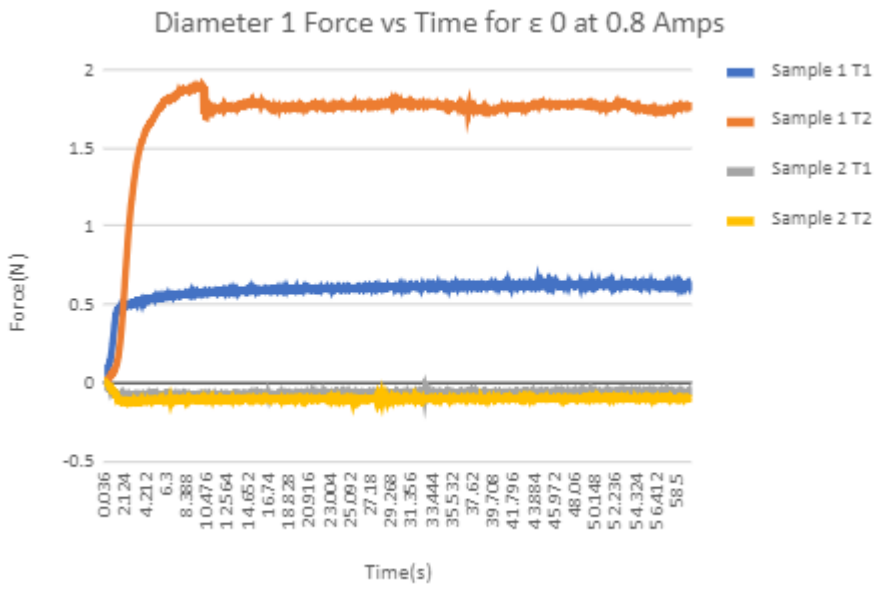

Figure 22:Graph of force vs. time from diameter1 at extensional strain of 0 depicting spring elongation

3.2.2 Time to reach maximum force

Using the force and time data, the time for each actuator to reach maximum force was recorded. The average maximum force, the standard deviation of the maximum force, and the range of maximum force was recorded for all samples and trials for each extensional strain and current setting. The average time for actuation, range of actuation

time, and standard deviation of actuation time were also recorded. Since the maximum force and time for actuation for 0 A is only noise, the values recorded were not represented. The values for D2E3 are shown below in Table 8Table 8, the remainder of the tables are in the appendix. A summary of the overall average time to maximum force for extensional strain of 0 to 2 for the 0.31mm and 0.38mm diameter wire is shown in Table 7. Figure 23-Figure 26 depict box and whisker graphs for a visual representation of the average and range of max force and time to max force. Figure 23 represents the average and range for all currents tested and all extensional strains for diameter 1 (0.31mm), Figure 24 shows the information for diameter 2(0.38mm), Figure 25 shows the range and average to achieve the maximum force for diameter 1, and Figure 26 shows the time to max force for diameter 2. Versions of these graphs separated out by diameter and extensional strain are in the appendix.

Table 7: Summary of total average time to the maximum force

Total Average Time to Maximum Force		
Diameter 0.31mm		
Extensional strain	Average	SD
ε 0	34.3878	20.69429
ε 0.5	41.7696	16.00829
ε 1.0	40.2394	14.90044
ε 1.5	38.9496	13.88186
ε 2.0	31.357	18.04702
Max Time Average	38.41778	
Diameter 0.38mm		
Extensional strain	Average	SD
ε 0	35.38517	23.00125
ε 0.5	48.922	14.31758
ε 1.0	45.853	15.39103
ε 1.5	40.62067	15.84019
ε 2.0	39.34972	15.67569
Max Time Average	42.02611	

0.1 A			**0.2 A**			**0.3 A**			**0.4 A**		
Trial	Max force (N)	Actuation time to max (S)	Trial	Max force (N)	Actuation time to max (S)	Trial	Max force (N)	Actuation time to max (S)	Trial	Max force (N)	Actuation time to max (S)
S1 T1	0.048151	54.684	S1 T1	0.159085	48.276	S1 T1	0.358109	51.912	S1 T1	0.768253	52.596
S1 T2	0.035644	35.028	S1 T2	0.155657	56.664	S1 T2	0.391514	56.592	S1 T2	0.928293	58.572
S1 T3	0.042814	30.24	S1 T3	0.133944	40.716	S1 T3	0.338749	47.988	S1 T3	0.670559	42.948
S1 T4	0.043378	48.24	S1 T4	0.179785	18.9	S1 T4	0.347444	55.656	S1 T4	0.729006	42.12
S2 T1	0.045706	57.528	S2 T1	0.388812	45.324	S2 T1	0.864997	55.332	S2 T1	0.419828	57.348
S2 T2	0.04533	57.204	S2 T2	0.196304	59.616	S2 T2	0.395829	51.588	S2 T2	0.764321	32.328
S2 T3	0.039756	51.3	S2 T3	0.159013	45.792	S2 T3	0.383252	56.232	S2 T3	0.767374	56.196
S2 T4	0.036523	51.3	S2 T4	0.154252	52.128	S2 T4	0.362177	54.18	S2 T4	0.729059	51.48
AVE	0.042163	43.6905	AVE	0.190856	45.927	AVE	0.430259	53.685	AVE	0.722087	49.1985
RANGE	0.012507	42.228	RANGE	0.254869	40.716	RANGE	0.526247	8.604	RANGE	0.508465	26.244
SD	0.004479	15.2855	SD	0.082098	12.56206	SD	0.176864	2.97074	SD	0.142728	9.21007
0.5 A			**0.6 A**			**0.7 A**			**0.8 A**		
Trial	Max force (N)	Actuation time to max (S)	Trial	Max force (N)	Actuation time to max (S)	Trial	Max force (N)	Actuation time to max (S)	Trial	Max force (N)	Actuation time to max (S)
S1 T1	2.108124	60	S1 T1	4.628794	60	S1 T1	6.947985	55.476	S1 T1	8.751187	59.328
S1 T2	2.698867	52.956	S1 T2	4.206271	57.564	S1 T2	6.63342	44.424	S1 T2	8.880727	50.616
S1 T3	1.294652	57.276	S1 T3	3.357055	50.616	S1 T3	5.244244	50.904	S1 T3	7.398974	55.188
S1 T4	1.899992	57.6	S1 T4	3.907981	59.616	S1 T4	5.732485	38.232	S1 T4	7.927141	45
S2 T1	2.179914	49.356	S2 T1	4.472947	55.116	S2 T1	6.290046	44.316	S2 T1	8.09582	46.44
S2 T2	1.716062	45.684	S2 T2	4.01062	51.66	S2 T2	6.230272	57.744	S2 T2	8.397757	38.628
S2 T3	1.743002	58.356	S2 T3	4.40206	56.34	S2 T3	5.76374	39.528	S2 T3	7.999237	31.248
S2 T4	1.64938	60	S2 T4	3.837828	56.952	S2 T4	6.294648	48.096	S2 T4	8.574269	32.616
AVE	1.911249	55.1535	AVE	4.102944	55.983	AVE	6.142105	47.34	AVE	8.253139	44.883
RANGE	1.404216	14.316	RANGE	1.271739	9.384	RANGE	1.703742	19.512	RANGE	1.481753	28.08
SD	0.421999	5.289274	SD	0.411745	3.404737	SD	0.542595	7.064418	SD	0.491506	10.18173

Table 8: Max force and actuation time for D2 E3 for all trials. Table includes average, range, and standard deviation.

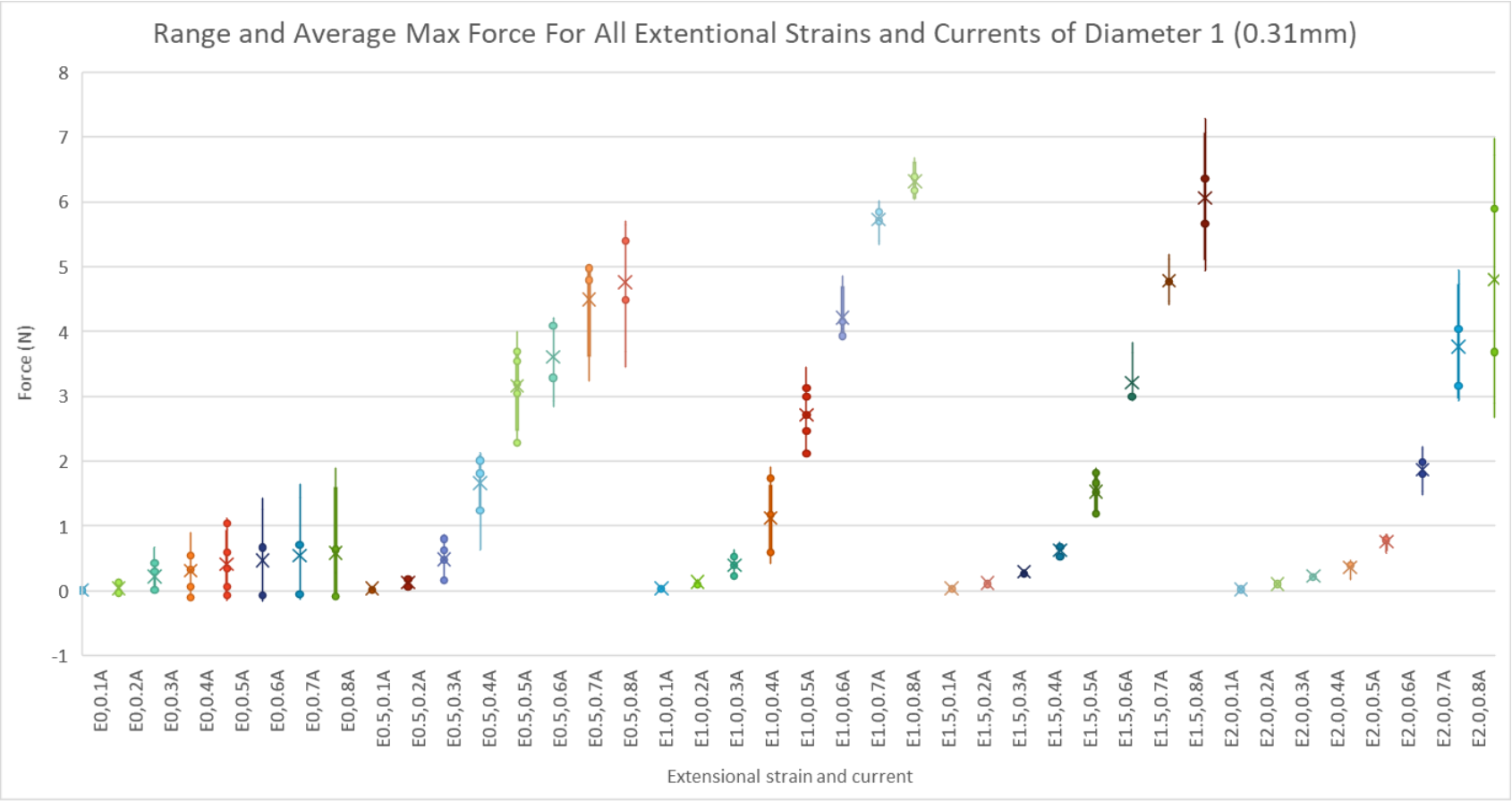

Figure 23: Box and whisker graph depicting range and average max force for all extensional strains and currents tested for diameter 1 (0.31mm).

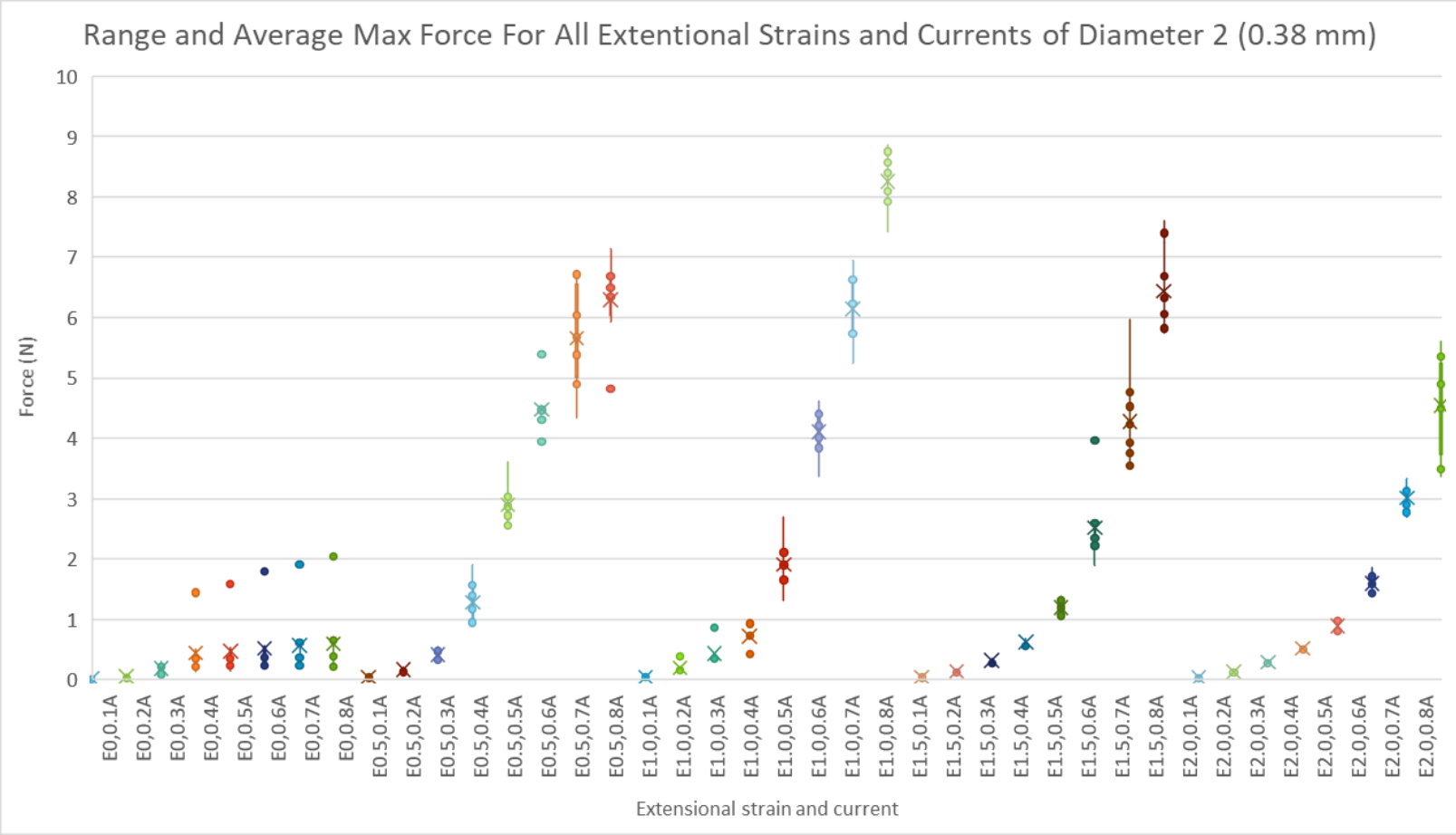

Figure 24:Box and whisker graph depicting range and average max force for all extensional strains and currents tested for diameter 2 (0.38mm).

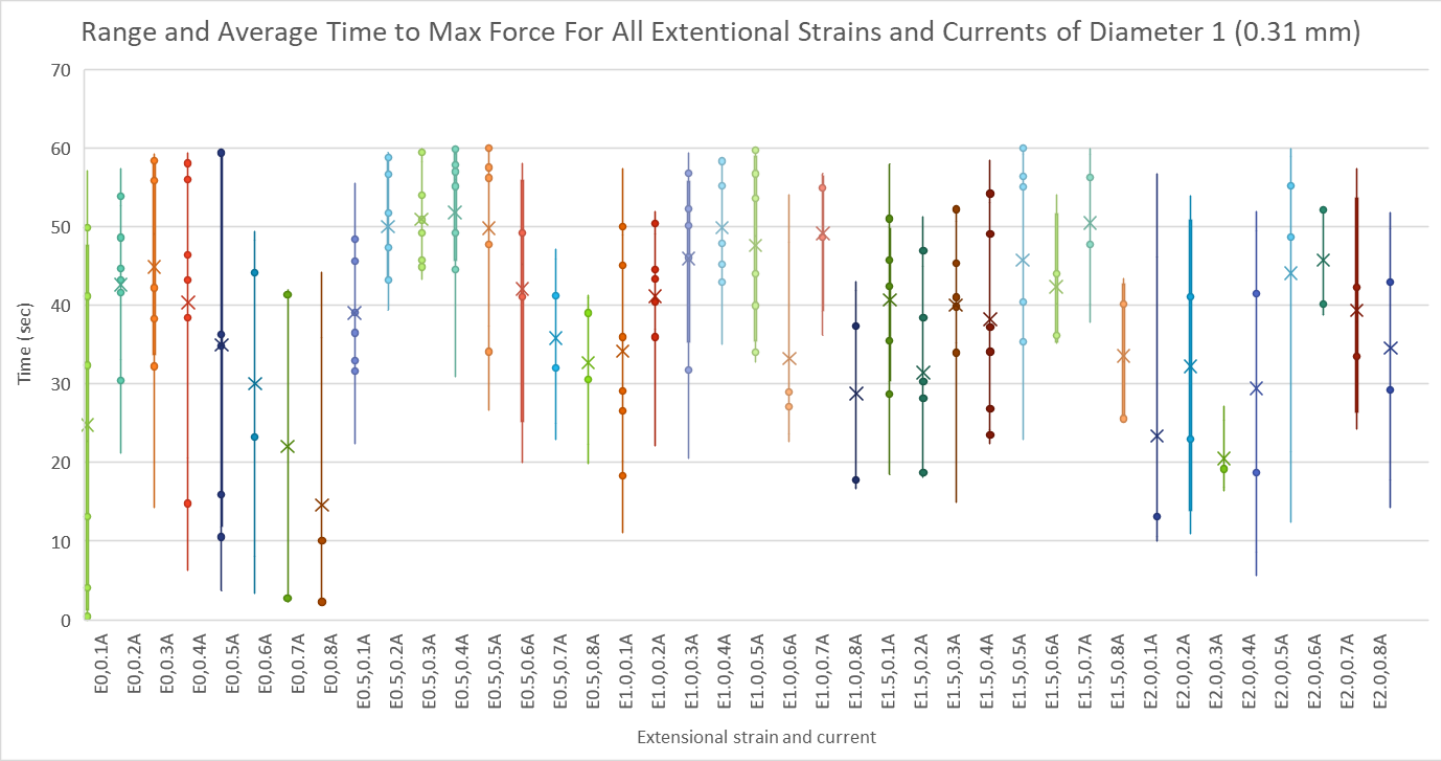

Figure 25:Box and whisker graph depicting range and average time to reach max force for all extensional strains and currents tested for diameter 1 (0.31mm).

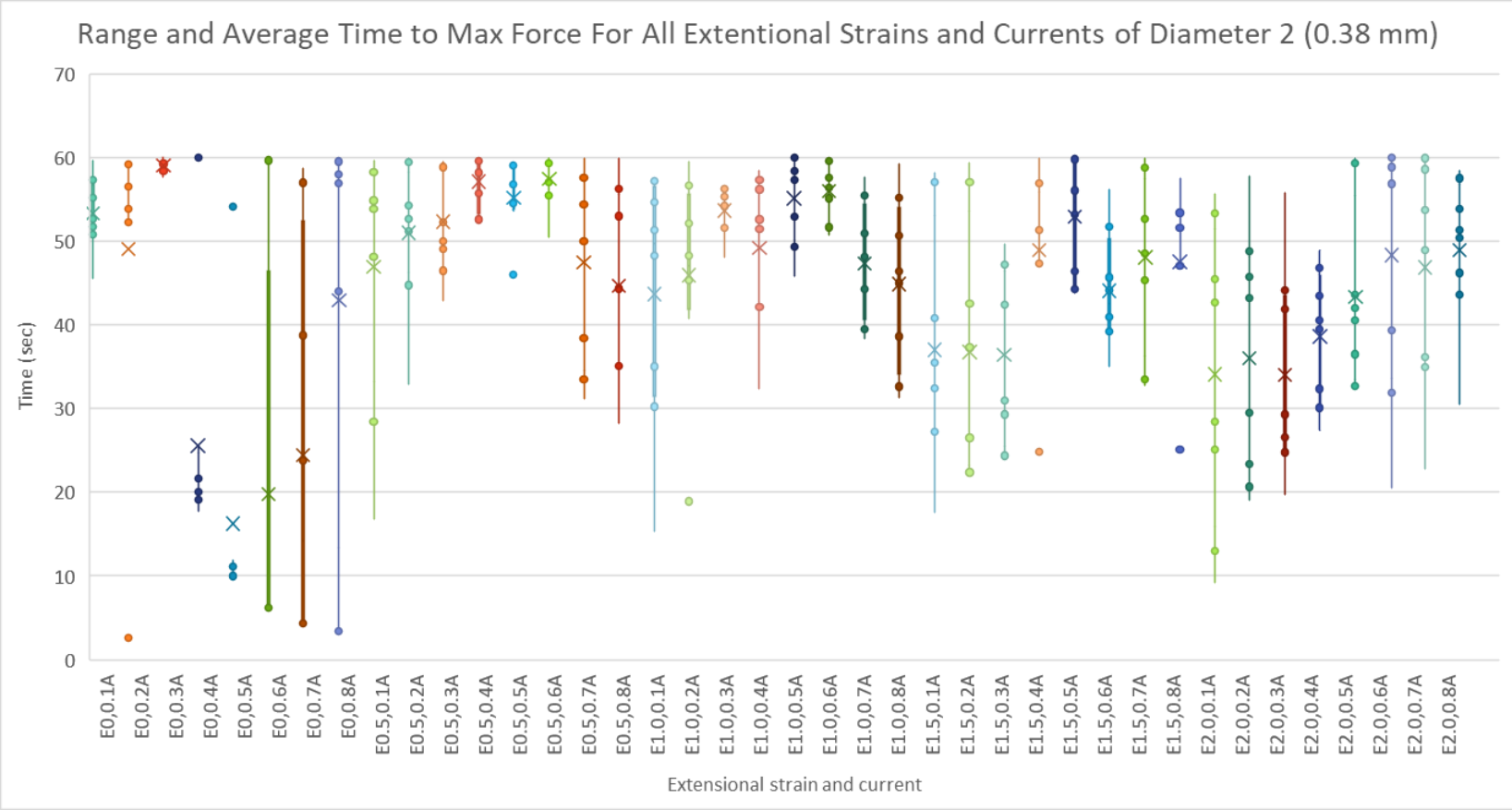

Figure 26:Box and whisker graph depicting range and average time to reach max force for all extensional strains and currents tested for diameter 2 (0.38mm).

3.2.3 Force vs. current vs. extensional strain

For the force vs current vs extensional strain graphs, the values used for the force are the average of the maximum force found in the last trial between samples.

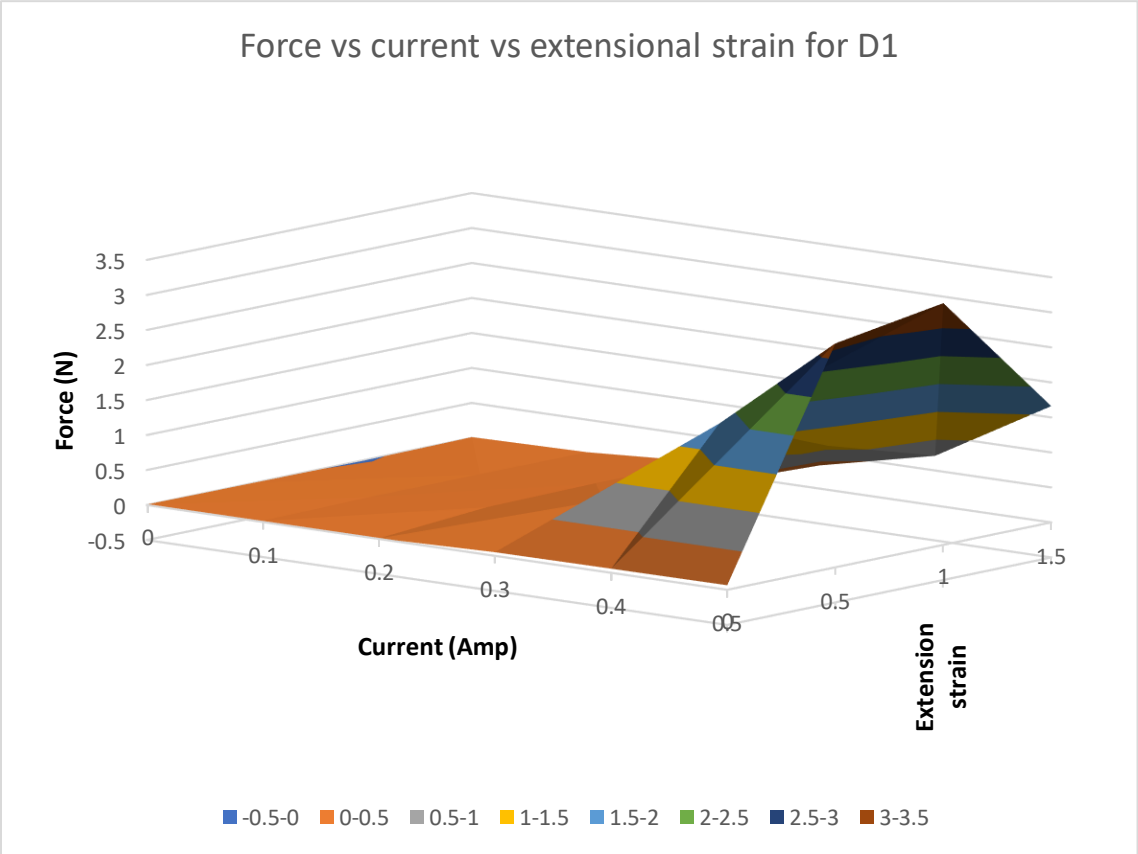

Figure 27: Graph depicting force vs current vs extensional strain for D1. Graph actually goes to extensional strain of 2.

The graph above depicts force vs. current vs. extensional strain for D1. This graph depicts how the current and extensional strain results in different forces and that at an extensional strain of 2, the forces decrease.

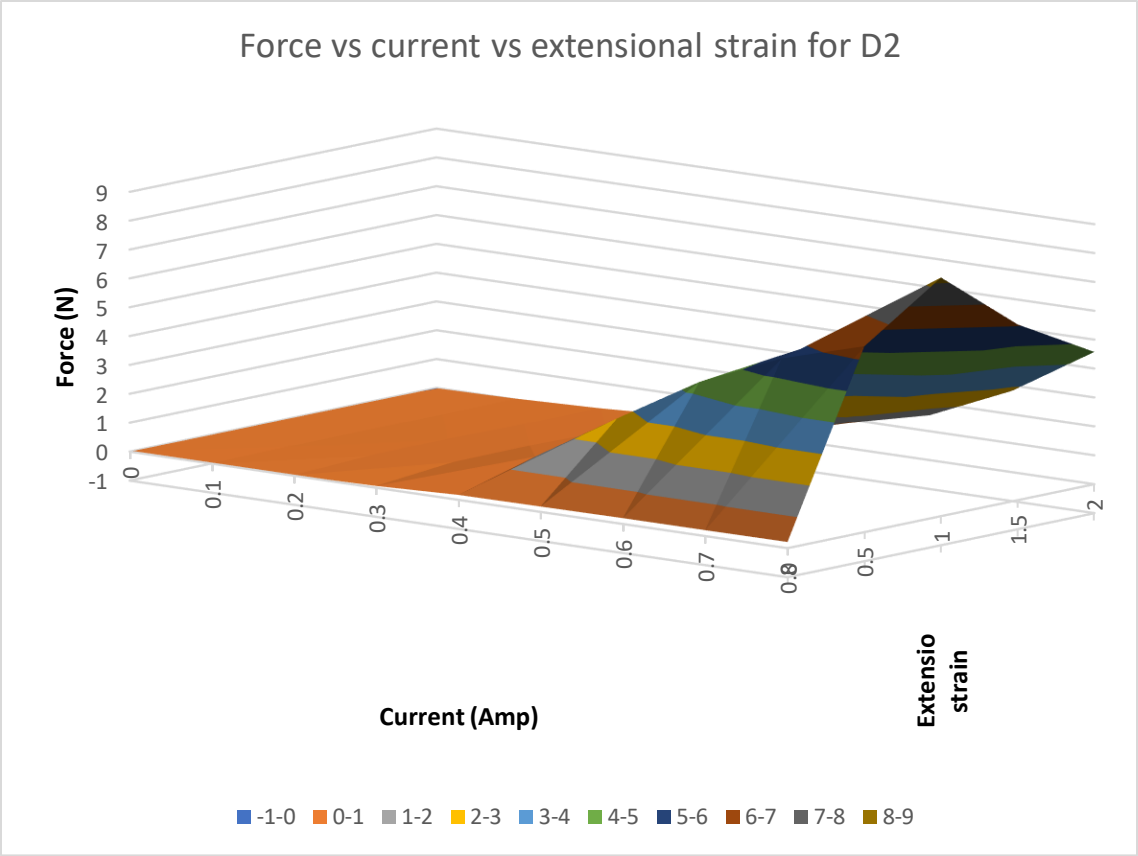

Figure 28: Graph depicting force vs current vs extensional strain for D2.

Figure 28 shows the same pattern as Figure 27 where the force decreases as extensional strain of 2.

3.2.4 Power and Resistance vs. Time

Using the Voltage data recorded from a Digital Multi Meter (DMM) and the set current, it was possible to create graphs of the change in resistance over time. Figure 29 depicts results for diameter 1. For the higher currents, the small fluctuation in the resistance is visible. More graphs of resistance vs. time are in Appendix A.

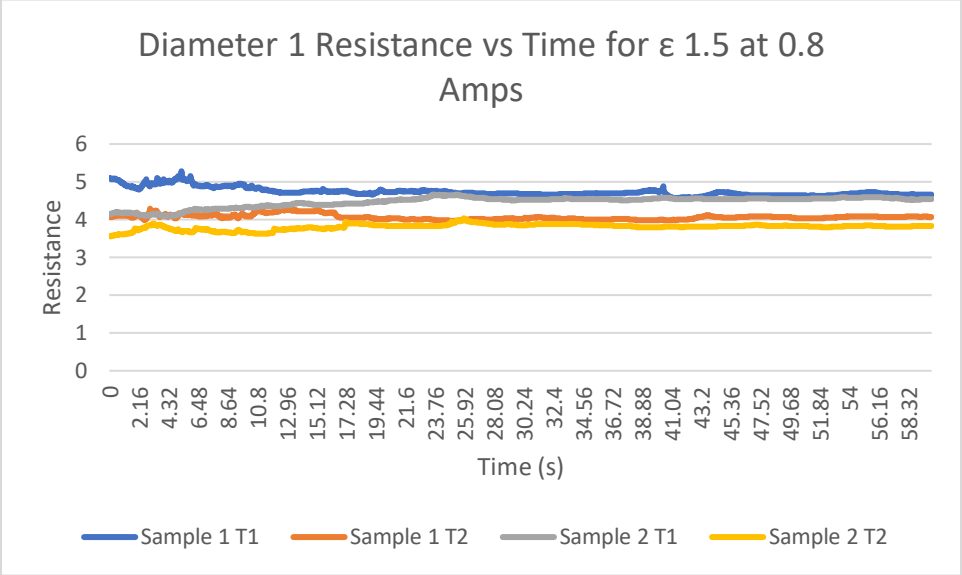

Figure 29: Resistance vs. time for diameter 1 extensional strain of 1.5 at .8 A.

In addition to the resistance vs time graphs, tables and box and whisker charts of the max, min, and difference between resistance were taken. The values for diameter 2 and extensional strain 2 are shown in Table 9. The rest of the tables are in the appendix. It is important to note that the outliers in the resistance for sample 1 diameter 1 (0.31 mm) are due to adjusting the sample between tests as memory decay occurred. This is further discussed in the discussion section of this chapter under the heading of memory loss.

0.1 A				0.2 A				0.3 A				0.4 A			
Trial	Min (Ω) Resistance	Max (Ω) Resistance	Diff (Ω) Resistance	Trial	Min (Ω) Resistance	Max (Ω) Resistance	Diff (Ω) Resistance	Trial	Min (Ω) Resistance	Max (Ω) Resistance	Diff (Ω) Resistance	Trial	Min (Ω) Resistance	Max (Ω) Resistance	Diff (Ω) Resistance
S1 T1	6.22655	6.49763	0.27108	S1 T1	5.23155	5.40961	0.17806	S1 T1	4.8967333	5.109933	0.2132	S1 T1	4.3099	4.9727	0.6628
S1 T2	4.70918	4.75787	0.04869	S1 T2	4.657255	4.83617	0.178915	S1 T2	4.4657333	4.597633	0.1319	S1 T2	3.92355	4.821075	0.897525
S2 T1	4.36199	4.36668	0.00469	S2 T1	4.355855	4.40282	0.046965	S2 T1	4.2577333	4.376333	0.1186	S2 T1	4.046425	4.519825	0.4734
S2 T2	3.53464	3.5408	0.00616	S2 T2	3.53563	3.63411	0.09848	S2 T2	3.5468733	3.626297	0.0794233	S2 T2	3.3062	3.660525	0.354325
S3 T1	6.15341	6.25471	0.1013	S3 T1	4.77701	4.823515	0.046505	S3 T1	4.5185333	4.6423	0.1237667	S3 T1	3.9593	4.831075	0.871775
S3 T2	4.66631	4.77388	0.10757	S3 T2	4.43022	4.53604	0.10582	S3 T2	4.1379333	4.338233	0.2003	S3 T2	3.66685	4.08135	0.4145
S3 T3	3.98385	3.99934	0.01549	S3 T3	3.95439	3.99114	0.03675	S3 T3	3.8455767	3.94603	0.1004533	S3 T3	3.525	4.754525	1.229525
S3 T4	4.91129	4.97808	0.06679	S3 T4	4.86636	5.5025	0.63614	S3 T4	4.7605333	5.084833	0.3243	S3 T4	4.043475	4.555875	0.5124
AVE			0.077721	AVE			0.165954	AVE			0.1614929	AVE			0.6770313
RANGE			0.26639	RANGE			0.59939	RANGE			0.2448767	RANGE			0.8752
SD			0.087932	SD			0.19809	SD			0.0804326	SD			0.300862
0.5 A				**0.6 A**				**0.7 A**				**0.8 A**			
Trial	Min (Ω) Resistance	Max (Ω) Resistance	Diff (Ω) Resistance	Trial	Min (Ω) Resistance	Max (Ω) Resistance	Diff (Ω) Resistance	Trial	Min (Ω) Resistance	Max (Ω) Resistance	Diff (Ω) Resistance	Trial	Min (Ω) Resistance	Max (Ω) Resistance	Diff (Ω) Resistance
S1 T1	4.08202	5.08344	1.00142	S1 T1	3.5415333	4.415017	0.873483	S1 T1	3.4983429	4.317314	0.8189714	S1 T1	3.3785625	4.261825	0.8832625
S1 T2	3.7495	4.44472	0.69522	S1 T2	3.6735167	4.1806	0.507083	S1 T2	3.5238571	4.068086	0.5442286	S1 T2	3.6663375	4.128738	0.4624
S2 T1	3.44592	4.20904	0.76312	S2 T1	3.3106667	3.931667	0.621	S2 T1	3.3328	4.109557	0.7767571	S2 T1	3.1680625	3.8986	0.7305375
S2 T2	3.20948	3.65448	0.445	S2 T2	3.0500833	3.796867	0.746783	S2 T2	2.9918571	3.556757	0.5649	S2 T2	3.3162125	3.9185	0.6022875
S3 T1	3.56368	4.27432	0.71064	S3 T1	3.2254667	4.123233	0.897767	S3 T1	3.5371571	4.525529	0.9883714	S3 T1	3.0644875	3.77975	0.7152625
S3 T2	3.5181	4.3321	0.814	S3 T2	3.3150833	4.19745	0.882367	S3 T2	3.2295	4.100371	0.8708714	S3 T2	3.0905875	3.8496	0.7590125
S3 T3	3.73556	4.5034	0.76784	S3 T3	3.3882667	4.5084	1.120133	S3 T3	3.2961429	4.001286	0.7051429	S3 T3	3.3621125	3.857275	0.4951625
S3 T4	3.85022	4.35406	0.50384	S3 T4	3.4802833	4.379533	0.89925	S3 T4	3.3532	4.156371	0.8031714	S3 T4	3.2483375	4.001738	0.7534
AVE			0.712635	AVE			0.818483	AVE			0.7590518	AVE			0.6751656
RANGE			0.55642	RANGE			0.61305	RANGE			0.4441429	RANGE			0.4208625
SD			0.175173	SD			0.189744	SD			0.1500912	SD			0.1434825

Table 9:Minimum and maximum resistance for D2E2. Average, range, and standard deviation for the difference in resistance are also shown.

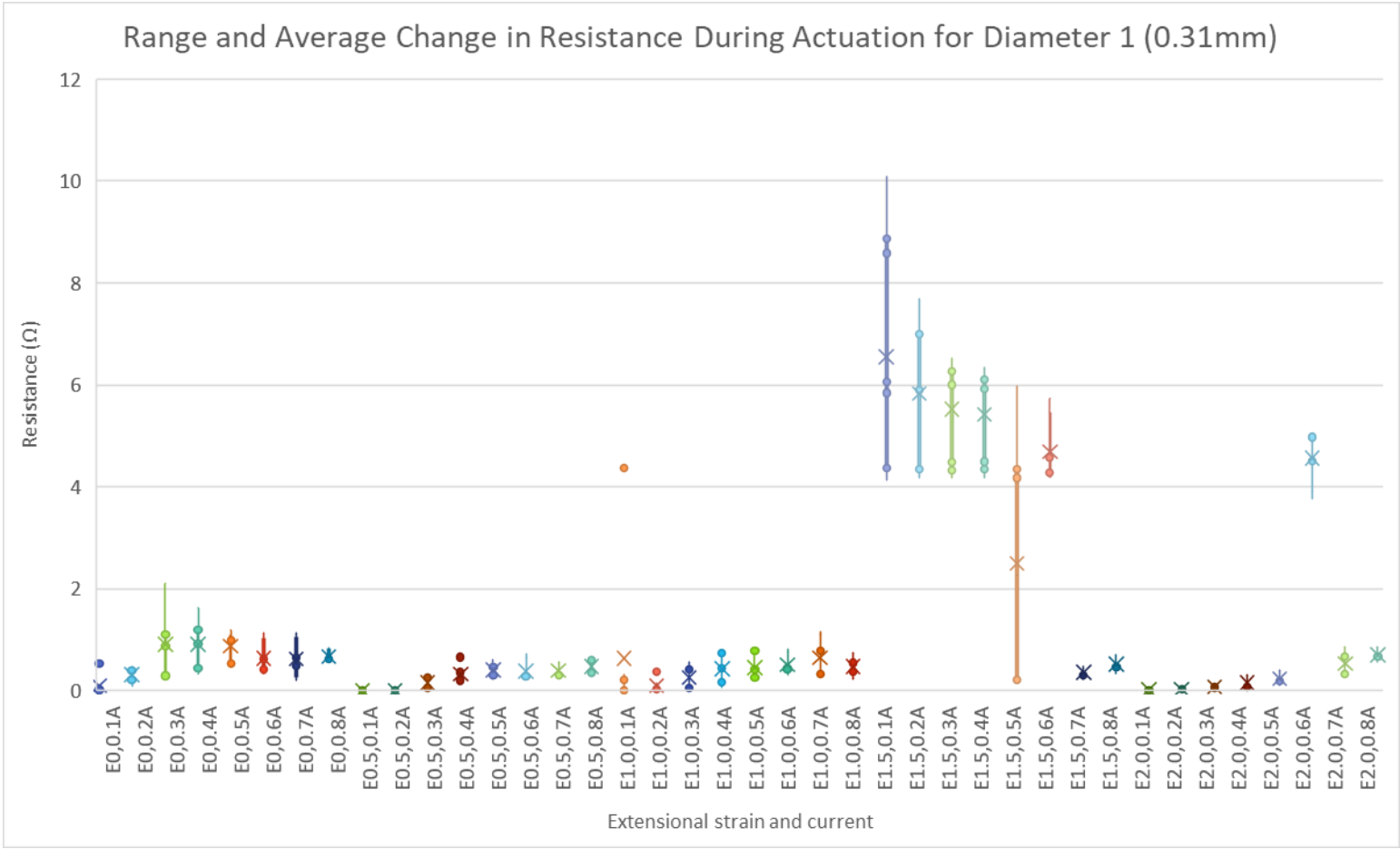

Figure 30: Box and whisker graph depicting range and average change in resistance for all extensional strains and currents tested for diameter 1 (0.31mm).

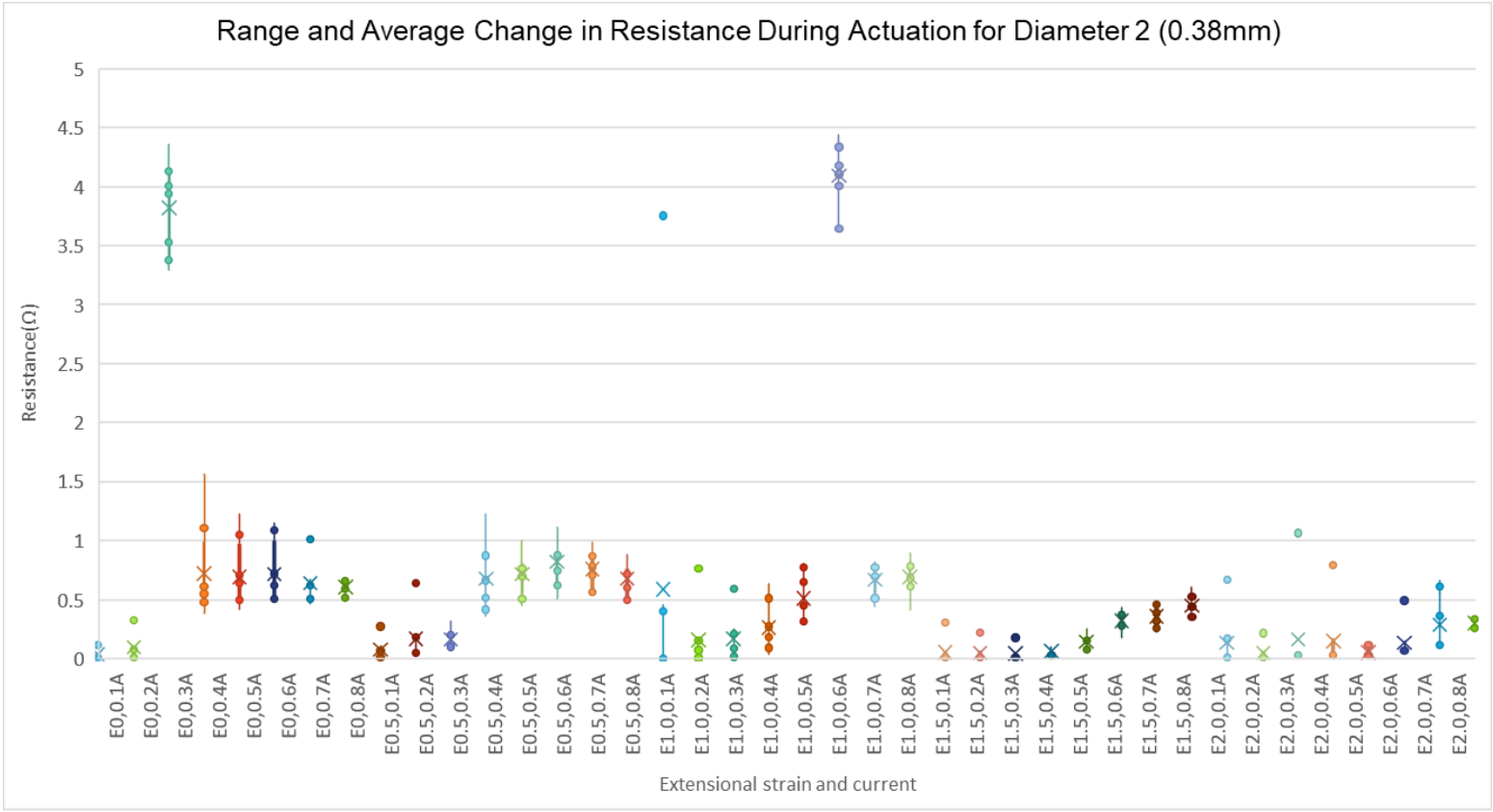

Figure 31: Box and whisker graph depicting range and average change in resistance for all extensional strains and currents tested for diameter 2 (0.381mm).

To visualize the difference in average maximum power, a summary table was created Table 10.

Table 10: Summary comparison of average maximum power.

		Average Max Power (Watts) for each current									
Extensional strain	Diameter	0A	0.1 A	0.2 A	0.3 A	0.4 A	0.5 A	0.6 A	0.7 A	0.8 A	
ε 0	0.31 mm	0	0.0078	0.0155923	0.10501898	0.446191	1.31740675	-	-	-	
ε 0	0.38 mm	0	1.76694	3.5039775	5.28186	7.198325	8.5798125	9.8184	10.8509275	12.08701	
ε .5	0.31 mm	0	0	0.0146	1.1327325	2.58198	4.8180375	-	-	-	
ε .5	0.38 mm	0	2.4894	4.3811175	6.05278125	8.254535	9.54505625	10.577445	11.8500813	12.57914	
ε 1	0.31 mm	0	4.73046	8.78659	12.413295	14.96302	17.4363625	-	-	-	
ε 1	0.38 mm	0	1.62393	3.2510225	4.9161825	6.40773	7.8869875	9.2506425	8.17326125	11.4792	
ε 1.5	0.31 mm	0	6.4	8.48169	11.4530175	14.37772	17.026825	-	-	-	
ε 1.5	0.38 mm	0	2.53899	4.0443175	5.52949875	7.17358	8.966975	10.096493	11.3114925	12.60271	
ε 2	0.38 mm	0	1.27973	2.8396625	4.186875	5.160705	6.45088125	7.9084275	9.52462875	10.75001	

3.2.5 Potential for spring fatigue and degradation

In addition to the recorded data, visual and measured length results to show the memory decay of the spring during testing. After the completion of the testing the samples were compressed to their maximum and measured to determine how much the compressed length changed (**Error! Reference source not found.**Figure 32).

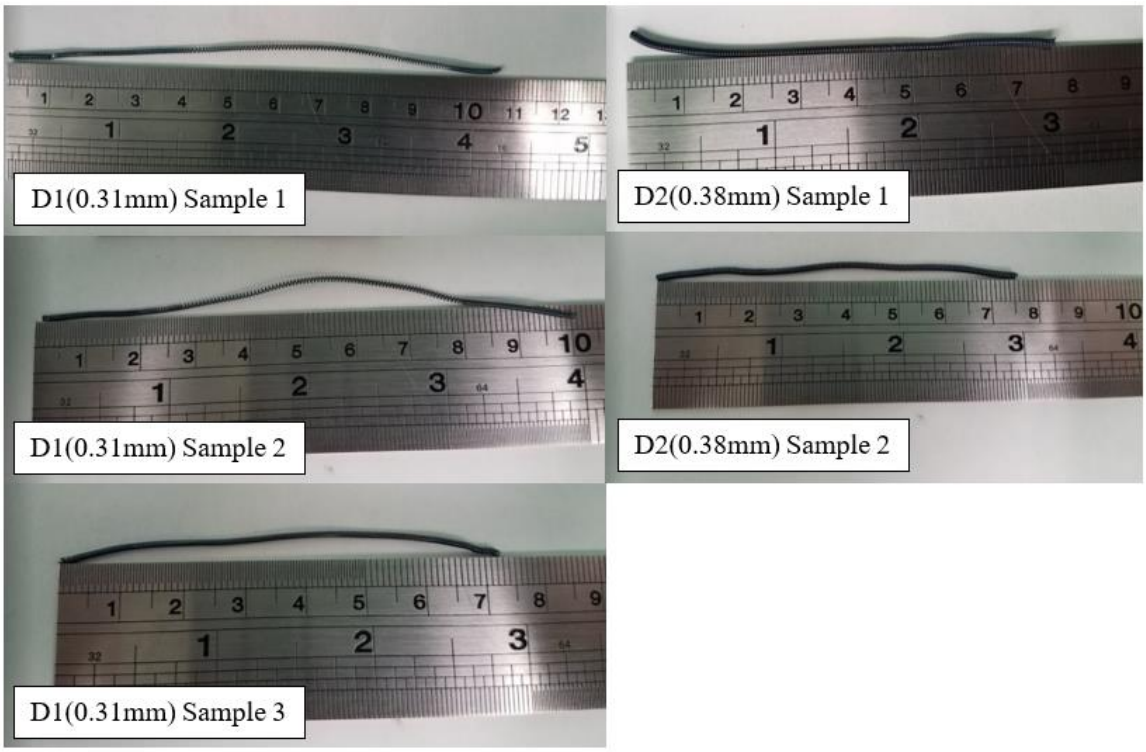

Figure 32: The final compressed length after completed testing.

All the samples did show some degree of memory loss (extension). All the samples were originally cut to 7 cm when fully compressed. After testing, D1 (0.31 mm) sample 1 was 11 cm, D1 (0.31 mm) sample 2 was 10.6 cm, D1(0.31 mm) sample 3 and D2 (0.38 mm) sample 1 were 7.5cm, and D2 (0.38 mm) sample 2 was 7.7 cm. Figure 32 is a good visual representation but the measurements are approximations as the springs kept buckling

when the images were being taken. The measurements listed above are the actual measurements when the springs are held against the ruler.

In the case of samples 1 and 2 for diameter 1, they experienced significant amount of decay with over 40% increase in length.

3.3 Discussion

The variables manipulated in this study were wire diameter, current, and extensional strain, to measure the time for actuation and actuation force.

Initial bench top testing eliminated D3 as an option as the memory degraded after a couple of cycles at the currents required to achieve the required temperature for actuation. This might have been due to the annealing temperature used for the wire. This wire has a higher starting actuation temperature and using the same annealing temperature and time for all actuators might have influenced the behavior. It is unknown what annealing temperature was used by Dynalloy for them to get the current rating of 3.4 A for 2 second actuation which is higher than the 1.95 A found in the bench top test. Further investigation and characterization of the larger diameter wire spring is needed as there are many uncontrollable variables. As such, full testing was only conducted on D1 and D2.

3.3.1 Maximum force and time to maximum force

The results from actuation characterization show that for a given power and extensional strain, the 0.31 mm diameter wire often produces equal or greater forces than the 0.38mm diameter wire spring. This behavior can be explained by the higher resistance of D1 which causes the wire to actuate more quickly and at lower currents than the D2 springs. Although initial analysis might lead one to believe that the D1 springs are best, further analysis and investigation reveal many factors that make the diameter less ideal

than D2 for the application for the exoskeleton. These factors used for comparison are behavior, force, and power.

Looking at time to achieve maximum force, for all samples, all diameters, all currents besides 0, and all extensional strains beyond 0.5, the average time to reach maximum force for wire diameter of 0.31 mm was 38.41778 seconds, and for diameter of 0.38 mm was 42.02611 seconds. Although this was the time to achieve maximum force, a closer look at the force vs. time graphs shows that the actuators begin to heat up and produce force nearly instantaneously with the largest rate of change in force occurring between 5 seconds and 10 seconds. At this point, the rate of change of force decreased. This shows that although it takes a long time for the actuators to reach maximum force, there is no preheating time where the actuators are standing idle waiting to heat up to a point where actuation can begin. As discussed at the end of this chapter in the section titled limitation, this thesis only focuses on SMA with an austenite starting temperature of 70 °C. It is possible that using a material with lower activation temperature might lead to shorter warming time but not activation time.

For all current settings, all samples, all diameters, forces increased with extensional strain until a 1.5 extensional strain, the forces for extensional strain 2 were consistently lower than extensional strain of 1.5. This is due to over extension of the actuators at extensional strain of 2 which begins to fatigue the spring [57] [45]. The force at extensional strain of 2 is lower than the force of extensional strain 1.5 even in the samples that were first tested at extensional strain of 2 and therefore had not yet experienced hysteresis from prior testing.

3.3.3 Power and resistance vs. time

Since the thinner diameter wire spring is only able to run for longer periods of time at 0.6 Amps and an extensional strain of 2, its maximum force that can repeatably be expected from the actuator is between 1.5 and 2 Newtons. The springs using D2 are able to run with higher currents for longer periods of time, are more repeatable, and are able to produce forces between 5 and 7 Newtons. The graph above depicts force vs. current vs. extensional strain

If the actuators were to be powered for 1 second for instantaneous actuation, with a control system that was to use pulse width modulation to control the power state of the actuators, then the actuators could theoretically be actuated for a longer period of time, in which case D1 might be used, but the temperature required to sustain the contraction of the required force would still damage the D1 actuators.

From a power perspective, the higher resistance of D1makes it such that the springs use more power for a given current. This relationship between power and resistance is given by $P=I^2 \cdot R$. At lower currents, the total power going through the actuators are approximately equal with D2 often consuming more power. The influence of the higher resistance is more noticeable at higher currents. For the current setting of 0.8 Amps, D1 consumed approximately 3.2 Watts where D2 consumed approximately 2.32. The thinner spring, therefore, consumes about 1 Watt more than the thicker wire. Tables of max power for each test and sample are included in the appendix.

3.3.4 Potential for spring fatigue and degradation

Fatigue from repeated cycles can lead to memory loss in shape memory alloys [60]. For example, Weber et al in *Vacancies of sphape memory alloys* mention that “Repeating the deformation and heating cycle in air reveals a rather rapid ‘memory loss’ after a few

cycles" and that "not every specimen performs within the desired specifications" [60]. The behavior of the SMAs influenced both the results and testing methods. Changes in the behavior of the spring are a limitation of the material and compensation for such effects might have also influenced results as testing methods had to change.

3.3.4.1 Memory loss

The 0.31mm diameter wire springs did not handle as much current or extensional strain as the 0.38 mm diameter wire springs. Both tested diameters experience hysteresis as described in the literature review. However, the hysteresis effects on the spring memory and spring length were greater in the thinner diameter wire spring. During the Instron testing, where the D2 diameter springs consistently held their memory and returned to their initial free spring length after every actuation, the D1 springs began to lose their memory. The loss of memory was detected even before completing the first full test cycle on the first two samples of D1 springs (testing of the third D1 sample was different since it was not tested in the higher extensional strains and higher currents, and therefore did not experience the same extreme behavior). The measurements of the free spring lengths of each sample after testing completion show this difference in memory loss. Where both samples 1 and 2 of D2 experience approximately 8.57% increase in length at the completion of testing, sample 1 of D1 experienced a 52.86% increase in length, sample 2 a 42.86% increase in length and sample 3 experienced a 4.29% increase in length.

3.3.4.2 Two-way SMA actuation

In addition to the memory loss, the memory state and behavior of the 0.31 mm diameter wire changed. Initially, only the packing density of the wire was changing. At the end of the first test the smaller actuators, at extensional strain 0, began to expand when the

current was applied but would compress back to the new starting length as they cooled. After the second test, the actuators memory was completely reset, and they began to expand fully when powered and would only compress if forced. Essentially it seems as if the springs transitioned from extension springs into compression springs. The reversal of memory state meant that the applied current was heating the springs hot enough to train them into an extra state.

The investigation into this reversed performance revealed that it may be consistent with a behavior known as two-way shape memory effect (TWSME). Multiple studies have been conducted on the training of NiTi SMA to have a two-way actuation without the need of an externally applied stress [61]–[65]. The TWSME is the result of thermomechanical loading (training) of traditional one-way shape memory effect (OWSME). Repeated deformation and heating between the austenite and martensite finishing temperatures cause a dislocation in the structure of the NiTi SMA [66].

There are four methods for training an OWSME actuator into a TWSME actuator, pseudoelastic cycling, shape memory cycling, combination pseudoelastic and shape memory cycling, over-deformation, and constrained temperature cycling [31], [34], [36]. Pseudoelastic cycling involves cycling loading and unloading at above austenite finishing temperature. Shape memory cycling is traditional SMA actuation, where the actuator is cooled below martensitic finishing temperature, deformed below the strain limit, and heated to austenite finishing temperature. Continual cycling to the same deformed condition will cause the actuator to creep towards the deformed condition while cooling. A combination of pseudoelastic and shape memory cycling is a combination of the two cycling methods. Over-deformation is observed when the actuator is deformed beyond the

strain limit at below the martensitic finishing temperature. By deforming beyond the strain limit, permanent deformation causes a loss in memory. After an over-deformed actuator compresses during heating, it will cool to the deformed state. The last method of developing two-way actuation, constrained temperature cycling, is the easiest to achieve, and most likely what caused the behavior during the characterization test. This method of training actuators involves stretching the actuators when below martensitic finishing temperature, constraining to not allow compression, and heating while constrained. Cycling cooling and heating while the actuator is constrained. When the actuator is unloaded and returned to the original memory position, subsequent heating will lead to extension of the spring into the deformed position, with cooling returning the spring to the compressed state [65].

The method used for testing the actuators in the characterization testing is the same method used for two-way actuation training under constrained temperature cycling. Using this method, two-way behavior can be observed after 5-20 cycles. After initial two-way memory was observed, continual deformation of the actuator beyond the strain limit led to a permanent reversal of memory state, similar to the effect of the over-deformation method.

The behavior was most notable for extensional strain of 0. At extensional strain of 0 as the actuator was heated it began to expand between the grips of the Instron, instead of compress. The way the forces are measured on the Instron is by looking at the force acting on the grips. As the spring extended, it was no longer in tension as the excess spring began to buckle, leading to negative forces. The negative forces recorded show this behavior, however, the magnitude of the negative forces is less than the actual negative forces produced by the expanding spring. As a spring expands, the force is going in opposing

directions. Instead of translating the force to both grippers, the reacting force on the two stationary grippers causes the spring to buckle, as the grippers force the expanding spring to compress. With the buckling, the load path changes, and more load is concentrated at the center of the bend (buckle) of the spring. As a result of the way the Instron collects data, it is unable to measure the force at the buckle, only that against the grips, so it is not possible to ascertain the actual magnitude of the force exerted by the expanding spring.

As a result of such extreme behavioral change, the first two samples of the thinnest diameter springs were only tested twice. By the second round of testing with each sample, the actuators began to expand instead of compress. To more accurately assess D1, a third sample of the 0.31 mm diameter wire was tested with a lower maximum current and extensional strain. This sample experienced a lesser change in packing density and memory loss than the previous samples. This sample also did not experience the same two-way actuation behavior

3.3.5 Temperature

The temperature testing was inconclusive. Four methods for measuring temperature were attempted, but none were able to determine the temperature accurately. The first method was to use a thermistor connected to an Arduino. The small diameter of the spring, combined with low packing density when stretched, and regional compression, prevented the thermistor from making good contact. Attempts were made to make better contact by using a flat thermistor instead of a domed thermistor, but the temperature was still unable to be read. Temperatures measured using the thermistor peaked at 42 °C, this is much lower than the temperature should have been considering that the activation temperature is 70 °C.

The temperature was also taken using a multimeter with a thermocouple. This device was more successful than the thermistor, but contact was still an issue. The

thermocouple was able to measure up to 135 °C in one instance, but incomplete contact prevented the measurement from being repeated. In an attempt to achieve better contact, the thermocouple was inserted into a small tube filled with thermal paste around the actuator. Better contact was achieved. However, the thermal paste and tube interfered with the behavior and heating of the spring and caused the region with the paste to overheat and compress, further expanding other regions of the spring.

The final attempt for temperature was a FLIR C2 thermal camera. From literature, thermal imaging is usually the only way to measure the temperature of SMA wire. In order to achieve accurate measurements, the emissivity of the SMA used must be known, and the thermal camera must have a high resolution [68]. The FLIR C2 had too low of a resolution to get an accurate measure of the temperature of the SMA.

For future testing, a method of welding thermocouples to the spring actuators should be explored. Other institutions are currently working on developing methods for measuring the temperature of straight wire using welded thermocouples, but to my knowledge, this technique has not been attempted for springs [69]. Additionally, a high-resolution thermal camera is recommended to gather more accurate images and thermal data.

Since temperature could not be measured, the approximation of temperature via joule heating was used as the estimate for the spring temperature.

3.3.3.6 Actuator choice conclusion

Based on the results of testing the wires of diameter 0.31 and 0.38 mm, it was determined that the 0.38 mm diameter wire was the best wire to use for subsequent testing in the elbow flexion exoskeleton rig. Where the 0.31 mm actuators had a maximum force of 3.21 N, the 0.38 mm wire had a higher max force of 8.88 N. Additionally, the 0.38 mm

actuators consumed less than half the power than the 0.31mm actuators. The final reason for choosing the 0.38mm wire actuators was that the actuators were more repeatable at the higher currents and extensional strain showing a smaller change in free spring length. It is important to note that these decisions are based on the comparison to only sample 3 of the 0.31 mm diameter wire actuators as the other two were deemed compromised. Although the samples 1 and 2 of the 0.31mm wire tested at higher currents displayed equal to higher forces than the 0.38 mm wire actuators, they were unreliable and decayed too quickly. Samples 1 and 2 also displayed a high change in free length which is not desirable.

3.4 Limitations of characterization studies

There are a number of limitations to the characterization studies. The first limitation is that the characterization focused on only two wire diameters of one alloy, set at one annealing temperature. There are other diameters and alloys that exist and could have been tested. Additionally, as mentioned in chapter 2, different annealing temperatures influence the actuation temperature. It is unknown how these variables might have influenced results.

The second limitation is the number of samples. Only three samples were tested for diameter 1 (0.381 mm). Although 3 were tested, only one was used for comparison as the others were adjusted during testing. Adjusting the samples might have influenced power and force readings as there was the same amount of current going through less wire. More investigation is necessary to discover the influence of readjusting the spring. Force and resistance graphs were included in the results to show the decay and the effects of higher currents and extensional strain on the first two samples of diameter 1. Since changing the

positions of the clamps might have influenced results for force and power, the data and results from the first two samples were not used when comparing the two diameters and was only included in this thesis to show the behavior observed during testing. Only sample 3, a new sample not tested to the extremes of temperature and extension, was compared to the diameter 2 (0.381 mm) springs. Besides the limitation of the number of samples of D1 (.31 mm) vs D2 (0.381 mm), there is a limitation on the overall number of samples. Ideally this study would have been done with more samples, however, there was a limitation on the number of samples that could be tested due to time.

While there are many limitations, one can still make observations. The 0.381 mm wire was more power efficient and produced more force than the 0.31 mm diameter wire spring. Although the sample of the 0.31 mm diameter used most for comparison was not tested to the same values as the 0.381 mm diameter wire, the best diameter chosen would be the same. Looking at the tables in the appendix for the force and power maximums for extensional strains of 2 and 1.5 and current of .8 A, using sample 2 for both cases as sample 2 was tested for these conditions first and were not adjusted or experienced any loss of memory yet, the maximum force was still produced at extensional strain of 1.5 for diameter of 0.381. The power is also less at diameter 0.381, approximately 1 Watt less, for all settings making it more power efficient.

3.5 Conclusions of characterization studies

The characterization test measured the output force and change in resistance during actuation for springs of two different diameter wires (0.31 mm wire and 0.381 mm wire). These were tested for extensional strains of 0 to 2 increasing at intervals of 0.5 and currents of 0.0-0.8 at intervals of 0.1. The springs of diameter 0.31 mm were tested at these

parameters for two samples. The samples began to exhibit fatigue and did not actuate back to the 7 mm starting length. Instead, they began to expand when heated instead of compressing. As a result, the samples were adjusted which influenced the results. These two samples were discarded and a new sample, (sample 3) was tested for the 0.31 mm wire spring. This sample was tested to lower extensional strains and current settings to reduce the memory loss effect.

Based on the results of testing, the 0.38mm diameter wire demonstrated the most reliable actuation with a smaller change in free spring length. This diameter wire spring also produced more force as it was capable of handling higher currents more reliably than the D1 actuators. Power wise, D2 was also more power-efficient than the D1 actuators.

It was also shown that for Diameter 2, the force at extensional strain 2 was less than the force at extensional strain of 1.5. This matches results from An et al. as discussed in chapter 2, where the maximum is less than 2. Theoretically the higher the extensional strain the higher the force, however, these results show that with other factors, the theory only holds until a certain point.

Chapter 4: Practical design testing

This chapter focuses on the third goal of the thesis: to test the general feasibility of using SMA spring actuators to actuate an elbow bend exoskeleton. To carry out the tests, two SMA actuator rig systems were built: A 1.5 extensional strain rig and a 3.0 extensional strain rig. In addition, a servo motor rig was built for purpose of comparison. The first section of this chapter describes the methods used. The second section sets forth the results of the tests carried out on the three rigs. The third section of this chapter is a discussion of those results. The fourth section describes various limitations to the rig test. The final section of the chapter is a summary of the chapter.

4.1 Methods

This methods section is divided into three parts. The first part describes the setup of the two SMA actuator testing rigs. The second part describes the setup of the servo motor rig. The third part describes the test procedures used to test the rig.

4.1.1 Set up of the SMA testing rigs

Two SMA balsa wood rigs were built to simulate the forearm, Elbow, and upper arm. Each SMA rig was fitted with 6 SMA spring actuators, which were wired in series. The actuators in one rig were set to 1.5 extensional strain, and the actuators in the second were set to 3.0 extensional strain. Each rig was also fitted with a computer fan.

The first part of this sub section describes the design of the lever arm used in the two SMA rigs. The servo motor rig discussed in subsection 4.1. 2, uses the same lever arm. The second part of this subsection discusses the setup of the SMA actuators on the rig.

4.1.1.1 Lever arm set up

The rigs are based on the average female forearm length from the elbow to the center of mass, which is 11.5 cm [24]. The location of the center of mass is also based on the anthropometric data. To accomplish the 4 cm lever arm determined for design, the lever arm on the test rig (skeletal model) was set to 8 cm. Since the joint is approximately 4 cm from the elbow surface at 90° angle, the lever arm is actually 8 cm from the pivot of the joint (Figure 33). The value of 4 cm comes from textbooks and biomechanical models used for determining the force exerted by the bicep [25]. Copaci et al also used this distance [35], [36].

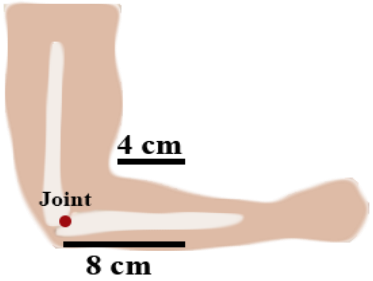

Figure 33: Lever arm showing 4 cm from elbow surface is approximately 8 cm from elbow joint

4.1.1.2 SMA actuator set up

The SMA actuator set up comprises of two plastic pieces supporting the springs located near the position of the bicep. The top plastic support is kept stationary and the bottom one is left to float. Attached to the bottom plastic support is a Kevlar cable that routes through hooks located at 8 cm on both sides of the hinge and ends at the wrist.

The system works by heating the springs until they compress and translating the linear stroke through the cable until the elbow flexes. Details of the individual components of the SMA actuator set up are detailed below.

4.1.1.2.1 Number of actuators

Based on the characterization study in chapter 3 and the literature review, each SMA rig was fitted with 6 SMA springs of 0.38 mm diameter NiTi alloy wire springs with an actuation temperature of 70 ℃. In choosing the number of SMA actuators to include in the SMA rig, the main constraint was the power supply needed to power the actuators. Based on the literature review, a limitation of 25 VDC power supply was imposed. Given this and the use of series configuration in the 6 SMA springs (discussed below), the number of actuators that could be used on the SMA rig was limited to 6. Increasing the number of actuators increases the voltage needed to power the actuators.

4.1.1.2.2 Series configuration of the SMA spring

The springs were wired in a series by alternating connections on the floating or fixed end (Figure 34) with both power leads at the top (fixed end) of the system.

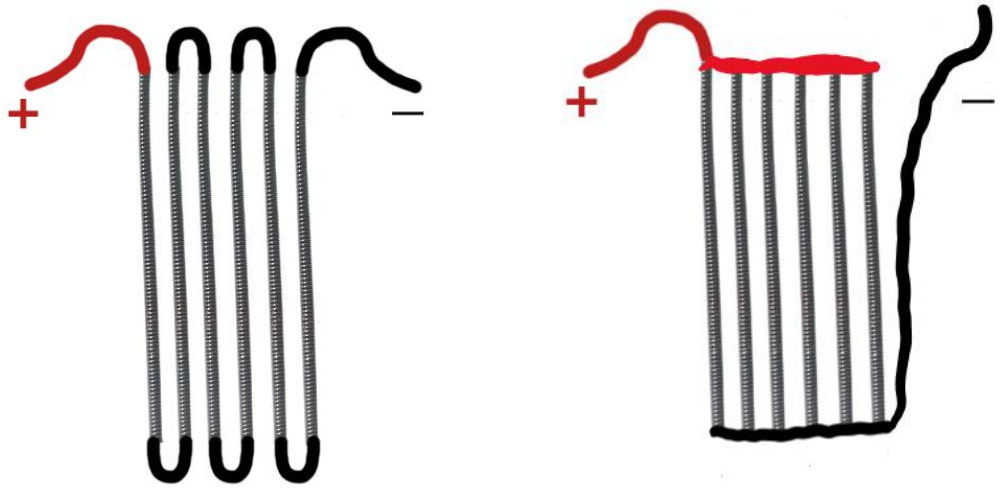

Figure 34: Left, Actuator series connection; right, actuator parallel connection.

The actuators were placed in a series to reduce the electrical current variability in the system during actuation. The actuation is being driven by current, and the circuit in series results in equal current through each spring. When actuators are placed in parallel

instead of in series, it is more difficult to assure that the current going through each actuator is the same. This is because resistance changes as actuators are heated, so even if each of the actuators have the same length, the current going through each of them may be different. Actuators with lower resistance will draw more current than those with higher resistance. This will lead to unequal forces through parallel actuators. It is possible to reduce the likelihood of unequal forces by fitting the start of each of the actuators with a properly sized resistor. However, if the rate of change of the actuator resistance across all actuators is not constant, the resistors will not ensure equal current. A second advantage of the electrically series actuator design is avoiding having excess lead wires in the system, which would be necessary if the system were electrically in parallel.

There is a tradeoff involved. The total voltage required for a parallel circuit is less than that required for a series circuit. However, given the challenges of the parallel circuits, it was determined that the series circuit was the best for this rig. This tradeoff is discussed in the limitation section of the chapter.

4.1.1.2.3 Actuator system actuator length

The biomechanical model was used to measure the total linear displacement for flexion at the elbow from 130° to 30°. The measured displacement was 10 cm. Data from actuator characterization showed that extensional strain, ε = 1.5 produced higher forces than ε = 2. Using extensional strain of 1.5 and displacement of 10 cm, the equation $\varepsilon = \delta / L_0$ was rearranged to give the desired free spring length (L_0).

$$L_0 = {}^{\delta}/_{\varepsilon}$$

$$6.67 = {}^{10}/_{1.5}$$

A second actuator system was created with shorter springs to evaluate the option of an alternative length that would require less power (Figure 35). The shorter springs were created to have an extensional strain of ε =3, which is equivalent to stretching the springs to four times their free spring length. For the same 10 cm displacement, the shorter springs were cut to 3.33 cm. It is important to note that the image below is of the system during testing, and the length of the springs spring actuators depicted is not the original cut length.

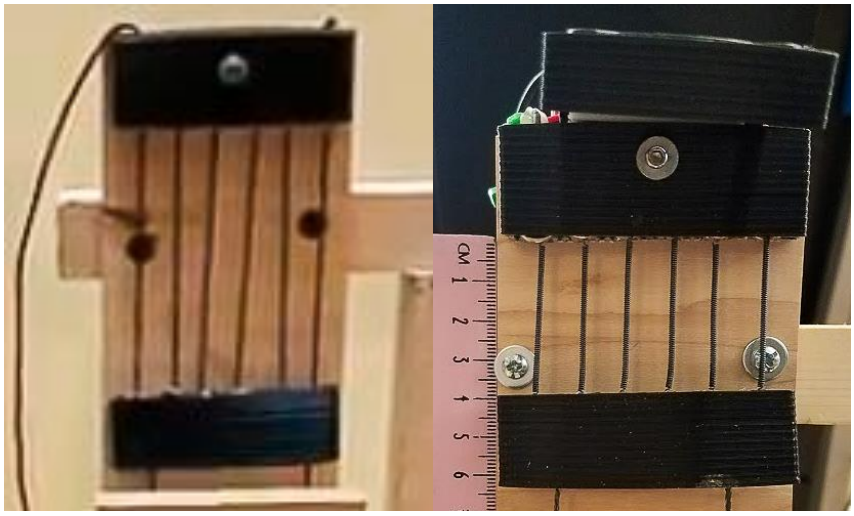

Figure 35: Two actuator lengths. Left extensional strain of 1.5 (6.66 cm compressed). Right original extensional strain of 3 (3.33 cm compressed), 40 cm during testing when image was taken.

4.1.2 Servo motor rig setup

For this project, a traditional cable and motor system was compared to the previously characterized SMA actuators. The cable system uses a pulley at the motor head to coil the cable as the motor turns, translating rotational motion into linear. Motors have an advantage in that they are able to produce high torque for relatively low power. The coiling of the cable on the pulley at the motor shaft also decreases the length of the cable and has a large stroke. The motor used is a HiTech HS5646WP servo. This motor has a

stall torque of 11.31 Kg*cm at 6 Volts and can theoretically provide a maximum of 108.244N vertical lift with a 20.5mm pulley at the shaft of the motor.

Mechanically, the set up for the servo actuator system is the same as the SMA systems, where there is a lever arm of 8 cm as shown in Figure 33. The difference is that there is only one cable running through the system. Additionally, instead of running through eyelets, the cable runs through a Bowden cable with one end near the actuator, and the other at the same position as the eyelet in the SMA system, 4 cm. Although there is a different number of cables, since both systems have the same lever arm and location where the weight is being applied, the total amount of force being transmitted to the servo actuator is the same as the total load being transmitted to the 6 SMA actuators.

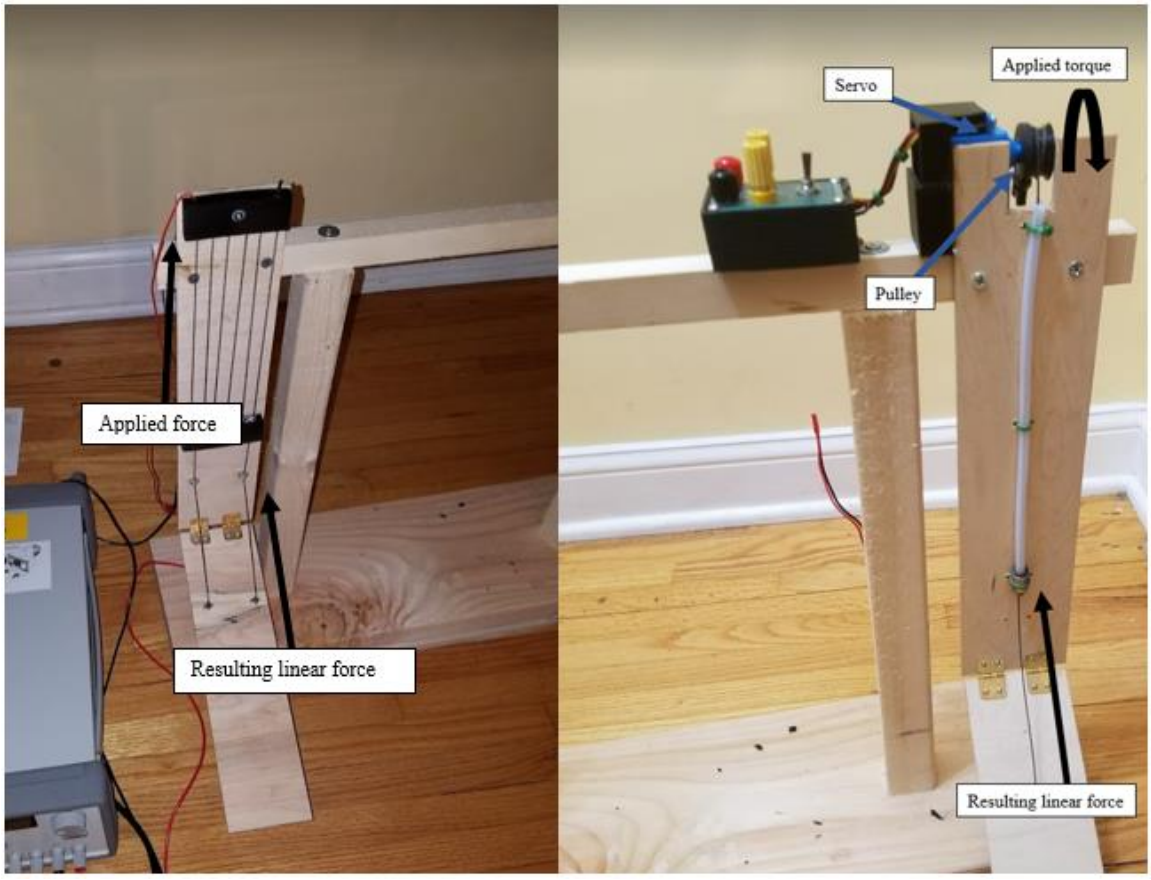

Figure 36:Right image depicts the loads of the SMA actuators with extensional strain of 1.5. Left image depicts components and loads of the servo system.

4.1.3 Test methods and data collection

The testing methods for the test rigs were developed based on the actuator characterization tests. Three tests were carried out. The first test was a benchmark test to characterize the maximum weight the three rigs could lift, current required to lift that weight, and actuation and cooling time. During the benchmark test, efficiency of the three rigs was calculated. The benchmark test and the efficiency calculations were done at the same time since the results from the benchmark test were needed to determine efficiency. At the end of the benchmark and efficiency test, actuators in the 1.5 and 3.0 extensional strain rigs began to burn due to the final testing parameters. Thus, the two SMA rigs were fitted with 6 new actuators each. The first and second set of actuators came from the same batch of SMA spring actuators. The parameters that caused the actuators to burn were not used in subsequent testing

The second test was a cycling test. The aim of this test was to observe any potential drift in total actuation. Total actuation is the difference between the fully stretched and fully compressed length of the spring. Another way of defining total actuation is the difference between the start and final position of the bottom end of the actuator set. This test was carried out because of the drift in maximum force and compressed length observed in the characterization test in chapter 3 with the SMA spring actuator with diameter 0.31 mm. This observed drift in the 0.31 mm spring actuators was one of the reasons that I use the 0.38 mm actuator in the SMA rig tests. The repeatability test aimed to determine whether the same drift would be observed under the test conditions of the SMA rig.

The third test, a load cycle test, was run after the third test. The load cycle test measured the force produced by the actuators at each mm of actuation. Load testing was

done to determine the force produced by the actuators when trying to lift a weight along the actuation cycle. The loading is different than with the Instron where the springs are kept extended in a static position and force is purely linear. In the rig, the springs are able to fully compress during actuation and although the actuation is linear, the forces experienced are not constant due to the geometry of the rig and the change in the exerted forces as the elbow bends.

Only the two SMA systems went through the repeatability and load cycle test since SMAs are the focus of this study and the servo used was factory tested and is rated to hundreds of thousands of cycles.

The variables being manipulated were amount of extensional strain in two SMA systems, amount of applied load, cooling method, type of actuator, and supplied current. The measured values were time for actuation, time for cooling, actuation force, total actuation, and efficiency. The purpose of total actuation is to also determine the drift in total actuation. Descriptions of each test and data analysis are discussed below.

4.1.3.1 Benchmark test: Setting parameters for maximum weight, actuation and cooling time, and current

This benchtop test used various weights to characterize the three test rigs as to the maximum amount of weight they could each lift, the actuation and cooling time at each weight, and the current and voltage requirements at each weight.

Weights were added to the center of mass of the 1.5 extensional strain SMA rig, the 3.0 extensional strain SMA rig, and the servo motor rig. The weights were 500g, 700g, 1.0 kg, 1.2 kg, and 1.5 kg. They were tested in this order and data was collected using a multimeter and a stopwatch. The actuators in each SMA rig were actuated with a 25VDC maximum voltage power supply. For the servo actuator, the rated voltage is 6VDC. The

current it draws only depends on the load applied to the servo. Increasing the voltage beyond 6VDC will create excess heat which will damage the servo. Additionally, due to the higher efficiency and lower power demand of the servo motor, less energy gets transformed into heat. This means the servo does not need active cooling in form of a fan.

At each weight, each SMA rig was actuated four times:

- 0.8 Amps without fan cooling
- 0.8 Amps with fan cooling
- 0.9 Amps without fan cooling
- 0.9 Amps with fan cooling.

At each weight the servo actuator rig was actuated once since there was only one testing condition.

Each weight was tested twice at the two different current settings (once with and once without fan cooling), recording time for actuation and return using a stopwatch. Actuation was considered complete when the angle between the forearm and upper arm was 30°, springs fully compressed. In cases where the actuators did not actuate all the way, actuation was considered complete 2 seconds after the actuator stopped moving. This 2 second buffer was added to the test in order to ensure that the actuators had fully stopped moving.

4.1.3.1.1 Efficiency of the two SMA rigs and the servo motor rig

Data for efficiency was collected at the same time as the data for the benchmark test. The peak voltage and current was recorded for each trial of each condition to use for determining the efficiency of the each of the three systems. The peak voltage was

determined from the power supply since the power supply was kept at a constant current. Choosing the peak voltage will give the worst-case efficiency. The average efficiency will be slightly higher, as discussed in section 4.4.1.1. Additional confirmation was taken by connecting a multimeter to probe locations near the power switches for the rigs. The efficiency of the two lengths of actuator systems and the servo system were calculated by using the max power consumed during actuation, the average time to actuate, and the total linear displacement at the end of actuation. For the two SMA systems, the data from the trial with 1kg load and 0.8 A was used. For the servo, since the voltage was constant, the trial was the 1 kg load. The efficiency calculations do not take into consideration the power used for the computer fan for the two SMA systems as efficiency is taken with the voltages and time during actuation and not cooling. The fans were only used when cooling. Since the time for cooling was not considered, and the cooling after actuation does not influence the actuation itself, the average time for actuation was calculated from the results of the test with and without the fan. To calculate the efficiency of the servo, a weight of 1 kilogram was lifted 4 times. Each time the time and peak current were recorded. An average was taken of both the time to lift the weight and the peak current.

Note that the efficiency test was only done with a constant load (1kg). Different loads will have slightly different efficiencies. However, the same conclusions still apply.

4.1.3.1.2 Data analysis: Benchmark and Efficiency

Table 11: Benchmark parameters

Dependent Variables	Independent Variables	Explanation

	Current	Tests were conducted using a current of 0.8 A and 0.9 A. This gives insight into how current affects produced force by the springs.
Actuation Time		Actuation time affects how fast actuators can cycle
Cooling Time		Cooling time had a big impact on cycle time
	Fan on/off	Fan had noticeable impact on cooling time
	Load	Load varied between 0.5kg - 2kg
	Extensional Strain	Tests were conducted for both systems (extensional strain of 1.5 and 3)

*Table 12: Efficiency test parameters to finish the efficiency calculation. For the efficiency test, the load was kept constant at 1kg. All the variables were required to calculate the efficiency for each system. *Name of the variables in the formulas used to calculate efficiency. Equations 13-15 show the formulas. ** this only applies for the servo system*

Dependent Variables	Independent Variables	Explanation
Current**	Current	Current needed to calculate power (I*)
Voltage	Voltage**	Voltage needed to calculate power (v*)
Time		Time needed to calculate energy consumption (t*)
	Distance center of mass moved	Used to calculate the potential energy (h*)
	Extensional Strain	Efficiency was calculated for both systems (extensional strain of 1.5 and 3)

4.1.3.1.2.1 Data analysis: Efficiency

The equations for calculating efficiency are shown below. In these equations I is current, V is voltage, t is time in seconds, F is force, h is displacement, m is mass, g is acceleration due to gravity. Although the torque is occurring at the elbow, the force for the energy calculation is taken as the linear displacement of the load, so $\theta = 0$. The reason that

it is not taken as torque is because the transmission of motion is not at the joint and is being produced by a linear motion offset from the axis of rotation, therefore, joint torque is converted to applied linear force [70].

Equation 13

$$\eta = {}^{W_{out}}/_{W_{in}}$$

Equation 14

$$W_{in} = Power\ (Watts) \cdot Time\ (s) = I \cdot V \cdot t$$

Equation 15

$$W_{out} = F \cdot h \cdot \cos\theta = \mathrm{Fd} = \mathrm{m} \cdot \mathrm{g} \cdot \mathrm{h}$$

In Equation 14, since all three actuator systems work on DC, the power (P) is just current * voltage (I*V). This means that the work in, the energy used to complete one actuation, is I*V*t.

To calculate the actual efficiency, the useful energy needs to be calculated. The only purpose of the exoskeleton is to lift the arm. Considering that one actuation brings the elbow from 120 degrees to 30 degrees, the potential energy, Equation 15, can be easily calculated using a statics model, Figure 37.

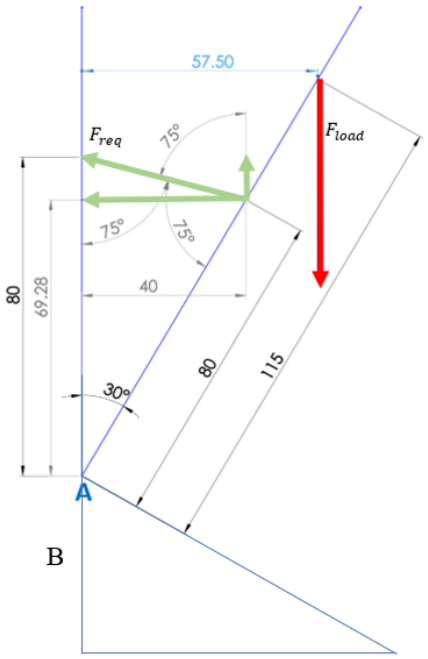

$$h = B + 69.28 = 80 * \cos(60) + 69.28 = 109.28\,mm = \ 0.10928\,m$$

Figure 37: Static model and equation to determine potential energy

From Figure 37, the center of mass was lifted by 109.28 mm or 0.10928 m. This means that the potential energy to lift 1 kg is:

$$W_{out} = 1kg * \frac{9.81m}{s^2} * 0.10928m = 1.07J$$

The efficiency of the three systems was calculated and compared against each other.

4.1.3.2 Repeatability testing for determining potential drift in 0.381 mm diameter wire spring

The characterization testing in chapter 3 found some drift in the maximum force and compressed length of the SMA actuators of 0.31 mm. The aim of the repeatability test was to determine whether the same drift would be observed when the SMA rig actuators were run over multiple cycles.

During the benchmark testing, it was determined that the 3.0 extensional strain rig was able to lift no more than 1.0 kg, as a result, the repeatability test was done with a 1 kg weight to ensure that the loading conditions for the 1.5 extensional strain and 3.0 extensional strain systems were the same.

This subsection begins by discussing the main changes to the SMA rig that were made for the repeatability test (and subsequently also used for the load cycle test). It then describes the testing method for the repeatability test. The test was run for a total of 100 cycles. The test was performed once using a new set of actuators for both the 1.5 and 3 extensional strain systems. The new set of actuators meant that they were not used in benchmark testing and had been pre-actuated 5 times as with the benchmark and characterization actuators.

4.1.3.2.1 Changes in rig set up for repeatability testing and load cycle testing

The SMA rigs were modified to include a load cell and linear encoder to record force and position (Figure 38 to Figure 42). A microcontroller (Arduino Nano) with a data logger was used to record all of the position, time, and load data. A 1.0 kg weight was placed at the center of mass. As stated above, this weight was used as the 3.0 extensional strain SMA rig began to but at higher weights.

The testing was performed on the test rig with a linear encoder from a printer attached to the side of rig frame. The sensor for the encoder was attached to the free end of the springs. As the spring compressed and decompressed, the data collected from the encoder was recorded on an SD card in a data logger on an Arduino nano. For the drift test, the data was set to record at the end of the actuation time, measuring the maximum location.

The Arduino nano was also used to control the actuation and cooling cycles by turning on/off relays. The cycle was set to 22 seconds of power and 30 seconds of forced air cooling. Cooling of 30 seconds with a fan provided sufficient time for stretching the actuators and rest before the next cycle. The timing for actuation was determined by a bench test with the encoder; actuation time was set to the time at which the encoder began to show a constant position at the 30-degree position. Although the benchmark test was meant to select the heating time, the new, fresh set of actuators were requiring more time to actuate, so 2 actuation cycles were completed using the encoder to determine the new time.

The Arduino code is included in the appendix.

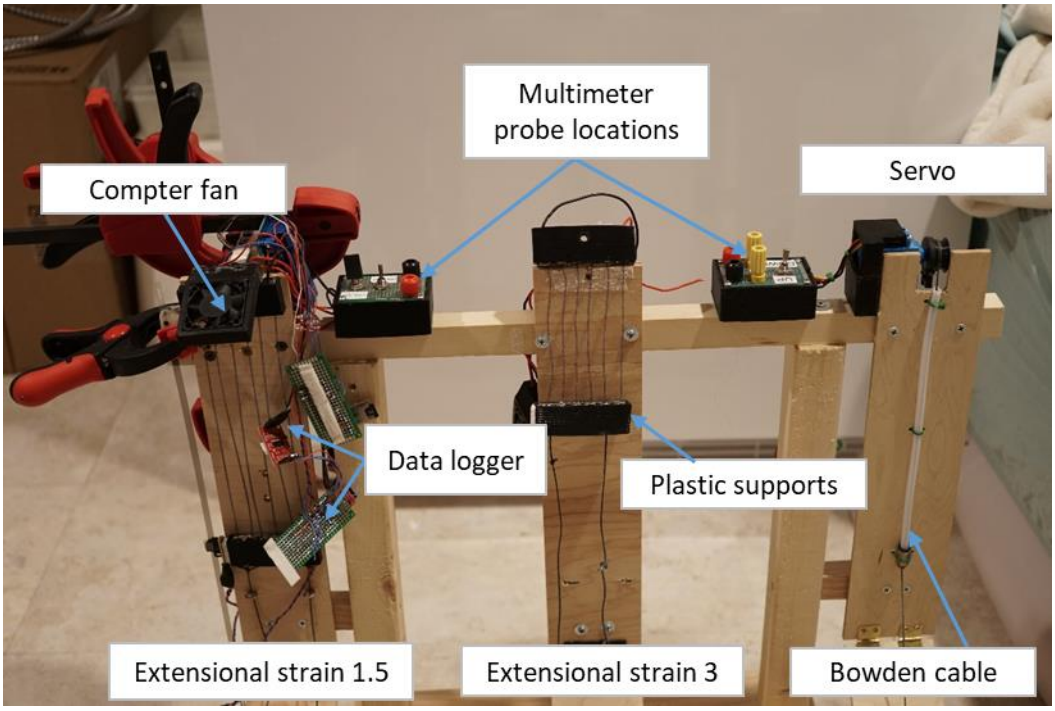

Figure 38: Right rig of SMA system extensional strain of 1.5, middle SMA system extensional strain of 3, and left servo motor system. Pictures show data logger, linear encoder, and computer fan.

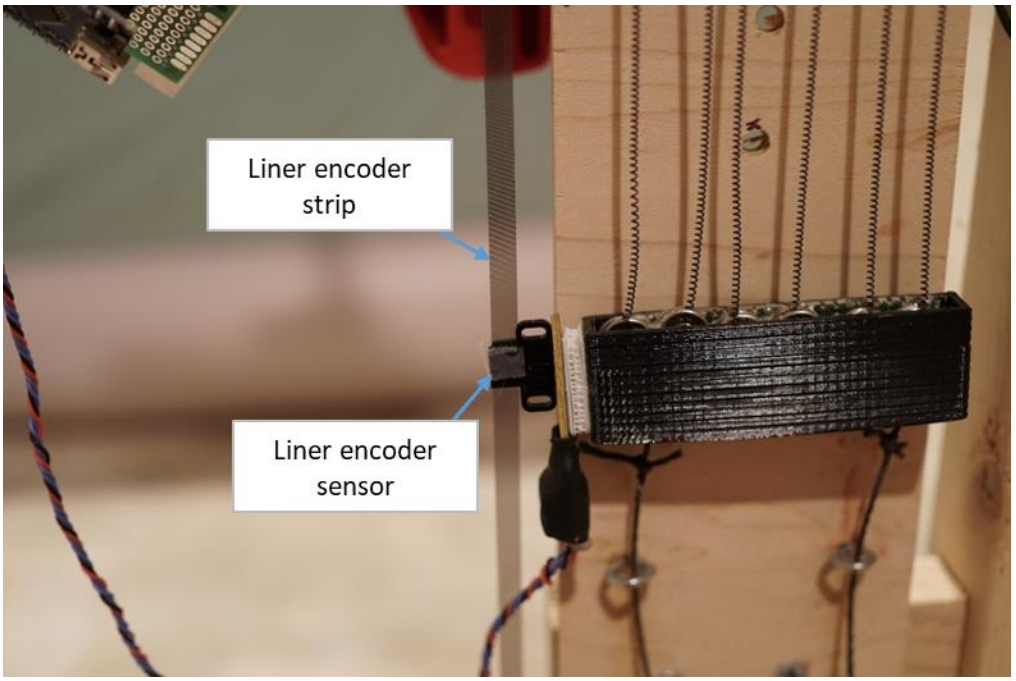

Figure 39: Linear encoder on SMA system of extensional strain of 1.5. The sensor was attached to the moving base of the SMA actuators.

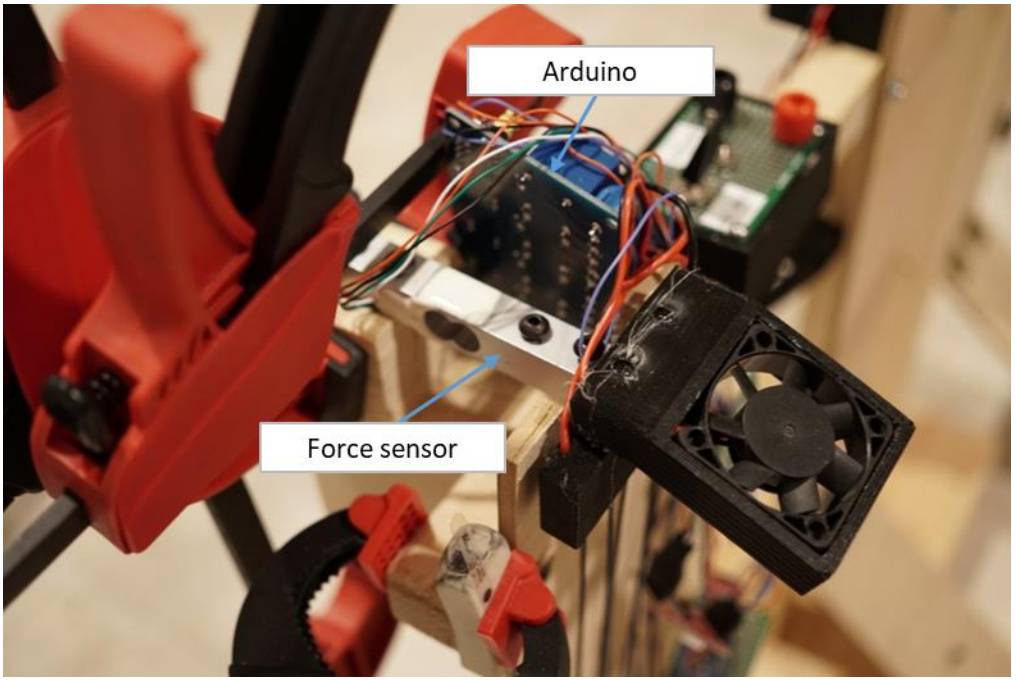

Figure 40: Load cell on the SMA system and cooling fan. Two Arduinos and data loggers were used. One was connected to the load cell and the other to the encoder.

Figure 41: Arm rig with extensional strain of 1.5 with a 1 kg weight.

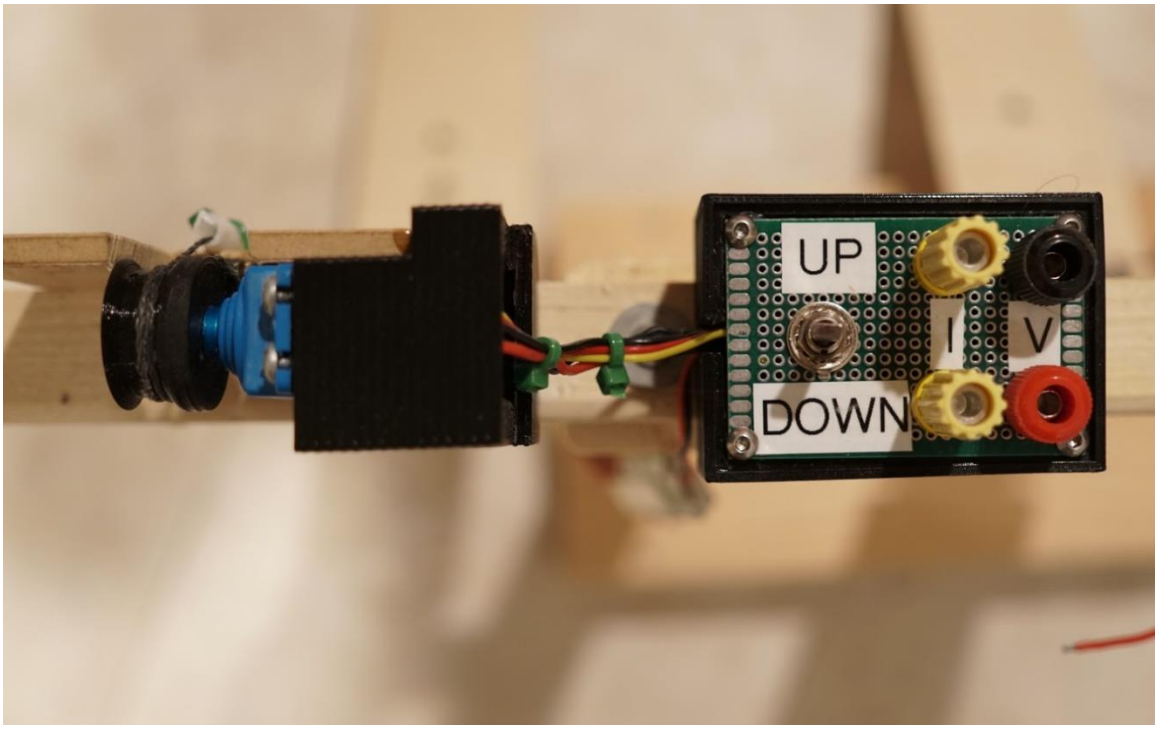

Figure 42: Up and down switch for servo motor with meter testing ports.

4.1.3.2.2 Methods for repeatability testing

Based on the information in the literature review about the decay in memory properties of SMAs, it was chosen to run a repeatability test with and without a stopper. The purpose of the stop was to limit the extensional strain of the actuators. Without the stopper, as actuation went on, the amount that the actuators extended with the weight of the arm shifted. This shift is due to two factors. First, the weight applied was sufficient to extend greater than 1.5 extensional strain. Second, the stiffness decreases the more the springs are actuated. The tests without the stopper measured the drift in the extension of the spring and the test with the stopper measured the shift in flexion. When actuator cycles are run without a stopper, it becomes easier for the actuators to stretch and harder to maintain the extensional strain [45]. The test was done with both conditions to measure the change in extensional strain.

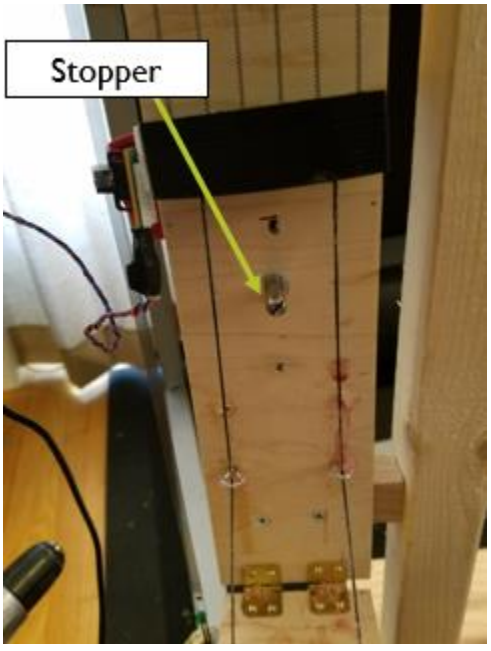

Figure 43:Stopper on rig of extensional strain of 1.5.

The 3.0 extensional strain SMA and the 1.5 extensional strain SMA were each run for 200 cycles with a stopper set at the same physical vertical position on each rig. Based on the literature review, the stoppers were set to stop the SMA rigs at 120 degrees of extension. It is important to note that, although a stopper was placed on the extensional strain of 3.0 rig, at this extensional strain the actuators were unable to be stretched all the way and did not reach the stopper.

Only the two SMA systems went through the repeatability test since SMAs are the focus of this study and the servo used was factory tested and is rated to hundreds of thousands of cycles. Further, as will be discussed in the section describing results of the benchmark test, at the end of the benchmark and efficiency test, actuators in both SMA rigs began to burn. As a result, before running the repeatability test, each SMA rig was fitted with a new set of actuators. The new set of actuators meant that they were not used in benchmark testing and had been pre-actuated 5 times as with the benchmark and characterization actuators. This same set of actuators was subsequently used for the load cycle testing.

The test was first performed with the stopper. For both the 1.5 extensional strain rig and the 3.0 extensional strain rig the repeatability test was run once for a total of 200 cycles between the two test conditions with exception of the no stopper condition for the 1.5 extensional strain. For the case of the extensional strain of 1.5, the repeatability test data without the stopper was collected at the same time as the load test data described in the next section and results for only 100 cycles were recorded. The reason why this specific case was only run 100 times is explained in the load test section.

4.1.3.2.2.1 Data analysis: Repeatability

During the repeatability test, different parameters were considered for the first cycle at the beginning of the repeatability test. This singular cycle aimed at observing the actuation distance over time.

Table 13: Parameters of one cycle of the repeatability test, one cycle.

Dependent Variables	Independent Variables	Explanation
Actuator Position		The position of the actuator sensor. Actuator position is equal to the output from the linear encoder. This is used to calculate the total actuation distance.
Actuation Time		Actuation time affects how fast actuators can cycle. Actuation time was measured using a stopwatch. The time measured was the time from when the power supply to the actuators was turned on to when the actuators were fully compressed. The fully compressed state was determined by when the actuators visibly stopped actuating for 2 seconds.
Cooling Time		The cooling time was measured using a stopwatch. The time was recorded from then the power supply was turned off to when the actuators were fully extended. Fully extended was determined if the actuator bottom reached the stopper or had visibly stopped extending further for 2 seconds.
	Fan on/off	Fan had noticeable impact on cooling time
	Extensional Strain	Tests were conducted for both systems (extensional strain of 1.5 and 3)

In this case the actuation distance is the same as the output from the linear encoder. This means no calculations required.

The rest of the repeatability test measured the following parameters over multiple cycles.

Table 14:Parameters for repeatability test.

Dependent Variables	Independent Variables	Explanation
Actuator Position		The position of the actuator sensor. Actuator position is equal to the output from the linear encoder. This is used to calculate the total actuation distance.
Stop Position		Position of the encoder sensor after 20 seconds of actuation. (The maximum position in the cycle)
Start Position		Position of the encoder sensor at the beginning of the cycle, fully extended. This is the position the sensor is at after the 30 seconds of cooling of the previous cycle.
	Number of Cycles	Every occurrence that the actuators fully compress and return to the start position counts as 1 cycle. The length of the cycle was set to 20 seconds of heating and 30 seconds of cooling. It is important to keep track of the number of cycles done. This keeps track of when any drift occurs.
	Time	Time is measured in seconds using the Arduino clock. The time is used to compare the amount of actuation at a certain moment of time along a given cycle.
	Stopper/No Stopper	Having a stopper limits the maximum length the springs can be stretched to. This only had an impact of the springs with an extensional strain of 1.5. The springs with an extensional strain of 3 never stretched long enough to reach the stopper.
	Extensional Strain	Tests were conducted for both systems (extensional strain of 1.5 and 3)

Calculated Parameters	Explanation
Total actuation distance	The total actuation distance is the difference between the start and stop positions.
Compressed length	The initial compressed length is either the 3.3cm or the 6.6cm (depends on which spring is used). The linear encoder was zeroed out when the actuator was stretched out by an extensional strain of 3 or 1.5 dependent on springs used). This means that the starting length for both actuators was 9.9cm. From there the linear encoder measures how much the actuation distance is. The starting length minus the actuated distance is the new compressed length. This gives a new compressed length for each cycle.
Extended length	The extended length is the total length of the spring when fully stretched. The extended length is found for each cycle. The extended length is calculated by adding the compressed length to the total actuation distance.
Drift of the compressed length (number of cycles required)	The compressed length for each cycle is subtracted from the initial compressed length from the previous cycle. At the end of testing, the difference between the compressed length of the first and last cycle was calculated, providing the drift of the compressed length for the test.
Drift of the extended length (number of cycles required)	The total extended length was calculated for each cycle and each test. As mentioned above, the initial extended length

	for both SMA springs is 9.9cm. This is where the linear encoder is zeroed out at. The total actuation distance is then measured (as it compresses) as well as the total extended length. The difference between the starting extended length in the first cycle and the extended length of the last cycle is the drift in extended length.
Extensional strain	The extensional strain for each cycle was calculated by subtracting the compressed length (L_0) at the end of the previous cycle with the extended length of the start of the current cycle, resulting in ΔL. Using the equation for extensional strain, $\varepsilon = \Delta L/L_0$, the result is the extensional strain for the beginning of the current actuation cycle.
Change in extensional strain (number of cycles required)	The extensional strain was calculated for each cycle. To calculate the change in extensional strain, the extensional strain of the first and last cycle was used. As the tests with and without the stopper were conducted using the same set of actuators, taking the average to compare the amount of drift with and without the stopper would not accurately depict the difference.

The total actuation distance is important in order to know if the actuator is done with its actuation (stops moving). Understanding the actuation time and cooling time is important to know how one cycle looks. The times measured were than used in the Arduino

code to set up the automated repeatability testing. Whether the fan was on or off had a big impact on the cooling time. The times used in the Arduino code was adjusted for tests with the fan on.

4.1.3.2.2.1.1 Linear position data

The linear encoder in Figure 39 was recovered from a broken inkjet printer. The sensor exists of two parts. The first part is a stationary encoder strip. This encoder strip has evenly spaced solid black lines along the whole length of the clear plastic strip. The other part of the sensor is called a photogate. This is mounted to the moving end of the actuator. The photogate has an LED emitter and an LED receiver. When the encoder strip is placed between the emitter and the receiver, there will be a HIGH signal if the clear plastic is in front of the emitter and the light can easily be received by the receiver. However, when a black line is placed in front of the emitter, the light gets blocked and the receiver won't receive the light. This results in a LOW signal. During actuation, the photogate will move along the strip constantly passing the black lines and the clear plastic parts. This results in a pulse train of HIGH and LOW signals. When this signal is fed into the microcontroller, the number of solid lines passed can be counted. After careful testing (moving the load cell a known distance and seeing how many lines (pulses) were passed), it was determined the lines are evenly space out by 85 µm. This relationship allows the connection to be made between the number of passed lines and the actual actuation distance. In our case, the linear encoder can also measure direction. This is because there is a second receiver in the photogate. When the photogate moves up over the encoder strip, the top receiver will see the black lines first (light gets blocked to the top receiver). At that moment the bottom receiver still receives light (not yet blocked by the line). Moving further, the light for the

bottom receiver gets now blocked while the top receiver receives light again. When the photogate moves down, the whole story reverses. This means that there are technically two pulse trains fed into the Arduino (with a light phase shift). Depending on which receiver 'sees' the line first, the direction the photogate moves over the encoder strip can be determined. The code on the Arduino counted up when the system was moving up and down when the system was moving down.

4.1.3.2.2.1.2 Graphical representation of data

For a visual depiction of the change in vertical actuation distance vs time, the position was continuously recorded over time for the duration of one cycle. Due to the high number of cycles tested, only one representation of actuation distance vs. time was created. To provide a summary of results of the total actuation distance per actuation cycle, graphs were created giving total actuation distance (in mm) vs number of cycles. To accommodate for the summary graph, the Arduino code was changed to record the start and end position of each cycle instead of the continuous position and time data.

The actuation distance vs number of cycles results for the testing with and without the stopper were overlaid into one graph to portray the difference. For the case of the extensional strain of 1.5 with a stopper, the data of the first 66 cycles was lost due to an issue with the data logger. A trend line was found using excel which gave an approximation of the results for the first 66 cycles.

4.1.3.3 Load cell testing

A load test was performed to measure the forces produced by the springs throughout the actuation cycle. This test was done for 60 cycles for each condition with the goal of determining the forces that must be produced by the springs to lift the applied load.

Although I calculated a theoretical value for the forces produced by the actuators, these calculations did not account for friction and other environmental factors that could influence the real-world force values. Due to these other uncontrolled variables, the forces produced by the SMA systems are higher than the theoretical value calculated. It is important to record the actual produced force over the actuation cycle.

Although the tests for the repeatability and load testing could have been conducted at the same time, the decision for the load test was decided after the first repeatability test. This means that for the 1.5 extensional strain system, the moment it was decided to do the load test, the first repeatability test with the stopper was already done. It was during this repeatability test that the most amount of decay was noticed (an important finding). Using the load test data to do the repeatability test would mean discarding the first repeatability test (and thus the first 200 cycles). This means the important decay phenomena would also be discarded.

The only condition where the load testing data was used for the repeatability test was for the 1.5 system without the stopper. This was because the load test was already done, and at this point the system was pretty much stabilized. Doing the repeatability test without stopper after the load test would have given similar results as the springs had stabilized at that point. Instead of doing that, I chose to move forward with using the same data for the two tests in this case.

A load cell was used to measure the variation in force produced by the actuators when trying to lift a weight along the actuation cycle. This load test differs from the benchmark load test previously done as the benchmark tested multiple applied loads and different currents without measuring force produced by the SMAs, and this test measures

the force produced by the spring actuators during actuation lifting a 1 kg weight at 0.8A. The only force calculated in the benchmark test was F_{load} for the purpose of efficiency. F_{load} is purely the force due to gravity on the mass and no measurement was needed or taken. As shown in Figure 44, the force being produced by the actuators, and measured by the load cell, is F_{req}. This force defers from F_{load} as the load path is not linear and the load is being transmitted at an angle. The active measurements give a more accurate representation of the force produced by the actuators than the Instron characterization test as they are compressing with an applied load. The lifting force of the actuators was recorded using a load cell for the two SMA systems. Like the repeatability test, the testing was done with a 1.0 kg weight. To measure the force, the rig was modified to include a load cell. The fixed end of the actuator system was mounted to the load cell instead of directly on the wooden arm frame. These data were recorded after the cycle testing with a stopper and focus on the measured load rather than the drift in position. This test was conducted for both SMA systems. Only the long actuator, extensional strain of 1.5, was tested with and without a stopper, starting with the no stopper condition. The short actuator was only tested without the stopper since, as with the cycle testing, the actuators with extensional strain of 3 were unable to extend all the way and did not reach the stopper. As mentioned in the previous section on the repeatability test, the position data recorded during the load testing for the 1.5 extensional strain system without a stopper was used for the repeatability test.

4.1.3.3.1 Methods for load testing

To measure the force over time and a given position during actuation, the data from a load cell was collected along with data from the linear encoder on a second Arduino nano (code in the appendix). The first Arduino nano was used to cycle actuation and cooling.

The test ran for an hour cycling between 30 seconds power and 30 seconds fan cooling. The time for actuation was once again changed to accommodate for testing without a stopper and to give the actuator more time to actuate. Since the decision for testing without a stopper was made after the repeatability test for extensional strain of 1.5 and 3 with the stopper was done, the time was not changed then. One test of 60 cycles was performed for each of 3 conditions: extensional strain of 1.5 with stopper, extensional strain of 1.5 without the stopper, and extensional strain of 3 without stopper. Since the position data for the extensional strain of 1.5 without a stopper was used for the repeatability test, the test for this condition was run for a longer amount of time and 100 cycles were reported.

4.1.3.3.1.1 Data analysis: Load cell

The load applied to the center of mass of the arm during the load cell testing was 1 kg.

Table 15: Load cell test parameters.

Dependent Variables	Independent Variables	Explanation
Actuator Position		The position of the actuator sensor. Actuator position is equal to the output from the linear encoder. This is used to calculate the total actuation distance.
Force		This is the force recorded by the load cell.
	Extensional Strain	Tests were conducted for both systems (extensional strain of 1.5 and 3)

4.1.3.3.1.1.1 Calculation of theoretical forces

Theoretical calculations were done prior to testing to determine the expected force that the actuators would have provide to lift the human forearm at 120 degrees, 30 degrees, and 90 degrees.

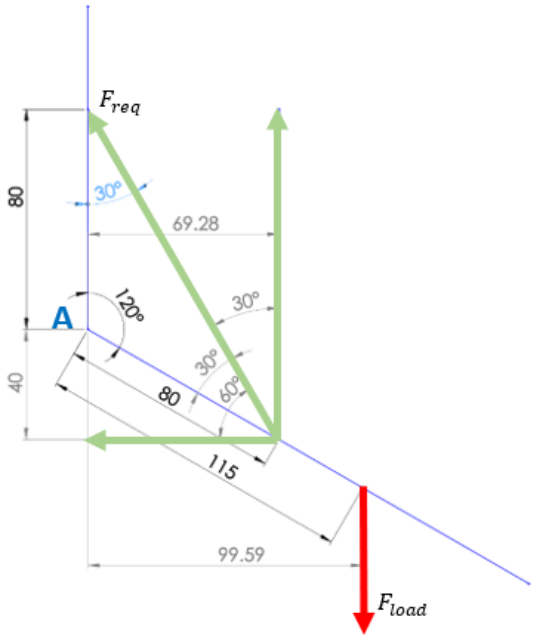

$$\sum M_A = 0$$

$$F_{req} * \cos(30°) * 69.28 - F_{req} * \cos(60°) * 40 - F_{load} * 99.59 = 0$$

$$F_{load} = 1kg * 9.81\frac{m}{s^2} = 9.81N$$

$$F_{req} = 24.4N \text{ or } 2.5kg$$

Figure 44: Force required to lift load at center of mass at 120 degree angle.

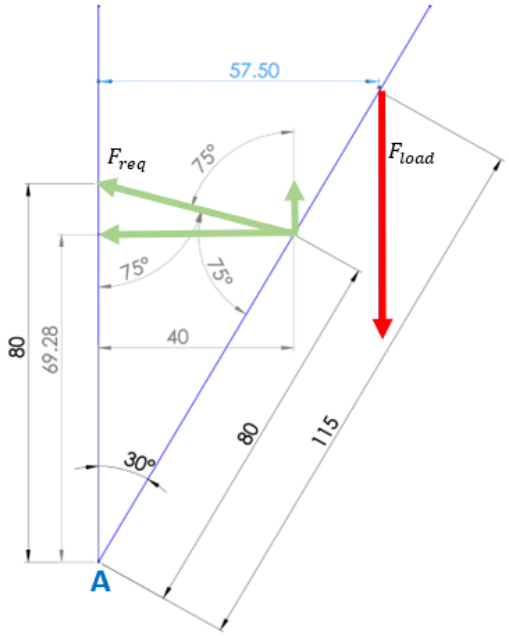

$$\sum M_A = 0$$

$$F_{req} * \cos(75°) * 40 + F_{req} * \sin(75°) * 69.28 - F_{load} * 57.50 = 0$$

$$F_{load} = 1kg * 9.81\frac{m}{s^2} = 9.81N$$

$$F_{req} = 7.3N \text{ or } 0.75kg$$

Figure 45:Force required to lift load at center of mass at a 30 degree angle.

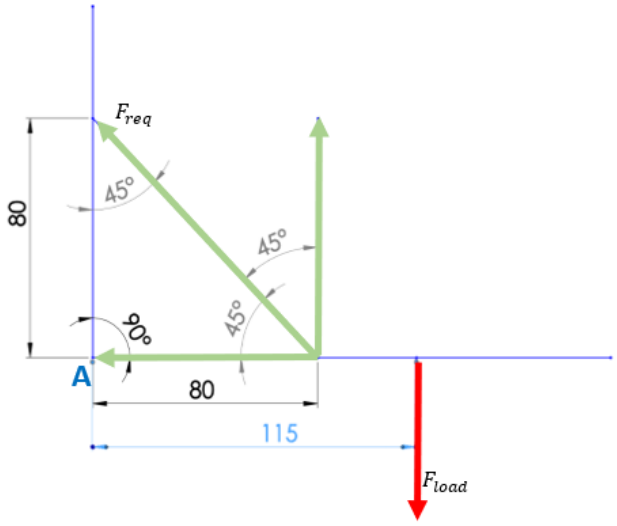

$$\sum M_A = 0$$

$$F_{req} * \cos(45°) * 80 - F_{load} * 115 = 0$$

$$F_{load} = 1kg * 9.81\frac{m}{s^2} = 9.81N$$

$$F_{req} = 19.9N \text{ or } 2kg$$

Figure 46:Force required to lift load at center of mass at a 90 degree angle.

4.1.3.3.1.1.2 Load cell calibration

The load cell used is a standard 10kg load cell bought from sparkfun. The load cell consists of a piece of Aluminum and 4 strain gauges connected in a Wheatstone bridge configuration. When a load is applied, the strain gauges change resistance and thus the voltage output of the Wheatstone bridge changes. These changes however are so small they can't be picked up by the microcontroller directly. To overcome this problem, an amplifier board (HX711) was used. The last step is to calibrate the load cell. To do this, a known weight needs to be applied on the load cell. The corresponding raw data output is then noted down, Table 16. When these steps are repeated for different weights, a calibration curve can be made, Figure 47. This curve relates the raw output with the actual load. The

spec sheet of the HX711 states the output should be linear, thus a linear trendline was fitted to the curve. The slope of the trendline is called the calibration factor. The calibration factor was then used in the Arduino code to relate the raw output to the applied load.

Table 16: Load cell raw data to load (kg).

Raw Data	Actual Load (kg)
-74190.9	0
-31589.9	0.2
238037.2	1.4653
382747.6	2.14525
476487.3	2.58405
565303.9	2.99985
624559.1	3.2776
715086.3	3.702
833859.7	4.2595

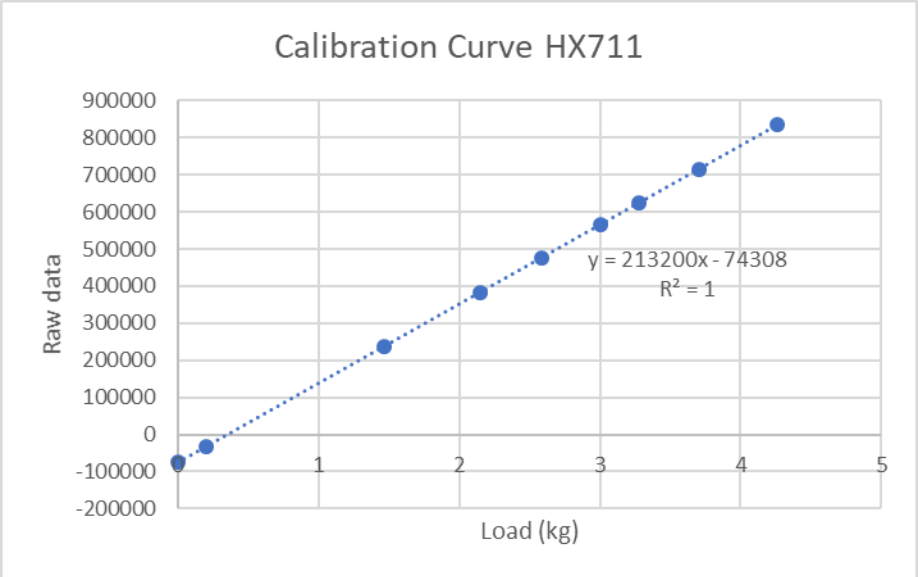

Figure 47: Load cell calibration curve and calibration factor.

4.1.3.3.1.1.2 Load cell data

The data collected from the load cell was load (kg) and the position of the bottom edge of the actuators. The load cell data was multiplied by the acceleration due to gravity,

9.81 m/s^2 to get the resulting force in N. This force was graphed against the position data for the tests with and without the stopper.

For the case of the test without the stopper for extensional strain of 1.5, the position data was separated and added to the results of the repeatability test.

4.3 Results

4.3.1 Benchmark test results: Setting parameters for maximum weight, actuation and cooling time, and current

Since the power supply was not able to provide the actuators with the desired current of 0.9 Amps for extensional strain of 1.5, the actual current measured was recorded in parenthesis in Table 17. The same is true for the values for extensional strain for extensional strain of 3. The actuators were unable to reach an extensional strain of 3 with the weights or with trying to extend the springs.

Testing stopped for extensional strain of 1.5 and 3 when the systems began to smoke. The weights tested were 500g 700g, 1kg, and 1.2kg. As the benchmark test was done visually using a stopwatch, there is no additional raw data besides what is shown in Table 17. The results showed that for the extensional strain of 1.5, the max weight the SMA system could lift was 1.5 kg at 0.8A, as at the higher current the current and mass the actuators began to smoke. The result for the extensional strain of 3 showed the maximum weight that could be lifted was 1 kg at 0.8A as similarly the actuators began to smoke. The Servo was able to lift the 2 kg weight.

*Table 17: Rig actuation testing for extensional strain of 1.5 and 3. Table depicts the measured current, max voltage, time to complexly actuate the elbow, and cooling time with and without a fan for each weight. * Denotes actuator did not reach desired extensional strain.*

Extensional strain	Current (A)	Voltage (V)	Time to actuate (s)	Time cool fan (s)	Time cool no fan (s)	Weight

1.5	0.8	23.3	9.64		50.2	500g
1.5	0.8	23.3	9.9	20		500g
1.5	.9(.86)	25	9		48.23	500g
1.5	.9(.86)	25	9.5	21.24		500g
1.5	0.8	23.3	9.96		46.5	700g
1.5	0.8	23.3	10.53	19.6		700g
1.5	.9(.84)	25	9.5		47.32	700g
1.5	.9(.85)	25	10.15	19.74		700g
1.5	0.8	23.3	10.81		41.23	1kg
1.5	0.8	23.3	11.37	16.09		1kg
1.5	.9(0.85)	25	9.22		46.62	1kg
1.5	.9(.86)	25	10.27	19.08		1kg
1.5	0.8	23.23	12.44		35.81	1.2kg
1.5	0.8	23.23	12.76	10.26		1.2kg
1.5	.9(.86)	25	10.75		32.88	1.2kg
1.5	.9(.864)	25	10.85	9.81		1.2kg
1.5	0.8	23.12	20.98		26.44	1.5kg
1.5	0.8	23.15	23.97	8.38		1.5kg
1.5	.9(.86)	25	30		Not measured	1.5kg
3(1.2) *	0.8	11.2	8		15.5 *	500g
3(1.2) *	0.8	11.2	8.2	12*		500g
3(1.4) *	0.9	12.8	8		20.15 *	500g
3(1.4) *	0.9	12.7	7	14.2*		500g
3(1.6) *	0.8	11	8.36		15.65*	700g
3(1.5) *	0.8	11.2	9.35	11.12*		700g
3(1.5) *	0.9	12.7	9.6		18.2*	700g
3(1.6) *	0.9	12.7	10	11.5*		700g
3 (2.36) *	0.8	11	16	13 *		1Kg
3 (2.06) *	0.8	11	10		Not recorded because began to smoke	1Kg
Servo	.6	6	2	-	-	500 g
Servo	.6	6	2	-	-	500g
Servo	.65	6	2	-	-	700 g
Servo	.65	6	2	-	-	700 g
Servo	.7	6	2	-	-	1 kg
Servo	.7	6	2	-	-	1 kg
Servo	.7	6	2	-	-	1.2 kg
Servo	.7	6	2	-	-	1.2 kg
Servo	.7	6	2	-	-	1.5 kg
Servo	.7	6	2	-	-	1.5 kg
Servo	.75	6	2	-	-	2 kg
Servo	.75	6	2	-	-	2 kg

4.3.1.1 Efficiency of the two SMA rigs and the servo motor rig

The maximum voltage, current, and time for actuation of 1kg from Table 17 can be found in Table 18 below with the resulting energy in Joules.

Table 18: Data collected during efficiency testing.

Actuator	Voltage (V)	Current (A)	Time (s)	Energy (J)
SMA ε=3 (short)	11 V	0.8A	13s	114.4
SMA ε=1.5 (long)	23.3 V	0.8A	11s	205.04
Servo	6 V	0.7A	2s	8.4

The efficiency for all the actuators is shown in Table 19.

*Table 19: Efficiency comparison of tested actuators. * During actual testing the short SMA was not able to actuate the full 15.5cm. However, for simplicity for the calculations, the actuated distance is kept the same. Since the actuation was shorter, the actual efficiency is also lower for the short springs*

Actuator	Energy (J)	Potential Energy E_{pot}	Efficiency (%) $\eta = \frac{E_{pot}}{E} * 100$
SMA ε= 3 (short)	114.4	1.07	0.93%*
SMA ε= 1.5 (long)	205.04	1.07	0.52%
Electric servo	8.4	1.07	12.74%

4.3.2 Repeatability testing for determining potential drift in 0.381 mm diameter wire spring

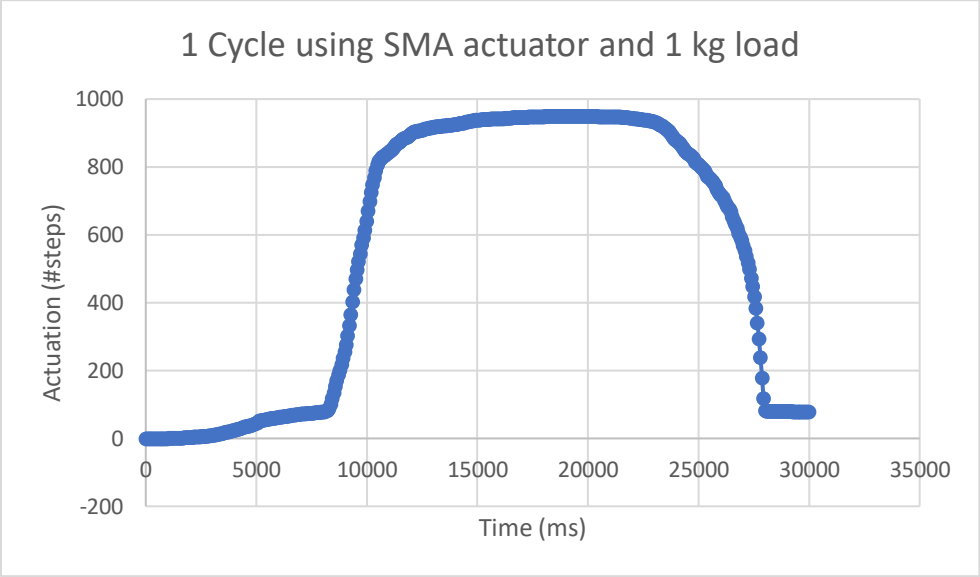

Figure 48: Graph of the path of actuation over time for extensional strain of 1.5 lifting 1kg at 0.8A. Power was supplied for 22 seconds and then cooled with a fan.

This graph shows what a cycle with an SMA actuator with ε =1.5 looks like. These data were recorded during the first few cycles when establishing the power on and off times for the repeatability test. At time 0, the power is turned on, and current starts flowing through the actuator. Although the actuator starts producing force soon after the power is turned on, as shown in the characterization test, it takes approximately 3 seconds until this current has finally heated up the Nitinol springs enough to produce forces necessary to actuate and start lifting the weight. However, it is not until approximately 8 seconds after turning on the power supply that the actuators experience a steep increase in rate of actuation over time. After this point, the actual actuation takes about 3 seconds until full compression is reached. This differs from the static Instron test since in the Instron characterization there was no applied mass and what was being observed was pure force and not actuation distance. At 11 seconds the actuator reached the fully compressed

position, the power to the SMA was turned off, and the SMA actuator starts cooling down. A fan blows extra air over the actuator to increase the cooling rate. It takes 12 seconds for the actuator to cool down enough so that it can stretch out again to the original state. One cycle takes almost 30 seconds on average. This is considering an extra cooling fan to cool down the actuator faster when the power is turned off.

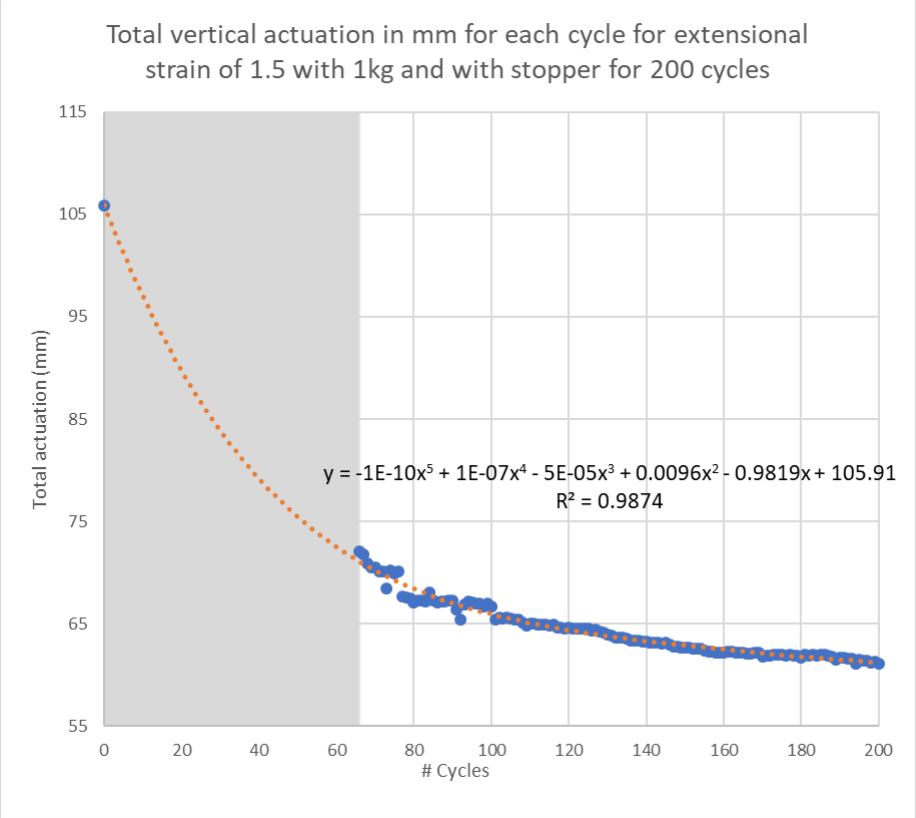

Figure 49:Graph depicting total actuation per cycle with a stopper for extensional strain of 1.5.

During testing of the 1.5 extensional strain system with a stopper, the first 66 cycles of testing did not log properly, and all values came back as 0. A trend line was created, and an equation found to plot an approximation of the lost data, Figure 49. The graph shows the total actuation, the difference between the fully extended and fully compressed, per cycle. The trendline tracks the starting value as 106mm of actuation which is close to the

actual known starting value of 99.9 mm. The data point at the starting point of this graph was placed to highlight the value of 106 mm total actuation approximated from the trendline.

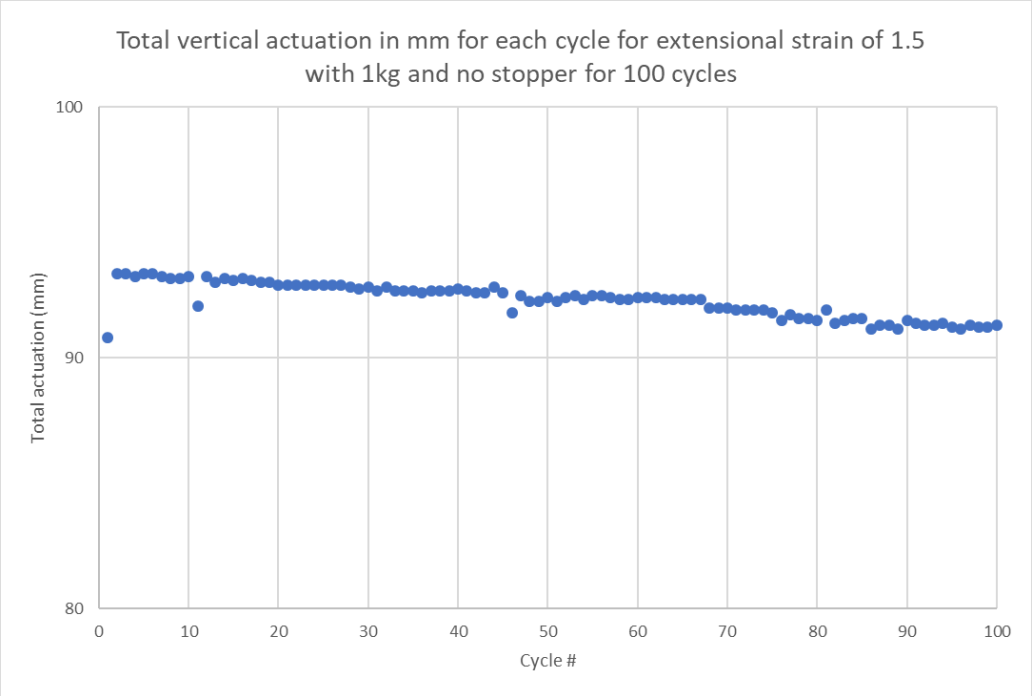

Figure 50: Graph depicting total actuation per cycle without a stopper for extensional strain of 1.5.

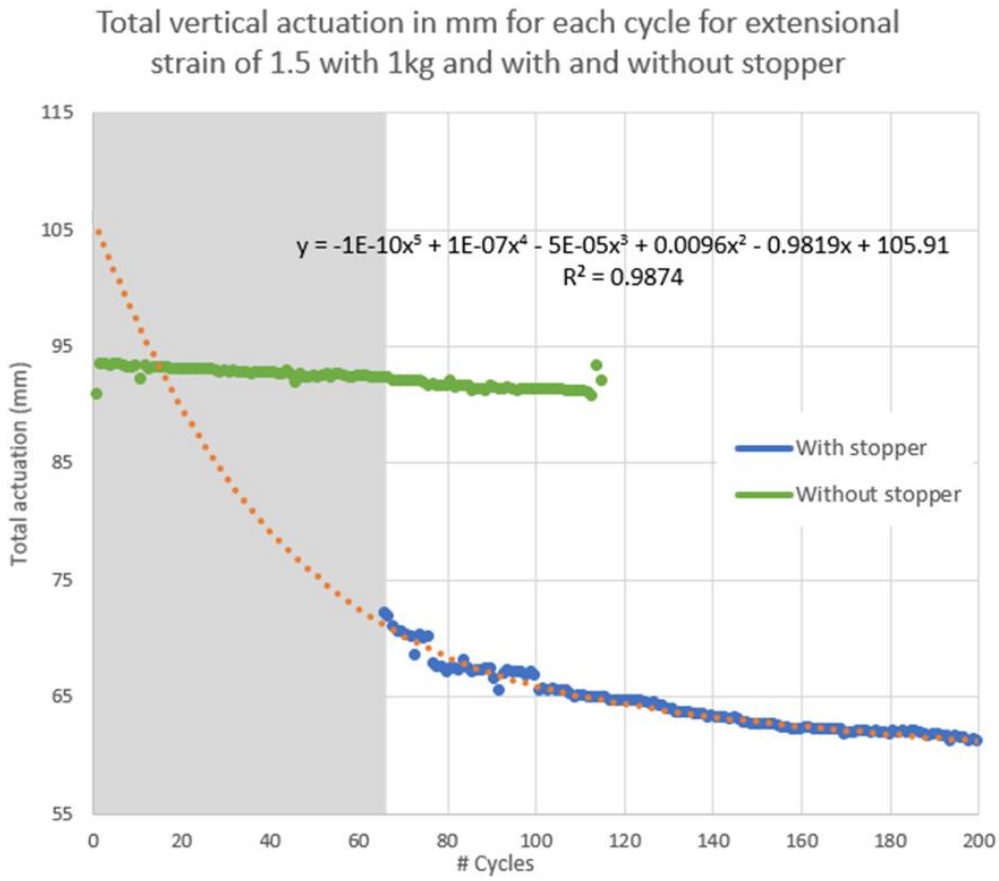

Figure 51: Graph of total actuation per cycle for 1.5 extensional strain system with and without a stopper.

The graph shown in Figure 51 shows the difference between total actuation with and without a stopper.

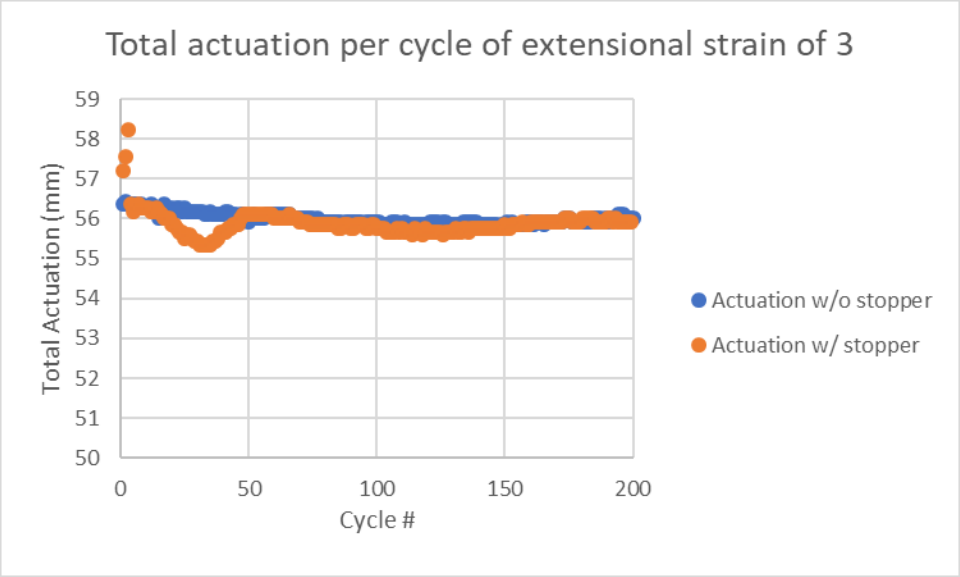

Figure 52: Total actuation per cycle of extensional strain of 3 with and without a stopper.

Similarly, the comparison of total actuation per cycle of extensional strain of 3 actuators was made between the cycle test with and without the stopper, Figure 52.

Actual drift was reported in Table 20 below. This table shows the starting and ending extensional strains, compressed length (free length), and total extended length for extensional strain of 1.5 and 3* with and without a stopper. Additionally, the difference between the corresponding stopper and no stopper conditions were represented.

Table 20: Start and end conditions of actuator systems.

Variable	Extensional strain 1.5 With stopper	Extensional strain 1.5 Without stopper	Diff. Stopper No Stopper	Extensional strain 3 With stopper	Extensional strain 3 Without stopper	Diff. Stopper No Stopper
Extensional Strain Start	1.50	0.917247	-0.59	1.71	1.33	-0.38
Extensional Strain Finish	0.61	0.869769	0.26	1.32	1.27	-0.05
Drift in Extensional Strain	-0.89	-0.047478	-	-0.39	-0.06	-
Compressed Length start	66.6 mm	101.76 mm	35.16 mm	33.3 mm	42.48 mm	9.18 mm

Compressed length final	107.94 mm	104.64 mm	-3.3 mm	42.48mm	44.10 mm	1.62 mm
Drift in Compressed Length	41.34 mm	2.88 mm	-	9.18	1.62	-
Total Extended Length Start	166.6 mm	195.44 mm	28.94	90.50 mm	98.84 mm	8.34
Total Extended Length final	166.6 mm	195.44 mm	28.94	98.41mm	100.03mm	1.62
Drift in Total Extended Length	0.00 mm	0.00mm	-	7.91 mm	1.19 mm	-

4.3.3 Load testing

The resulting data were graphed to display force vs. linear displacement.

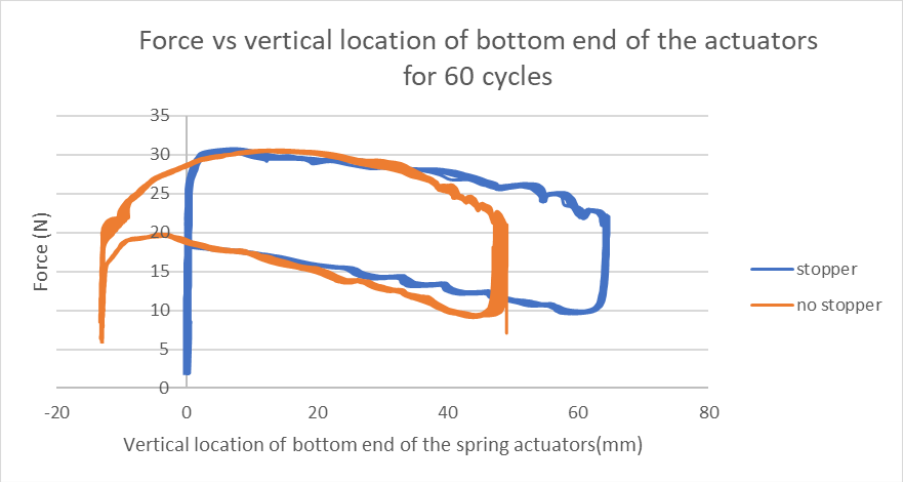

Figure 53: Graph depicting force vs vertical location of the bottom end of the actuators, with and without a stopper for extensional strain of 1.5. All 60 cycles for each test were plotted on top of each other.

This graph shows how the cycle of the actuator and the forces required. At time 0 there is no actuation and almost no force. The force in the actuator needs to rise to almost 30N (3 kg) before the actuator can lift the 1 kg load. The force needed in the beginning (at the biggest angle) will always be the greatest. It moves upwards until the max actuation of

65mm is reached. While doing this, the angle decreases, and so does the force required to lift the 1 kg weight. There the power is turned off, and the actuator starts to cool. This means that the force of the actuator starts dropping until about 1 kg is reached. At that point, the load is bigger than the force of the actuator and the arm moves back down until it reached its starting point.

The test was repeated with extensional strain of 3.

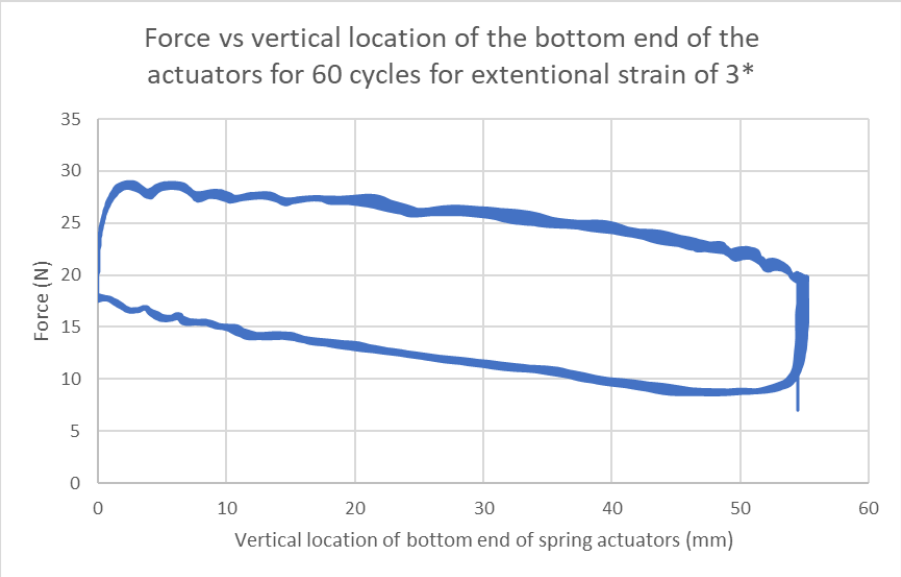

Figure 54: Graph depicting force vs vertical location of the bottom end of the SMA actuators for extensional strain of 3. All 60 cycles for each test were plotted on top of each other. *Although extensional strain of 3 was desired, it was not achieved.*

4.4 Discussion

4.4.1 Benchmark test: Setting parameters for maximum weight, actuation and cooling time, and current

The maximum load that the extensional strain of 1.5 system, 6.66 cm compressed, was able to lift was 1.5 kg at 0.8 Amps. Although the system was able to lift this weight, the system was not able to actuate completely and began to smoke. Smoking also occurred when the system attempted to lift 1.2 kg with an input of 0.86 Amps. These issues led to

the rest of the testing being completed using a 1 kg weight. Even though the weight used was less than half the weight of a female's arm, with system 1, the 1 kg weight was enough to stretch the actuators to the desired elongation.

Although 0.9 Amps was attempted, the voltage of the power supply used maxed out with an input of 0.85-0.86 Amps. The reason that the current maxed out was that the maximum voltage the power supply could provide is 25VDC. With the higher resistance of all of the actuators in series, the maximum current was 0.86 Amps. Even though the system was current driven, since it could not reach the set current, the current drifted as the actuators were compressed and the resistance of the actuators changed.

Looking at power consumption, the servo actuator used less power, only using a peak of 4.5 Watts. This is less that the power consumed in both of the SMA rigs. The SMA with extensional strain of 1.5 used a peak of 18.64 Watts at 0.8A and 21.5 Watts at 0.9 (0.86)A. The extensional strain of 3 actuators used a peak of 8.96 Watts at 0.8A and 11.52 Watts at 0.9A. The applied load had an impact on the measured current, however this impact was relatively small. For example, the total current used to actuate the servo with a 1 kg attached weight was only 0.05 A less than the current measured for the 2 kg testing condition. This means that for a 100% increase in load, there is only a 7% increase in current and thus power. This indicates that the servo system will get more efficient at higher loads.

The peak power consumption was used for safety and reliability reasons. The system will need to be designed to handle the worst-case power consumption while still staying safe and reliable (i.e. batteries need to be able to supply enough current for the worst case). Using the data in Table 9, for a bigger diameter spring at 0.8A there is about

a 25% resistance decrease as the SMA's temperature goes up. When the resistance decreases about 25%, so does the voltage (ohms law). Therefore following Equation 13 to Equation 15, it is clear that the power consumption and efficiency also change by 25%. Peak power is always observed in the beginning when the SMAs are heating up.

Additionally, the servo was able to lift more weight than SMA systems. The Servo lifted 2 kg, the 1.5 extensional strain SMA lifted 1.5kg, and the extensional strain 3.0 SMA lifted 1kg.

Time for actuation and cooling was taken for each test using a stopwatch. Full actuation was defined as the point at which the angle between the forearm and upper arm of the rig reached 30 °. In cases where the actuator did not actuate all the way, actuation was considered complete 2 seconds after the actuator stopped moving. The 2 seconds were added to encompass small, non-visible, movements. Table 17 shows the results from this test. Further analysis of these results shows that the time for actuation increases per cycle and added weight. For example, for the extensional strain of 1.5 and 1kg load, the time to actuate was 10.81 seconds and the following cycle with the same conditions took 11.37 seconds. This is as expected as an increase in applied weight requires higher forces to be generated by the SMAs and therefore longer waiting time for the actuators to be able to produce the force. Furthermore, pushing the SMA material to the material's limits through phenomena such as overheating, overstretching, and fatiguing; will further worsen the cycle time. Additionally, the tests at or around 0.9A actuated faster than the 0.8A tests. Higher currents lead to an increase temperature in the actuators and therefore, they generate

a given force faster than a lower current. As decay stabilized during the repeatability test, the time to actuate also stabilized.

Where actuation time increased with every cycle, cooling time decreased. One explanation is that the applied load is increasing every cycle, therefore the force due to gravity increases and extends the spring quicker. Overall, cooling of the actuators takes a long time. For 1 kg at extensional strain of 1.5, it took 41.23 seconds for the actuators to extend to the starting position without a fan, and 16.09 seconds with a fan.

4.4.1.1 Efficiency of the two SMA rigs and the servo motor rig

The efficiency of the 6.66 cm actuators of system 1 (extensional strain of 1.5) is 0.52%. As stated in the previous section, this is the worst-case efficiency. In the best case it is about 25% higher or 0.65%. Without knowing the actual efficiency of system 2 (extensional strain of 3*), since it did not complete actuation, the efficiency of the two SMA systems cannot be compared. The energy required for the SMA actuator is over an order of magnitude bigger than that for a motor and cable system. Further testing would have to be done as the limitations of my study might have influenced the results.

The low efficiency of the SMA actuators is due to the loss of energy in the form of heat and the relatively higher power requirements, this is a known setback of SMAs. As expected [11] [52], the efficiency of the servo system, is greater than that of either SMA system and has an efficiency of 12.74%.

Different alloys might have improved efficiencies and should be investigated. If the time for heating the actuators decreases and is not included in the efficiency calculations, the efficiency would increase. Assuming the actuators have the same power consumption as the ones discussed in this thesis, but only take 3 seconds to actuate (from 13 seconds for the extensional strain of 3* and 11 seconds for extensional strain of 1.5), the efficiency

would increase by approximately a factor of 4. This means the efficiency of the extensional strain of 3* would go from 0. 93% to 4.03%. The extensional strain of 1.5 actuators would go from 0.52% to 1.9%. SMA's with a lower power consumption might be able to greater increase the efficiency.

4.4.2 Repeatability testing for determining potential drift in 0.381 mm diameter wire spring

For extensional strain of 1.5 with the stopper, the repeatability test shows that the total amount of actuation decreases significantly with the number of actuated cycles. The decay in the first 100 cycles occurred at a higher rate, showing approximately 11 mm of reduced actuation. Although the data for the first 66 cycles were not collected, a trend line following the path of the data reaches approximately the same starting total actuation length that was recorded before testing began. The starting position concluded from the trendline is 106 mm of actuation which is off from the starting 99.9 mm. This variation is due to the fact that the real data does not have perfectly follow a curve, however, the approximation is sufficient to depict the lost data.

Once the stopper was removed, the actuators were also allowed to drift in the direction of extension. The total drift in extended length between the stopper and no stopper conditions for extensional strain of 1.5 is 39 mm. Compressed length is 41.16 mm, and the drift in extensional strain is +0.9. The results show that there is a difference in terms of drift between a system with and without a stopper.

In the case of extensional strain, the starting extentional strain of no stopper system is greater than the final extensional strain of the stopper system because without the stopper, the actuator is able to stretch out further, and as it still returns to the same compressed length, the total stroke, and therefore the extentional strain is greater. Other

studies have found similar decay with SMA actuators, and this is still an area of active research [60].

Looking at the graph for the total stroke of the extensional strain of 3 system with and without the stopper, it appears that there is nearly no drift since even in the case with the stopper, the actuators don't extend far enough to reach it. However, taking a close look at Table 20, the difference in extensional strain, compressed length and extended length shows the drift. Additional information was taken from the position data results and actual extensional strains were found. For the extensional strain of 3 system, the actual starting extensional strain was 1.71. Due to the large decay in compression (9.18 mm total) and extension (10.5 mm total),the extensional strain at the end of testing was 1.37, showing a decay of 0.44 extensional strain.

Based on the results, the extensional strain does change during each cycle. Since the extensional strain of 3 system never reaches an extensional strain of 3, only reaching a maximum of 1.71, there is nearly no difference between the results from test with the stopper and without. On the other hand, the results of the testing for 1.5 extentional strain system shows a greater difference between the stopper and no stopper tests.

4.4.3 Load testing

This test was only 60 cycles. By the time this testing began, the actuator sets were already starting to stabilize, and the drift in total actuation was less as is shown in the graphs depicted in Figure 53 and Figure 54. During this test, the location data was recorded. Since the max and min positions for each test remain almost the same (overlapping data points), it means that there is little, if any drift in actuation. There is also little drift in the force produced by the actuators. The total drift in force for a given position is less than 0.5 N. In Figure 54, the point outside of the normal path might be noise.

The system with extensional strain of 1.5 generated greater forces than the system of extensional strain of 3. This is mostly due to the fact that the extensional strain of 3 actuators were unable to reach the desired extensional strain and thus could not extend beyond 90 degrees. Besides the end range of the actuation, the remainder of the forces per position are very similar for the two different extensional strains. This makes sense as the force being measured is just what the actuator has to supply to lift the arm, it does not measure the maximum capability of the actuators.

There is an additional difference between the extensional strain of 1.5 and extensional strain of 3 systems. This is that the extensional strain of 1.5 experiences a period of 0 kg loads every cycle. This is because both with and without the stopper, the weight was always supported when the actuator is fully extended as opposed to the 3.0 extensional strain system where the system never made it to the stopper or the table.

When it comes to the analysis of the load data with and without the stopper, the data for the extensional strain of 3 system is the same with and without the stopper. Since the system does not achieve the extensional strain of 3, it does not reach the stopper. I chose not to repeat the test since there is no true stopper condition and the tests would therefore be the same. As for the system with extensional strain of 1.5, the load becomes the same, but they differ in the amount of total actuation and position at which max force is observed. When the system without the stopper was extended, the weight would rest on the ground and with the stopper, when the system hit the stopper. Additionally, the reasoning behind why the actuator reaches peak force after a greater amount of actuation is because the load cell does not start detecting the load until the weight is no longer being supported on the ground. For the stopper case, it is at approximately .5cm. For the case with no stopper, the

weight rests on the ground and there was slack in the string attaching the weight to the arm. As the springs began to actuate, the arm bent, resulting in a non-zero load recorded by the load cell at approximately .5 cm, however, maximum load occurred closer to a net of 3.5 cm, the approximate length of the string attaching the weight to the center of mass of the rig.

The same difference in total actuation between the stopper and no stopper cases is observed for extensional strain 1.5 as with the repeatability test.

The load applied by the actuators was very consistent over the 60 cycles tested, differing only by approximately 0.1 kg over all cycles for all extensional stains and setups. Even though the amount of actuation drifted, the experienced load remained the same. Again, this is because the load is based on the mass of the arm, the position, and the force due to gravity at each position. The drift in position was also less than in the repeatability test as the actuators began to stabilize. The total amount of reduced stroke was 1.7 mm for the 1.5 extensional strain with a stopper, and 3 mm without a stopper. For both the cases with and without the stopper for extensional strain of 3, the drift was 0.75 mm

The results from the load cell are comparable to the theoretical calculations. The theoretical value was 24.4 N; however, the recorded data showed a max of approximately 30.4 N. There are a couple of reasons why there is a higher force (over 30 N) from our experiment. In the calculation the effect of the weight of the wood is not taken into account. Also, the friction between the Kevlar cable and O ring had been neglected in the calculations. The linear encoder is a contactless sensor. The sensor moves over the encoder strip without touching it. This means there is no friction or energy loss due to the sensor.

As with the actuation cycle testing, testing on the forces should be further studied to determine the limitations of the materials.

4.4.4 Space needed to fit the actuators

Although size, and thus space to mount actuators, is a drawback of female arms, a benefit of the lighter arm of a female is that the actuators are not required to generate as much force to accomplish elbow bend as would be required for males, and thus, not as many SMA actuators would be needed.

As set forth in Table 2, the space available to mount actuators in a female upper arm is approximately 4.43 – 5.25 cm (2.5 in) in females. Thus, the space available in the female upper arm is approximately 0.77 to 1.66 cm less than the space available in the male upper arm. Some space should be left between the edge of the arm and the placement of the actuator. Spacing is desired to prevent the actuators from shorting during actuation and assist with heat dissipation. According to a paper by De Laurentis et al. on the optimal design of SMA actuator bundles, the spacing between the actuators should be approximately 3 times the outer diameter of the actuator to provide sufficient spacing for airflow and heat dissipation [71]. The outer diameter of the 0.381 mm wire spring is 1.52 mm, requiring a spacing of approximately 4.56 mm between the springs. This number was rounded to 5.0 mm between the actuators.

The spring for the 0.012 in (.31 mm) diameter wire has a diameter of 1.24 mm and the spring for the 0.015 in (.381 mm) diameter wire is 1.52 mm. This fact creates a number of critical design issues that require considering a number of trade-off. One possible elbow-flexion exoskeleton design would fit the most actuators possible to create the most force. In theory, it is possible to fit approximately 28 actuators of the 1.24 mm diameter springs and approximately 22 of the 1.52 mm spring. However, some spacing is needed between

actuators as discussed above. It should be noted that, although there is literature on spacing between SMAs in a bundle, there is no set standard in the literature for the optimal spacing of SMA actuators on a human body. Although bicep width chosen was for the average female population, the system would probably still work for the 5th percentile. Using the spacing from Laurentis et al. [71], the 5th percentile arm has a bicep width of 3.78 cm can fit the 6 actuators tested in the rig. However, if more actuators are needed to lift more mass, there will not be sufficient space to add more actuators with the 0.5 cm spacing.

In determining the number of SMA actuators too include in an elbow-flexion exoskeleton, is necessary to consider a number of factors various tradeoffs. One factor is power. As the number of actuators increase, so does the power needed to run the exoskeleton. SMA actuators are known to be "power hungry" [72]. Another factor is cooling ability and the potential for overheating. These were specific concerns for the SMA alloy used in this study. As the number of actuators increase, so does the amount of heat generate by the system. Overheating is also more likely when there is little or no separation between SMA actuators. This is because separating the actuators helps increase the rate of cooling and thus reduces the likelihood of overheating. Overheating can create safety issues in wearable devices. This problem is made worse when the user has a medical disability. Overheating and safety concerns is something that SMA researchers testing on human subjects take into account. For example, Yarosh et al. describe the testing of SMA squeeze bands in which bands had to be temporarily deactivated twice due to overheating when the user's hand overlapped, and the bands were activated for a period of more than three minutes. This overheating only occurred with a couple of subjects under a very specific content [73]. Overheating can be mitigated with the assistance of a control system such as

Pulse Width Modulation (PWM). Copaci et al. used a PWM system controlled by a bilinear proportional-integral-derivative controller (BPID) on the straight wire SMA. This type of controller is necessary due to the hysteresis of the material. Although this type of control system can be used, extra challenges can occur due to the more complex geometry (for example section 4.1.1.2.2 Series configuration of the SMA spring, where the difference between series and parallel configuration is explained).

Another factor is the potential shorting of the system. As one decreases the separation between SMA actuators one increases the likelihood that they will touch each other and short the system. Avoiding such a short is important when designing a medical exoskeleton to be used for rehabilitation where reliability and safety are important design factors. A solution would be to add insulation between the actuators, however, this would also add thickness and extra space between the actuators. The system still has to be insulated, but insulating the whole system is more space efficient than insulating each actuator. Another factor in choosing the numbers of actuators to include in an exoskeleton is the frequency of cycles. As one increases the separation between SMA actuators one increases the rate of cooling and thus increases the frequency of cycles. Finally, some separation between actuators is needed given that the attachment method requires space.

4.5 Limitations

There are a number of limitations to the practical design testing portion of this study. First, the rig used only one diameter wire which was set at one annealing temperature resulting in a high activation temperature, i.e. a 0.381 mm diameter wire spring annealed at 450 °C. Other alloys with lower activation temperatures were not considered. An SMA

with a lower activation temperature would require less power, thus holding everything else equal, it would improve the efficiency and it would also allow more actuators to fit in the elbow-flexion exoskeleton.

The second limitation is that only one test was run for each condition. Due to time and limited resources, each test was only able to be run once. Additionally, the repeatability and load tests with and without the stopper were conducted using the same set of actuators. This means that there are no other results to compare against and validate results.

The third limitation is the testing set up. The way the testing was conducted, there is room for noise and possible drift in the sensor. This is most noticeable when looking at the results and comparison of the extensional strain of 1.5 with and without the stopper. Along with the testing set up, human error in how the data was recorded might have influenced the results, more specifically with regards to the actuation time, cooling time, compressed length, and extended length. Error in these measurements could influence the resulting drift values as well as efficiency.

The fourth limitation is that an error occurred during testing and data for the first 66 cycles of the repeatability test for the extensional strain of 1.5 with a stopper was lost. A trendline had to be created to approximate the results. Although it is a good approximation, without these 66 cycles, the true behavior remains unknown.

The practical design testing aimed to study actuators with an extensional strain of 3. However, due to the small size and diameter of the springs, they were not able to stretch to that extensional strain. The highest extensional strain, that was able to be produced was 2.36, which was after I attempted to stretch it out using as much force as I could push on the rig.

The time for which the repeatability and load test cycles ran were controlled. Since the time needed for actuation changes with decay over cycles, controlling the time might not fully demonstrate the behavior. However, since the amount of total actuation is changing, the method for determining complete actuation during the benchmark testing, measuring the spring and stopping the time when it returned to the original compressed length, could not be used. It was decided to keep a consistent set cycle time to give enough time for actuation.

An additional limitation to the load test was that the rig was rebuild between the testing. Before the second repeatability test was done, the system was broken down to place the linear encoder on the rig with an extenstional strain of 3. Later the load cell was added to the system with an extensional strain of 3. After the testing for extensional strain of 3 was completed, the 1.5 extenstions strain system was rebuilt to finish the load and repeatability test. This might have influenced some of the results (one thing that could have happened was a slight relocation of the linear encoder). Without further testing, I am not aware of the extent (if any) of the impact.

4.6 Conclusion of practical design testing

This study focused on looking at the efficiency of, the load capabilities, drift/decay in the actuators, and generated forces of a set of SMA spring actuator assemblies. Although there are limitations to this study as noted in the section above, observations based on the data collected are useful in understanding SMA systems more generally. First, the maximum load that could be lifted with the system design evaluated here was 1 Kg. Additionally, when comparing the efficiency of the SMA system with extensional strain of 1.5 and an SMA system with extensional strain of 3* to a servo motor, the servo is most

efficient. The efficiencies of these systems are as follows: extensional strain of 1.5, 0.52 % efficiency; extensional strain of 3, 0.93% efficiency; and servo motor, 12.74. Further investigation must be done to determine methods of increasing efficiency. Efficiency would increase if the time needed to heat up and actuate decreases, since efficiency is time dependent. Another approach to improving efficiency is to decrease the amount of power used by the system. Some areas that could be investigated to accomplish these improvements in actuation time and power requirements are: different alloys and annealing temperature, which could lead to lower actuation temperature; larger wire diameters, which could be more power efficient and produce greater forces; and optimize the controls system, limiting the amount of time the current is being applied to the actuators.

The second part of this study focused on the repeatability of the actuators. Over the more than 400 cycles of testing, the SMA actuators showed drift in extensional strain, compressed length, and extended length. The greatest amount of drift occurred during the first 100 cycles, at which point the amount of decay began to decrease until it began to stabilize after about 160 cycles. Implications of this decay are that the actuators might need to be pre-fatigued before being cut and installed in the exoskeleton. Further investigation and testing should be done to characterize the springs behavior and the maximum force output after 160 cycles. Additionally, testing must be done to determine the life of the actuators, after how many cycles they must be changed.

Finally, from the load testing, it can be confirmed that the force produced by the actuators is equal and opposite to that produced by an applied mass at the center of mass. By the time these tests were conducted, the SMA actuators of both extensional strains had begun to stabilize and the drift was not as great as during previous tests. The force exerted

by the extensional strain of 1.5 actuators matches those of the extensional strain of 3 actuators as the load on the actuators (due to the mass of the arm) stays the same (ignoring minor differences in acceleration during the actuation stroke).

Chapter 5: Conclusion and future work

5.1 Overview

The purpose of this study was to characterize and evaluate SMA spring actuators for their use in a wearable elbow-flexion exoskeleton that can lift a female arm and assist in completing ADLs. The study makes two contributions. First it provides further characterization of the properties of SMA actuators. This is important given that we still do not have a full understanding of the complex non-linear relationships involved in SMA actuations, including the relationships between stress and the SMA's transformation temperature [52]. The second contribution is testing a practical rig to observe important metrics such as efficiency, repeatability, and load capabilities.

5.1.1 Characterization test

Results from the characterization test provided insight as to the relationship between extensional strain, applied current, and output force for two different diameter wires (0.31 mm wire and 0.381 mm wire). To cover a range of tested extensional strains and currents, 2 samples each of the selected wire diameters were tested at extensional strains of 0 to 2 and currents of 0.0-0.8. Due to fatigue from overstretching and overheating, the samples of the 0.31mm diameter wires began to expand when heated instead of compressing. As a result, the samples were adjusted which influenced the results and created the need to test a 3rd sample for this wire diameter. This sample was tested to lower extensional strains and current settings to reduce the memory loss effect.

5.1.2 Practical design test

The practical design test focused on observing the behavior of the spring actuators on a rig. The observations from this study are summarized here. First, the maximum load that could be lifted was 1 Kg. Additionally, when comparing the efficiency of the SMA system with extensional strain of 1.5 and an SMA system with extensional strain of 3* to servo motor, the servo is most efficient. The efficiencies of these systems are as follows: extensional strain of 1.5, 0.52 % efficiency; extensional strain of 3, 0.93% efficiency; and servo motor, 12.74. Further investigation must be done to determine methods of increasing efficiency. As far as the cycle testing, after the more than 400 cycles of testing, the SMA actuators showed drift in extensional strain, compressed length, and extended length. Determining the drift is important as SMAs exhibit exponential decay which should be studied to find ways of minimizing the decay.

An additional observation from the practical design test is that the force produced by the actuators is equal to that produced by an applied mass at the center of mass. Results showed that the extensional strain of 3 actuators and the extensional strain of 1.5 actuators experience the same forces as they are measuring the forces at the center of mass and that the actuators must produce to lift the arm.

5.2 Future work

5.2.1 Spring actuator considerations

5.2.1.1 Types of SMAs

If the spring configuration is to be used, further investigation into material properties and the effect of the annealing temperature, actuation temperature, and actuation time are necessary. This study only focused on one annealing temperature. Studies have

shown that the annealing temperature can impact the strength and forces of the SMA. In the future, I suggest that different materials and compositions also be investigated.

The actuators tested used springs with an extensional strain of 3 and were unable to flex the simulated joint beyond 90 degrees. Longer actuators may allow flex beyond 90 degrees. Finally, the system took approximately 1 minute for a full cycle (extend to heat, contract to cool, return to extend) without the use of a fan. With a fan, the cycle time went down to an average of 30 seconds for a full cycle. This is a very unnatural timing and would make the performance of tasks impractical. One way of improving the timing for actuation would be to use an SMA with a lower activation temperature. For cooling, a system with liquid nitrogen or more active cooling could be investigated.

Additionally, the straight wire configuration of the SMA might be a better route for exploration due to the higher potential forces. Alternative options using a cable driven system with small motors as replacements for SMA actuators should also be investigated.

5.2.1.2 Behavior

As a result of the complexity of SMAs, characterizing their behavior and isolating all influencing variables is difficult. For this reason, I believe that further investigation into the behavior and uses of SMA is necessary. One such area where further research should be done is the decay of the SMA memory and drift in the spring actuators. Due to the limitations of this study, more in-depth analysis of memory loss and drift were not done. Therefore, one option for further investigation would be to go beyond the 400 cycles tested and determine after how many cycles the actuators begin to stabilize, and how long they remain stabilized. This is important to ensure that the actuators are properly trained and that the actuators maintain a complete range of motion.

5.2.2 Elbow-flexion exoskeleton considerations

As of now, there is no universal set list of requirements that an upper-body exoskeleton must meet as set by the FDA or another organization. Without known requirements, there is no given metric as to the minimum torque needed for each joint, how many degrees of freedom the exoskeleton should aid with, weight requirements, and other such factors that need to be considered. A review by Veale and Xie on wearable robotic orthosis, identified the main user requirements are cost, ease of maintenance, operability, effectiveness, durability, physical comfort, portability, reliability, and safety [11]. Although these requirements are not considered in this study, knowledge of these requirements is important for any future work and for understanding. While addressing user requirements will be important in building an actual wearable elbow flexion exoskeleton, they are beyond the scope of this study.

Additionally, there is a need for further investigation into anchoring and control systems which were beyond the scope of this thesis. The placement of the anchoring points is important as is the method for distributing loads. One option might be to route cables through a garment that would terminate and be affixed to a belt at the waist. A program could be developed for the controls, that uses a closed-loop system with feedback to control the position of the actuators.

5.3 Conclusion

In conclusion, while SMAs have proven to have some amazing characteristics (many of which were replicated in this thesis), in the end the SMA configuration tested in this thesis was not successfully implemented as an effective elbow flexion exoskeleton. In particular the power required for actuation was too high and the cycling time was too low, and the forces created were too limited to lift the female arm. A decay in the actuation

stroke was observed over time. Changes to the design of the elbow-flexion exoskeleton for a female must be made to facilitate effective actuation. There are many different ways of configuring SMAs including changing the alloy composition, the annealing temperature or the physical shape (spring vs straight wire), all of which can change the properties of the SMAs dramatically.

Results from this study can be used towards future investigations and characterizations of SMA for their application in elbow-flexion exoskeletons. Although the rig built was unable to lift an adult female's arm, power and material limitations may have influenced results. Changing the SMA alloy, number of actuators, and power supply might provide different results. In the future, more lower temperature actuators should be tested and characterize.

Bibliography

[1] H. Herr, “Exoskeletons and orthoses: classification, design challenges and future directions,” *J. Neuroeng. Rehabil.*, vol. 6, no. 1, p. 21, Jun. 2009.

[2] S. Crowe, “Wearable Robots Hope to Improve Minimally Invasive Surgery - Robotics Business Review,” *Robotics Business Review*, 2017. [Online]. Available: https://www.roboticsbusinessreview.com/rbr/wearable_robots_hope_to_improve_minimally_invasive_surgery/.

[3] C.-J. Yang, J.-F. Zhang, Y. Chen, Y.-M. Dong, and Y. Zhang, “A review of exoskeleton-type systems and their key technologies,” *Proc. Inst. Mech. Eng. Part C J. Mech. Eng. Sci.*, vol. 222, no. 8, pp. 1599–1612, Aug. 2008.

[4] J. M. Wiener and R. J. Hanley, “Measuring the Activities of Daily Living: Comparisons Across National Surveys | ASPE,” *U.S. Department of Health and Human Services*, 1990. [Online]. Available: https://aspe.hhs.gov/basic-report/measuring-activities-daily-living-comparisons-across-national-surveys.

[5] D. H. Gates, L. S. Walters, J. Cowley, J. M. Wilken, and L. Resnik, “Range of Motion Requirements for Upper-Limb Activities of Daily Living.,” *Am. J. Occup. Ther.*, vol. 70, no. 1, pp. 7001350010p1-7001350010p10, 2016.

[6] R. E. Petrea, A. S. Beiser, S. Seshadri, M. Kelly-Hayes, C. S. Kase, and P. A. Wolf, “Gender differences in stroke incidence and poststroke disability in the Framingham heart study.,” *Stroke*, vol. 40, no. 4, pp. 1032–7, Apr. 2009.

[7] R. J. Nudo, “Recovery after brain injury: mechanisms and principles.,” *Front. Hum. Neurosci.*, vol. 7, p. 887, Dec. 2013.

[8] N. Yozbatiran *et al.*, “Robotic training and clinical assessment of upper extremity

movements after spinal cord injury: A single case report," *J. Rehabil. Med.*, vol. 44, no. 2, pp. 186–188, 2012.

[9] M. H. Rahman, M. Saad, J. P. Kenne, and P. S. Archambault, "Exoskeleton robot for rehabilitation of elbow and forearm movements," in *18th Mediterranean Conference on Control and Automation, MED'10*, 2010, pp. 1567–1572.

[10] H. F. Harbo, R. Gold, and M. Tintoré, "Sex and gender issues in multiple sclerosis.," *Ther. Adv. Neurol. Disord.*, vol. 6, no. 4, pp. 237–48, Jul. 2013.

[11] A. J. Veale and S. Q. Xie, "Towards compliant and wearable robotic orthoses: A review of current and emerging actuator technologies," *Med. Eng. Phys.*, vol. 38, pp. 317–325, 2016.

[12] J. C. Duvall, N. Schleif, L. E. Dunne, and B. Holschuh, "Dynamic Compression Garments for Sensory Processing Disorder Treatment Using Integrated Active Materials," *J. Med. Device.*, 2019.

[13] R. A. R. C. Gopura, D. S. V. Bandara, K. Kiguchi, and G. K. I. Mann, "Developments in hardware systems of active upper-limb exoskeleton robots: A review," *Rob. Auton. Syst.*, vol. 75, pp. 203–220, Jan. 2016.

[14] C. C. Norkin, D. J. White, and R2 Library (Online service), *Measurement of joint motion : a guide to goniometry*. .

[15] M. Schünke, E. Schulte, U. Schumacher, L. M. Ross, and E. D. Lamperti, *Thieme atlas of anatomy. General anatomy and musculoskeletal system*. Stuttgart ; New York: Thieme, 2006.

[16] R. L. Brookham, E. E. Middlebrook, T. Grewal, and C. R. Dickerson, "The utility of an empirically derived co-activation ratio for muscle force prediction through

optimization," *J. Biomech.*, vol. 44, no. 8, pp. 1582–1587, May 2011.

[17] R. L. Huston, *Principles of biomechanics*. CRC Press, 2009.

[18] C. C. Gordon *et al.*, "Anthropometric Survey of U.S. Army Personnel: Summary Statistics, Interim Report for 1988." 1989.

[19] I. Dianat, J. Molenbroek, and H. I. Castellucci, "A review of the methodology and applications of anthropometry in ergonomics and product design," *Ergonomics*, vol. 61, no. 12. Taylor and Francis Ltd., pp. 1696–1720, 02-Dec-2018.

[20] M. R. Grosso, R. D. Quach, E. Otani, and J. H. Zhao Susanna Wei Pei-Hwa Jiahe Lu Norman I Badler, "ANTHROPOMETRY F OR COMPUTER GRAPHICS HUMAN FIGURES."

[21] N. Jarrassé and G. Morel, "On the Kinematic Design of Exoskeletons and Their Fixations with a Human Member."

[22] R. L. Smith, J. Lobo-Prat, H. van der Kooij, and A. H. A. Stienen, "Design of a perfect balance system for active upper-extremity exoskeletons," in *2013 IEEE 13th International Conference on Rehabilitation Robotics (ICORR)*, 2013, vol. 2013, pp. 1–6.

[23] T.-M. Wu and D.-Z. Chen, "Biomechanical study of upper-limb exoskeleton for resistance training with three-dimensional motion analysis system," *J. Rehabil. Res. & Dev.*, vol. 51, no. 1, pp. 111–127, Jan. 2014.

[24] P. de Leva, "Adjustments to Zatsiorsky-Seluyanov's segment inertia parameters," *J. Biomech.*, vol. 29, no. 9, pp. 1223–1230, Sep. 1996.

[25] OpenStax College, *Forces and Torques in Muscles and Joints - College Physics - OpenStax CNX*. 2014.

[26] B. van Ninhuijs, L. A. van der Heide, J. W. Jansen, B. L. J. Gysen, D. J. van der Pijl, and E. A. Lomonova, "Overview of Actuated Arm Support Systems and Their Applications," *Actuators*, vol. 2, no. 4, pp. 86–110, Oct. 2013.

[27] V. Power *et al.*, "Exploring User Requirements for a Lower Body Soft Exoskeleton to Assist Mobility."

[28] C. Pylatiuk, A. Kargov, I. Gaiser, T. Werner, S. Schulz, and G. Bretthauer, "Design of a flexible fluidic actuation system for a hybrid elbow orthosis," in *2009 IEEE International Conference on Rehabilitation Robotics*, 2009, pp. 167–171.

[29] B. F. Morrey, L. J. Askew, and E. Y. Chao, "A biomechanical study of normal functional elbow motion.," *J. Bone Joint Surg. Am.*, vol. 63, no. 6, pp. 872–7, Jul. 1981.

[30] "Brush Teeth - American Dental Association." [Online]. Available: https://www.mouthhealthy.org/en/az-topics/b/brushing-your-teeth.

[31] B. S. Rupal, S. Rafique, A. Singla, E. Singla, M. Isaksson, and G. S. Virk, "Lower-limb exoskeletons," *Int. J. Adv. Robot. Syst.*, vol. 14, no. 6, p. 172988141774355, Nov. 2017.

[32] T. Rahman *et al.*, "Passive exoskeletons for assisting limb movement," *JRRD*, vol. 43, no. 5, pp. 583–590, 2006.

[33] L. Cappello, Dinh Khanh Binh, Shih-Cheng Yen, and L. Masia, "Design and preliminary characterization of a soft wearable exoskeleton for upper limb," in *2016 6th IEEE International Conference on Biomedical Robotics and Biomechatronics (BioRob)*, 2016, pp. 623–630.

[34] A. T. Asbeck, R. J. Dyer, A. F. Larusson, and C. J. Walsh, "Biologically-inspired

soft exosuit," in *2013 IEEE 13th International Conference on Rehabilitation Robotics (ICORR)*, 2013, pp. 1–8.

[35] D. Copaci, E. Cano, L. Moreno, and D. Blanco, "New Design of a Soft Robotics Wearable Elbow Exoskeleton Based on Shape Memory Alloy Wire Actuators," *Appl. Bionics Biomech.*, vol. 2017, pp. 1–11, Sep. 2017.

[36] A. Villoslada, A. Flores, D. Copaci, D. Blanco, and L. Moreno, "High-displacement flexible Shape Memory Alloy actuator for soft wearable robots," *Rob. Auton. Syst.*, vol. 73, pp. 91–101, Nov. 2015.

[37] P. K. Kumar and D. C. Lagoudas, "Introduction to Shape Memory Alloys."

[38] J. M. Gallardo Fuentes, P. Gümpel, and J. Strittmatter, "Phase change behavior of nitinol shape memory alloys," *Adv. Eng. Mater.*, vol. 4, no. 7, pp. 437–452, Jul. 2002.

[39] F. DAĞDELEN, S. BUYTOZ, M. KÖK, and E. ERCAN, "Heat treatment effects on thermal cycle, transition temperature, and microstructure of NiTi shape memory alloy (SMA)," *Erciyes Üniversitesi Fen Bilim. Enstitüsü Fen Bilim. Derg.*, vol. 31, no. 3, pp. 115–120, Jun. 2015.

[40] L. Petrini and F. Migliavacca, "Biomedical Applications of Shape Memory Alloys," *J. Metall.*, vol. 2011, pp. 1–15, 2011.

[41] R. Granberry, K. Eschen, B. Holschuh, and J. Abel, "Functionally Graded Knitted Actuators with NiTi-Based Shape Memory Alloys for Topographically Self-Fitting Wearables," *Adv. Mater. Technol.*, vol. 4, no. 11, Nov. 2019.

[42] "Technical Characteristics of Flexinol Actuator Wires."

[43] J. Mohd Jani, M. Leary, A. Subic, and M. A. Gibson, "A review of shape memory

alloy research, applications and opportunities," 2014.

[44] J. Mohd Jani, "Design Optimisation of Shape Memory Alloy Linear Actuator Applications," 2016.

[45] B. Holschuh, E. Obropta, and D. Newman, "Low Spring Index NiTi Coil Actuators for Use in Active Compression Garments," *IEEE/ASME Trans. Mechatronics*, vol. 20, no. 3, pp. 1264–1277, Jun. 2015.

[46] S. J. Yates and A. L. Kalamkarov, "Experimental Study of Helical Shape Memory Alloy Actuators: Effects of Design and Operating Parameters on Thermal Transients and Stroke," *Metals (Basel).*, vol. 3, no. 1, pp. 123–149, Feb. 2013.

[47] "Module 7 Design of Springs."

[48] "Earthquake Glossary." [Online]. Available: https://earthquake.usgs.gov/learn/glossary/?term=shear stress. [Accessed: 20-Jul-2019].

[49] "The Ideal Spring and Simple Harmonic Motion." [Online]. Available: http://demo.webassign.net/ebooks/cj6demo/pc/c10/read/ssg/c10x10_1.htm. [Accessed: 20-Jul-2019].

[50] "Mechanical Design of a Shaft - S.B.A Invent." [Online]. Available: https://sbainvent.com/mechanical-design/mechanical-design-of-a-shaft/. [Accessed: 20-Jul-2019].

[51] M. A. Savi, P. M. C. L. Pacheco, M. S. Garcia, R. A. A. Aguiar, L. F. G. De Souza, and R. B. Da Hora, "Nonlinear geometric influence on the mechanical behavior of shape memory alloy helical springs," *Smart Mater. Struct.*, 2015.

[52] "Mohammad H. Elahinia Nonlinear Control of a Shape Memory Alloy Actuated

Manipulator," 2002.

[53] L. Masia, M. Xiloyannis, D. B. Khanh, A. C. Wilson, S. Contu, and K. G. Yongtae, "Chapter 4 – Actuation for robot-aided rehabilitation: Design and control strategies," *Rehabil. Robot.*, pp. 47–61, 2018.

[54] J. Matovic and K. Reichenberger, "Two - way SMA actuators for space application: performances and reliability," *Procedia Eng.*, vol. 5, pp. 1372–1375, Jan. 2010.

[55] D. J. Hartl and D. C. Lagoudas, "Thermomechanical Characterization of Shape Memory Alloy Materials," in *Shape Memory Alloys*, 2008.

[56] G. Scirè Mammano and E. Dragoni, "Functional fatigue of shape memory wires under constant-stress and constant-strain loading conditions," in *Procedia Engineering*, 2011.

[57] S.-M. An, J. Ryu, M. Cho, and K.-J. Cho, "Engineering design framework for a shape memory alloy coil spring actuator using a static two-state model," *Smart Mater. Struct.*, vol. 21, no. 5, p. 055009, May 2012.

[58] R. G. (Richard G. Budynas, J. K. Nisbett, and J. E. Shigley, *Shigley's mechanical engineering design*. McGraw-Hill, 2008.

[59] K. P. Menard, *Dynamic mechanical analysis : a practical introduction*. CRC Press, 2008.

[60] M. H. Weber, T. Ablekim, and K. G. Lynn, "Vacancies in NiTi shape memory alloys," *J. Phys. Conf. Ser.*, vol. 505, no. 1, p. 012006, Apr. 2014.

[61] Y. Liu, Y. Liu, and J. Van Humbeeck, "Two-way shape memory effect developed by martensite deformation in NiTi," *Acta Mater.*, vol. 47, no. 1, pp. 199–209, Dec. 1998.

[62] C. Lexcellent, S. Leclercq, B. Gabry, and G. Bourbon, “The two way shape memory effect of shape memory alloys: an experimental study and a phenomenological model,” *Int. J. Plast.*, vol. 16, no. 10–11, pp. 1155–1168, Jan. 2000.

[63] A. Falvo, F. Furgiuele, and C. Maletta, “Two-way shape memory effect of a Ti rich NiTi alloy: experimental measurements and numerical simulations,” *Smart Mater. Struct.*, vol. 16, no. 3, pp. 771–778, Jun. 2007.

[64] Y. X. Tong *et al.*, “Two-way shape memory effect of TiNiSn alloys developed by martensitic deformation,” *Mater. Sci. Eng. A*, vol. 550, pp. 434–437, Jul. 2012.

[65] F. Auricchio, V. Massarotti, and E. Zanaboni, “One Way and Two Way–Shape Memory Effect: Thermo–Mechanical Characterization of Ni–Ti wires,” 2007.

[66] A. Falvo, F. Furgiuele, and C. Maletta, “Hysteresis modeling of two-way shape memory effect in NiTi alloys,” *Meccanica*, vol. 43, pp. 165–172, 2008.

[67] K. C. Atli, I. Karaman, R. D. Noebe, and D. Gaydosh, “The effect of training on two-way shape memory effect of binary NiTi and NiTi based ternary high temperature shape memory alloys,” *Mater. Sci. Eng. A*, vol. 560, pp. 653–666, Jan. 2013.

[68] T. C. Da Silva, M. V. C. Sá, E. P. Da Silva, and F. C. Da Silva, “Emissivity Measurements on Shape Memory Alloys.”

[69] H. Ma, “Thermal Modeling of Shape Memory Alloy Wire Actuators for Automotive Applications,” University of Waterloo, 2010.

[70] J. Ortiz, T. Poliero, G. Cairoli, E. Graf, and D. G. Caldwell, “Energy Efficiency Analysis and Design Optimization of an Actuation System in a Soft Modular Lower Limb Exoskeleton,” *IEEE Robot. Autom. Lett.*, vol. 3, no. 1, pp. 484–491, Jan. 2018.

[71] K. J. De Laurentis, A. Fisch, J. Nikitczuk, and C. Mavroidis, “Optimal Design of Shape Memory Alloy Wire Bundle Actuators.”

[72] B. T. Holschuh and D. J. Newman, “Morphing Compression Garments for Space Medicine and Extravehicular Activity Using Active Materials,” *Aerosp. Med. Hum. Perform.*, 2016.

[73] S. Yarosh *et al.*, “SqueezeBands,” *Proc. ACM Human-Computer Interact.*, 2017.

[74] “Human Anatomy Muscles Upper Limb Back Of Arm Muscle Diagram | World Of Diagrams - Anatomy Of Diagram.” [Online]. Available: https://anatomyofdiagram.com/human-anatomy-muscles-upper-limb/human-anatomy-muscles-upper-limb-back-of-arm-muscle-diagram-world-of-diagrams/.

[75] “Definition of a Shape Memory Alloy.” [Online]. Available: http://smart.tamu.edu/overview/smaintro/simple/definition.html. [Accessed: 03-May-2018].

[76] H. Song, E. Kubica, and R. Gorbet, “RESISTANCE MODELLING OF SMA WIRE ACTUATORS,” 2011.

Appendix A

Force vs time for Extensional strain of 0

Diameter 1

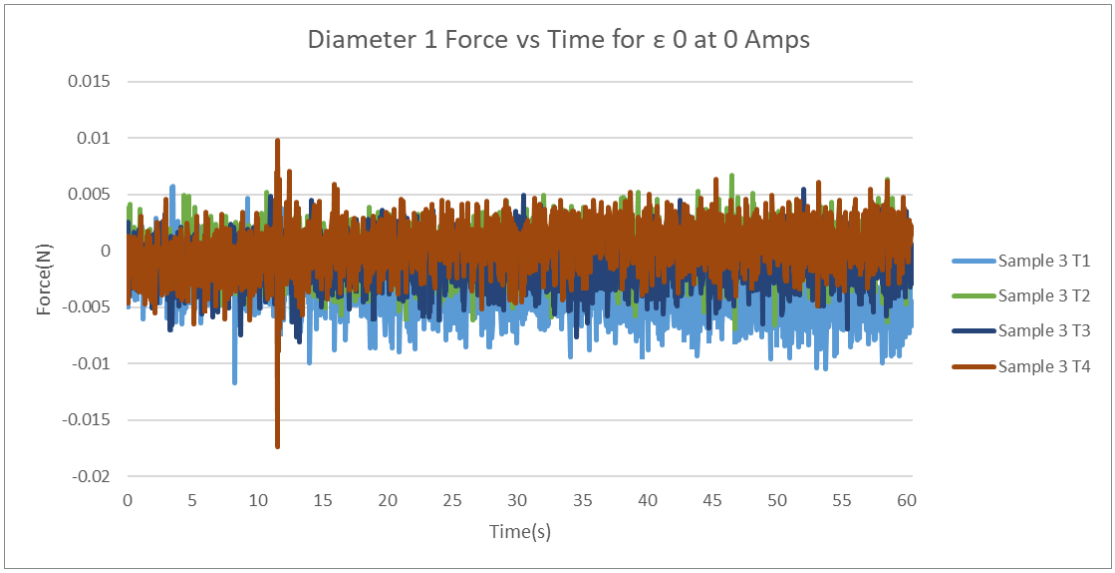

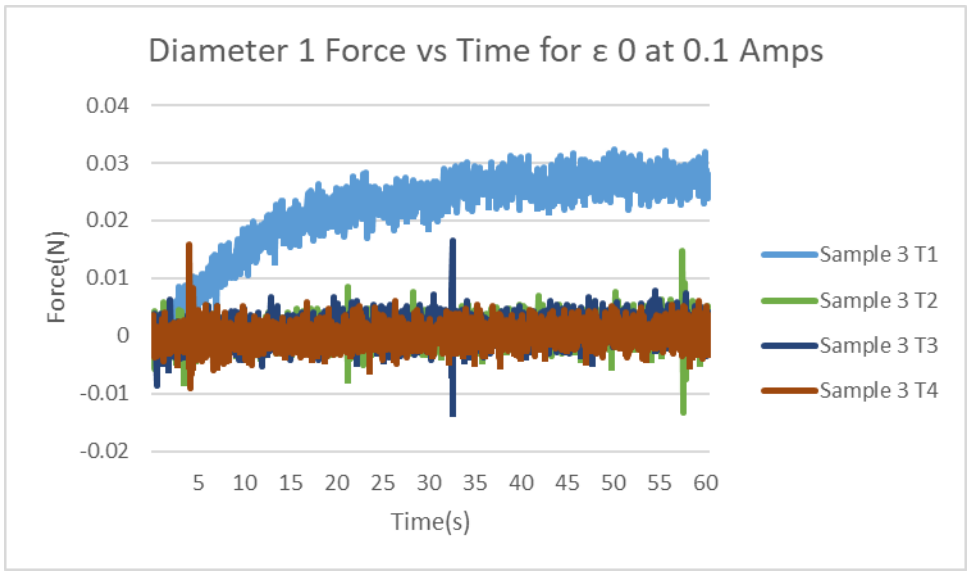

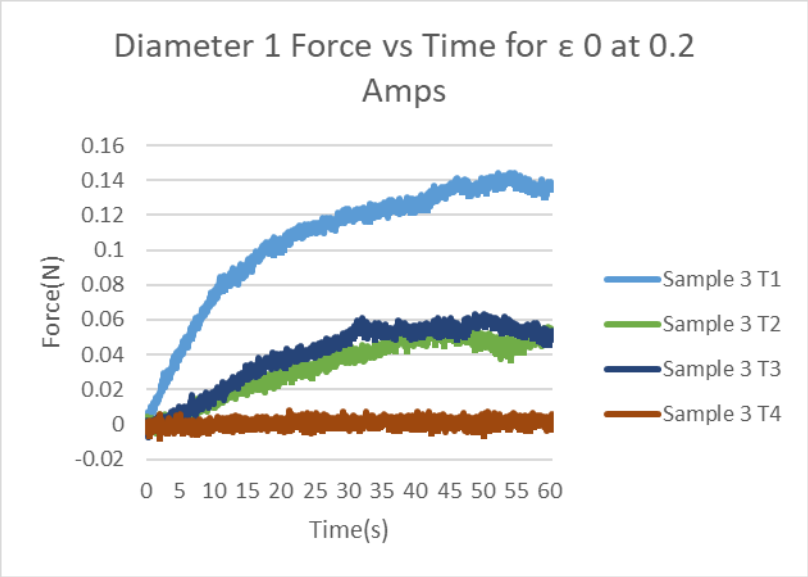
Diameter 1 Force vs Time for ε 0 at 0.2 Amps
Force(N)
0.16
0.14
0.12
0.1
0.08
0.06
0.04
0.02
0
-0.02
0 5 10 15 20 25 30 35 40 45 50 55 60
Time(s)
Sample 3 T1
Sample 3 T2
Sample 3 T3
Sample 3 T4

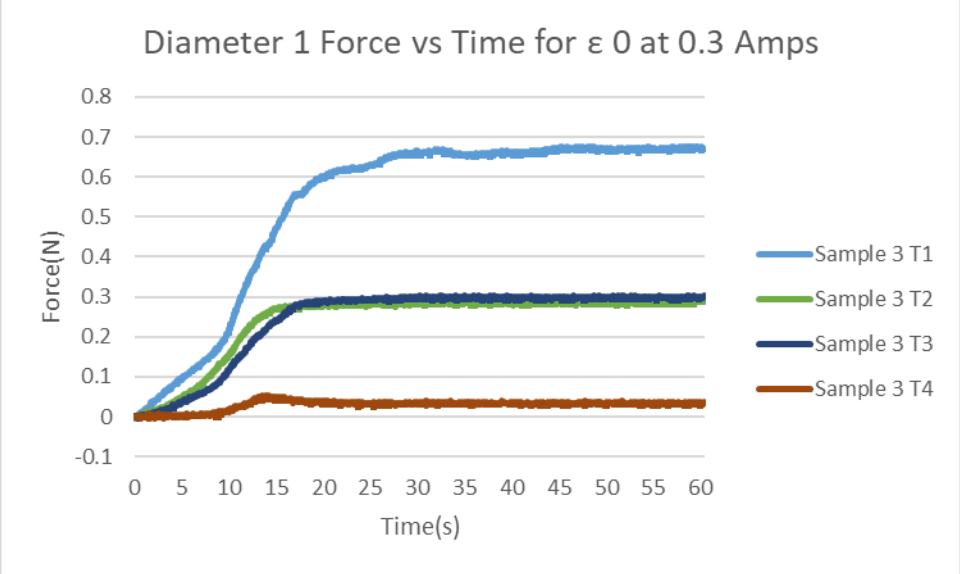
Diameter 1 Force vs Time for ε 0 at 0.3 Amps
Force(N)
0.8
0.7
0.6
0.5
0.4
0.3
0.2
0.1
0
-0.1
0 5 10 15 20 25 30 35 40 45 50 55 60
Time(s)
Sample 3 T1
Sample 3 T2
Sample 3 T3
Sample 3 T4

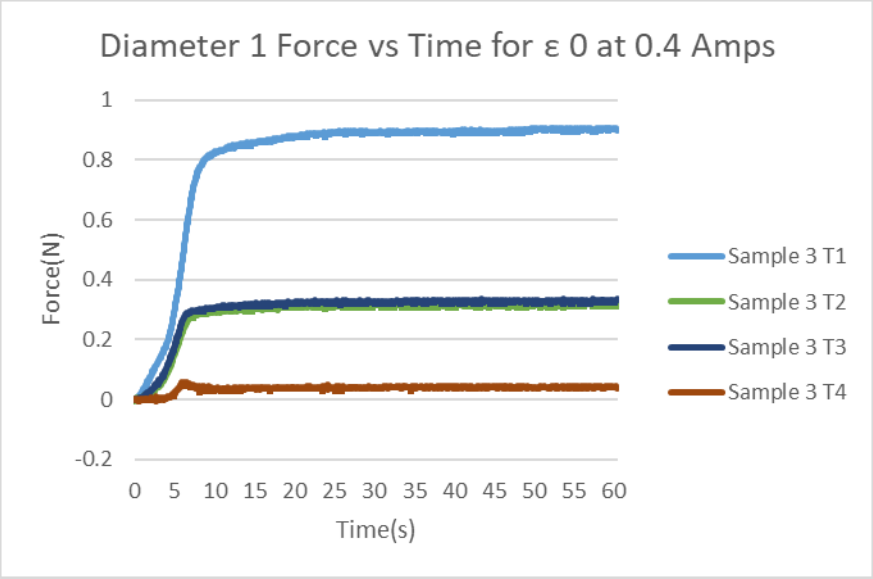
Diameter 1 Force vs Time for ε 0 at 0.4 Amps
Force(N)
1
0.8
0.6
0.4
0.2
0
-0.2
0 5 10 15 20 25 30 35 40 45 50 55 60
Time(s)
Sample 3 T1
Sample 3 T2
Sample 3 T3
Sample 3 T4

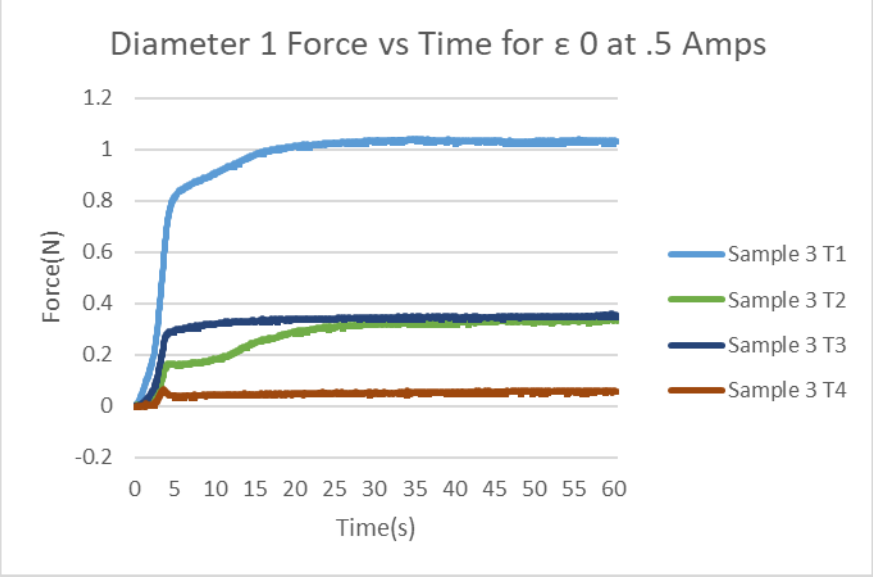
Diameter 1 Force vs Time for ε 0 at .5 Amps
Force(N)
1.2
1
0.8
0.6
0.4
0.2
0
-0.2
0 5 10 15 20 25 30 35 40 45 50 55 60
Time(s)
Sample 3 T1
Sample 3 T2
Sample 3 T3
Sample 3 T4

Diameter 2

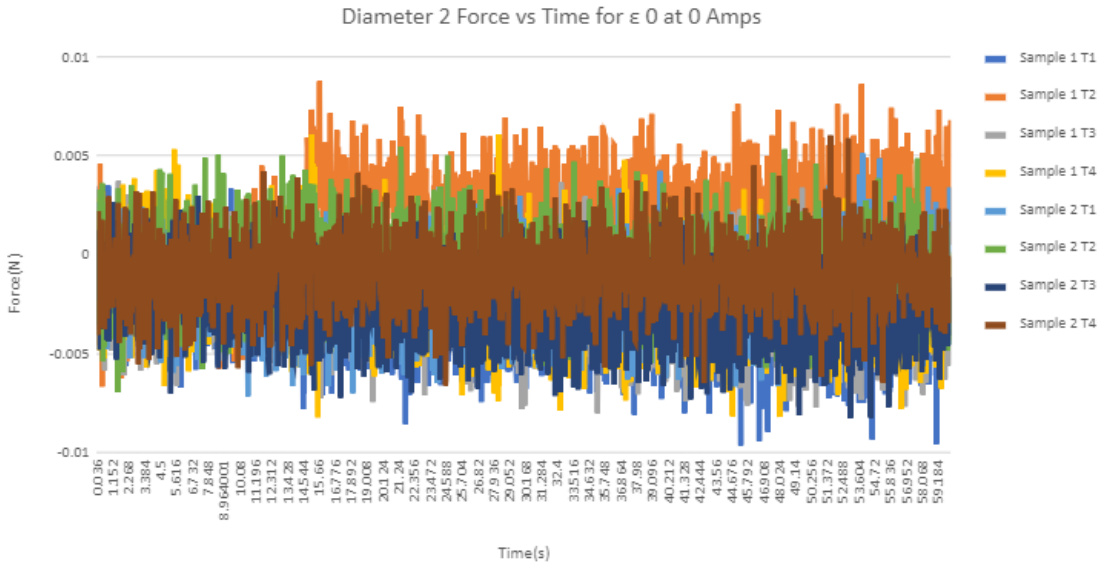
Diameter 2 Force vs Time for ε 0 at 0 Amps
Force(N)
Time(s)
Sample 1 T1
Sample 1 T2
Sample 1 T3
Sample 1 T4
Sample 2 T1
Sample 2 T2
Sample 2 T3
Sample 2 T4

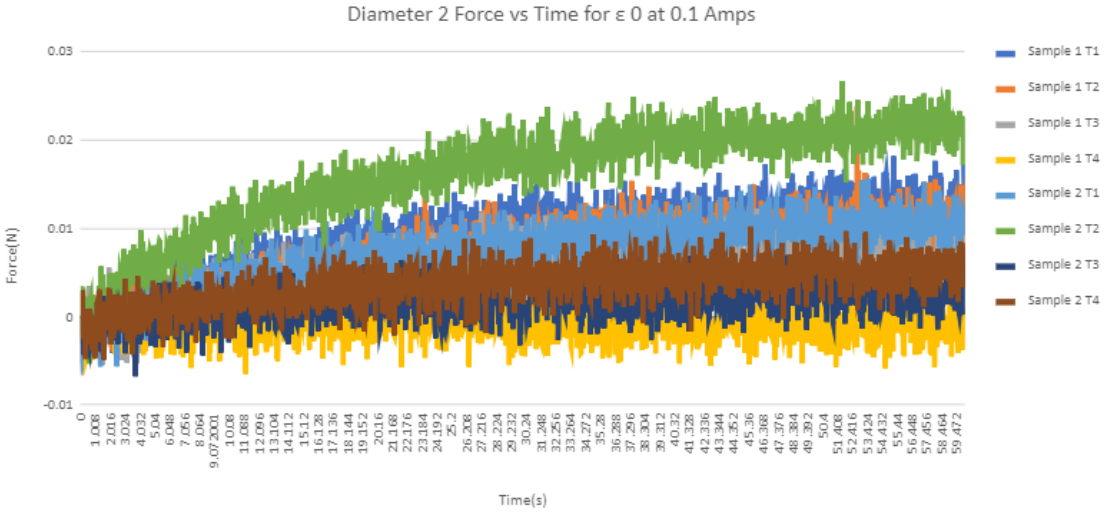
Diameter 2 Force vs Time for ε 0 at 0.1 Amps
Force(N)
Time(s)
Sample 1 T1
Sample 1 T2
Sample 1 T3
Sample 1 T4
Sample 2 T1
Sample 2 T2
Sample 2 T3
Sample 2 T4

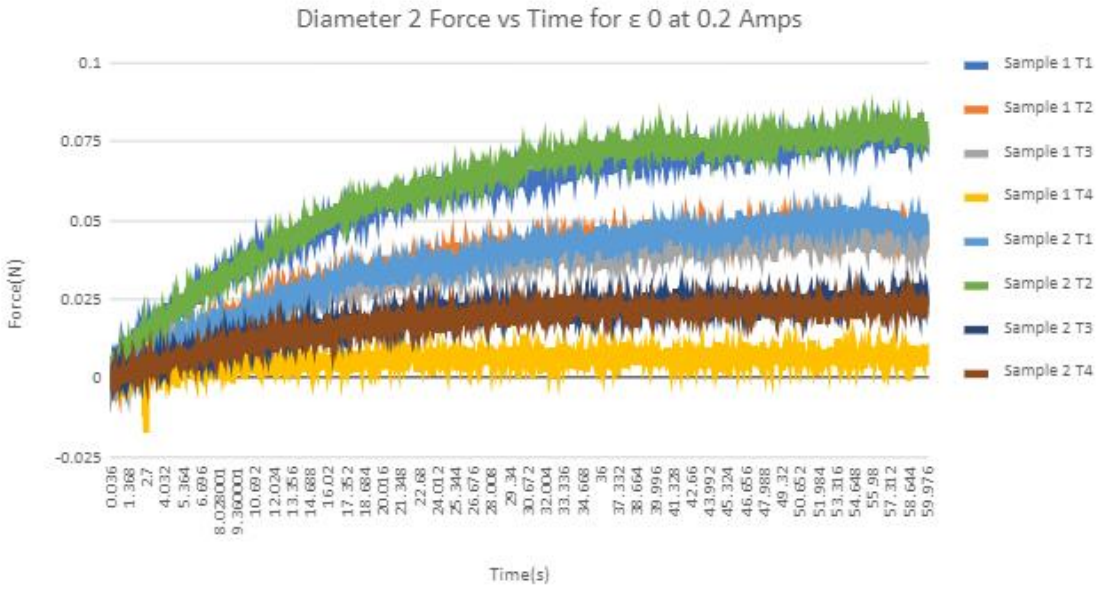
Diameter 2 Force vs Time for ε 0 at 0.2 Amps
Force(N)
Time(s)
Sample 1 T1
Sample 1 T2
Sample 1 T3
Sample 1 T4
Sample 2 T1
Sample 2 T2
Sample 2 T3
Sample 2 T4

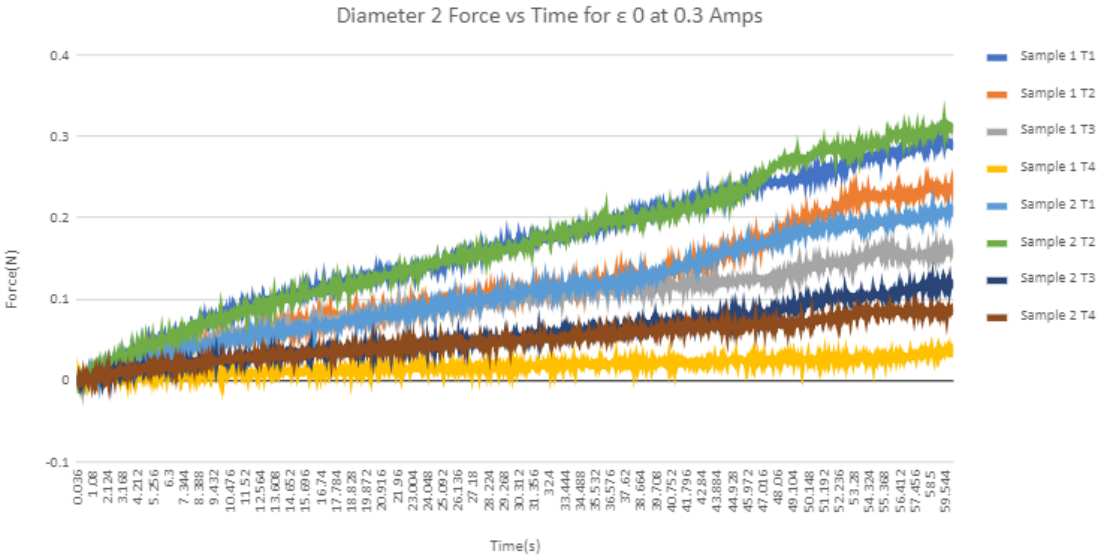
Diameter 2 Force vs Time for ε 0 at 0.3 Amps
Force(N)
Time(s)
Sample 1 T1
Sample 1 T2
Sample 1 T3
Sample 1 T4
Sample 2 T1
Sample 2 T2
Sample 2 T3
Sample 2 T4

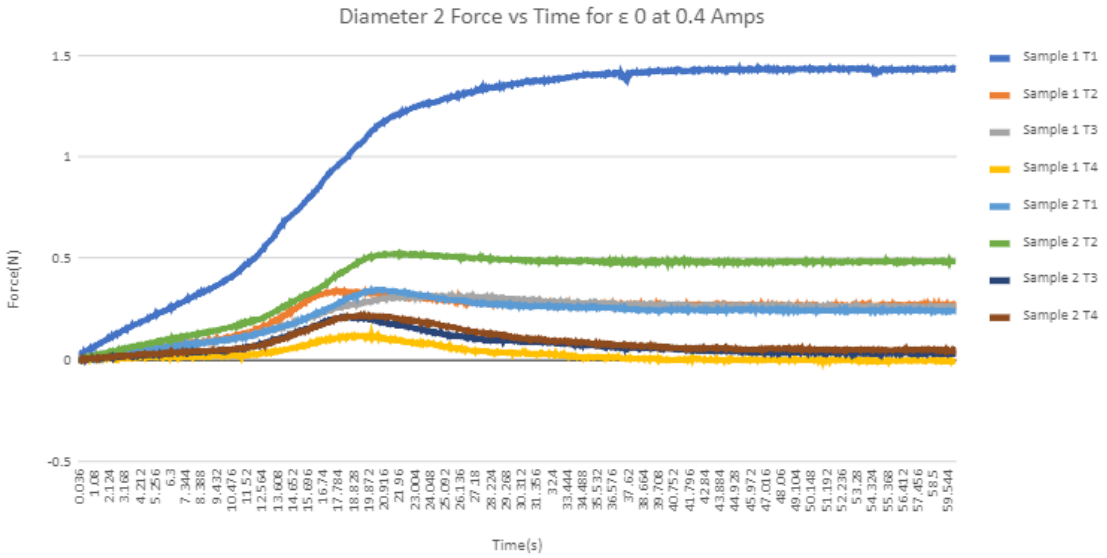
Diameter 2 Force vs Time for ε 0 at 0.4 Amps
Force(N)
Time(s)
Sample 1 T1
Sample 1 T2
Sample 1 T3
Sample 1 T4
Sample 2 T1
Sample 2 T2
Sample 2 T3
Sample 2 T4

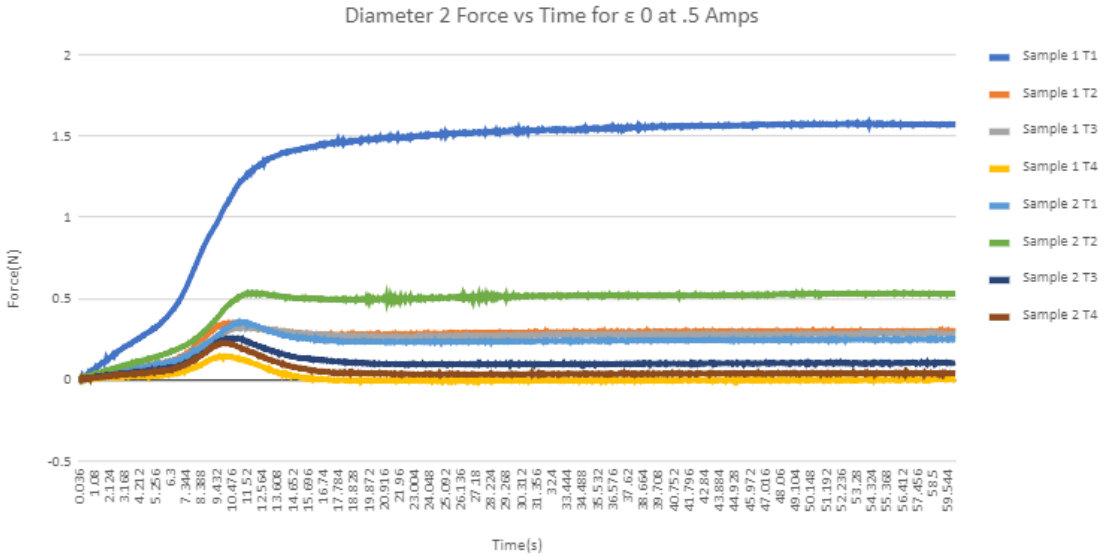
Diameter 2 Force vs Time for ε 0 at .5 Amps
Force(N)
Time(s)
Sample 1 T1
Sample 1 T2
Sample 1 T3
Sample 1 T4
Sample 2 T1
Sample 2 T2
Sample 2 T3
Sample 2 T4

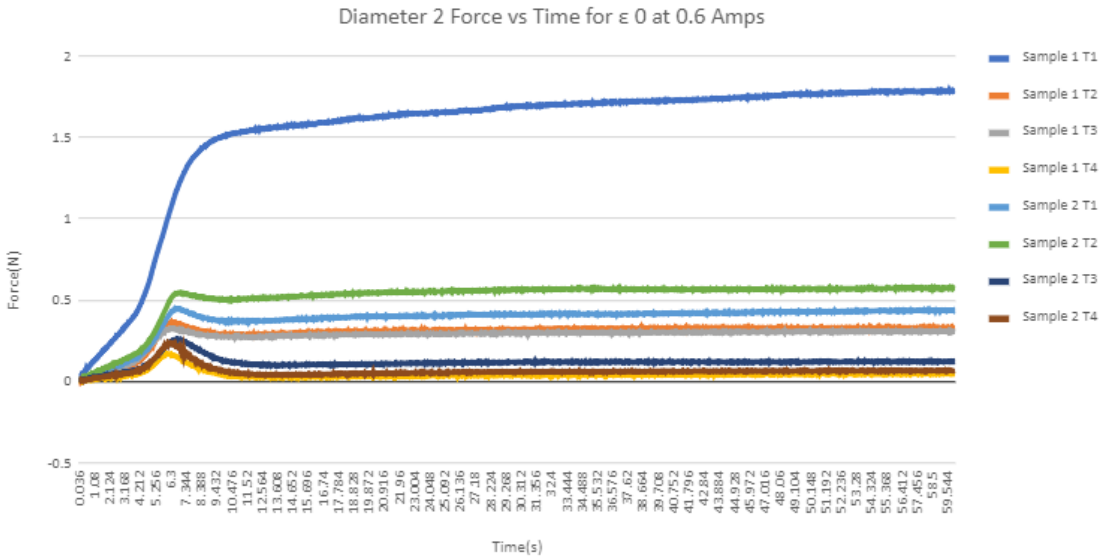
Diameter 2 Force vs Time for ε 0 at 0.6 Amps
Force(N)
Time(s)
Sample 1 T1
Sample 1 T2
Sample 1 T3
Sample 1 T4
Sample 2 T1
Sample 2 T2
Sample 2 T3
Sample 2 T4

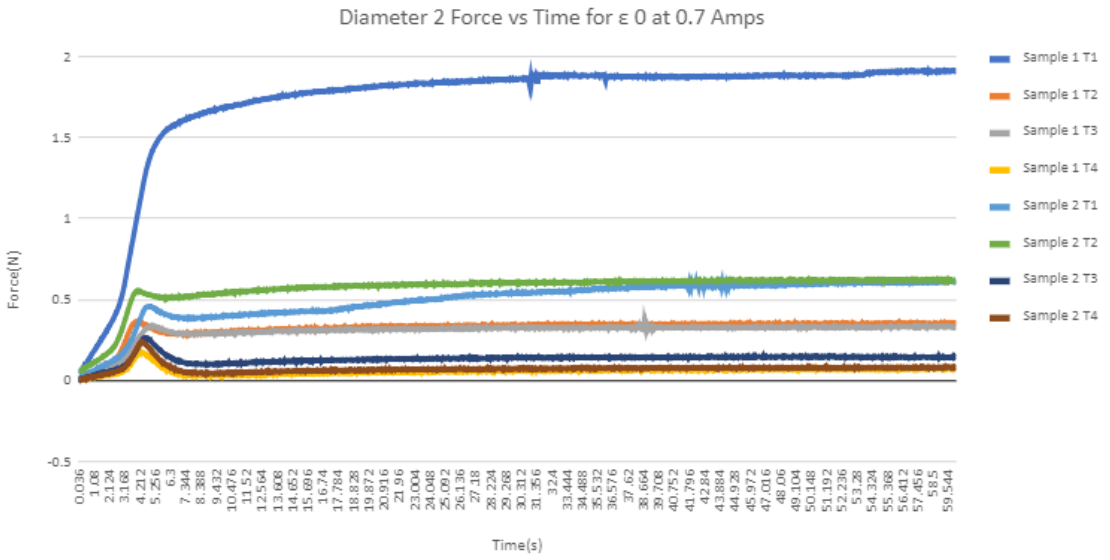
Diameter 2 Force vs Time for ε 0 at 0.7 Amps
Force(N)
Time(s)
Sample 1 T1
Sample 1 T2
Sample 1 T3
Sample 1 T4
Sample 2 T1
Sample 2 T2
Sample 2 T3
Sample 2 T4

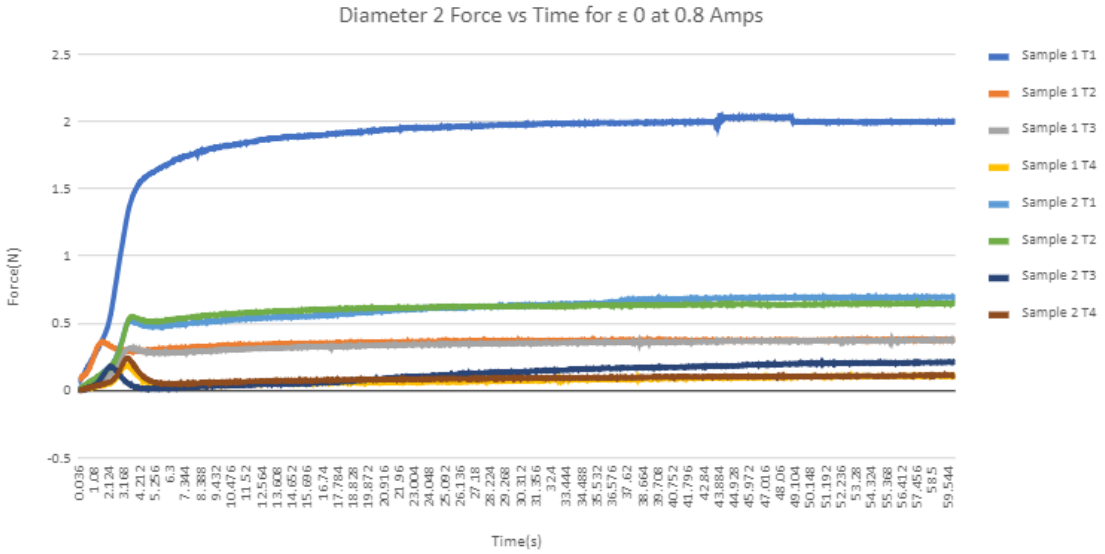

Force vs time for extensional strain of .5

Diameter 1

Diameter 2

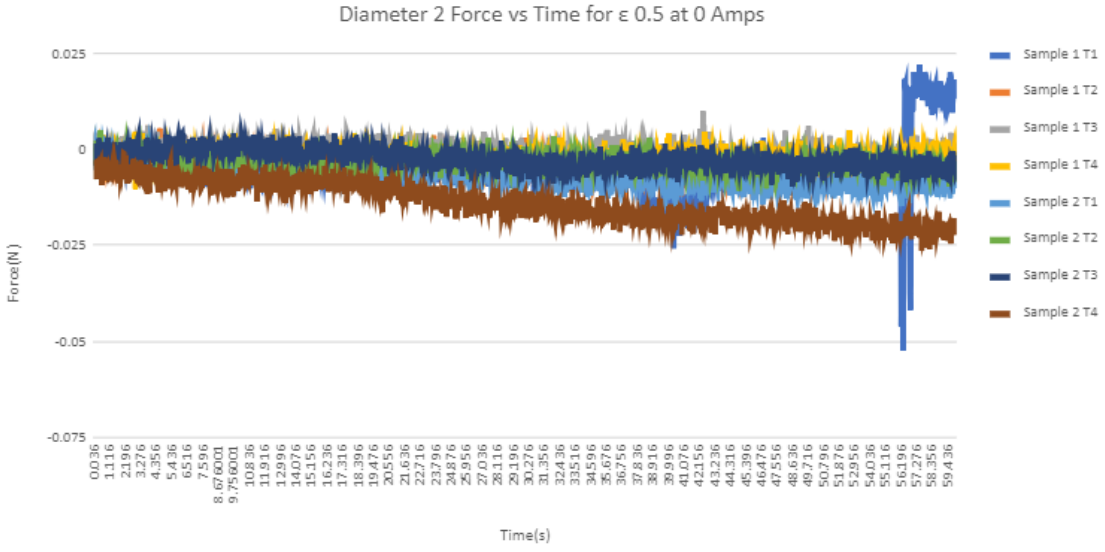

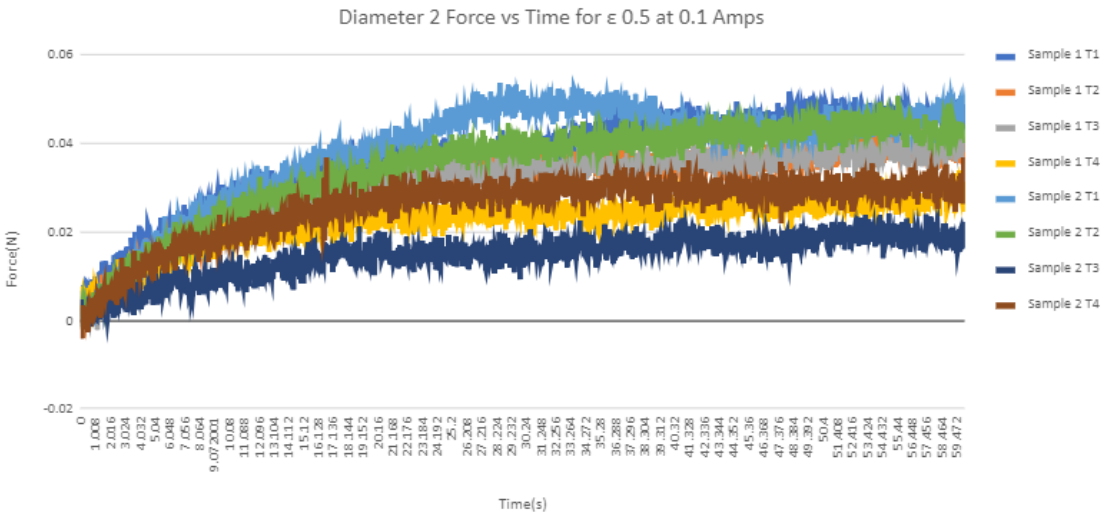
Diameter 2 Force vs Time for ε 0.5 at 0.1 Amps
Force(N)
Time(s)
Sample 1 T1
Sample 1 T2
Sample 1 T3
Sample 1 T4
Sample 2 T1
Sample 2 T2
Sample 2 T3
Sample 2 T4

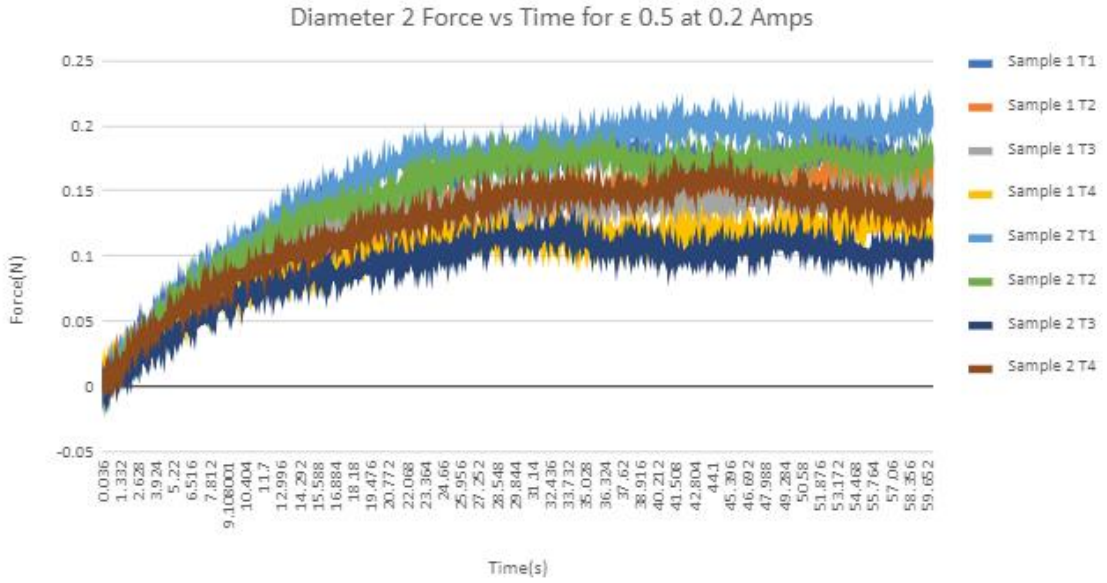
Diameter 2 Force vs Time for ε 0.5 at 0.2 Amps
Force(N)
Time(s)
Sample 1 T1
Sample 1 T2
Sample 1 T3
Sample 1 T4
Sample 2 T1
Sample 2 T2
Sample 2 T3
Sample 2 T4

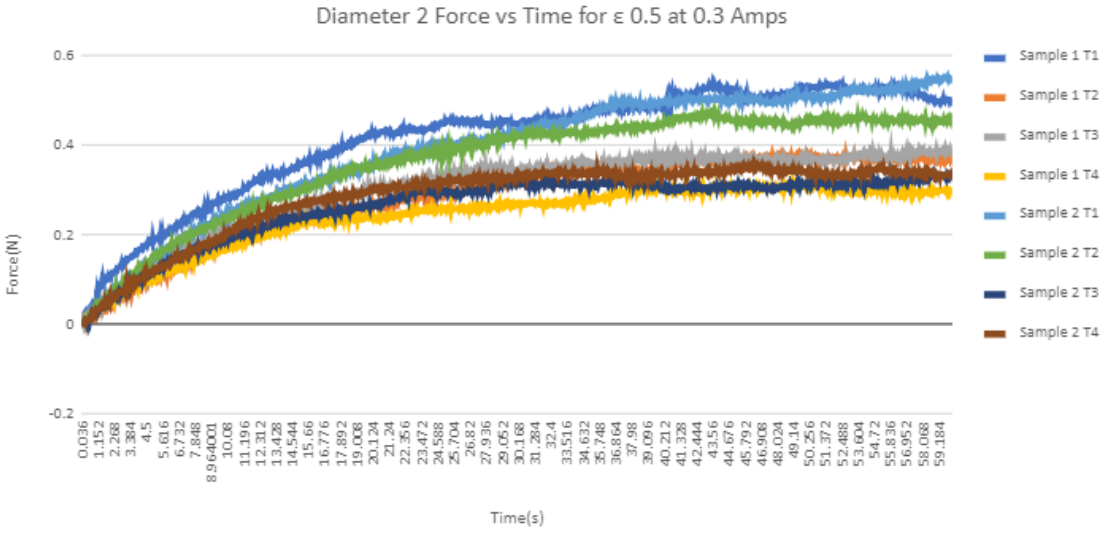
Diameter 2 Force vs Time for ε 0.5 at 0.3 Amps
Force(N)
Time(s)
Sample 1 T1
Sample 1 T2
Sample 1 T3
Sample 1 T4
Sample 2 T1
Sample 2 T2
Sample 2 T3
Sample 2 T4

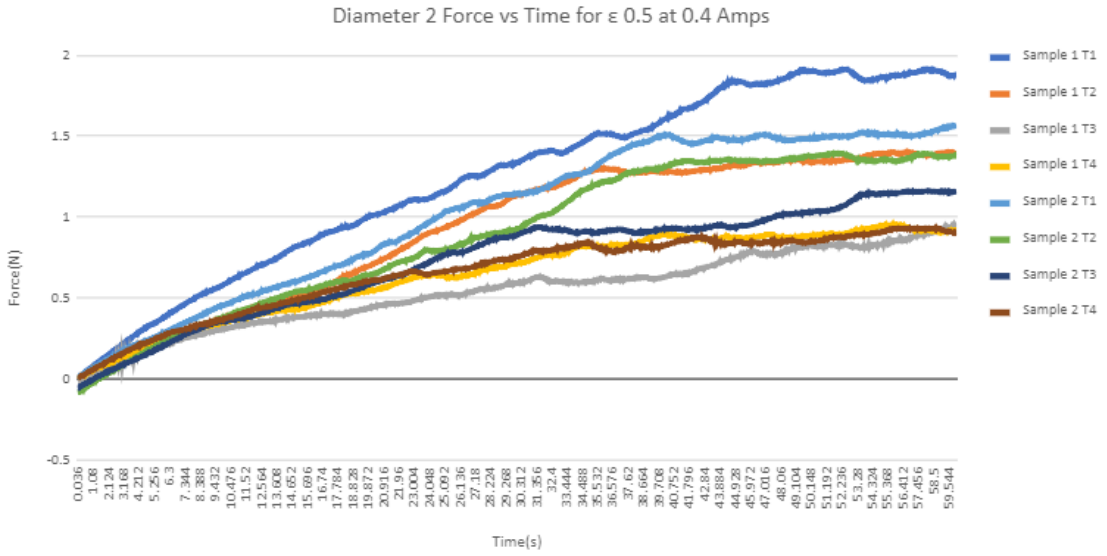
Diameter 2 Force vs Time for ε 0.5 at 0.4 Amps
Force(N)
Time(s)
Sample 1 T1
Sample 1 T2
Sample 1 T3
Sample 1 T4
Sample 2 T1
Sample 2 T2
Sample 2 T3
Sample 2 T4

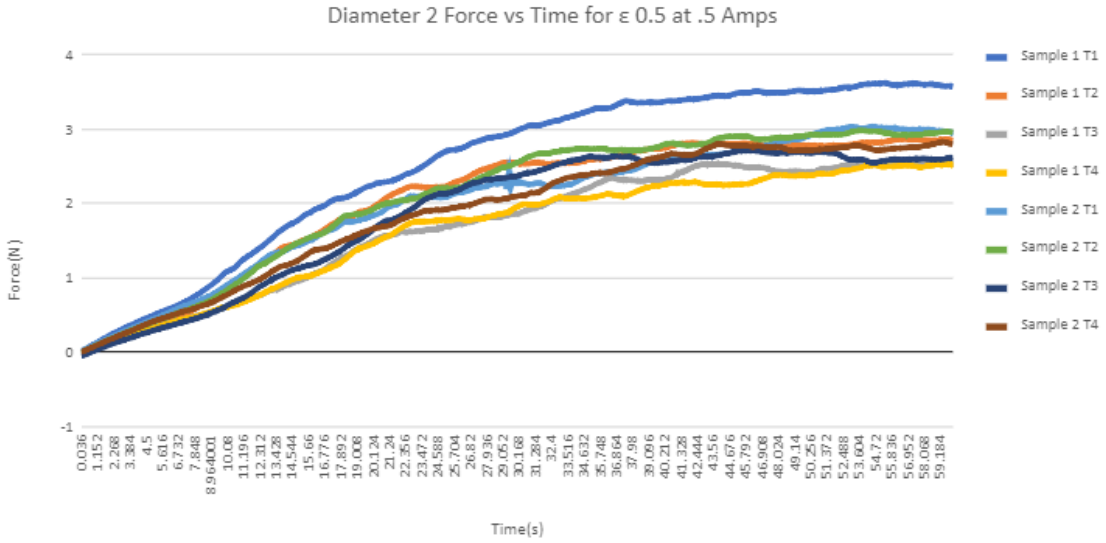
Diameter 2 Force vs Time for ε 0.5 at .5 Amps
Force(N)
Time(s)
Sample 1 T1
Sample 1 T2
Sample 1 T3
Sample 1 T4
Sample 2 T1
Sample 2 T2
Sample 2 T3
Sample 2 T4

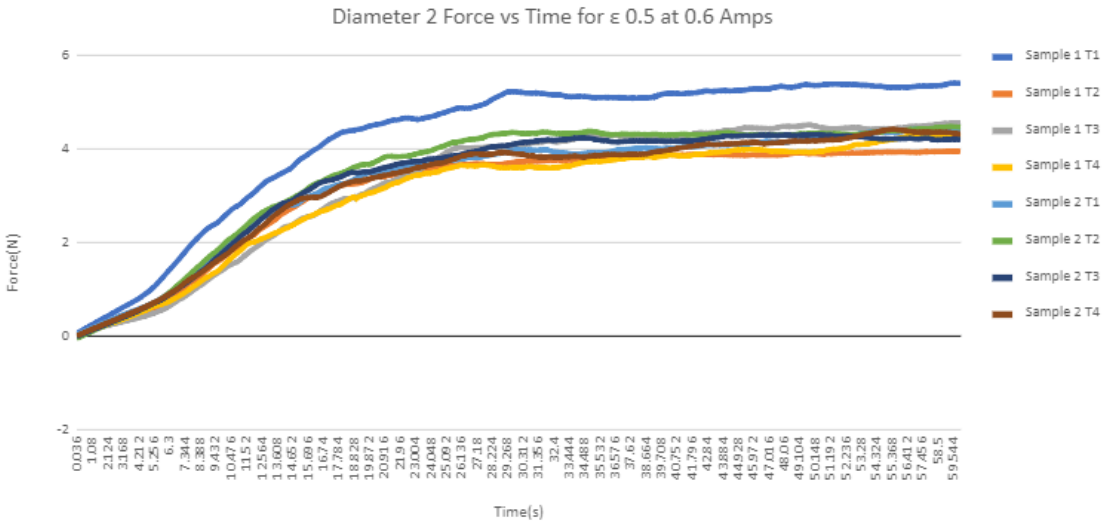
Diameter 2 Force vs Time for ε 0.5 at 0.6 Amps
Force(N)
Time(s)
Sample 1 T1
Sample 1 T2
Sample 1 T3
Sample 1 T4
Sample 2 T1
Sample 2 T2
Sample 2 T3
Sample 2 T4

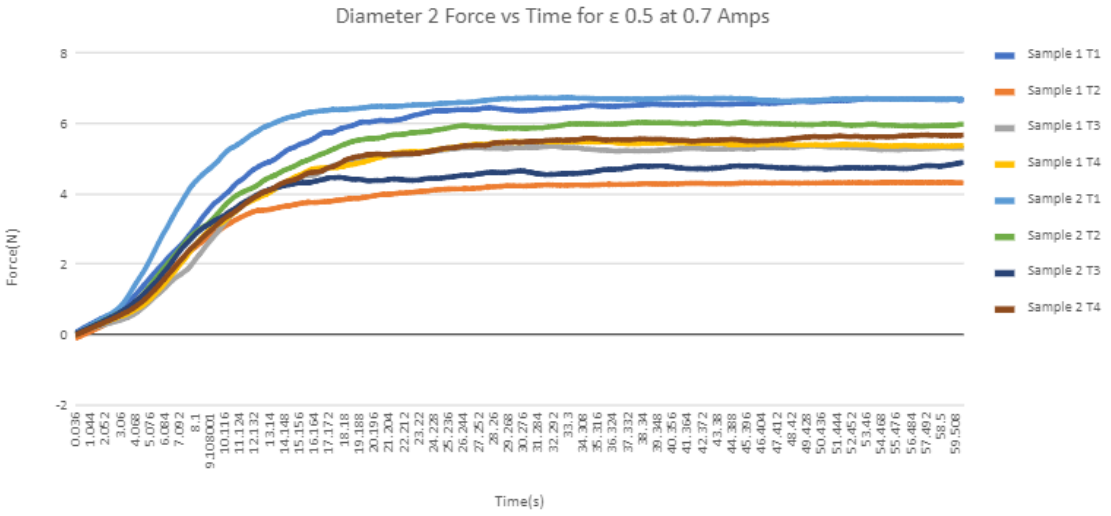
Diameter 2 Force vs Time for ε 0.5 at 0.7 Amps
Force(N)
Time(s)
Sample 1 T1
Sample 1 T2
Sample 1 T3
Sample 1 T4
Sample 2 T1
Sample 2 T2
Sample 2 T3
Sample 2 T4

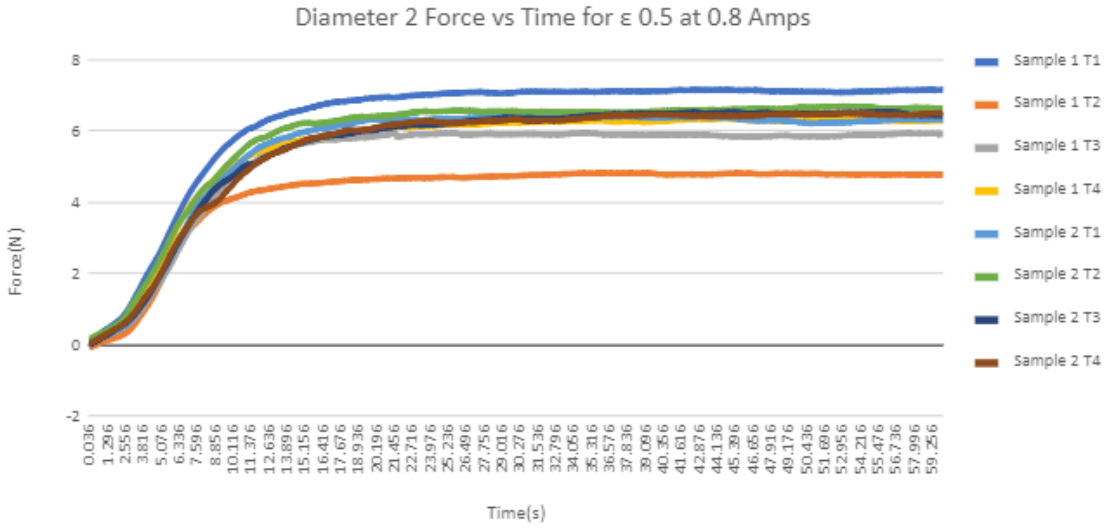
Diameter 2 Force vs Time for ε 0.5 at 0.8 Amps
Force(N)
Time(s)
Sample 1 T1
Sample 1 T2
Sample 1 T3
Sample 1 T4
Sample 2 T1
Sample 2 T2
Sample 2 T3
Sample 2 T4

Force vs. time for extensional strain of 1

Diameter 1

Diameter 2

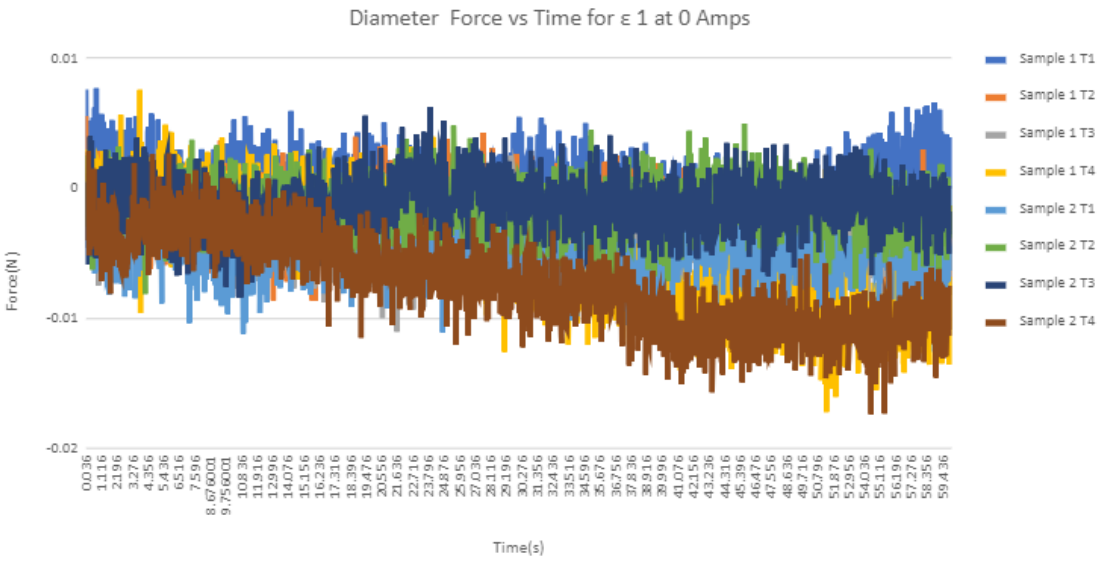

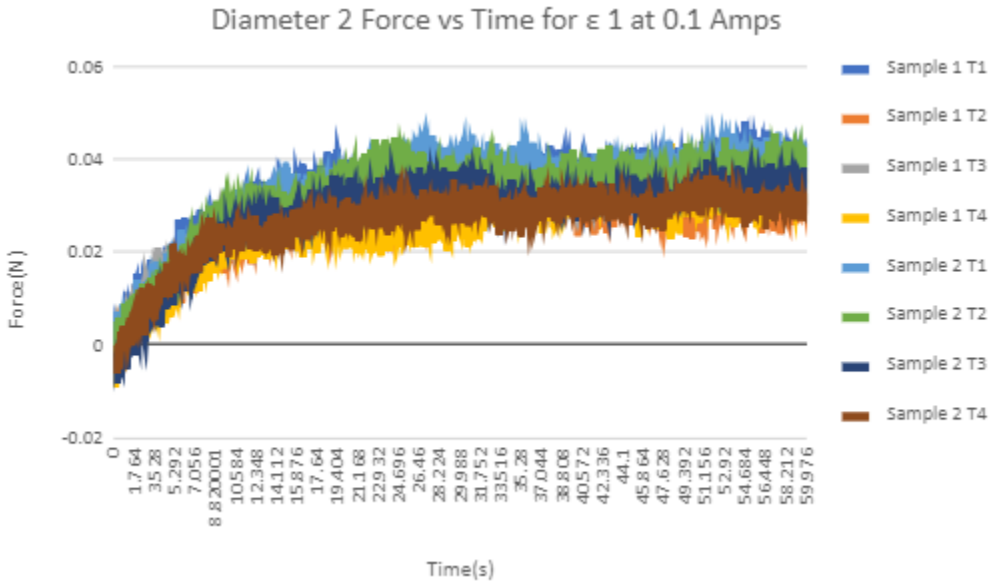

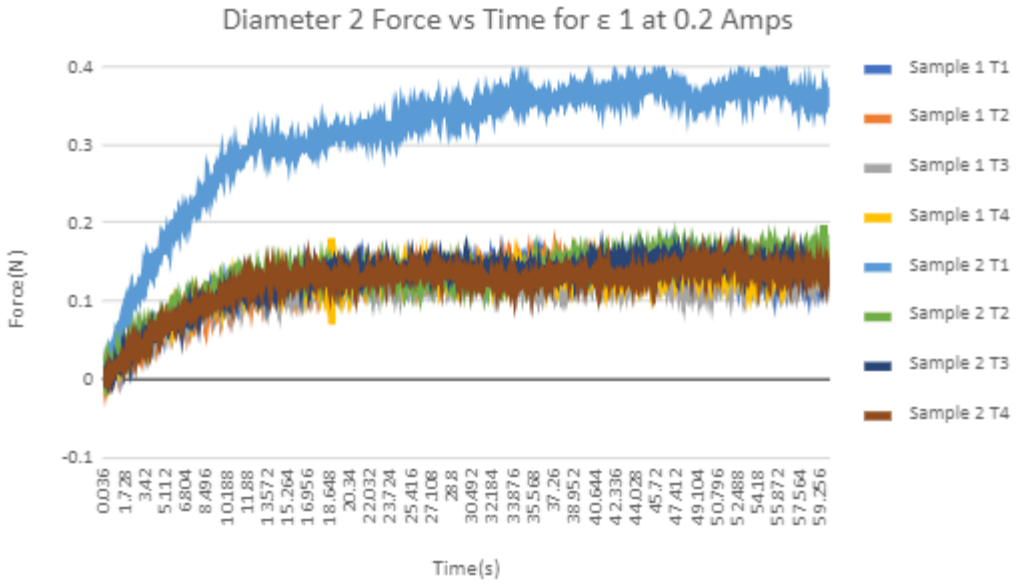
Diameter 2 Force vs Time for ε 1 at 0.2 Amps
Force(N)
0.4
0.3
0.2
0.1
0
-0.1
0.036
1.728
3.42
5.112
6.804
8.496
10.188
11.88
13.572
15.264
16.956
18.648
20.34
22.032
23.724
25.416
27.108
28.8
30.492
32.184
33.876
35.568
37.26
38.952
40.644
42.336
44.028
45.72
47.412
49.104
50.796
52.488
54.18
55.872
57.564
59.256
Time(s)
Sample 1 T1
Sample 1 T2
Sample 1 T3
Sample 1 T4
Sample 2 T1
Sample 2 T2
Sample 2 T3
Sample 2 T4

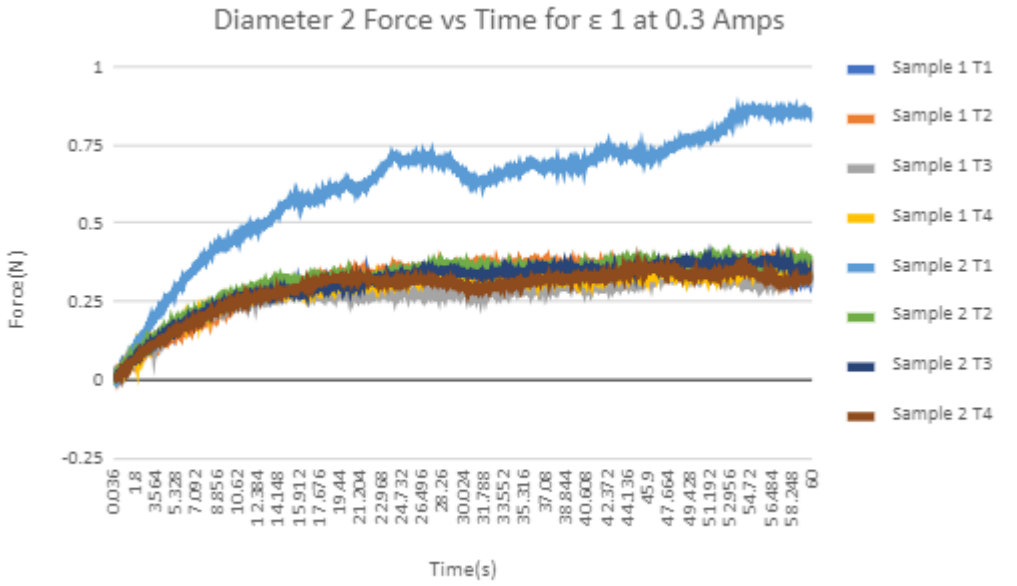
Diameter 2 Force vs Time for ε 1 at 0.3 Amps
Force(N)
1
0.75
0.5
0.25
0
-0.25
0.036
1.8
3.564
5.328
7.092
8.856
10.62
12.384
14.148
15.912
17.676
19.44
21.204
22.968
24.732
26.496
28.26
30.024
31.788
33.552
35.316
37.08
38.844
40.608
42.372
44.136
45.9
47.664
49.428
51.192
52.956
54.72
56.484
58.248
60
Time(s)
Sample 1 T1
Sample 1 T2
Sample 1 T3
Sample 1 T4
Sample 2 T1
Sample 2 T2
Sample 2 T3
Sample 2 T4

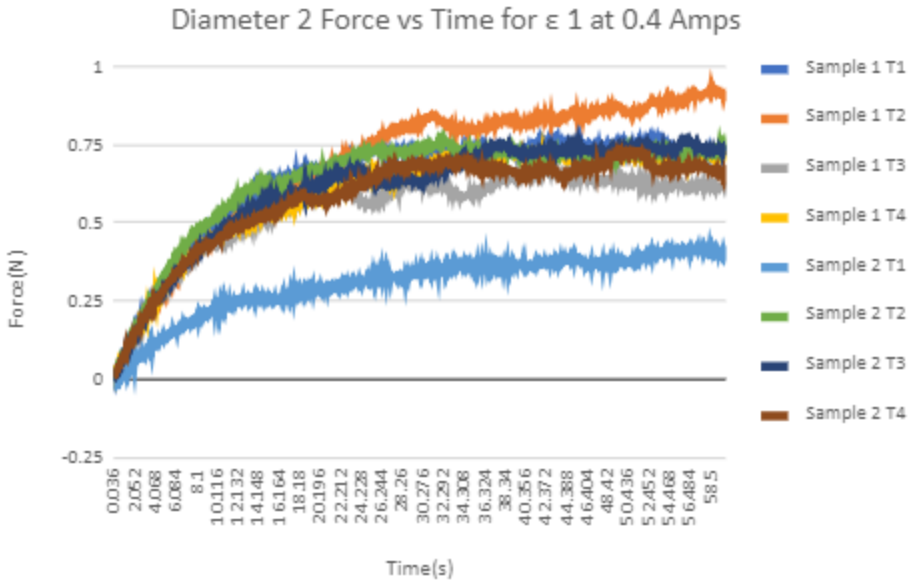
Diameter 2 Force vs Time for ε 1 at 0.4 Amps
Force(N)
Time(s)
Sample 1 T1
Sample 1 T2
Sample 1 T3
Sample 1 T4
Sample 2 T1
Sample 2 T2
Sample 2 T3
Sample 2 T4

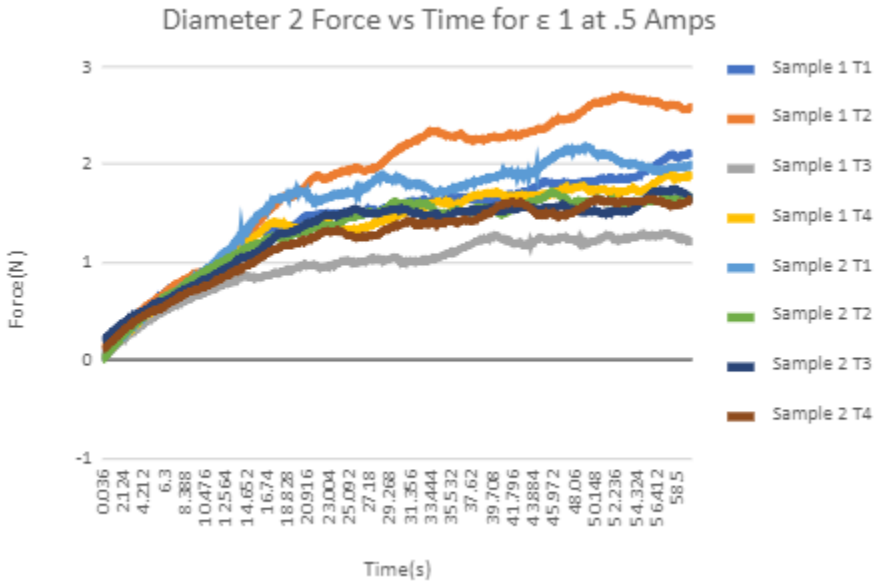
Diameter 2 Force vs Time for ε 1 at .5 Amps
Force(N)
Time(s)
Sample 1 T1
Sample 1 T2
Sample 1 T3
Sample 1 T4
Sample 2 T1
Sample 2 T2
Sample 2 T3
Sample 2 T4

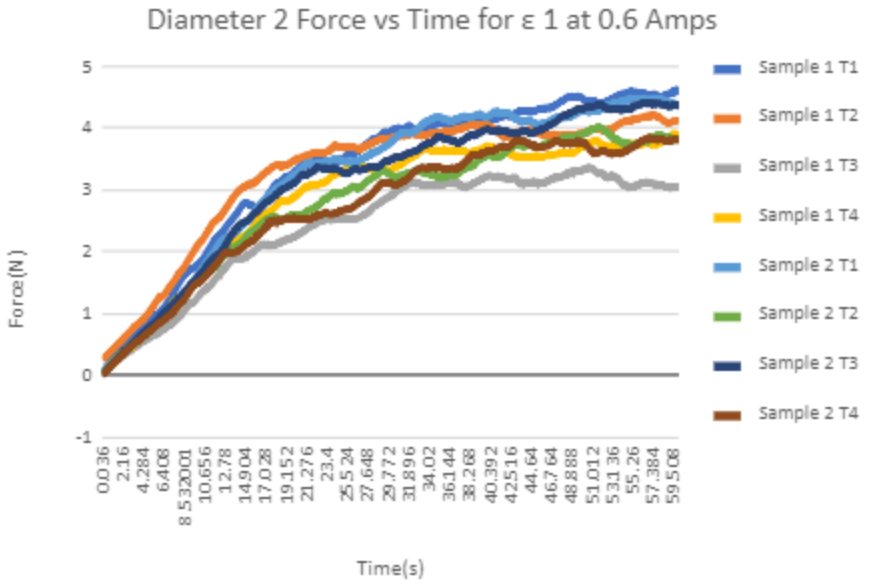
Diameter 2 Force vs Time for ε 1 at 0.6 Amps
Force(N)
Time(s)
Sample 1 T1
Sample 1 T2
Sample 1 T3
Sample 1 T4
Sample 2 T1
Sample 2 T2
Sample 2 T3
Sample 2 T4

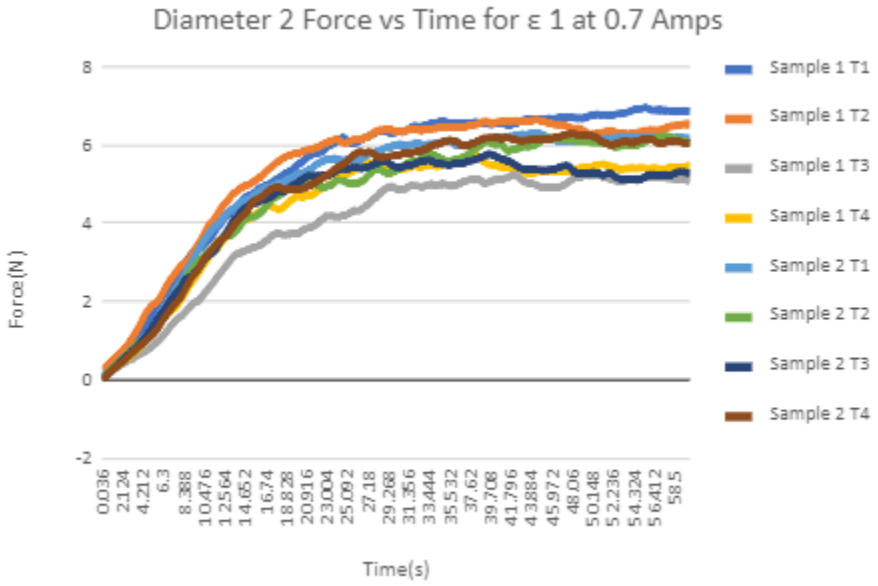
Diameter 2 Force vs Time for ε 1 at 0.7 Amps
Force(N)
Time(s)
Sample 1 T1
Sample 1 T2
Sample 1 T3
Sample 1 T4
Sample 2 T1
Sample 2 T2
Sample 2 T3
Sample 2 T4

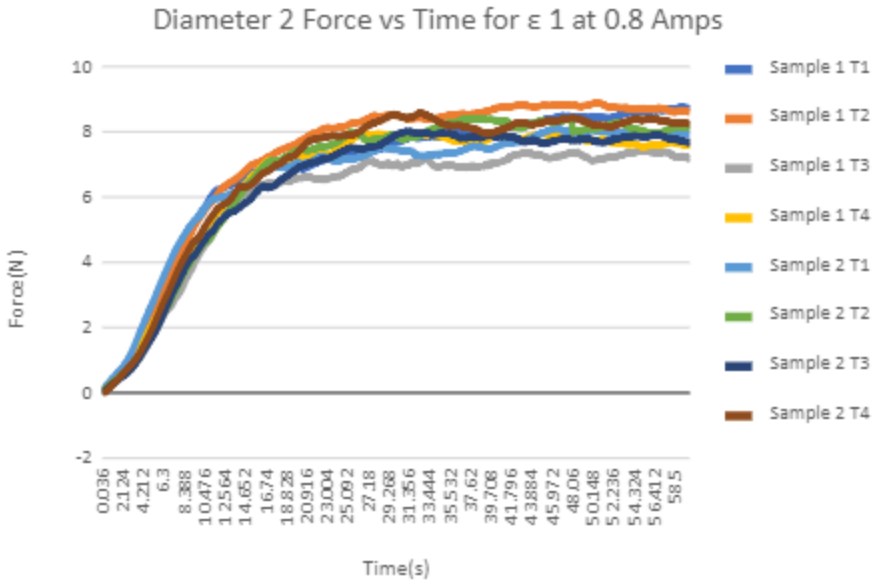

Force vs. time for extensional strain of 1.5

Diameter 1

Diameter 2

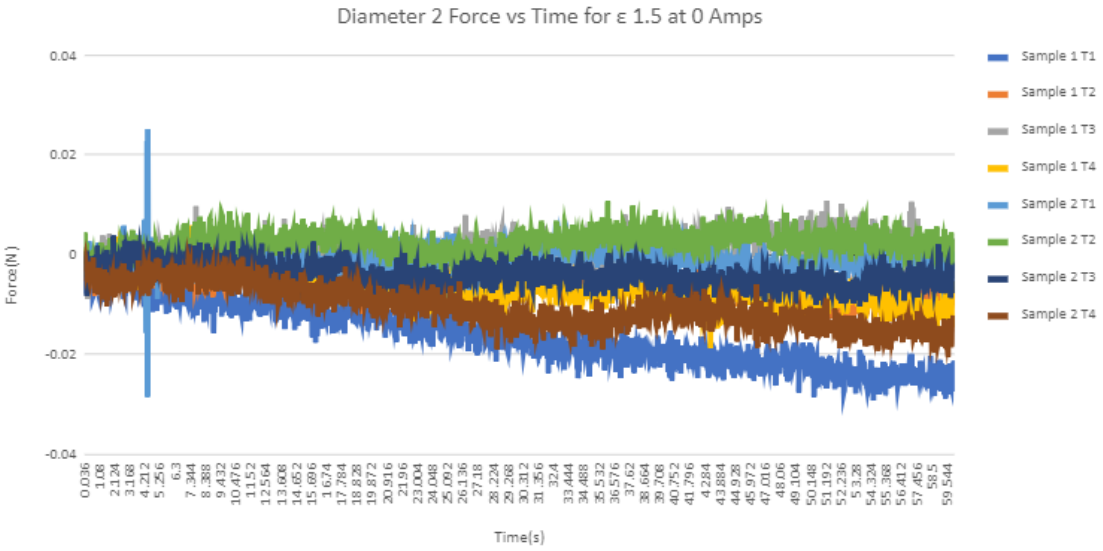

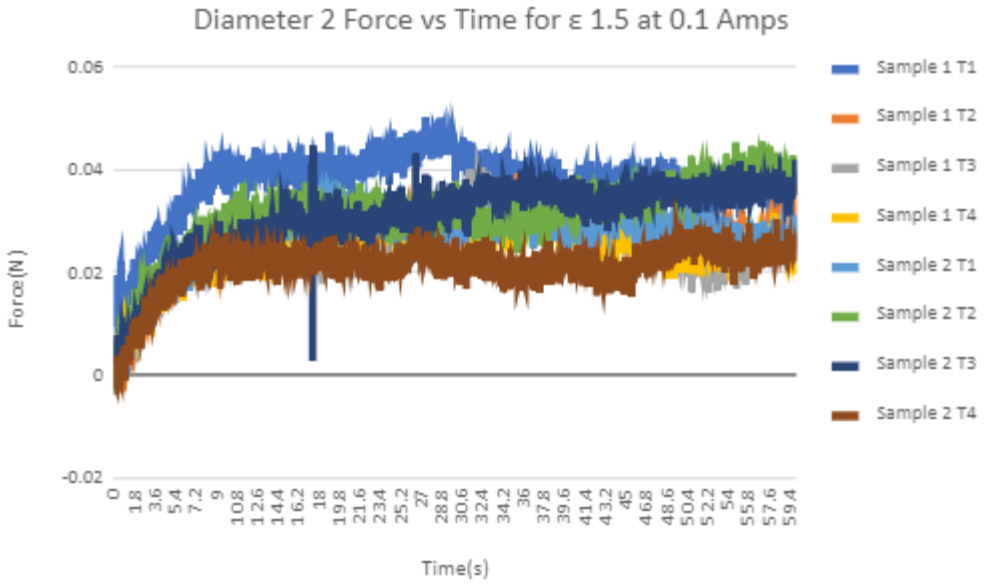
Diameter 2 Force vs Time for ε 1.5 at 0.1 Amps
Force(N)
Time(s)
Sample 1 T1
Sample 1 T2
Sample 1 T3
Sample 1 T4
Sample 2 T1
Sample 2 T2
Sample 2 T3
Sample 2 T4

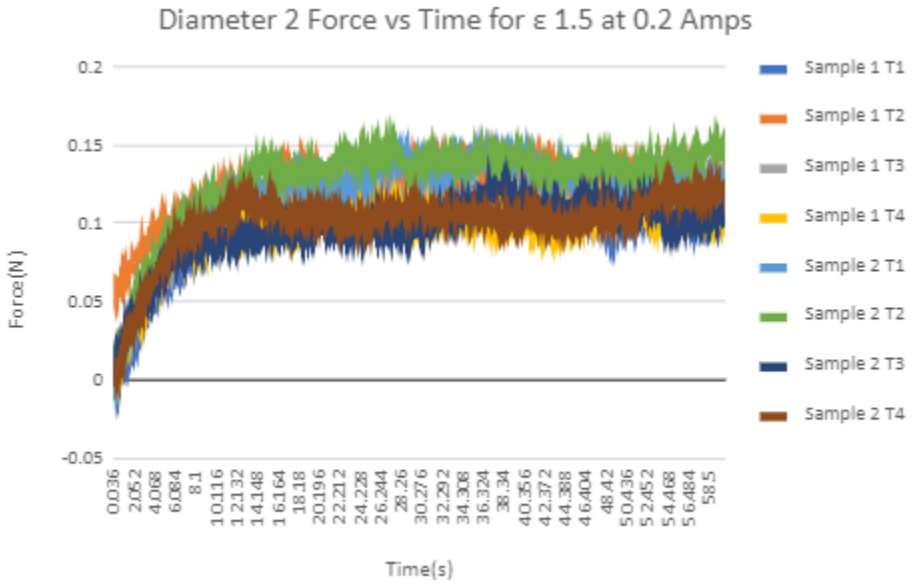
Diameter 2 Force vs Time for ε 1.5 at 0.2 Amps
Force(N)
Time(s)
Sample 1 T1
Sample 1 T2
Sample 1 T3
Sample 1 T4
Sample 2 T1
Sample 2 T2
Sample 2 T3
Sample 2 T4

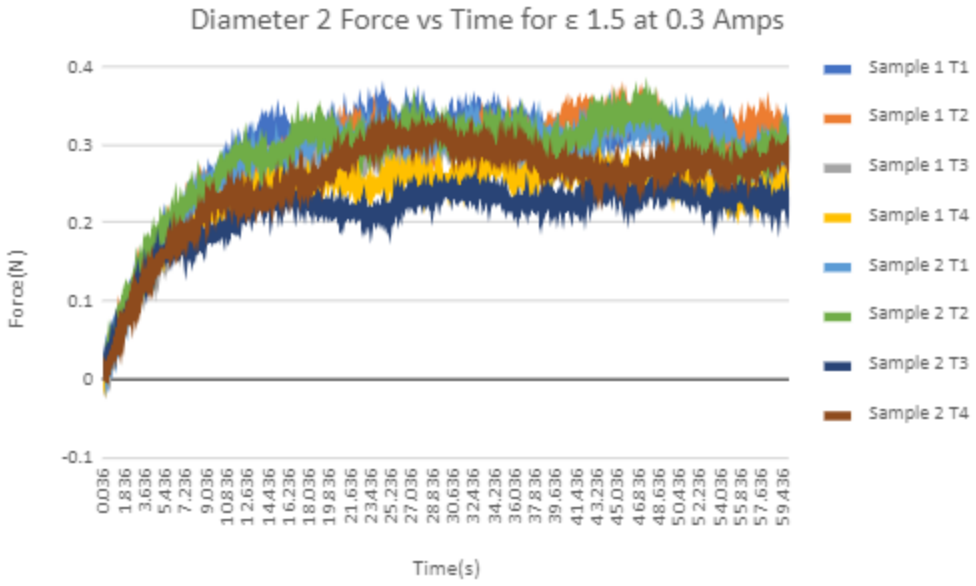
Diameter 2 Force vs Time for ε 1.5 at 0.3 Amps
Force(N)
0.4
0.3
0.2
0.1
0
-0.1
0.036
1.836
3.636
5.436
7.236
9.036
10.836
12.636
14.436
16.236
18.036
19.836
21.636
23.436
25.236
27.036
28.836
30.636
32.436
34.236
36.036
37.836
39.636
41.436
43.236
45.036
46.836
48.636
50.436
52.236
54.036
55.836
57.636
59.436
Time(s)
Sample 1 T1
Sample 1 T2
Sample 1 T3
Sample 1 T4
Sample 2 T1
Sample 2 T2
Sample 2 T3
Sample 2 T4

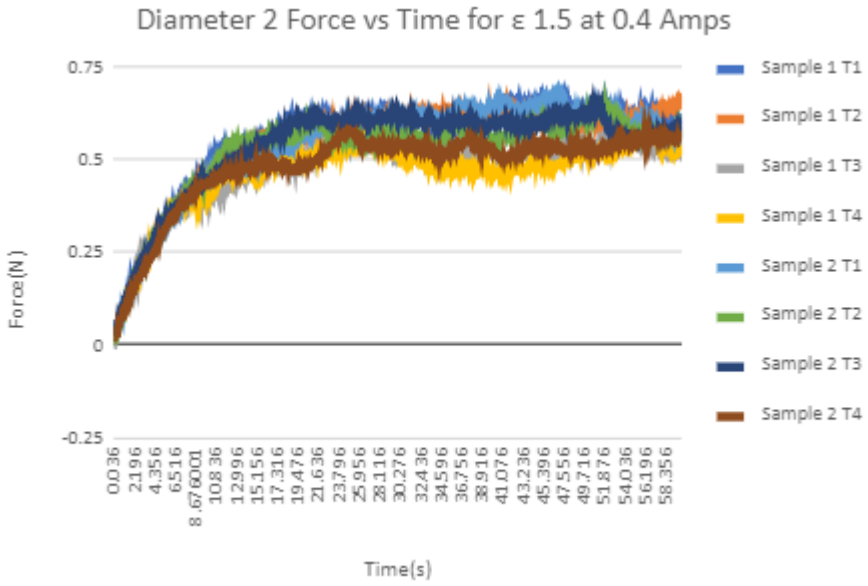
Diameter 2 Force vs Time for ε 1.5 at 0.4 Amps
Force(N)
0.75
0.5
0.25
0
-0.25
0.036
2.196
4.356
6.516
8.676001
10.836
12.996
15.156
17.316
19.476
21.636
23.796
25.956
28.116
30.276
32.436
34.596
36.756
38.916
41.076
43.236
45.396
47.556
49.716
51.876
54.036
56.196
58.356
Time(s)
Sample 1 T1
Sample 1 T2
Sample 1 T3
Sample 1 T4
Sample 2 T1
Sample 2 T2
Sample 2 T3
Sample 2 T4

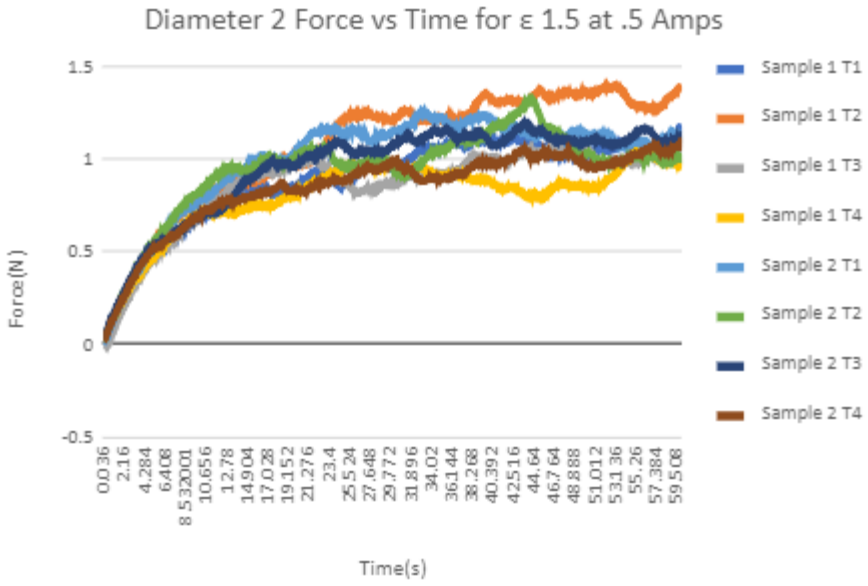
Diameter 2 Force vs Time for ε 1.5 at .5 Amps
Force(N)
Time(s)
Sample 1 T1
Sample 1 T2
Sample 1 T3
Sample 1 T4
Sample 2 T1
Sample 2 T2
Sample 2 T3
Sample 2 T4

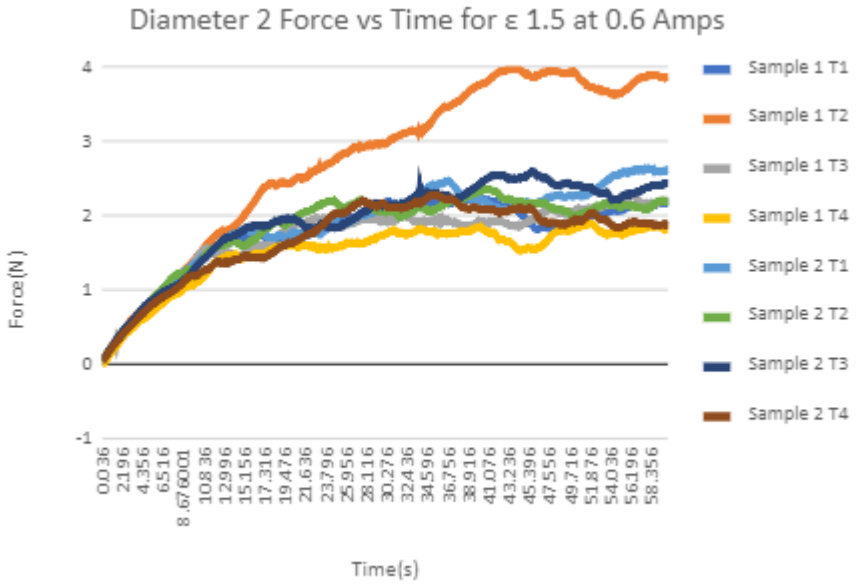
Diameter 2 Force vs Time for ε 1.5 at 0.6 Amps
Force(N)
Time(s)
Sample 1 T1
Sample 1 T2
Sample 1 T3
Sample 1 T4
Sample 2 T1
Sample 2 T2
Sample 2 T3
Sample 2 T4

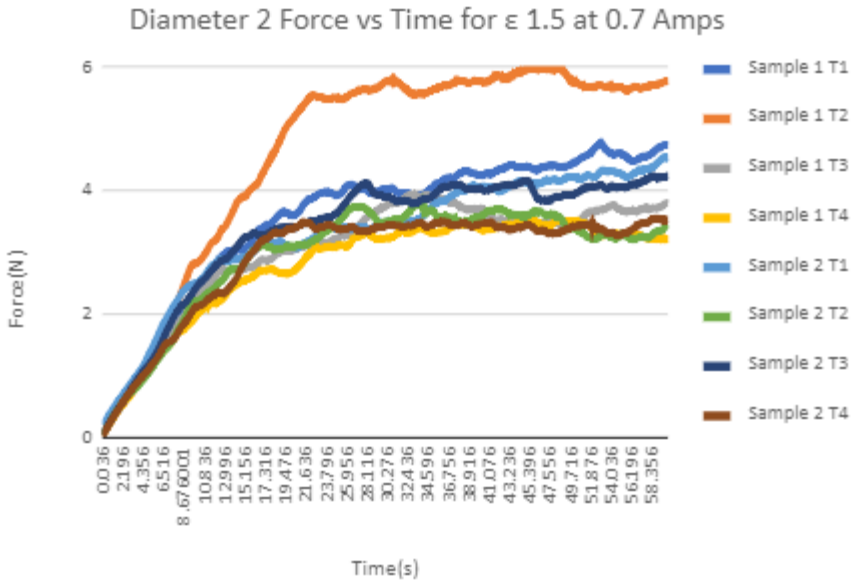
Diameter 2 Force vs Time for ε 1.5 at 0.7 Amps
Force(N)
Time(s)
Sample 1 T1
Sample 1 T2
Sample 1 T3
Sample 1 T4
Sample 2 T1
Sample 2 T2
Sample 2 T3
Sample 2 T4

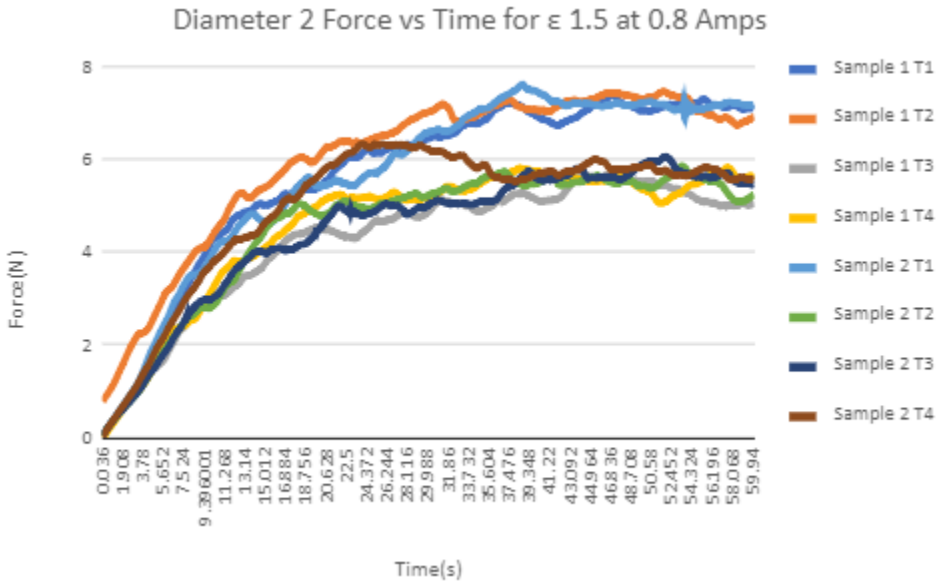
Diameter 2 Force vs Time for ε 1.5 at 0.8 Amps
Force(N)
Time(s)
Sample 1 T1
Sample 1 T2
Sample 1 T3
Sample 1 T4
Sample 2 T1
Sample 2 T2
Sample 2 T3
Sample 2 T4

Force vs. time extensional strain of 2

Diameter 1

Diameter2

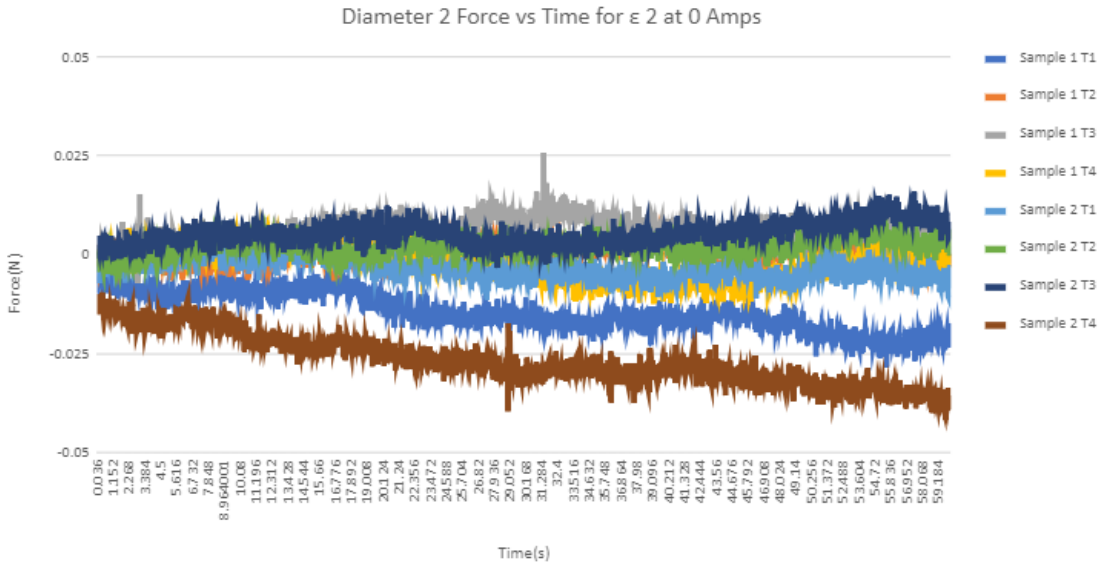

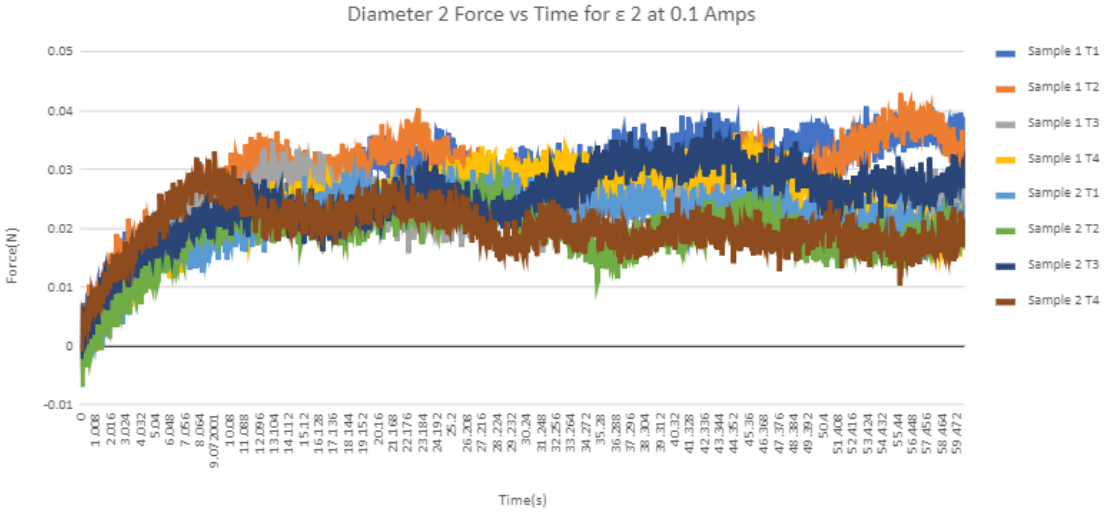

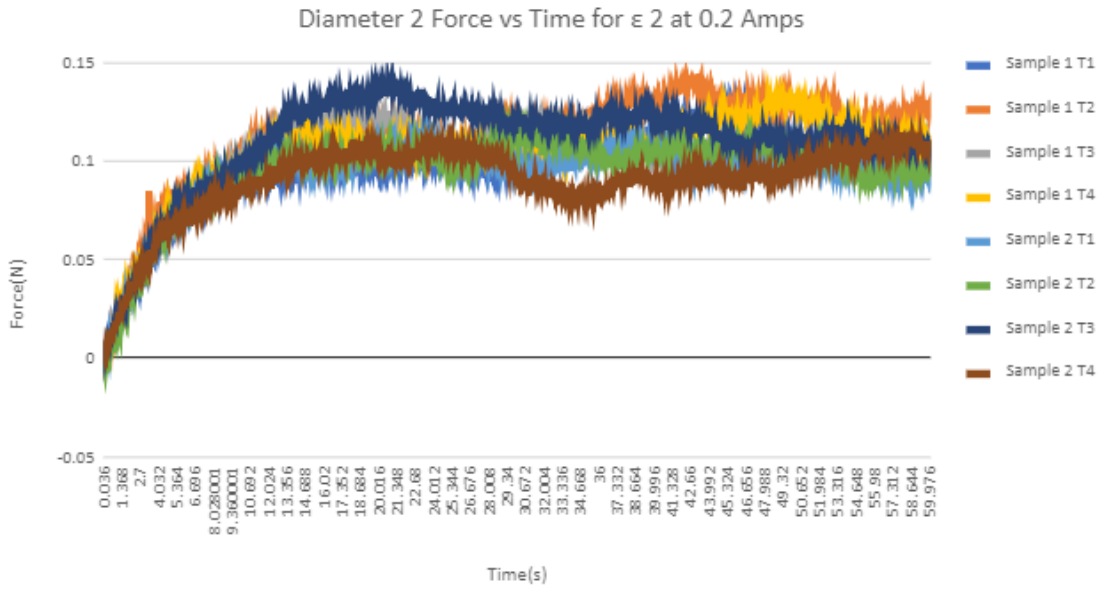
Diameter 2 Force vs Time for ε 2 at 0.2 Amps
Force(N)
Time(s)
Sample 1 T1
Sample 1 T2
Sample 1 T3
Sample 1 T4
Sample 2 T1
Sample 2 T2
Sample 2 T3
Sample 2 T4

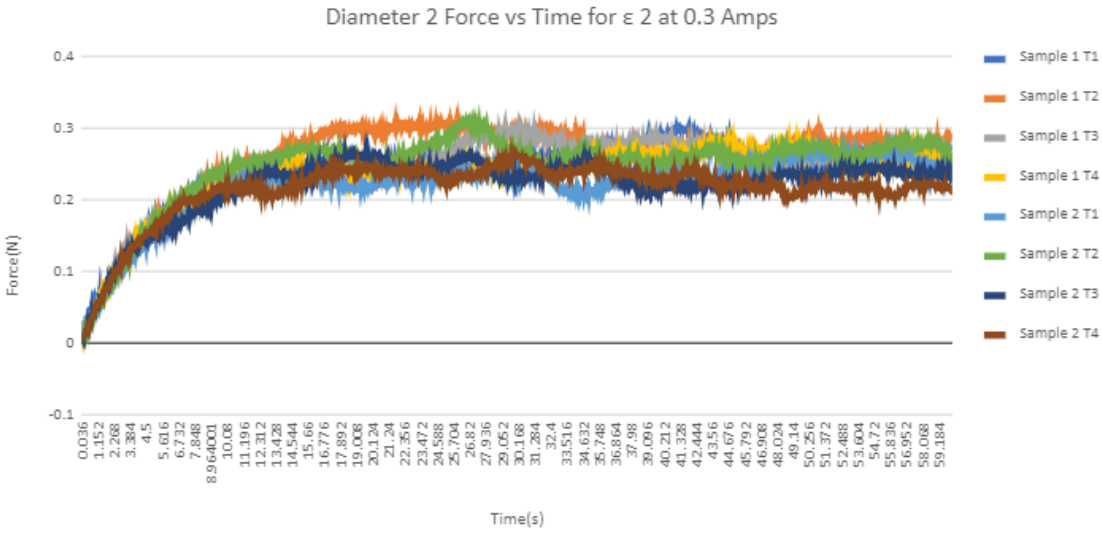
Diameter 2 Force vs Time for ε 2 at 0.3 Amps
Force(N)
Time(s)
Sample 1 T1
Sample 1 T2
Sample 1 T3
Sample 1 T4
Sample 2 T1
Sample 2 T2
Sample 2 T3
Sample 2 T4

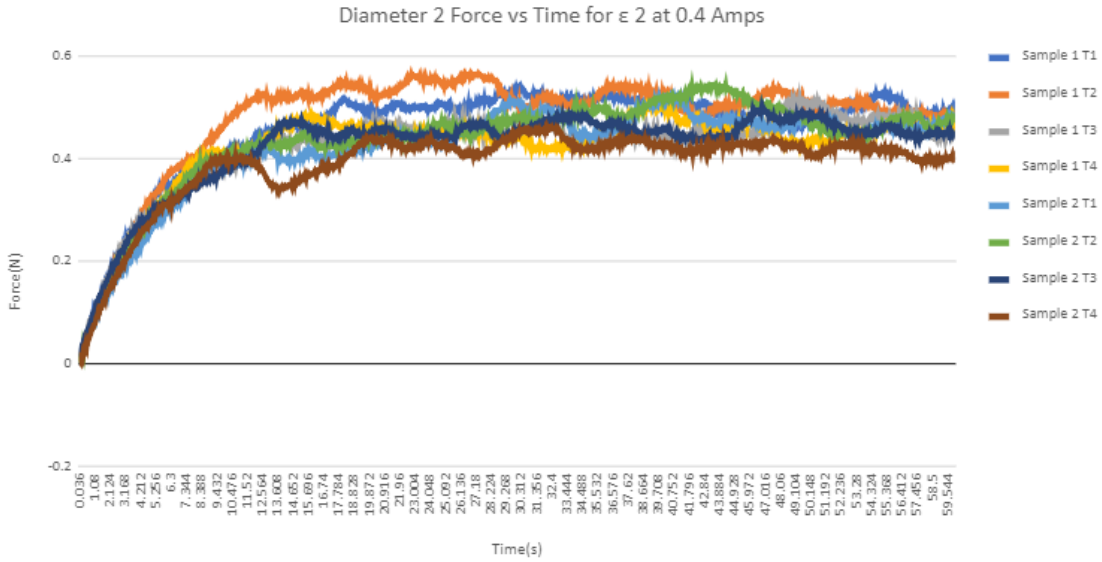
Diameter 2 Force vs Time for ε 2 at 0.4 Amps
Force(N)
Time(s)
Sample 1 T1
Sample 1 T2
Sample 1 T3
Sample 1 T4
Sample 2 T1
Sample 2 T2
Sample 2 T3
Sample 2 T4

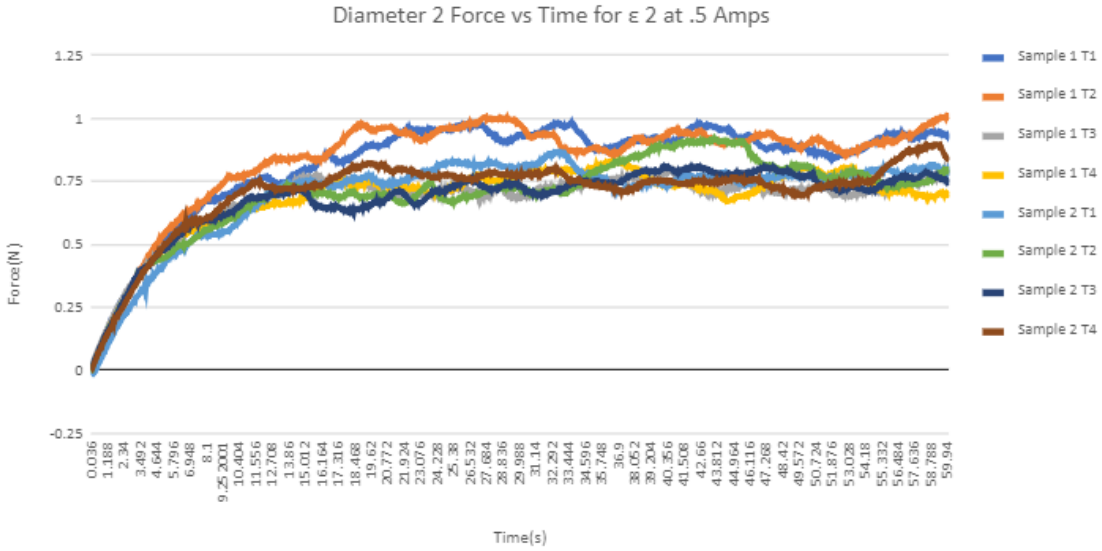
Diameter 2 Force vs Time for ε 2 at .5 Amps
Force(N)
Time(s)
Sample 1 T1
Sample 1 T2
Sample 1 T3
Sample 1 T4
Sample 2 T1
Sample 2 T2
Sample 2 T3
Sample 2 T4

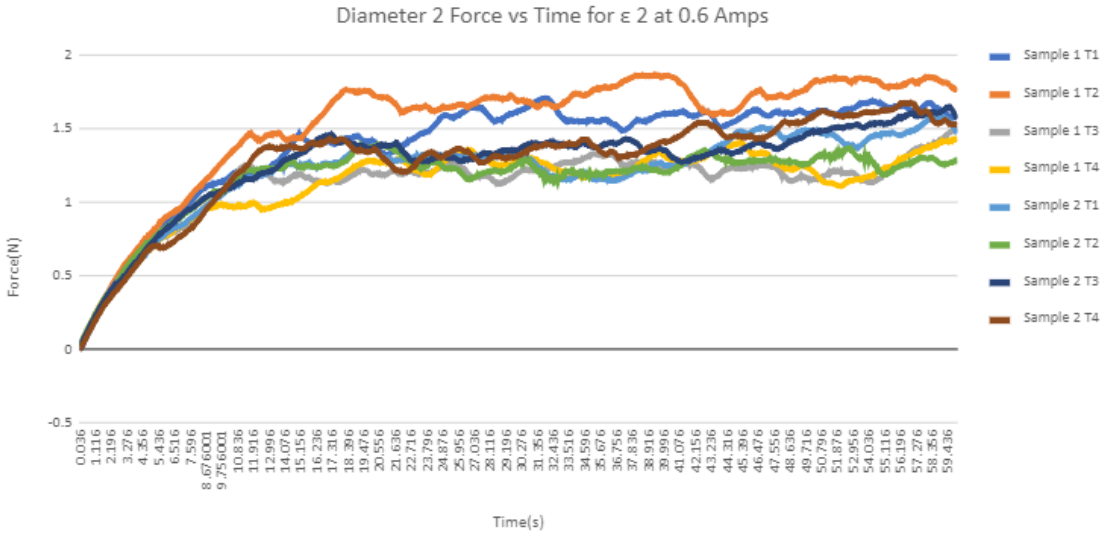
Diameter 2 Force vs Time for ε 2 at 0.6 Amps
Force(N)
Time(s)
Sample 1 T1
Sample 1 T2
Sample 1 T3
Sample 1 T4
Sample 2 T1
Sample 2 T2
Sample 2 T3
Sample 2 T4

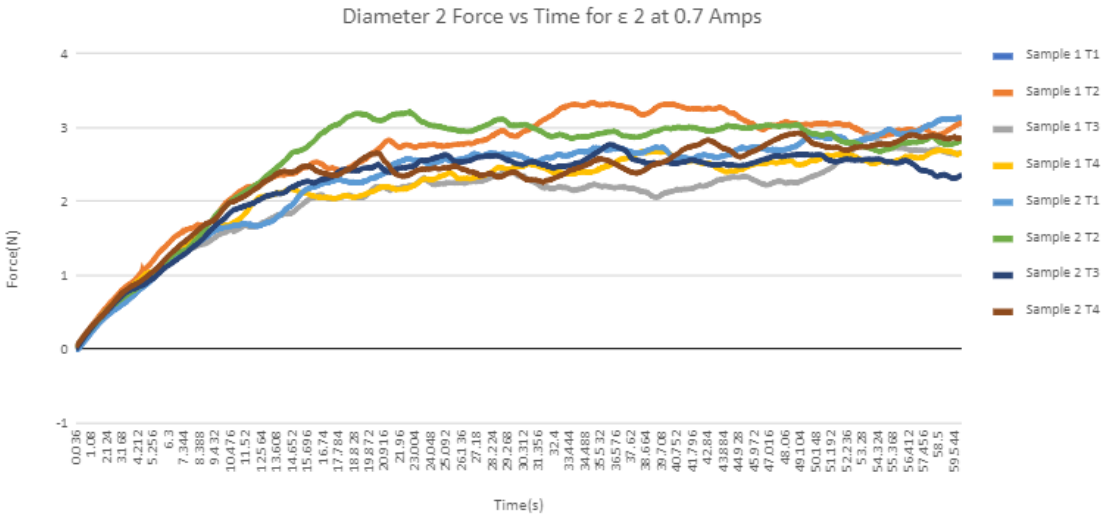
Diameter 2 Force vs Time for ε 2 at 0.7 Amps
Force(N)
Time(s)
Sample 1 T1
Sample 1 T2
Sample 1 T3
Sample 1 T4
Sample 2 T1
Sample 2 T2
Sample 2 T3
Sample 2 T4

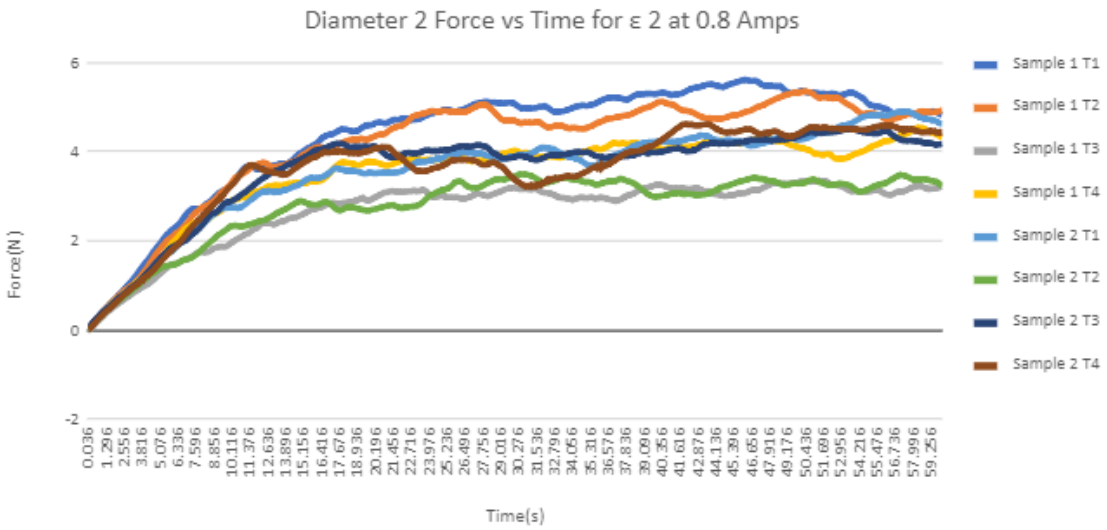

Resistance vs. time for extensional strain of 0

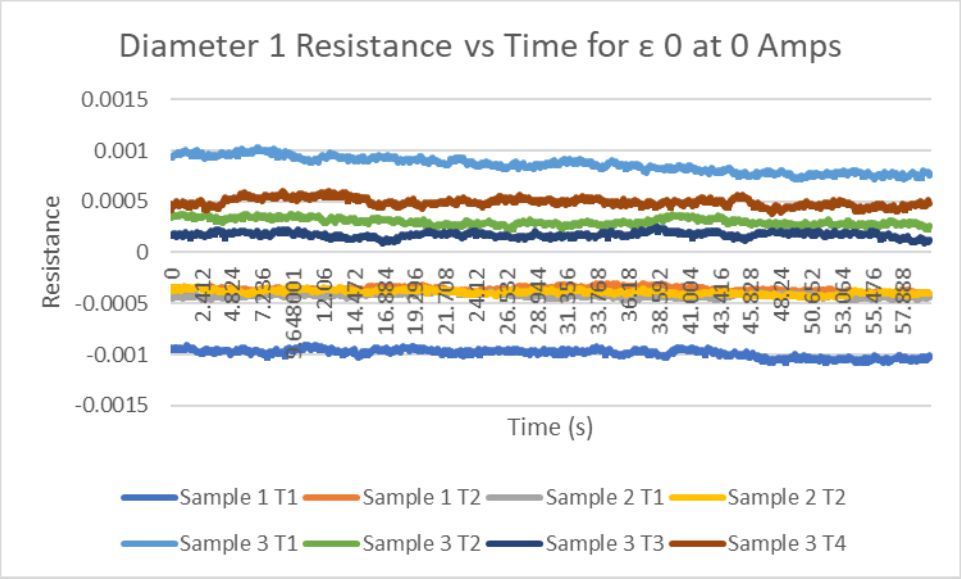
Diameter 1 Resistance vs Time for ε 0 at 0 Amps
Resistance
0.0015
0.001
0.0005
0
-0.0005
-0.001
-0.0015
Time (s)
Sample 1 T1
Sample 1 T2
Sample 2 T1
Sample 2 T2
Sample 3 T1
Sample 3 T2
Sample 3 T3
Sample 3 T4

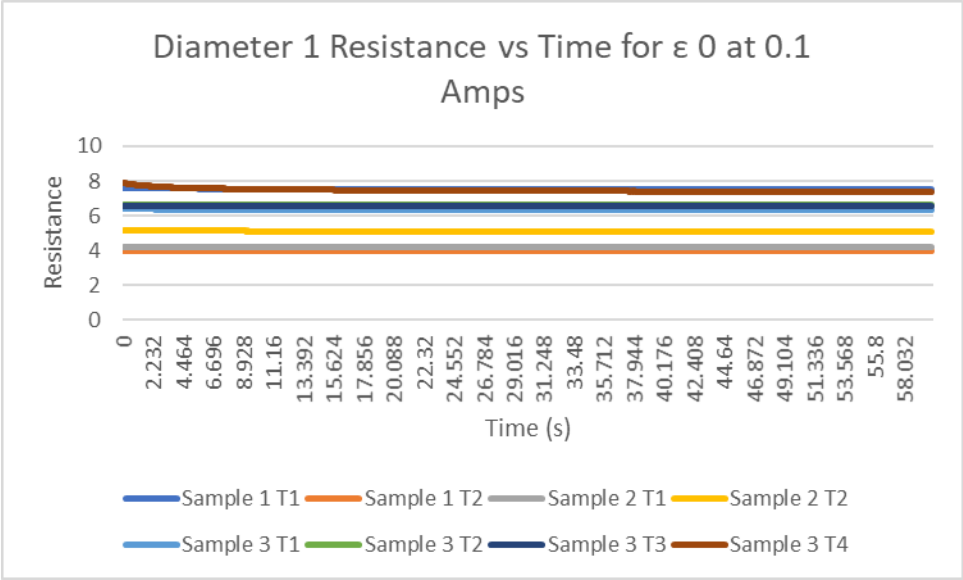
Diameter 1 Resistance vs Time for ε 0 at 0.1 Amps
Resistance
10
8
6
4
2
0
Time (s)
Sample 1 T1
Sample 1 T2
Sample 2 T1
Sample 2 T2
Sample 3 T1
Sample 3 T2
Sample 3 T3
Sample 3 T4

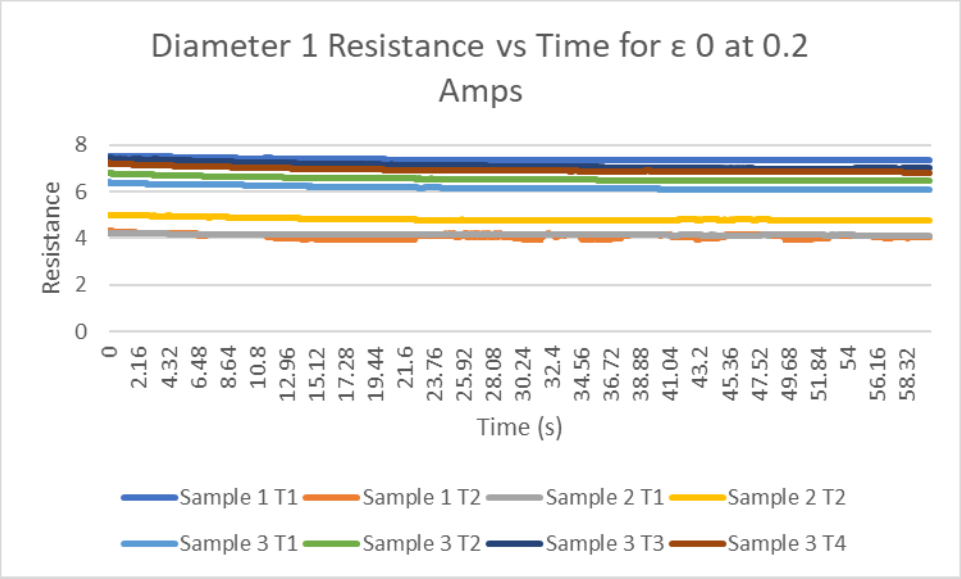
Diameter 1 Resistance vs Time for ε 0 at 0.2 Amps
Resistance
Time (s)
Sample 1 T1
Sample 1 T2
Sample 2 T1
Sample 2 T2
Sample 3 T1
Sample 3 T2
Sample 3 T3
Sample 3 T4

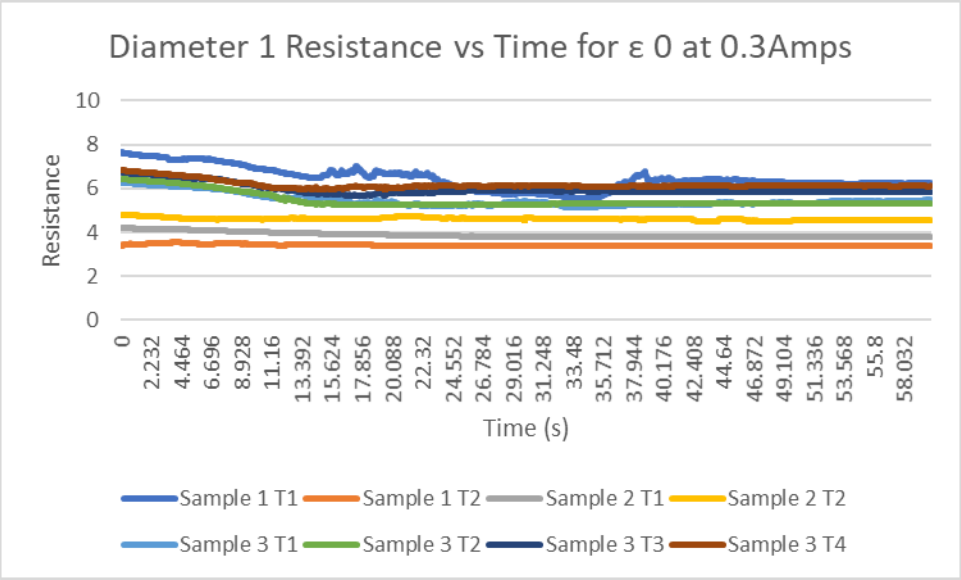
Diameter 1 Resistance vs Time for ε 0 at 0.3Amps
Resistance
Time (s)
Sample 1 T1
Sample 1 T2
Sample 2 T1
Sample 2 T2
Sample 3 T1
Sample 3 T2
Sample 3 T3
Sample 3 T4

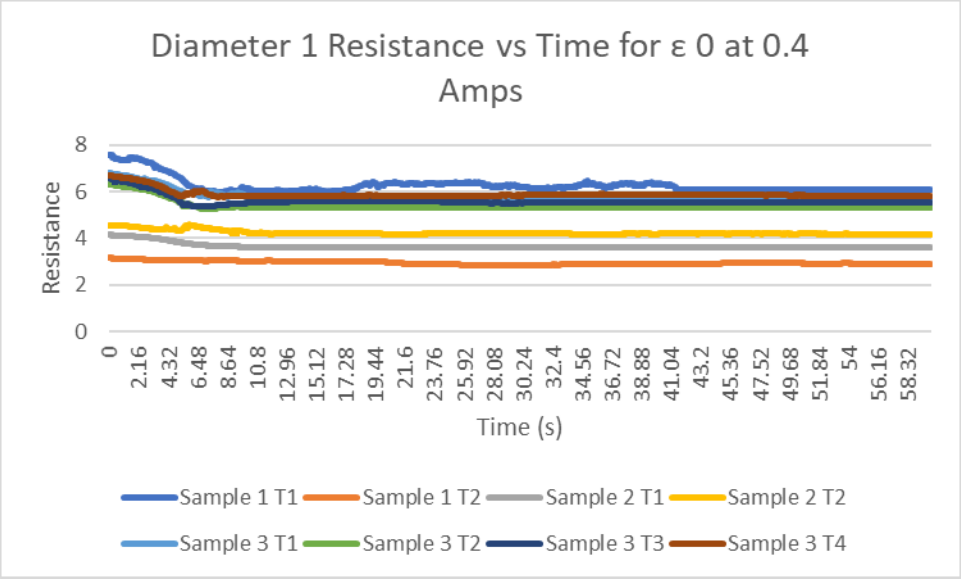
Diameter 1 Resistance vs Time for ε 0 at 0.4 Amps
Resistance
Time (s)
Sample 1 T1
Sample 1 T2
Sample 2 T1
Sample 2 T2
Sample 3 T1
Sample 3 T2
Sample 3 T3
Sample 3 T4

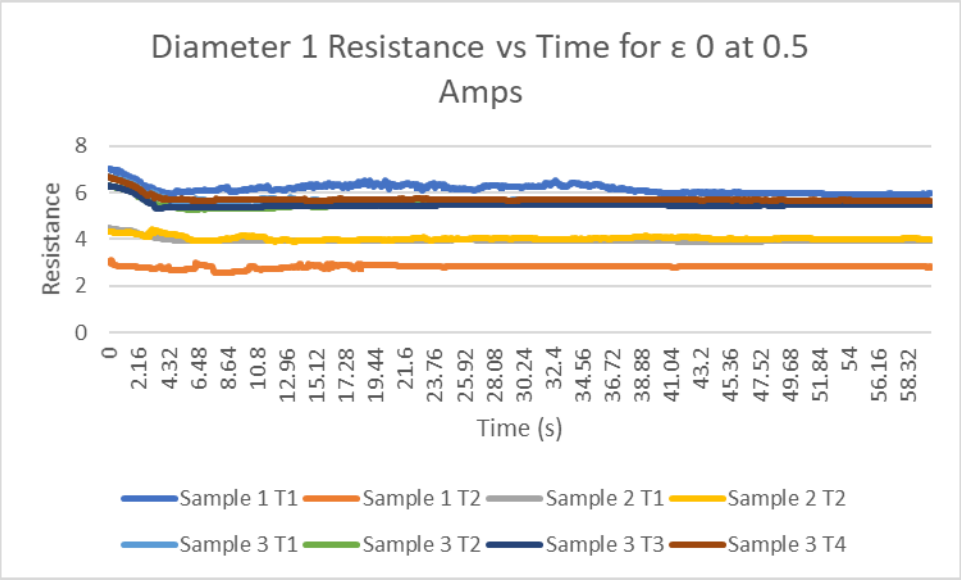
Diameter 1 Resistance vs Time for ε 0 at 0.5 Amps
Resistance
Time (s)
Sample 1 T1
Sample 1 T2
Sample 2 T1
Sample 2 T2
Sample 3 T1
Sample 3 T2
Sample 3 T3
Sample 3 T4

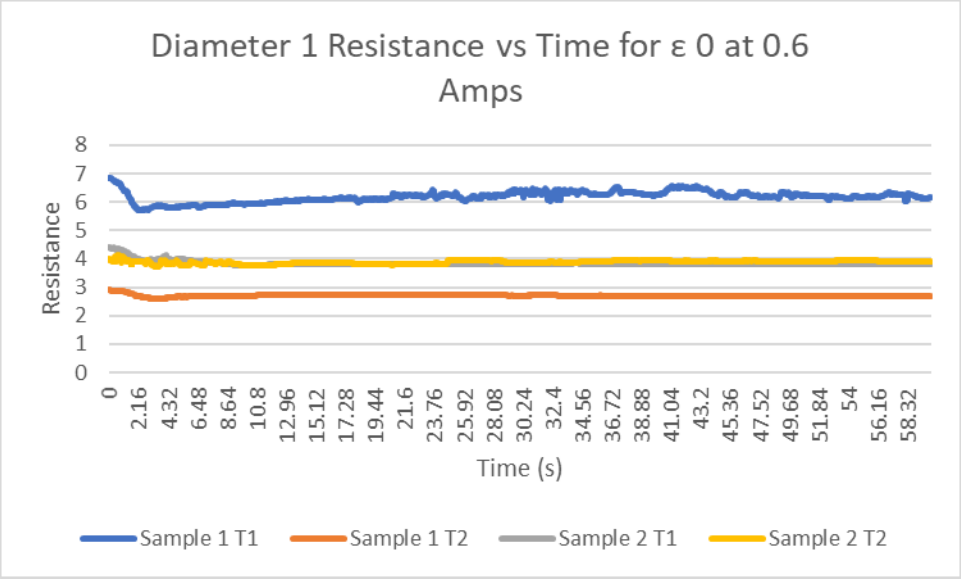
Diameter 1 Resistance vs Time for ε 0 at 0.6 Amps
Resistance
Time (s)
Sample 1 T1
Sample 1 T2
Sample 2 T1
Sample 2 T2

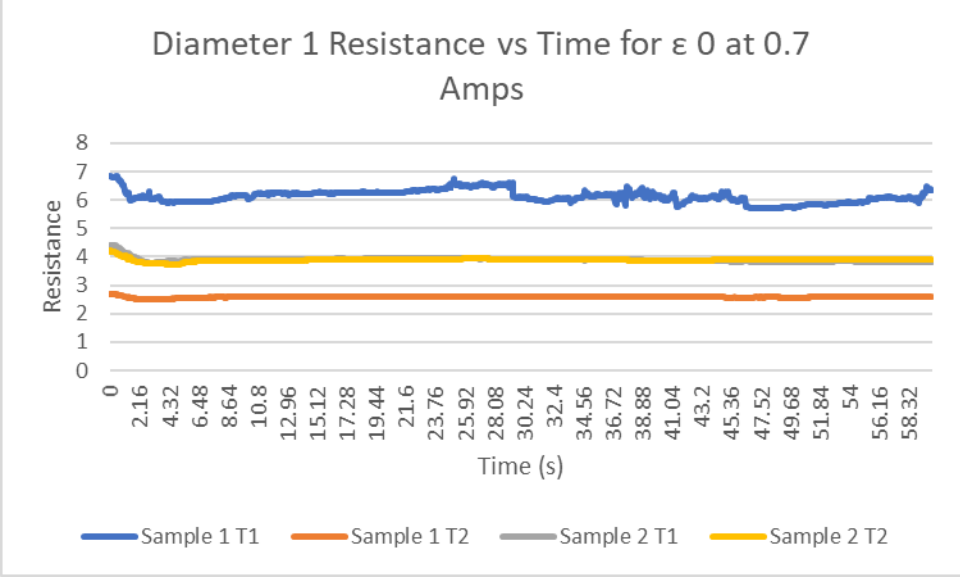
Diameter 1 Resistance vs Time for ε 0 at 0.7 Amps
Resistance
Time (s)
Sample 1 T1
Sample 1 T2
Sample 2 T1
Sample 2 T2

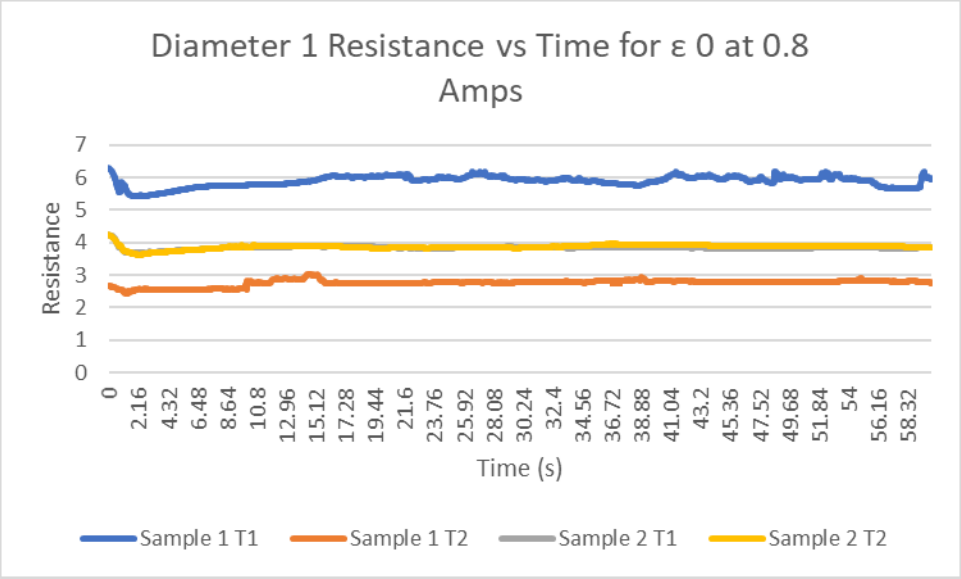
Diameter 1 Resistance vs Time for ε 0 at 0.8 Amps
Resistance
Time (s)
Sample 1 T1
Sample 1 T2
Sample 2 T1
Sample 2 T2

Diameter 2

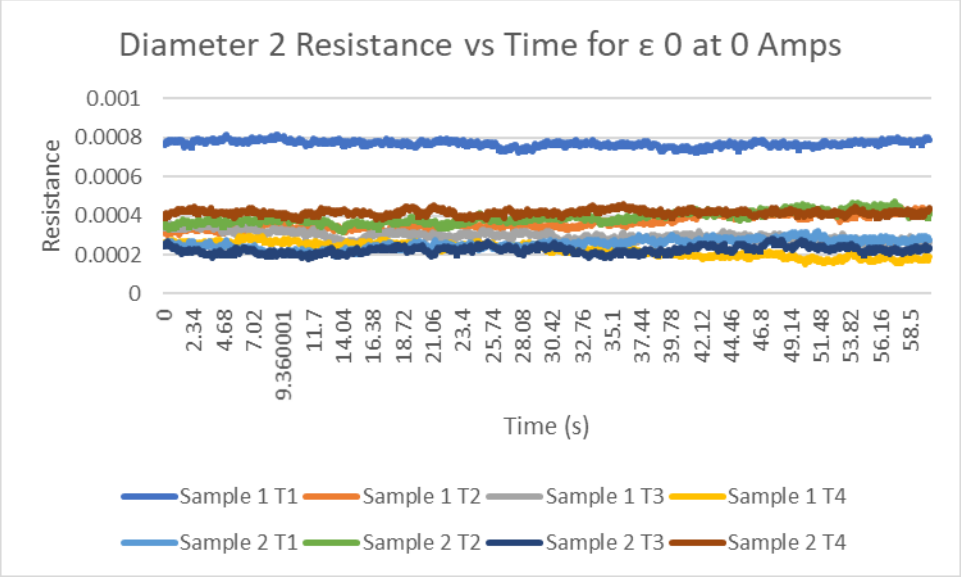
Diameter 2 Resistance vs Time for ε 0 at 0 Amps
Resistance
Time (s)
Sample 1 T1
Sample 1 T2
Sample 1 T3
Sample 1 T4
Sample 2 T1
Sample 2 T2
Sample 2 T3
Sample 2 T4

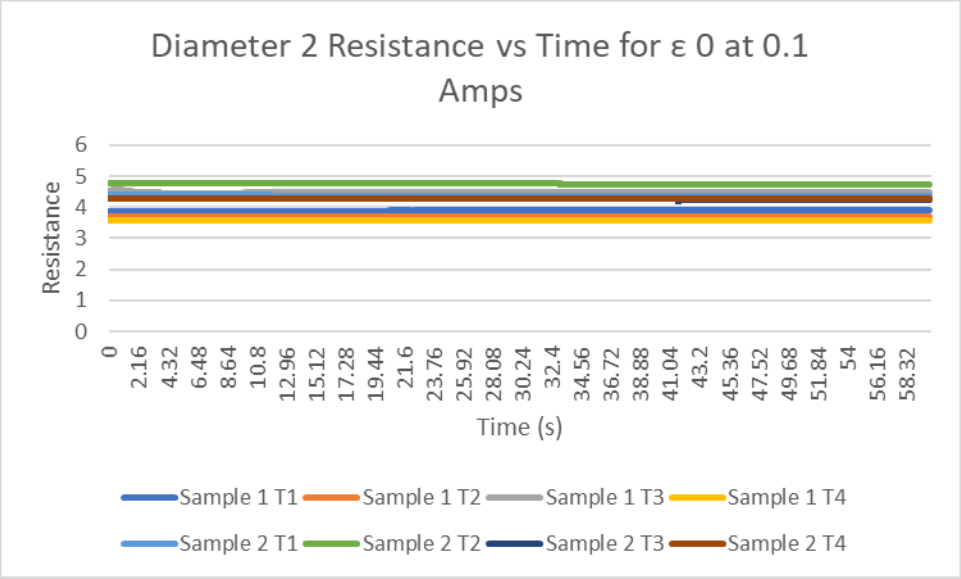
Diameter 2 Resistance vs Time for ε 0 at 0.1 Amps
Resistance
0
1
2
3
4
5
6
0
2.16
4.32
6.48
8.64
10.8
12.96
15.12
17.28
19.44
21.6
23.76
25.92
28.08
30.24
32.4
34.56
36.72
38.88
41.04
43.2
45.36
47.52
49.68
51.84
54
56.16
58.32
Time (s)
Sample 1 T1
Sample 1 T2
Sample 1 T3
Sample 1 T4
Sample 2 T1
Sample 2 T2
Sample 2 T3
Sample 2 T4

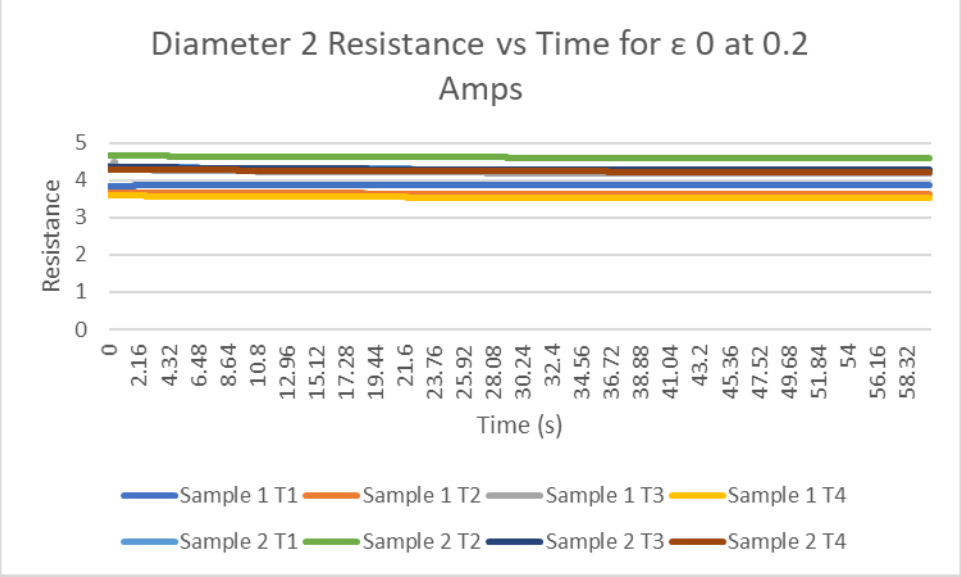
Diameter 2 Resistance vs Time for ε 0 at 0.2 Amps
Resistance
0
1
2
3
4
5
0
2.16
4.32
6.48
8.64
10.8
12.96
15.12
17.28
19.44
21.6
23.76
25.92
28.08
30.24
32.4
34.56
36.72
38.88
41.04
43.2
45.36
47.52
49.68
51.84
54
56.16
58.32
Time (s)
Sample 1 T1
Sample 1 T2
Sample 1 T3
Sample 1 T4
Sample 2 T1
Sample 2 T2
Sample 2 T3
Sample 2 T4

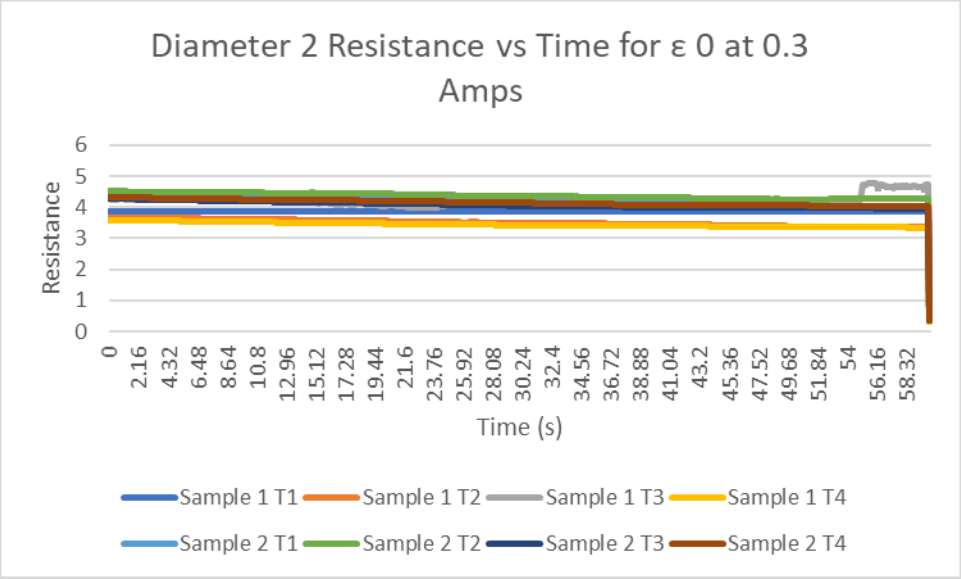
Diameter 2 Resistance vs Time for ε 0 at 0.3 Amps
Resistance
0
1
2
3
4
5
6
0
2.16
4.32
6.48
8.64
10.8
12.96
15.12
17.28
19.44
21.6
23.76
25.92
28.08
30.24
32.4
34.56
36.72
38.88
41.04
43.2
45.36
47.52
49.68
51.84
54
56.16
58.32
Time (s)
Sample 1 T1
Sample 1 T2
Sample 1 T3
Sample 1 T4
Sample 2 T1
Sample 2 T2
Sample 2 T3
Sample 2 T4

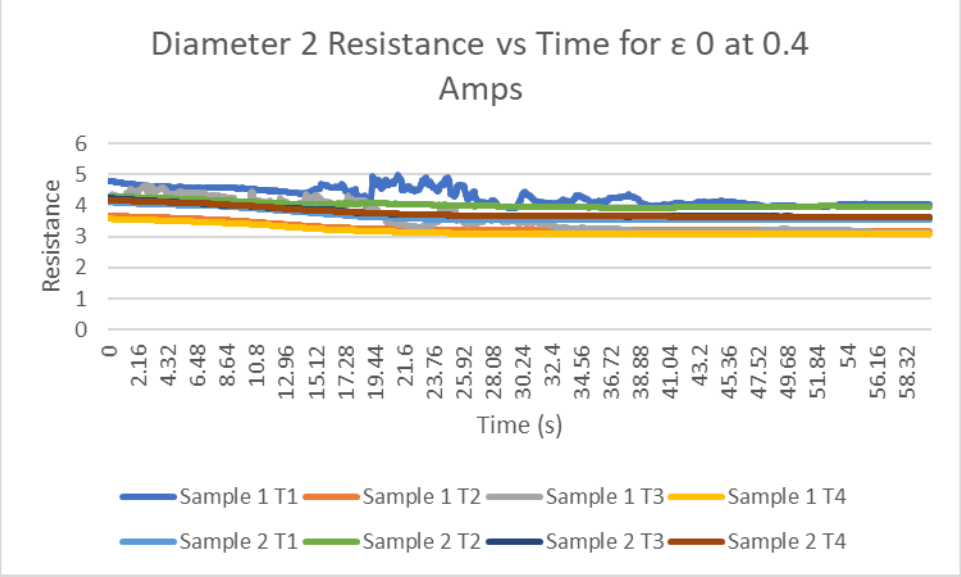
Diameter 2 Resistance vs Time for ε 0 at 0.4 Amps
Resistance
0
1
2
3
4
5
6
0
2.16
4.32
6.48
8.64
10.8
12.96
15.12
17.28
19.44
21.6
23.76
25.92
28.08
30.24
32.4
34.56
36.72
38.88
41.04
43.2
45.36
47.52
49.68
51.84
54
56.16
58.32
Time (s)
Sample 1 T1
Sample 1 T2
Sample 1 T3
Sample 1 T4
Sample 2 T1
Sample 2 T2
Sample 2 T3
Sample 2 T4

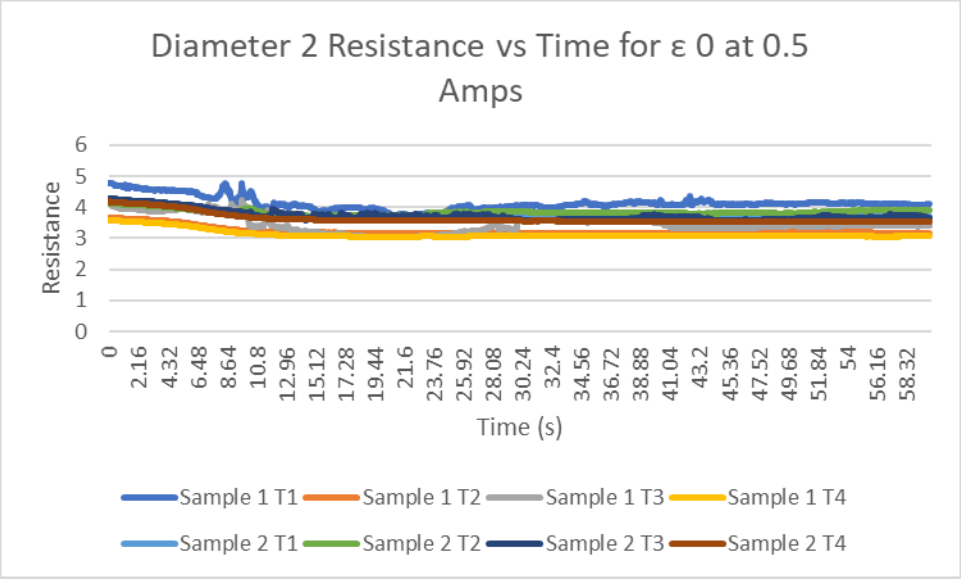
Diameter 2 Resistance vs Time for ε 0 at 0.5 Amps
Resistance
0
1
2
3
4
5
6
0
2.16
4.32
6.48
8.64
10.8
12.96
15.12
17.28
19.44
21.6
23.76
25.92
28.08
30.24
32.4
34.56
36.72
38.88
41.04
43.2
45.36
47.52
49.68
51.84
54
56.16
58.32
Time (s)
Sample 1 T1
Sample 1 T2
Sample 1 T3
Sample 1 T4
Sample 2 T1
Sample 2 T2
Sample 2 T3
Sample 2 T4

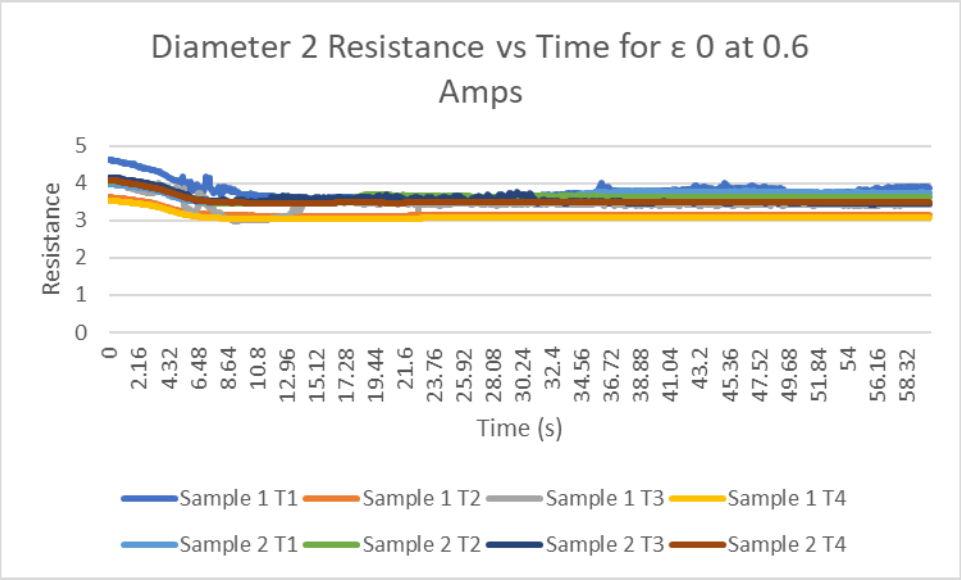
Diameter 2 Resistance vs Time for ε 0 at 0.6 Amps
Resistance
0
1
2
3
4
5
0
2.16
4.32
6.48
8.64
10.8
12.96
15.12
17.28
19.44
21.6
23.76
25.92
28.08
30.24
32.4
34.56
36.72
38.88
41.04
43.2
45.36
47.52
49.68
51.84
54
56.16
58.32
Time (s)
Sample 1 T1
Sample 1 T2
Sample 1 T3
Sample 1 T4
Sample 2 T1
Sample 2 T2
Sample 2 T3
Sample 2 T4

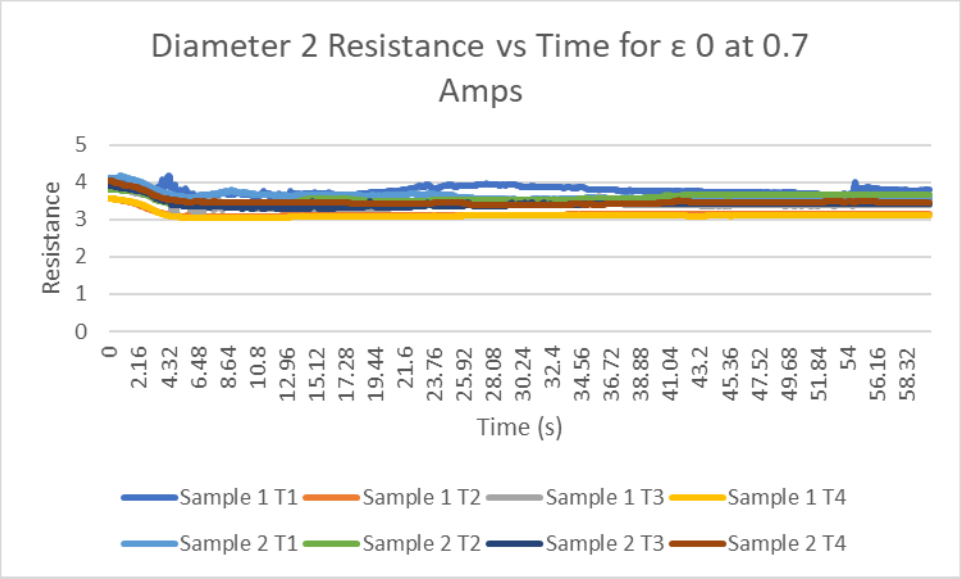

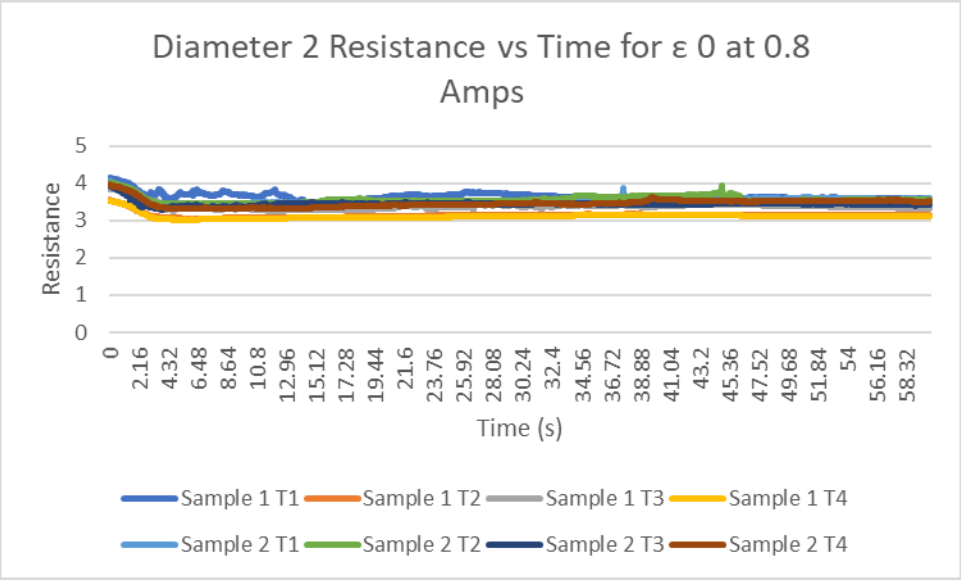

Resistance vs. time for extensional strain of 0.5

Diameter 1

Diameter 2

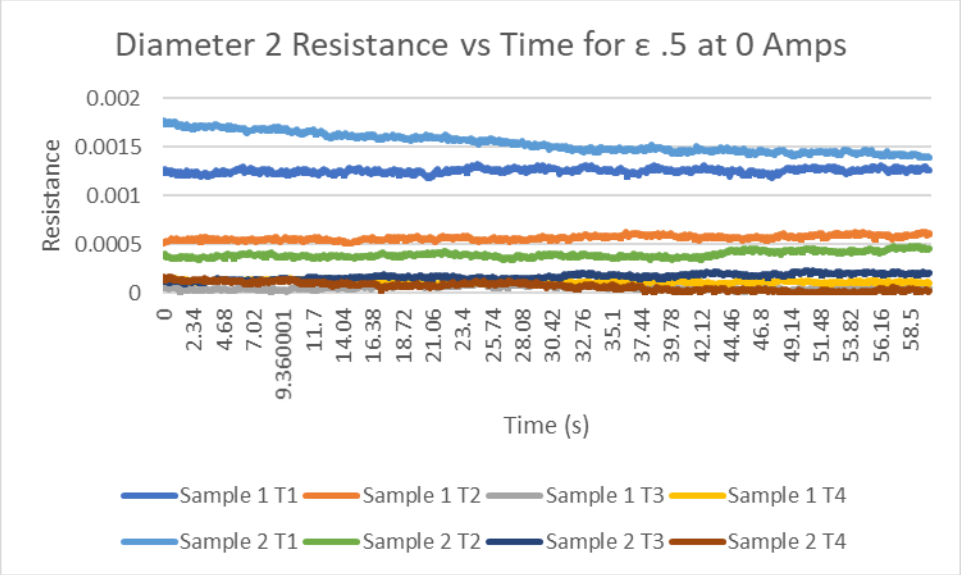
Diameter 2 Resistance vs Time for ε .5 at 0 Amps
Resistance
0.002
0.0015
0.001
0.0005
0
0
2.34
4.68
7.02
9.360001
11.7
14.04
16.38
18.72
21.06
23.4
25.74
28.08
30.42
32.76
35.1
37.44
39.78
42.12
44.46
46.8
49.14
51.48
53.82
56.16
58.5
Time (s)
Sample 1 T1
Sample 1 T2
Sample 1 T3
Sample 1 T4
Sample 2 T1
Sample 2 T2
Sample 2 T3
Sample 2 T4

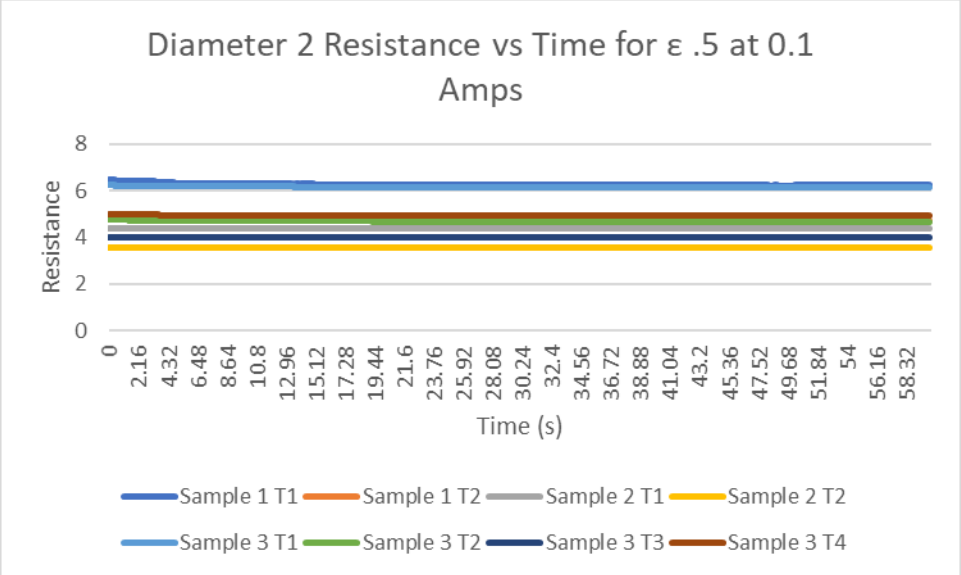
Diameter 2 Resistance vs Time for ε .5 at 0.1 Amps
Resistance
8
6
4
2
0
0
2.16
4.32
6.48
8.64
10.8
12.96
15.12
17.28
19.44
21.6
23.76
25.92
28.08
30.24
32.4
34.56
36.72
38.88
41.04
43.2
45.36
47.52
49.68
51.84
54
56.16
58.32
Time (s)
Sample 1 T1
Sample 1 T2
Sample 2 T1
Sample 2 T2
Sample 3 T1
Sample 3 T2
Sample 3 T3
Sample 3 T4

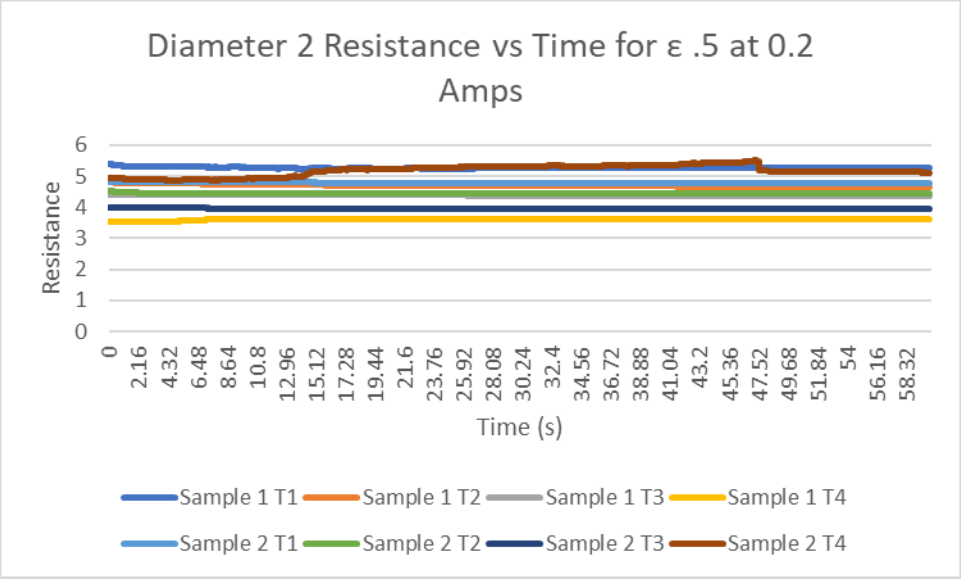
Diameter 2 Resistance vs Time for ε .5 at 0.2 Amps
Resistance
0
1
2
3
4
5
6
0
2.16
4.32
6.48
8.64
10.8
12.96
15.12
17.28
19.44
21.6
23.76
25.92
28.08
30.24
32.4
34.56
36.72
38.88
41.04
43.2
45.36
47.52
49.68
51.84
54
56.16
58.32
Time (s)
Sample 1 T1
Sample 1 T2
Sample 1 T3
Sample 1 T4
Sample 2 T1
Sample 2 T2
Sample 2 T3
Sample 2 T4

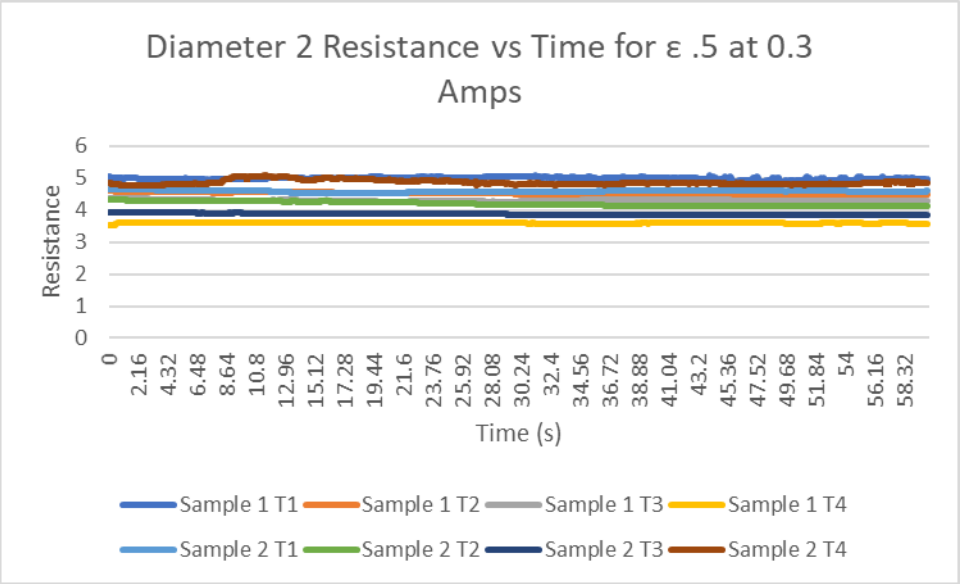
Diameter 2 Resistance vs Time for ε .5 at 0.3 Amps
Resistance
0
1
2
3
4
5
6
0
2.16
4.32
6.48
8.64
10.8
12.96
15.12
17.28
19.44
21.6
23.76
25.92
28.08
30.24
32.4
34.56
36.72
38.88
41.04
43.2
45.36
47.52
49.68
51.84
54
56.16
58.32
Time (s)
Sample 1 T1
Sample 1 T2
Sample 1 T3
Sample 1 T4
Sample 2 T1
Sample 2 T2
Sample 2 T3
Sample 2 T4

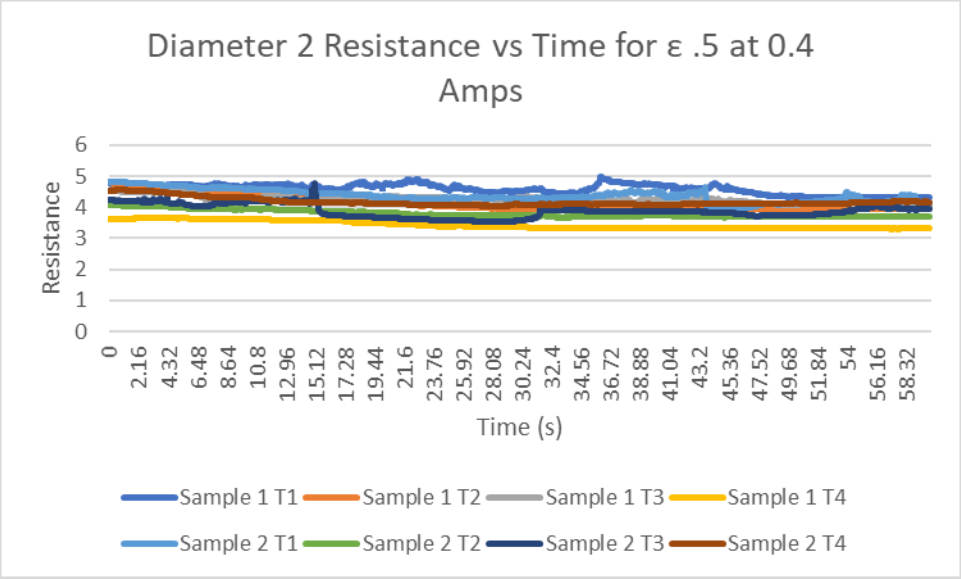
Diameter 2 Resistance vs Time for ε .5 at 0.4 Amps
Resistance
0
1
2
3
4
5
6
0
2.16
4.32
6.48
8.64
10.8
12.96
15.12
17.28
19.44
21.6
23.76
25.92
28.08
30.24
32.4
34.56
36.72
38.88
41.04
43.2
45.36
47.52
49.68
51.84
54
56.16
58.32
Time (s)
Sample 1 T1
Sample 1 T2
Sample 1 T3
Sample 1 T4
Sample 2 T1
Sample 2 T2
Sample 2 T3
Sample 2 T4

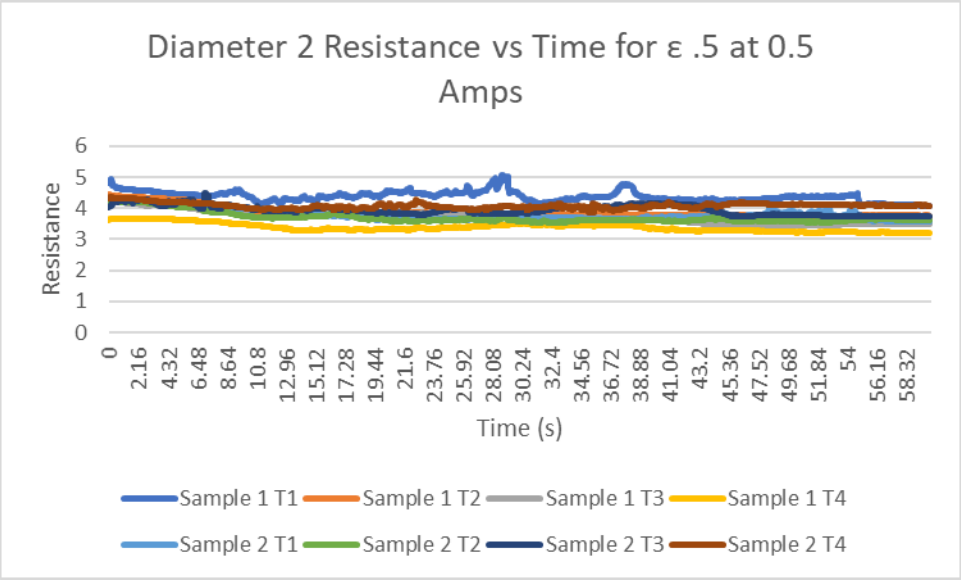
Diameter 2 Resistance vs Time for ε .5 at 0.5 Amps
Resistance
0
1
2
3
4
5
6
0
2.16
4.32
6.48
8.64
10.8
12.96
15.12
17.28
19.44
21.6
23.76
25.92
28.08
30.24
32.4
34.56
36.72
38.88
41.04
43.2
45.36
47.52
49.68
51.84
54
56.16
58.32
Time (s)
Sample 1 T1
Sample 1 T2
Sample 1 T3
Sample 1 T4
Sample 2 T1
Sample 2 T2
Sample 2 T3
Sample 2 T4

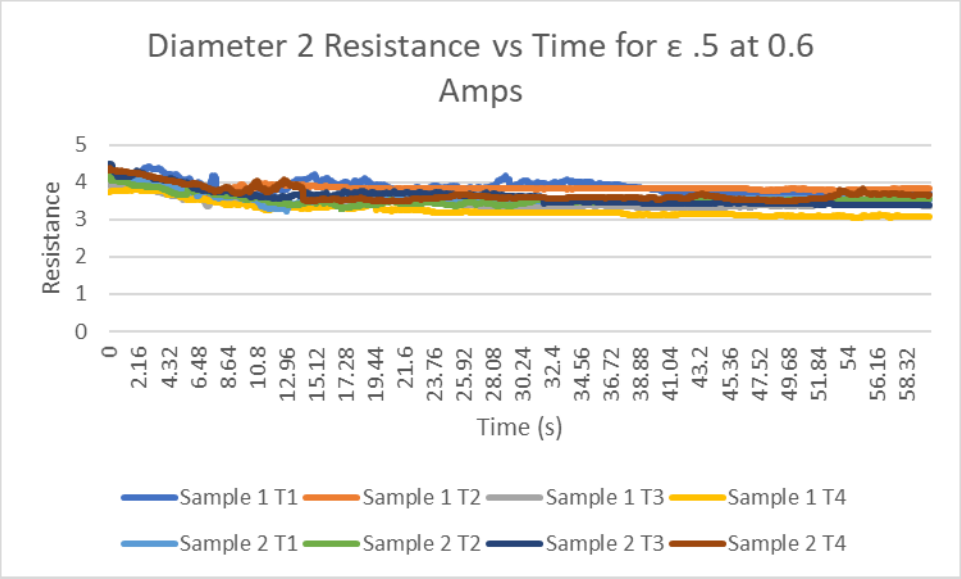
Diameter 2 Resistance vs Time for ε .5 at 0.6 Amps
Resistance
0
1
2
3
4
5
0
2.16
4.32
6.48
8.64
10.8
12.96
15.12
17.28
19.44
21.6
23.76
25.92
28.08
30.24
32.4
34.56
36.72
38.88
41.04
43.2
45.36
47.52
49.68
51.84
54
56.16
58.32
Time (s)
Sample 1 T1
Sample 1 T2
Sample 1 T3
Sample 1 T4
Sample 2 T1
Sample 2 T2
Sample 2 T3
Sample 2 T4

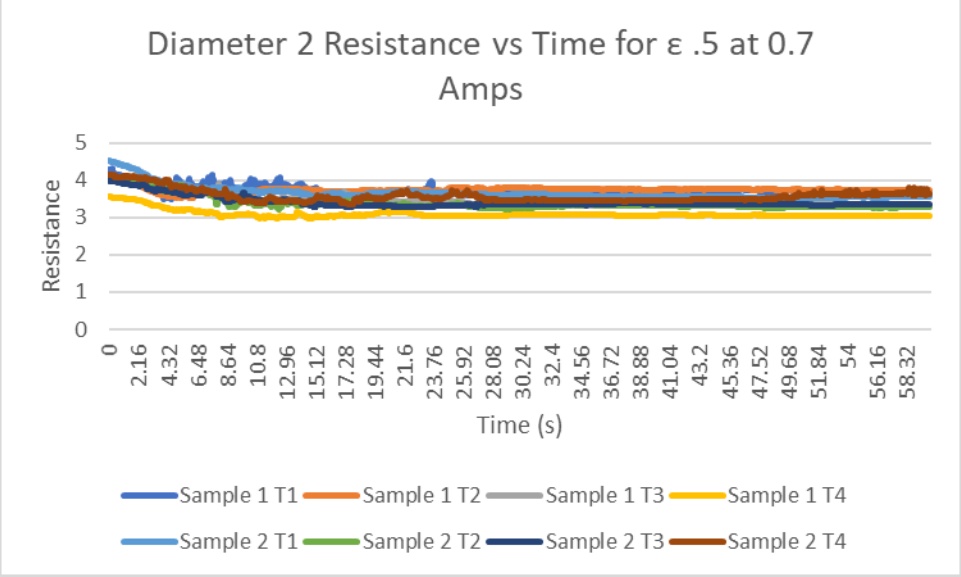
Diameter 2 Resistance vs Time for ε .5 at 0.7 Amps
Resistance
0
1
2
3
4
5
0
2.16
4.32
6.48
8.64
10.8
12.96
15.12
17.28
19.44
21.6
23.76
25.92
28.08
30.24
32.4
34.56
36.72
38.88
41.04
43.2
45.36
47.52
49.68
51.84
54
56.16
58.32
Time (s)
Sample 1 T1
Sample 1 T2
Sample 1 T3
Sample 1 T4
Sample 2 T1
Sample 2 T2
Sample 2 T3
Sample 2 T4

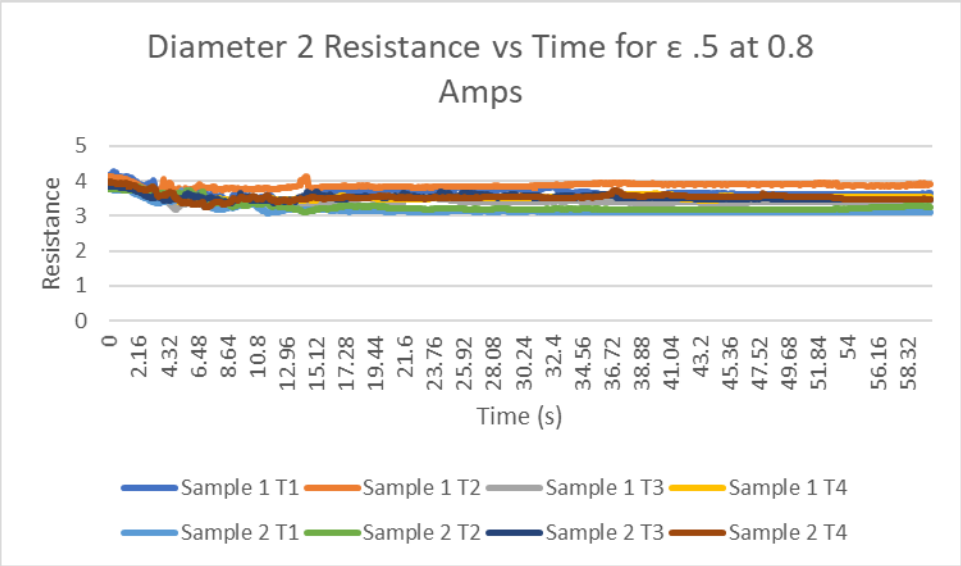

Resistance vs. time for extensional strain of 1

Diameter 1

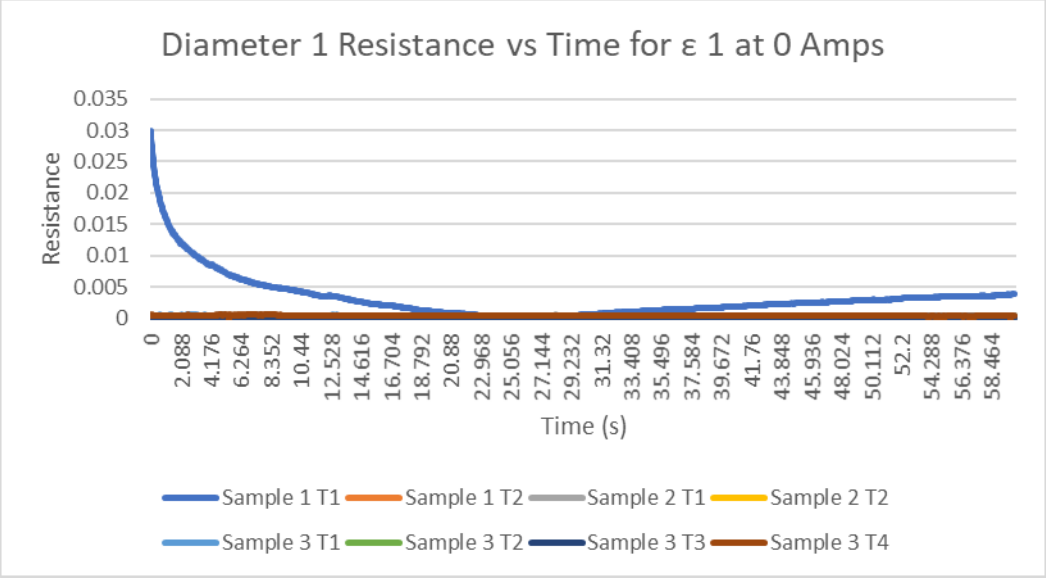

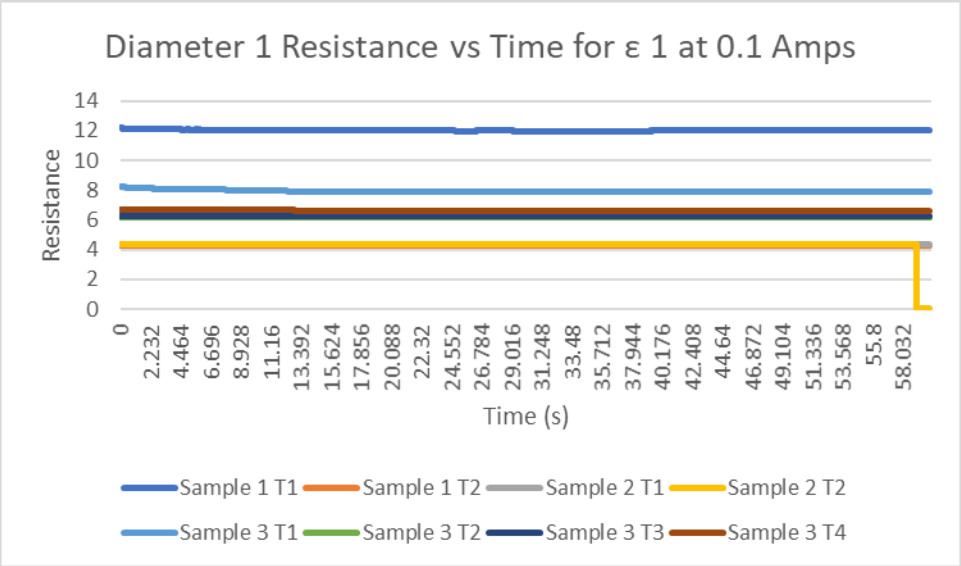
Diameter 1 Resistance vs Time for ε 1 at 0.1 Amps
Resistance
14
12
10
8
6
4
2
0
0
2.232
4.464
6.696
8.928
11.16
13.392
15.624
17.856
20.088
22.32
24.552
26.784
29.016
31.248
33.48
35.712
37.944
40.176
42.408
44.64
46.872
49.104
51.336
53.568
55.8
58.032
Time (s)
Sample 1 T1
Sample 1 T2
Sample 2 T1
Sample 2 T2
Sample 3 T1
Sample 3 T2
Sample 3 T3
Sample 3 T4

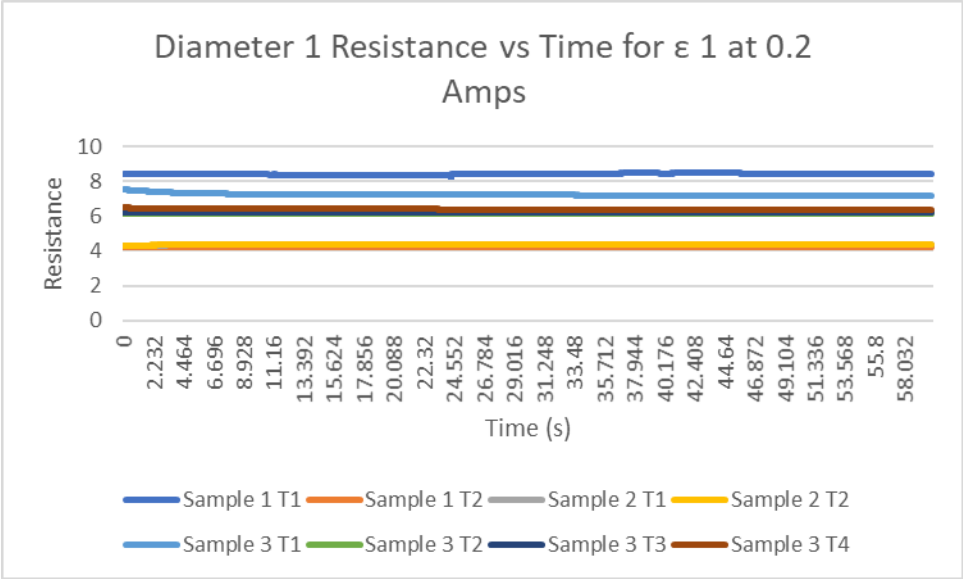
Diameter 1 Resistance vs Time for ε 1 at 0.2 Amps
Resistance
10
8
6
4
2
0
0
2.232
4.464
6.696
8.928
11.16
13.392
15.624
17.856
20.088
22.32
24.552
26.784
29.016
31.248
33.48
35.712
37.944
40.176
42.408
44.64
46.872
49.104
51.336
53.568
55.8
58.032
Time (s)
Sample 1 T1
Sample 1 T2
Sample 2 T1
Sample 2 T2
Sample 3 T1
Sample 3 T2
Sample 3 T3
Sample 3 T4

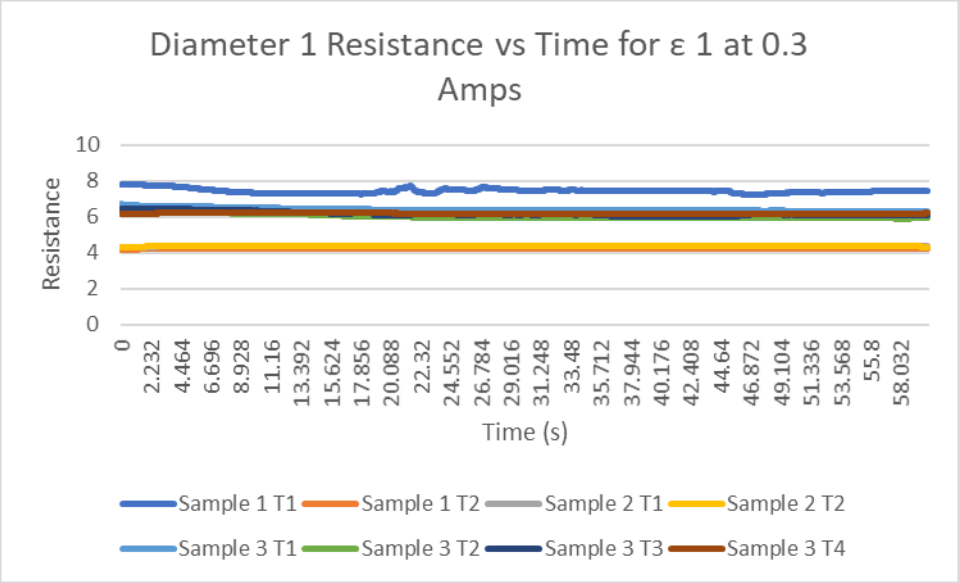
Diameter 1 Resistance vs Time for ε 1 at 0.3 Amps
Resistance
10
8
6
4
2
0
0
2.232
4.464
6.696
8.928
11.16
13.392
15.624
17.856
20.088
22.32
24.552
26.784
29.016
31.248
33.48
35.712
37.944
40.176
42.408
44.64
46.872
49.104
51.336
53.568
55.8
58.032
Time (s)
Sample 1 T1
Sample 1 T2
Sample 2 T1
Sample 2 T2
Sample 3 T1
Sample 3 T2
Sample 3 T3
Sample 3 T4

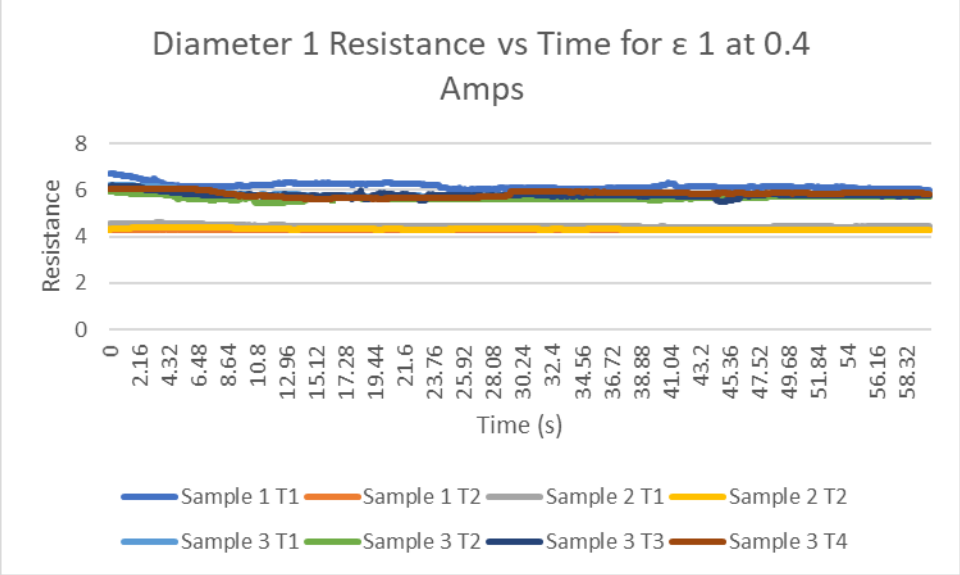
Diameter 1 Resistance vs Time for ε 1 at 0.4 Amps
Resistance
8
6
4
2
0
0
2.16
4.32
6.48
8.64
10.8
12.96
15.12
17.28
19.44
21.6
23.76
25.92
28.08
30.24
32.4
34.56
36.72
38.88
41.04
43.2
45.36
47.52
49.68
51.84
54
56.16
58.32
Time (s)
Sample 1 T1
Sample 1 T2
Sample 2 T1
Sample 2 T2
Sample 3 T1
Sample 3 T2
Sample 3 T3
Sample 3 T4

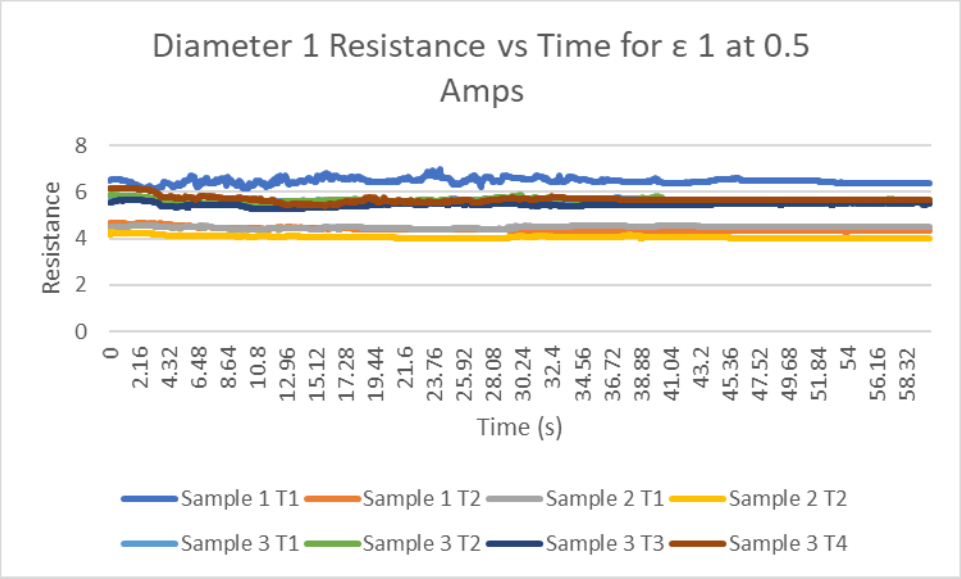
Diameter 1 Resistance vs Time for ε 1 at 0.5 Amps
Resistance
Time (s)
Sample 1 T1
Sample 1 T2
Sample 2 T1
Sample 2 T2
Sample 3 T1
Sample 3 T2
Sample 3 T3
Sample 3 T4

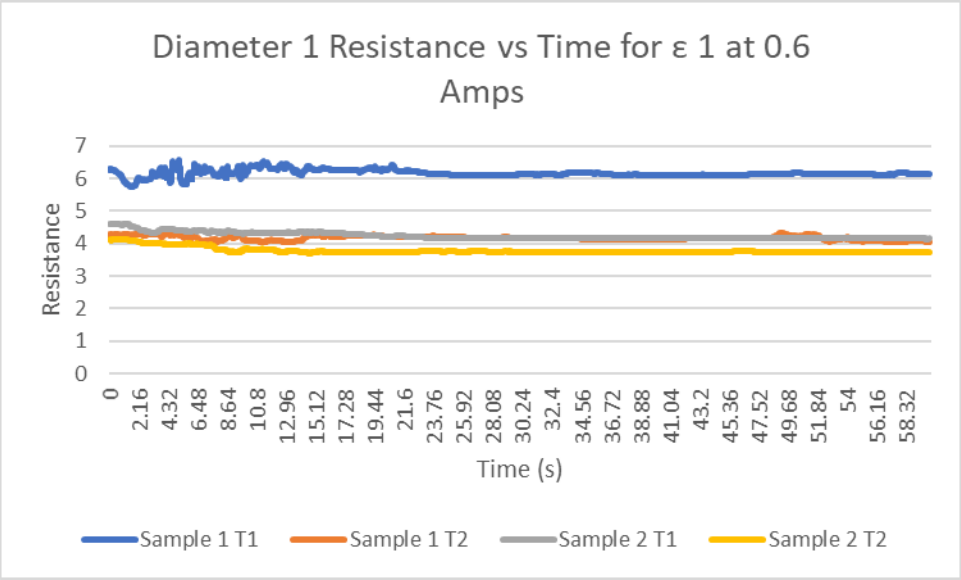
Diameter 1 Resistance vs Time for ε 1 at 0.6 Amps
Resistance
Time (s)
Sample 1 T1
Sample 1 T2
Sample 2 T1
Sample 2 T2

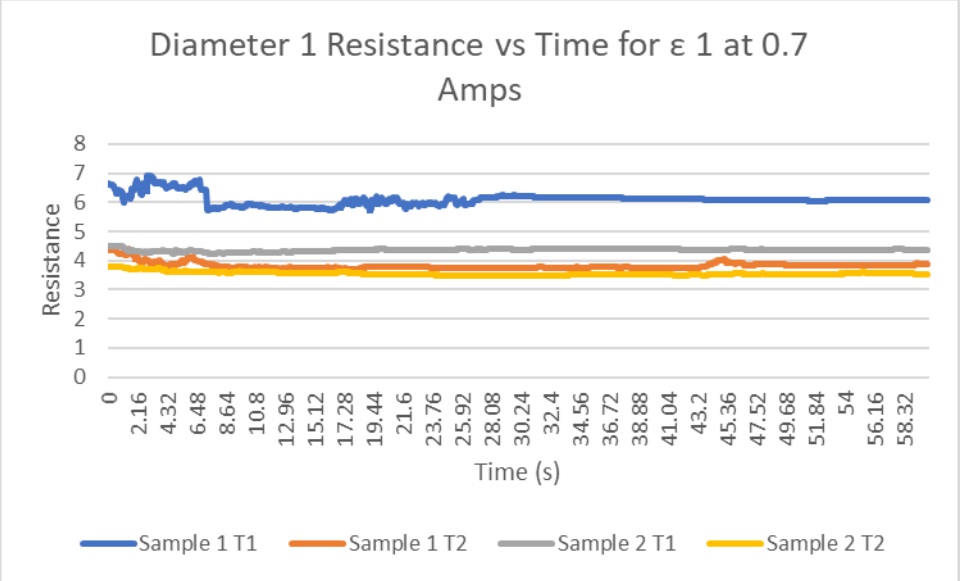
Diameter 1 Resistance vs Time for ε 1 at 0.7 Amps
Resistance
Time (s)
Sample 1 T1
Sample 1 T2
Sample 2 T1
Sample 2 T2

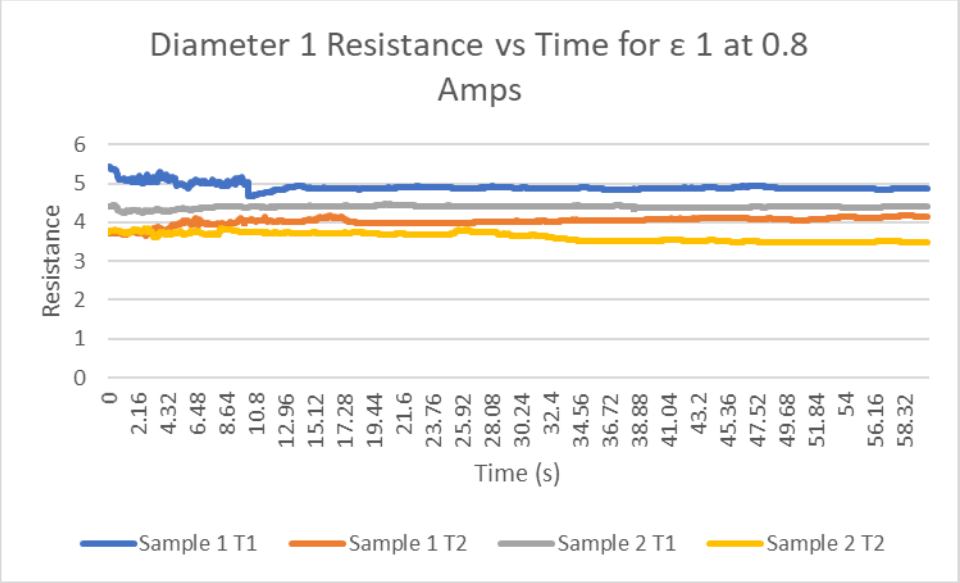
Diameter 1 Resistance vs Time for ε 1 at 0.8 Amps
Resistance
Time (s)
Sample 1 T1
Sample 1 T2
Sample 2 T1
Sample 2 T2

Resistance vs. time for extensional strain of 1.5

Diameter1

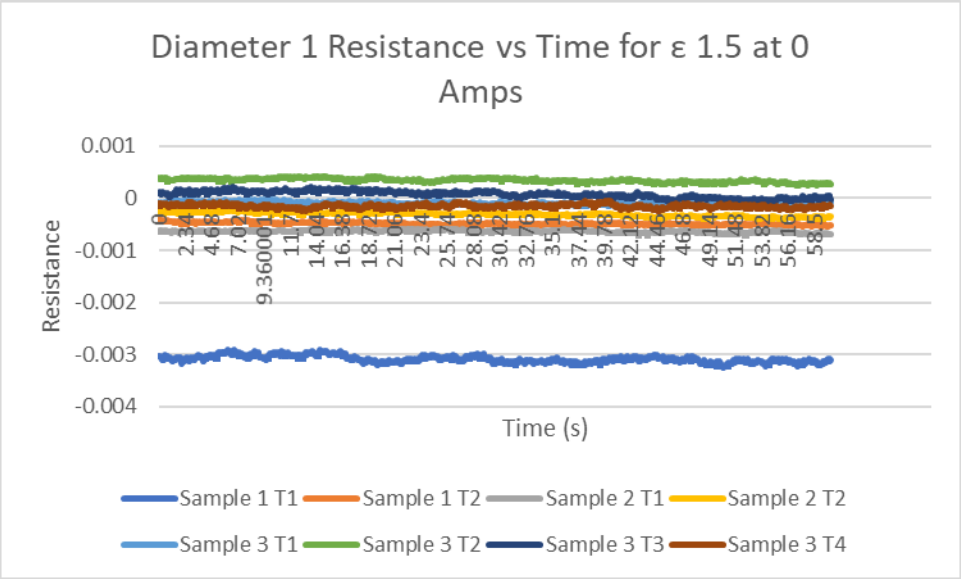

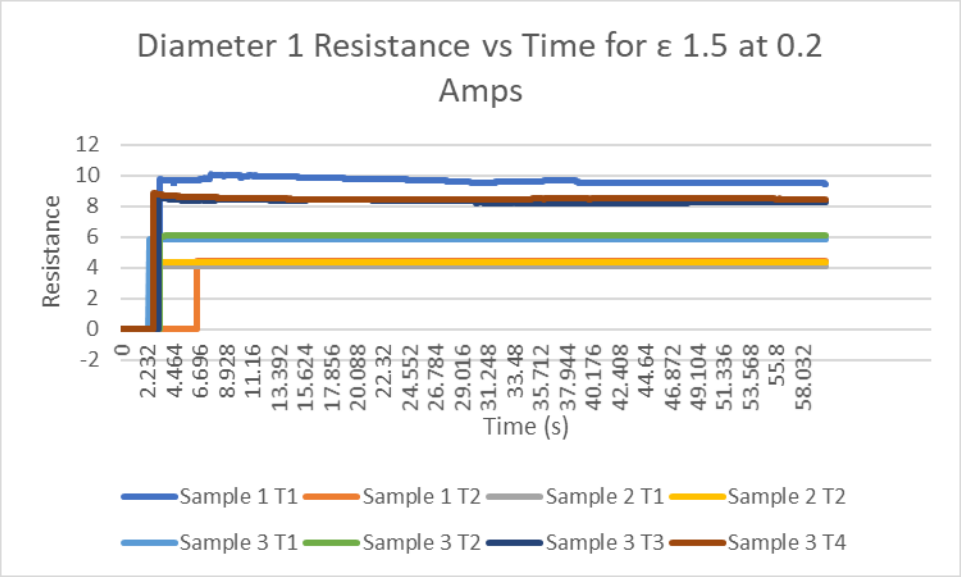

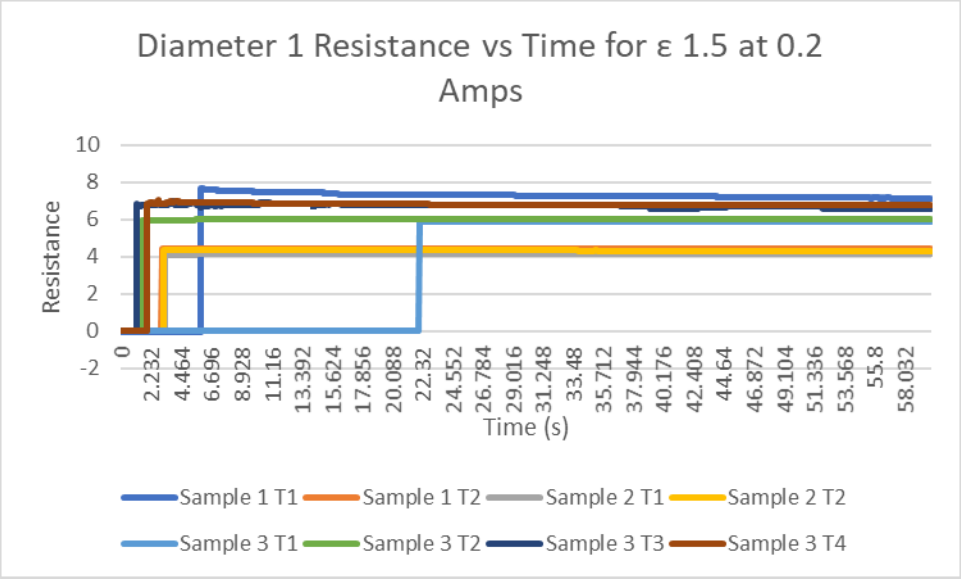
Diameter 1 Resistance vs Time for ε 1.5 at 0.2 Amps
Resistance
Time (s)
Sample 1 T1
Sample 1 T2
Sample 2 T1
Sample 2 T2
Sample 3 T1
Sample 3 T2
Sample 3 T3
Sample 3 T4

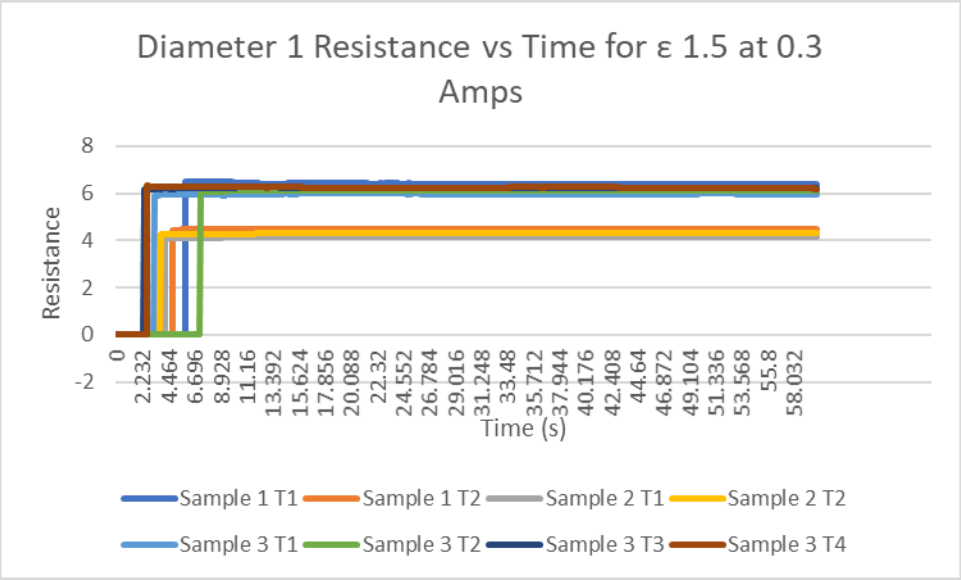
Diameter 1 Resistance vs Time for ε 1.5 at 0.3 Amps
Resistance
Time (s)
Sample 1 T1
Sample 1 T2
Sample 2 T1
Sample 2 T2
Sample 3 T1
Sample 3 T2
Sample 3 T3
Sample 3 T4

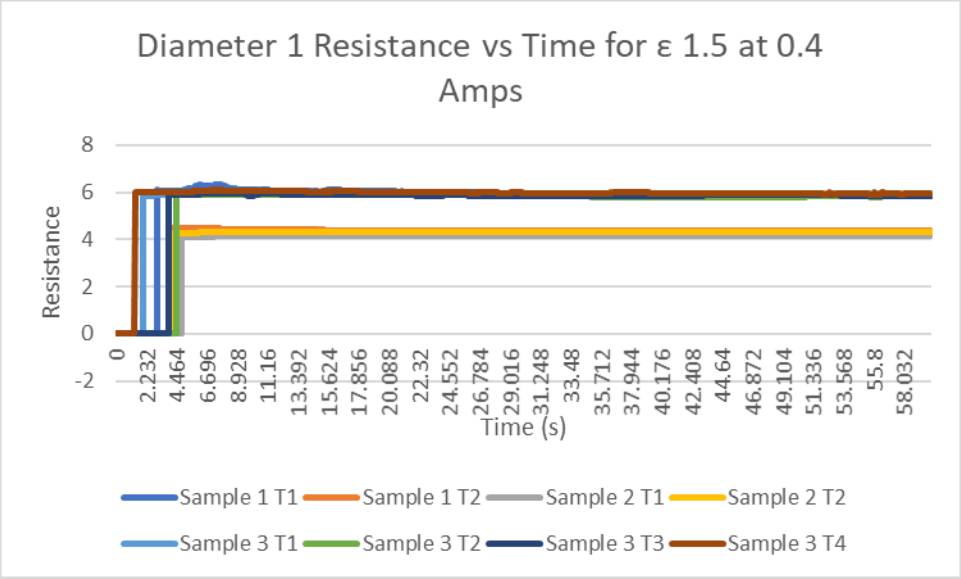
Diameter 1 Resistance vs Time for ε 1.5 at 0.4 Amps
Resistance
8
6
4
2
0
-2
0
2.232
4.464
6.696
8.928
11.16
13.392
15.624
17.856
20.088
22.32
24.552
26.784
29.016
31.248
33.48
35.712
37.944
40.176
42.408
44.64
46.872
49.104
51.336
53.568
55.8
58.032
Time (s)
Sample 1 T1
Sample 1 T2
Sample 2 T1
Sample 2 T2
Sample 3 T1
Sample 3 T2
Sample 3 T3
Sample 3 T4

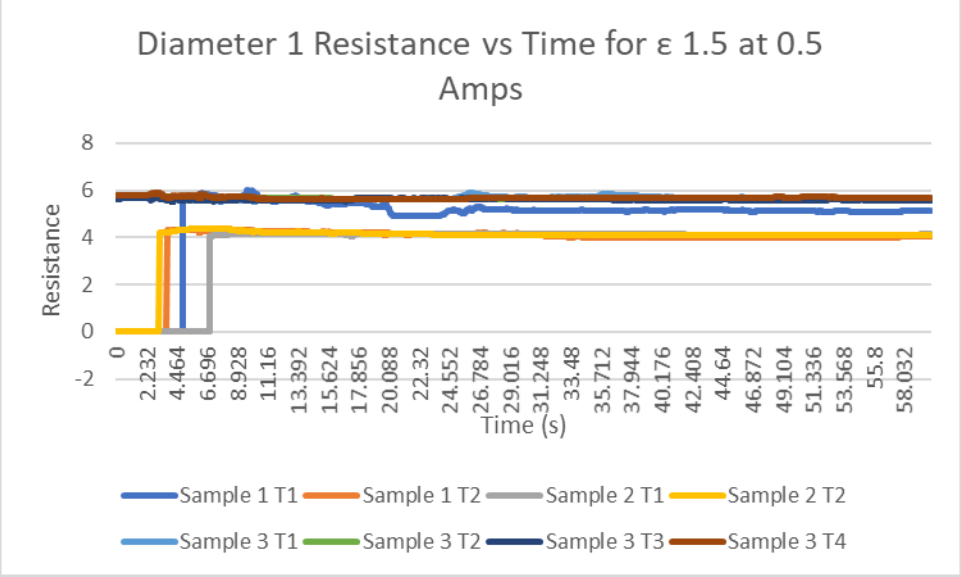
Diameter 1 Resistance vs Time for ε 1.5 at 0.5 Amps
Resistance
8
6
4
2
0
-2
0
2.232
4.464
6.696
8.928
11.16
13.392
15.624
17.856
20.088
22.32
24.552
26.784
29.016
31.248
33.48
35.712
37.944
40.176
42.408
44.64
46.872
49.104
51.336
53.568
55.8
58.032
Time (s)
Sample 1 T1
Sample 1 T2
Sample 2 T1
Sample 2 T2
Sample 3 T1
Sample 3 T2
Sample 3 T3
Sample 3 T4

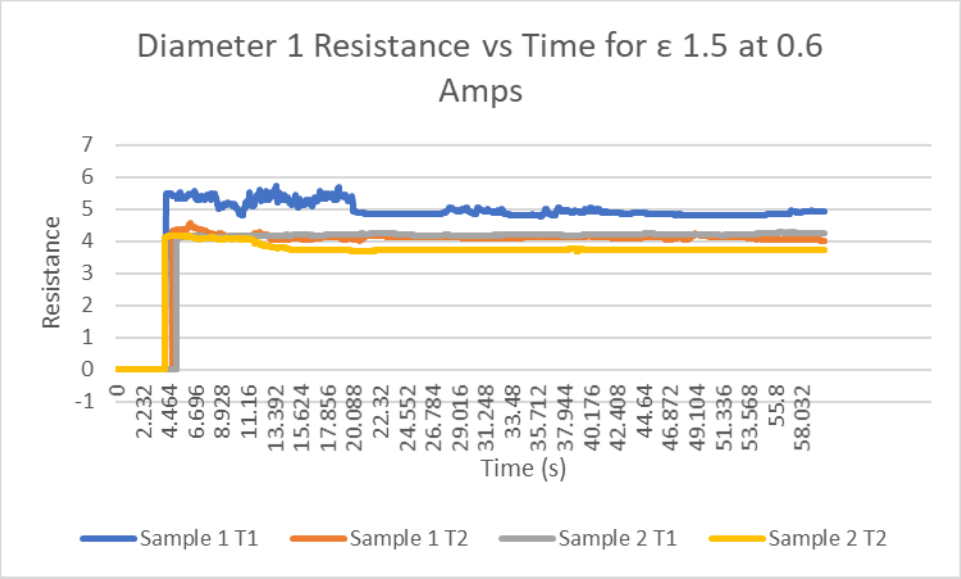
Diameter 1 Resistance vs Time for ε 1.5 at 0.6 Amps
Resistance
7
6
5
4
3
2
1
0
-1
0
2.232
4.464
6.696
8.928
11.16
13.392
15.624
17.856
20.088
22.32
24.552
26.784
29.016
31.248
33.48
35.712
37.944
40.176
42.408
44.64
46.872
49.104
51.336
53.568
55.8
58.032
Time (s)
Sample 1 T1
Sample 1 T2
Sample 2 T1
Sample 2 T2

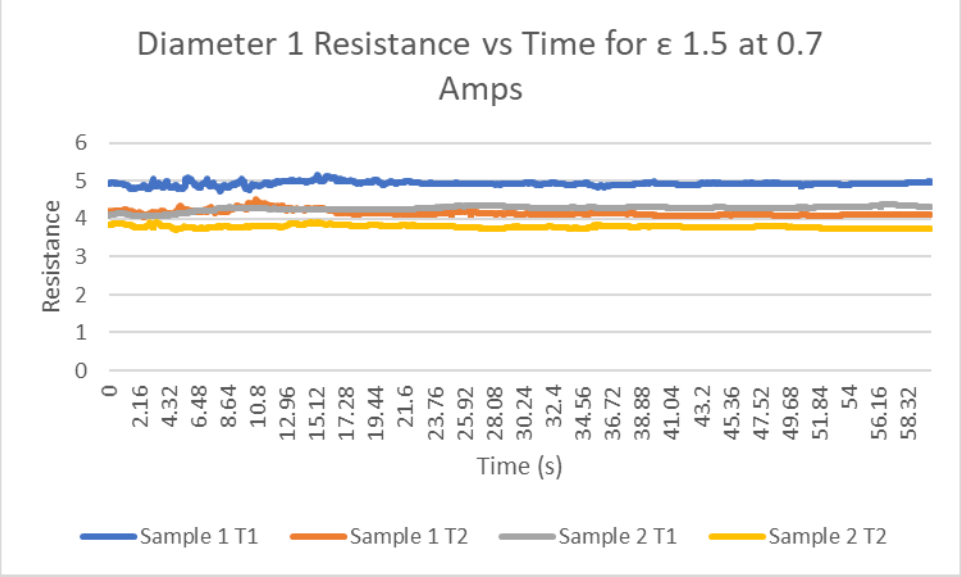
Diameter 1 Resistance vs Time for ε 1.5 at 0.7 Amps
Resistance
6
5
4
3
2
1
0
0
2.16
4.32
6.48
8.64
10.8
12.96
15.12
17.28
19.44
21.6
23.76
25.92
28.08
30.24
32.4
34.56
36.72
38.88
41.04
43.2
45.36
47.52
49.68
51.84
54
56.16
58.32
Time (s)
Sample 1 T1
Sample 1 T2
Sample 2 T1
Sample 2 T2

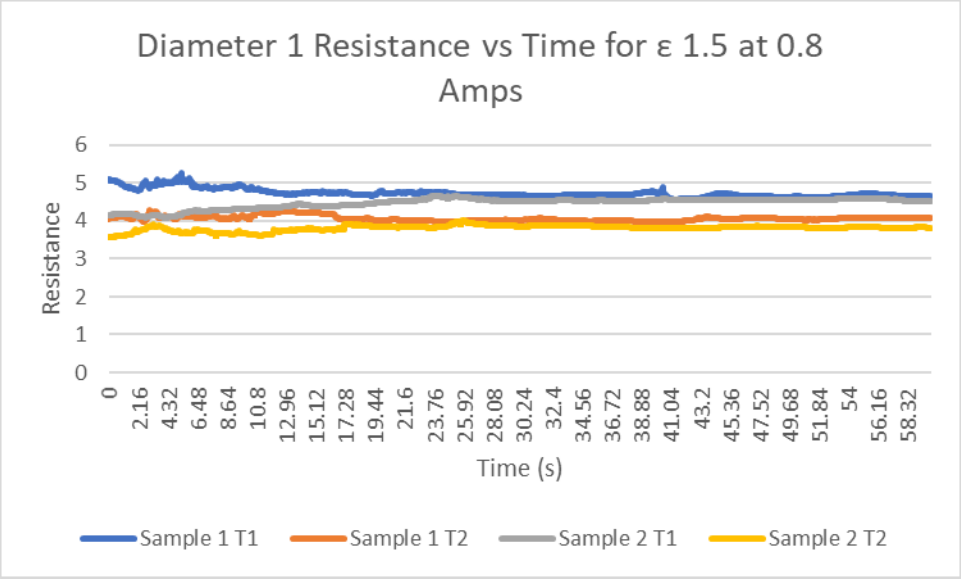
Diameter 1 Resistance vs Time for ε 1.5 at 0.8 Amps
Resistance
Time (s)
Sample 1 T1
Sample 1 T2
Sample 2 T1
Sample 2 T2

Diameter 2

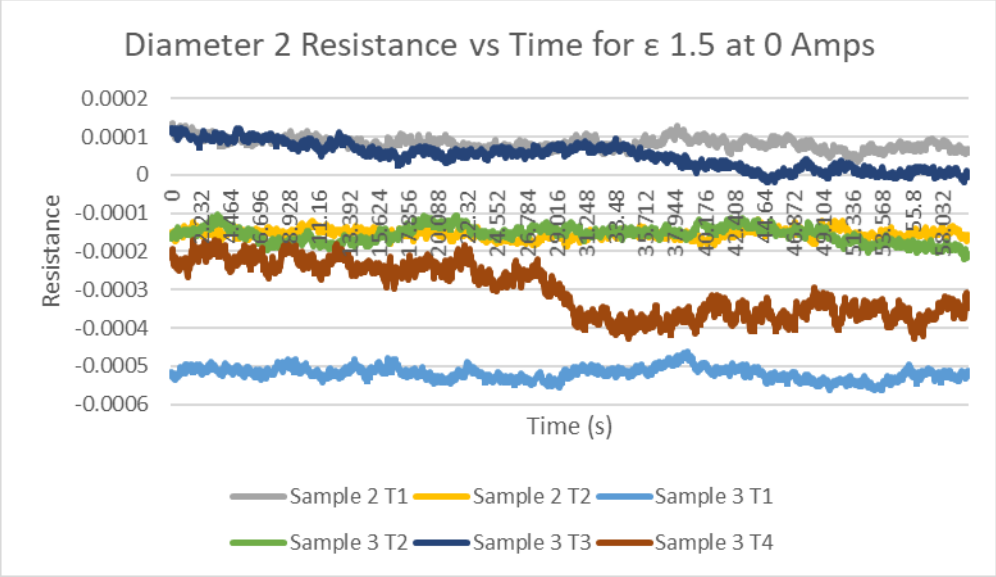
Diameter 2 Resistance vs Time for ε 1.5 at 0 Amps
Resistance
Time (s)
Sample 2 T1
Sample 2 T2
Sample 3 T1
Sample 3 T2
Sample 3 T3
Sample 3 T4

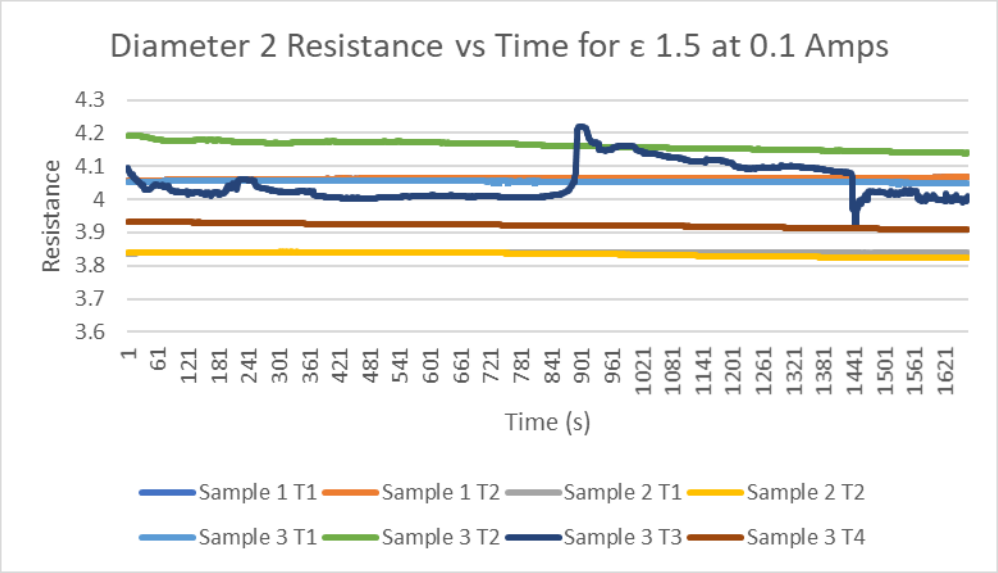
Diameter 2 Resistance vs Time for ε 1.5 at 0.1 Amps
Resistance
4.3
4.2
4.1
4
3.9
3.8
3.7
3.6
1
61
121
181
241
301
361
421
481
541
601
661
721
781
841
901
961
1021
1081
1141
1201
1261
1321
1381
1441
1501
1561
1621
Time (s)
Sample 1 T1
Sample 1 T2
Sample 2 T1
Sample 2 T2
Sample 3 T1
Sample 3 T2
Sample 3 T3
Sample 3 T4

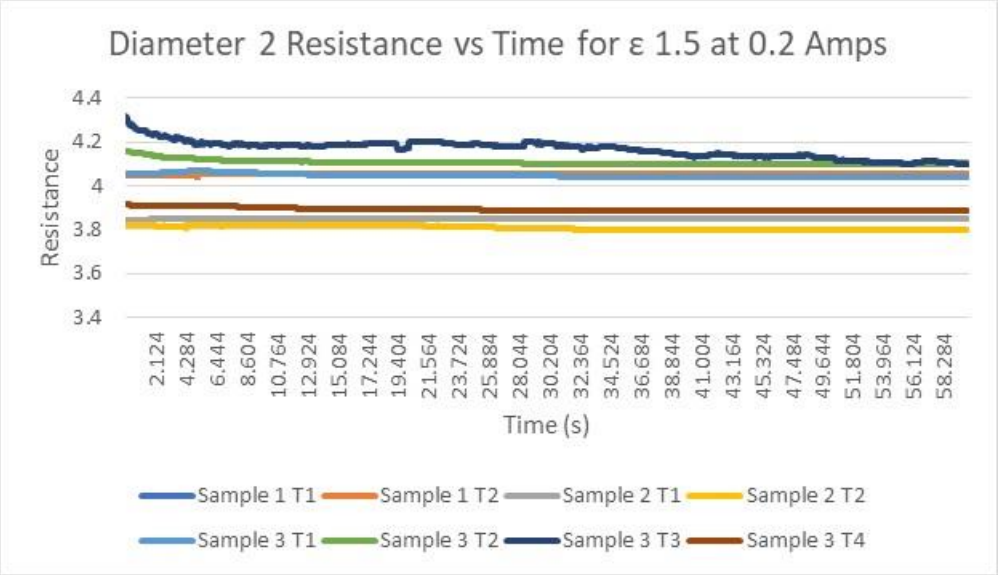
Diameter 2 Resistance vs Time for ε 1.5 at 0.2 Amps
Resistance
4.4
4.2
4
3.8
3.6
3.4
2.124
4.284
6.444
8.604
10.764
12.924
15.084
17.244
19.404
21.564
23.724
25.884
28.044
30.204
32.364
34.524
36.684
38.844
41.004
43.164
45.324
47.484
49.644
51.804
53.964
56.124
58.284
Time (s)
Sample 1 T1
Sample 1 T2
Sample 2 T1
Sample 2 T2
Sample 3 T1
Sample 3 T2
Sample 3 T3
Sample 3 T4

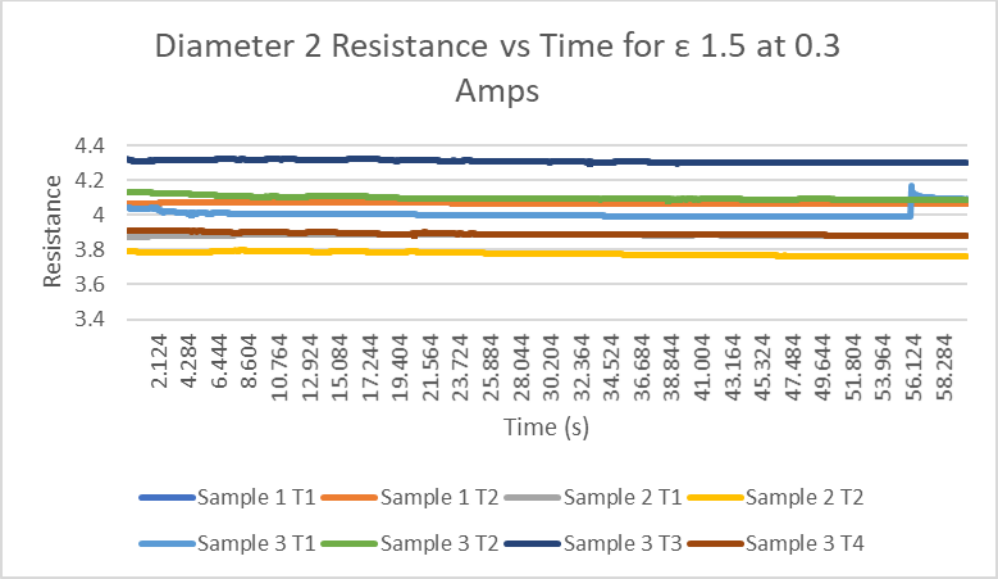
Diameter 2 Resistance vs Time for ε 1.5 at 0.3 Amps
Resistance
4.4
4.2
4
3.8
3.6
3.4
2.124
4.284
6.444
8.604
10.764
12.924
15.084
17.244
19.404
21.564
23.724
25.884
28.044
30.204
32.364
34.524
36.684
38.844
41.004
43.164
45.324
47.484
49.644
51.804
53.964
56.124
58.284
Time (s)
Sample 1 T1
Sample 1 T2
Sample 2 T1
Sample 2 T2
Sample 3 T1
Sample 3 T2
Sample 3 T3
Sample 3 T4

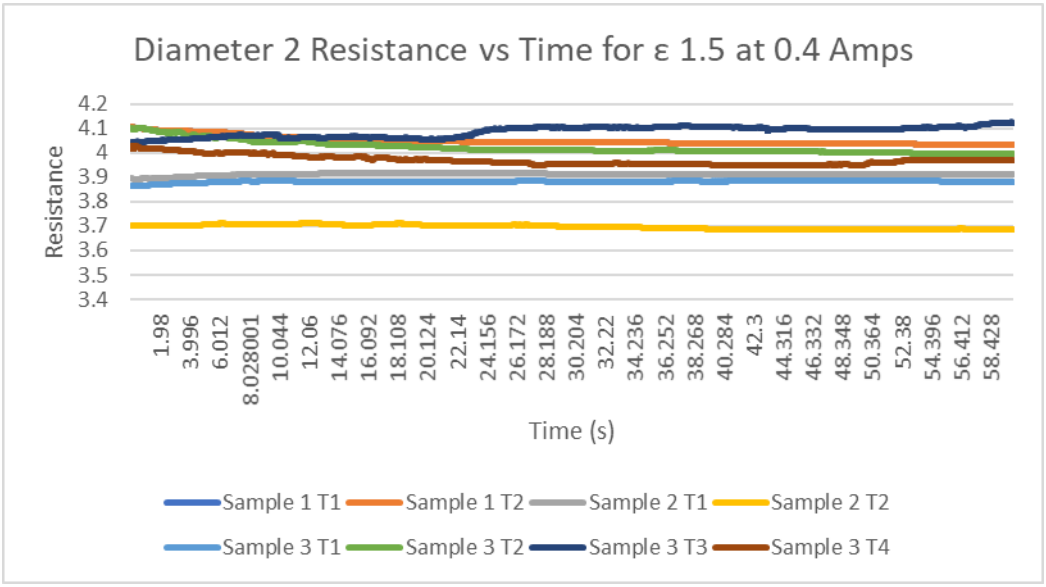
Diameter 2 Resistance vs Time for ε 1.5 at 0.4 Amps
Resistance
4.2
4.1
4
3.9
3.8
3.7
3.6
3.5
3.4
1.98
3.996
6.012
8.028001
10.044
12.06
14.076
16.092
18.108
20.124
22.14
24.156
26.172
28.188
30.204
32.22
34.236
36.252
38.268
40.284
42.3
44.316
46.332
48.348
50.364
52.38
54.396
56.412
58.428
Time (s)
Sample 1 T1
Sample 1 T2
Sample 2 T1
Sample 2 T2
Sample 3 T1
Sample 3 T2
Sample 3 T3
Sample 3 T4

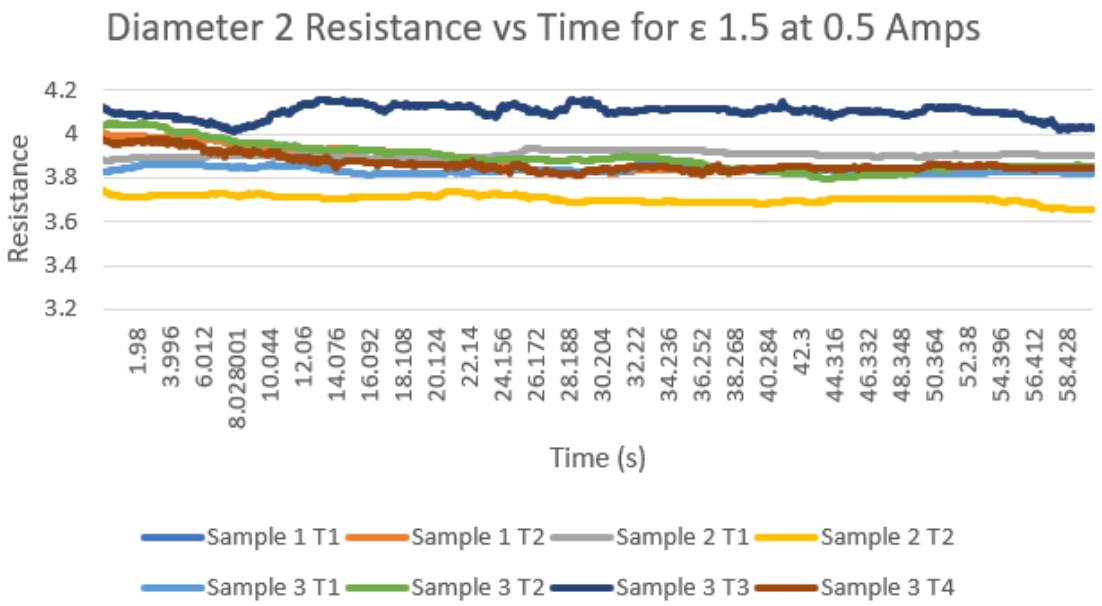
Diameter 2 Resistance vs Time for ε 1.5 at 0.5 Amps
Resistance
4.2
4
3.8
3.6
3.4
3.2
1.98
3.996
6.012
8.028001
10.044
12.06
14.076
16.092
18.108
20.124
22.14
24.156
26.172
28.188
30.204
32.22
34.236
36.252
38.268
40.284
42.3
44.316
46.332
48.348
50.364
52.38
54.396
56.412
58.428
Time (s)
Sample 1 T1
Sample 1 T2
Sample 2 T1
Sample 2 T2
Sample 3 T1
Sample 3 T2
Sample 3 T3
Sample 3 T4

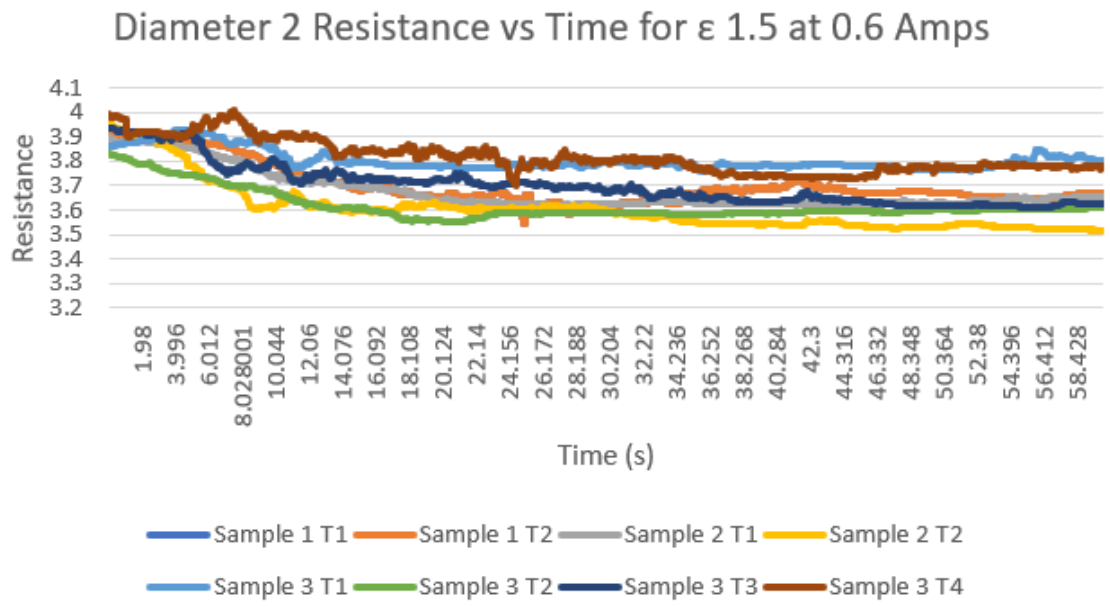
Diameter 2 Resistance vs Time for ε 1.5 at 0.6 Amps
Resistance
4.1
4
3.9
3.8
3.7
3.6
3.5
3.4
3.3
3.2
1.98
3.996
6.012
8.028001
10.044
12.06
14.076
16.092
18.108
20.124
22.14
24.156
26.172
28.188
30.204
32.22
34.236
36.252
38.268
40.284
42.3
44.316
46.332
48.348
50.364
52.38
54.396
56.412
58.428
Time (s)
Sample 1 T1
Sample 1 T2
Sample 2 T1
Sample 2 T2
Sample 3 T1
Sample 3 T2
Sample 3 T3
Sample 3 T4

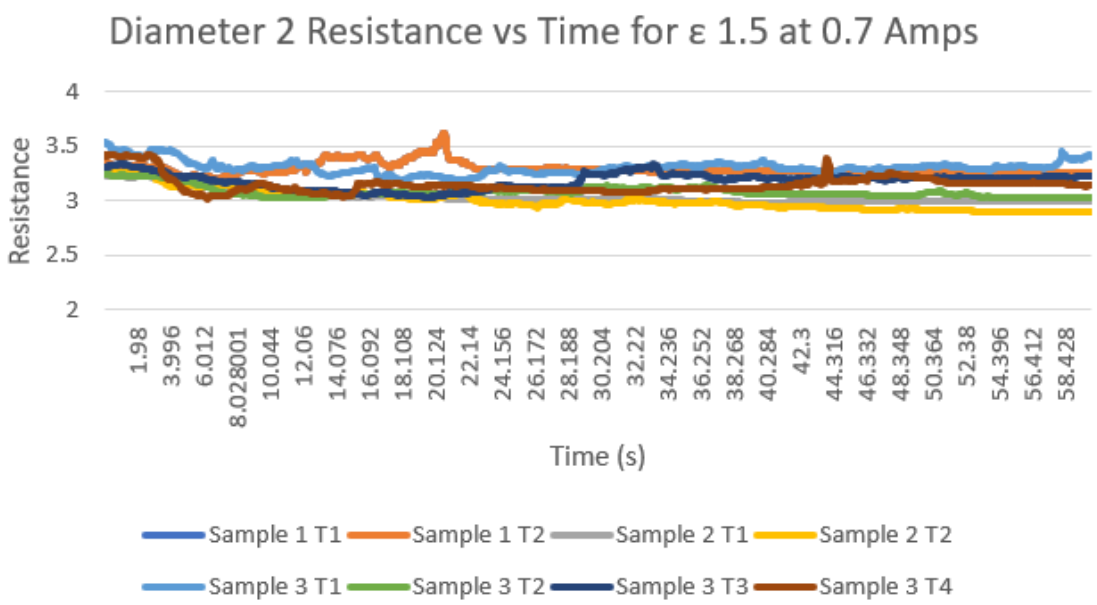

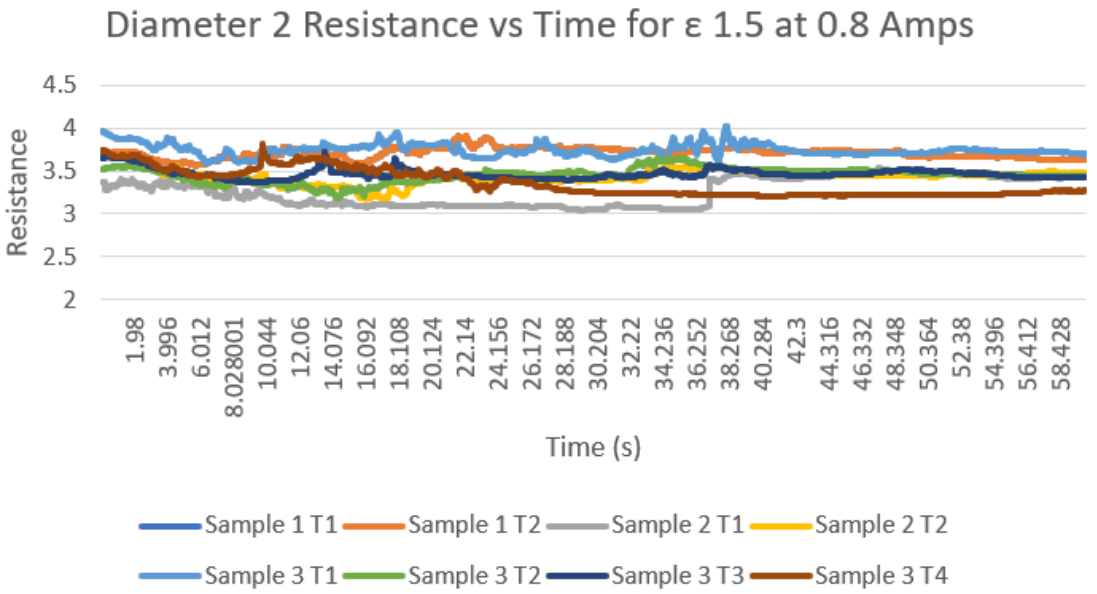

Resistance vs Time for Extensional strain of 2

Diameter 1

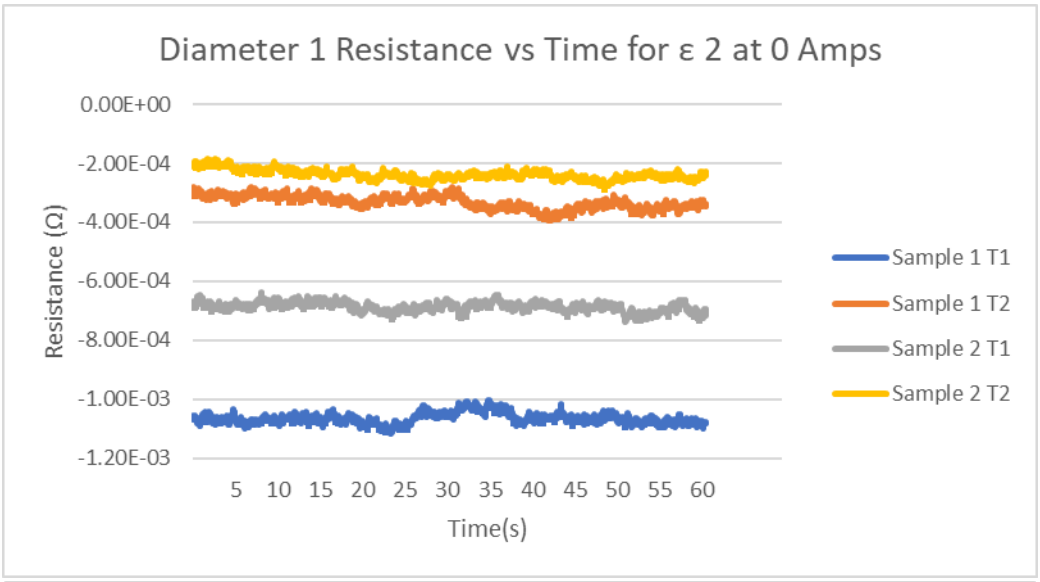
Diameter 1 Resistance vs Time for ε 2 at 0 Amps
0.00E+00
-2.00E-04
-4.00E-04
-6.00E-04
-8.00E-04
-1.00E-03
-1.20E-03
Resistance (Ω)
5 10 15 20 25 30 35 40 45 50 55 60
Time(s)
Sample 1 T1
Sample 1 T2
Sample 2 T1
Sample 2 T2

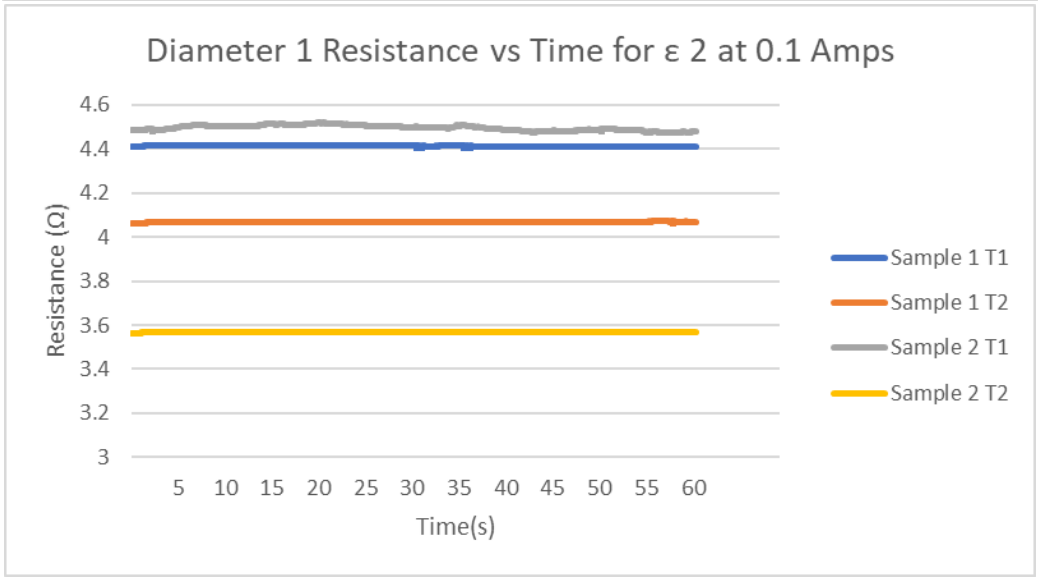
Diameter 1 Resistance vs Time for ε 2 at 0.1 Amps
4.6
4.4
4.2
4
3.8
3.6
3.4
3.2
3
Resistance (Ω)
5 10 15 20 25 30 35 40 45 50 55 60
Time(s)
Sample 1 T1
Sample 1 T2
Sample 2 T1
Sample 2 T2

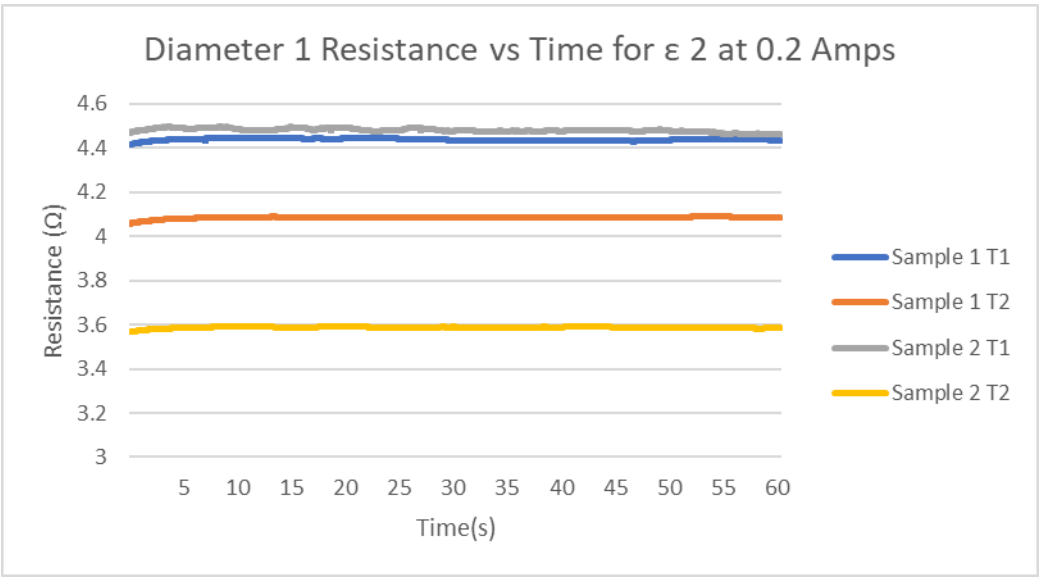
Diameter 1 Resistance vs Time for ε 2 at 0.2 Amps
4.6
4.4
4.2
4
3.8
3.6
3.4
3.2
3
Resistance (Ω)
5 10 15 20 25 30 35 40 45 50 55 60
Time(s)
Sample 1 T1
Sample 1 T2
Sample 2 T1
Sample 2 T2

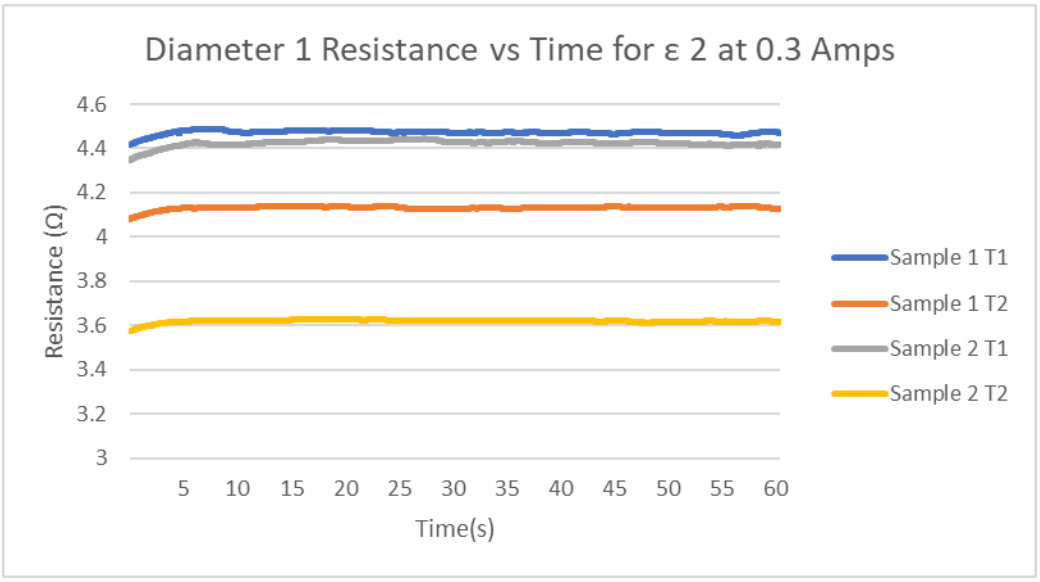
Diameter 1 Resistance vs Time for ε 2 at 0.3 Amps
Resistance (Ω)
4.6
4.4
4.2
4
3.8
3.6
3.4
3.2
3
5 10 15 20 25 30 35 40 45 50 55 60
Time(s)
Sample 1 T1
Sample 1 T2
Sample 2 T1
Sample 2 T2

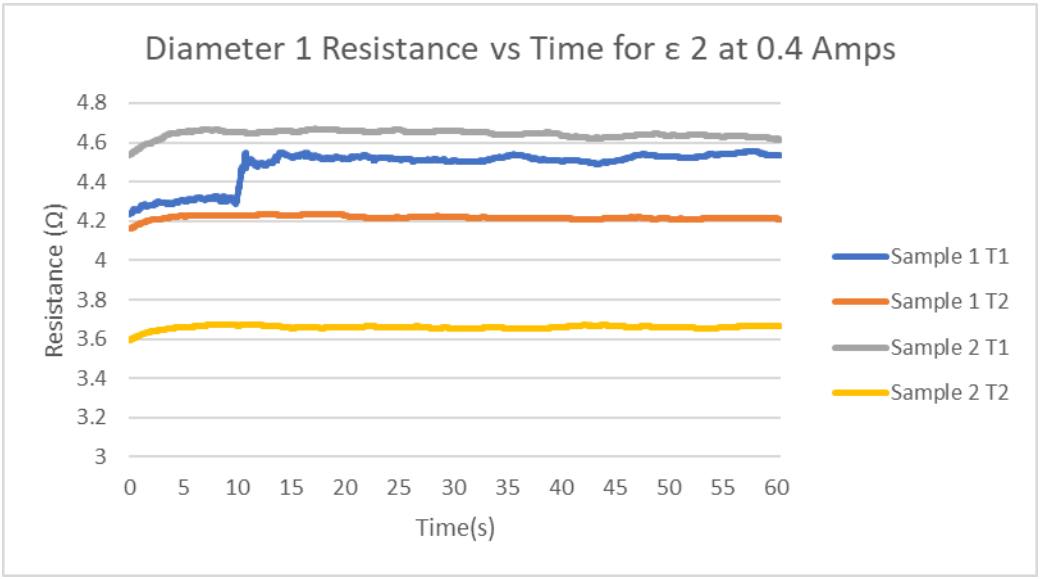
Diameter 1 Resistance vs Time for ε 2 at 0.4 Amps
Resistance (Ω)
4.8
4.6
4.4
4.2
4
3.8
3.6
3.4
3.2
3
0 5 10 15 20 25 30 35 40 45 50 55 60
Time(s)
Sample 1 T1
Sample 1 T2
Sample 2 T1
Sample 2 T2

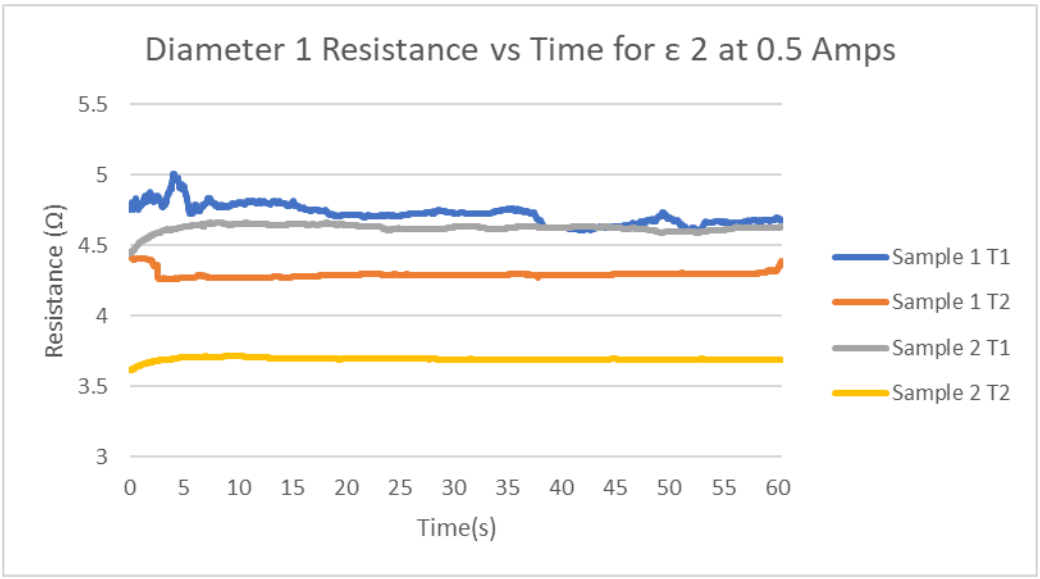
Diameter 1 Resistance vs Time for ε 2 at 0.5 Amps
Resistance (Ω)
5.5
5
4.5
4
3.5
3
0 5 10 15 20 25 30 35 40 45 50 55 60
Time(s)
Sample 1 T1
Sample 1 T2
Sample 2 T1
Sample 2 T2

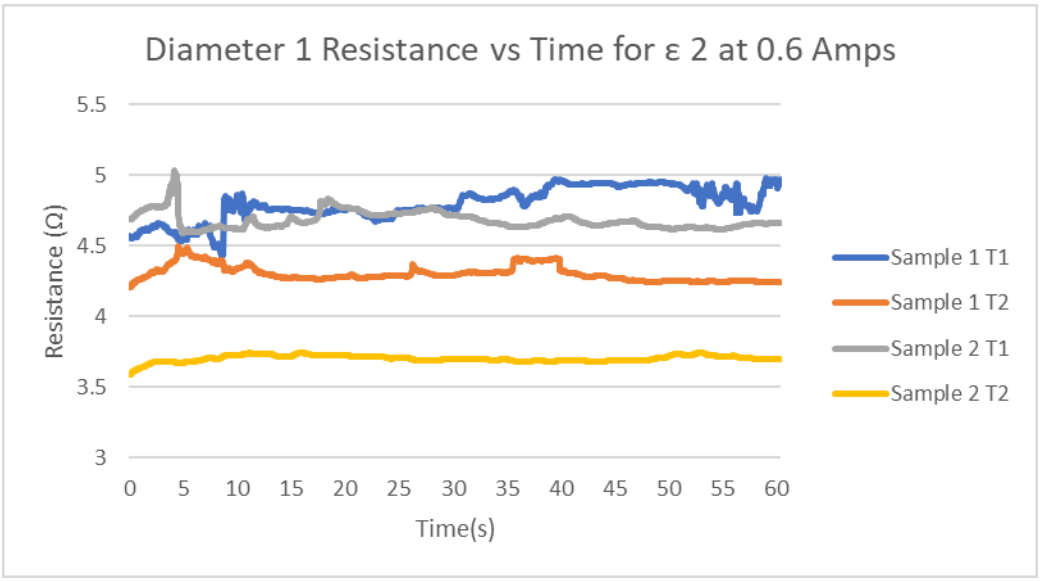
Diameter 1 Resistance vs Time for ε 2 at 0.6 Amps
Resistance (Ω)
5.5
5
4.5
4
3.5
3
0 5 10 15 20 25 30 35 40 45 50 55 60
Time(s)
Sample 1 T1
Sample 1 T2
Sample 2 T1
Sample 2 T2

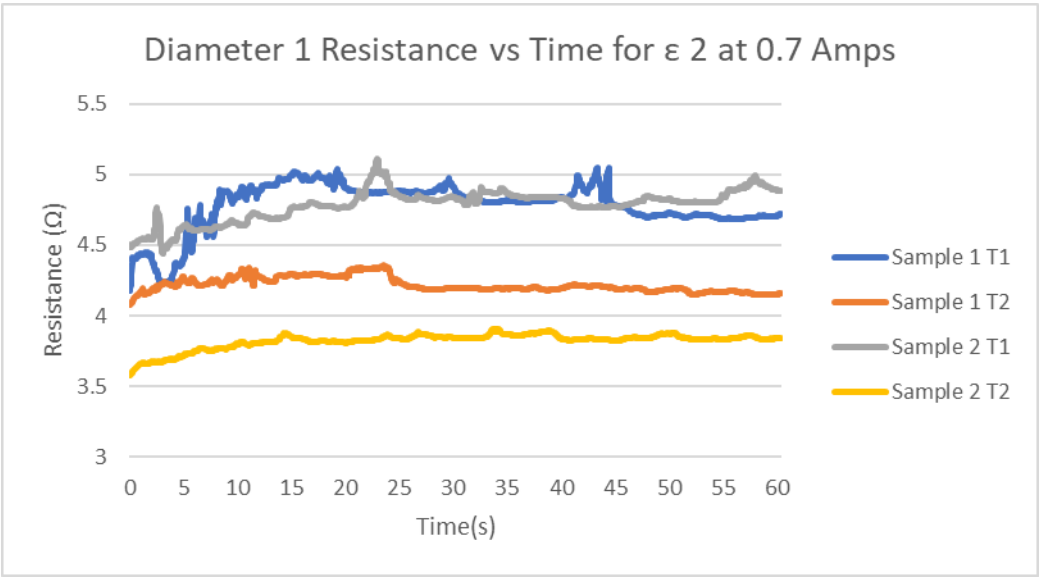
Diameter 1 Resistance vs Time for ε 2 at 0.7 Amps
Resistance (Ω)
5.5
5
4.5
4
3.5
3
0 5 10 15 20 25 30 35 40 45 50 55 60
Time(s)
Sample 1 T1
Sample 1 T2
Sample 2 T1
Sample 2 T2

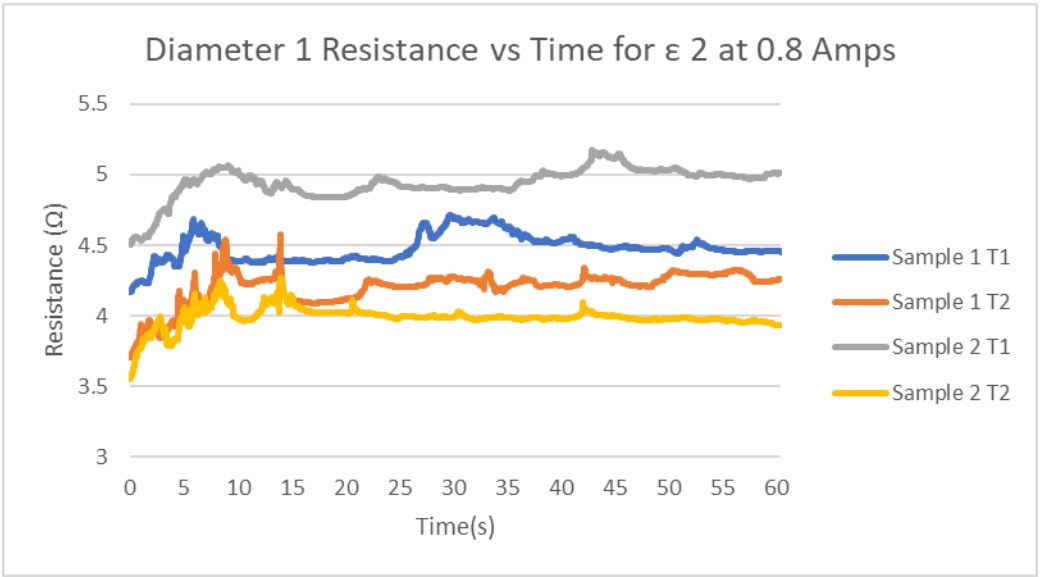
Diameter 1 Resistance vs Time for ε 2 at 0.8 Amps
Resistance (Ω)
5.5
5
4.5
4
3.5
3
0 5 10 15 20 25 30 35 40 45 50 55 60
Time(s)
Sample 1 T1
Sample 1 T2
Sample 2 T1
Sample 2 T2

Diameter 2

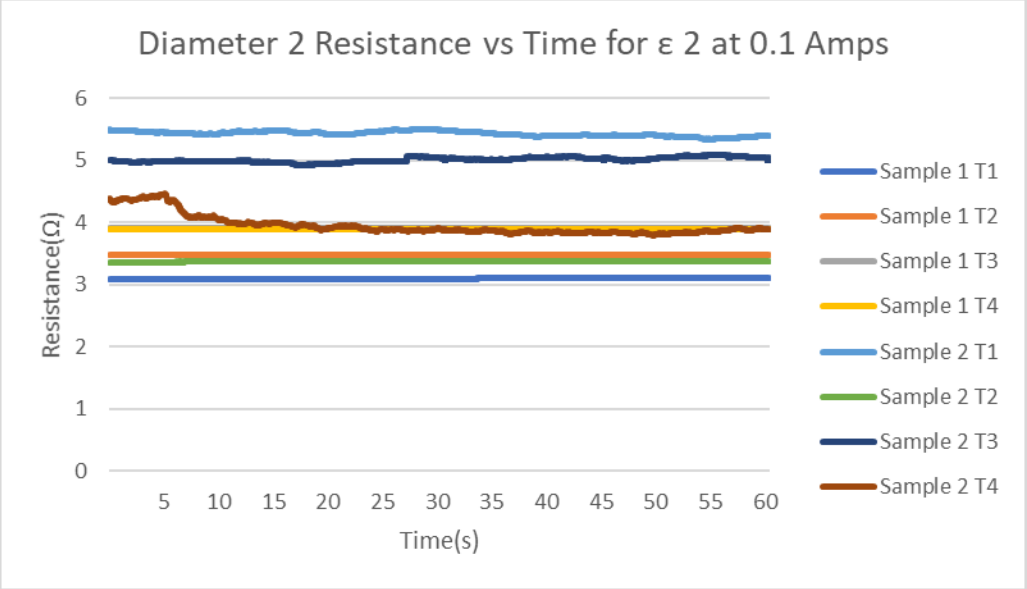
Diameter 2 Resistance vs Time for ε 2 at 0.1 Amps
Resistance(Ω)
Time(s)
0
1
2
3
4
5
6
5 10 15 20 25 30 35 40 45 50 55 60
Sample 1 T1
Sample 1 T2
Sample 1 T3
Sample 1 T4
Sample 2 T1
Sample 2 T2
Sample 2 T3
Sample 2 T4

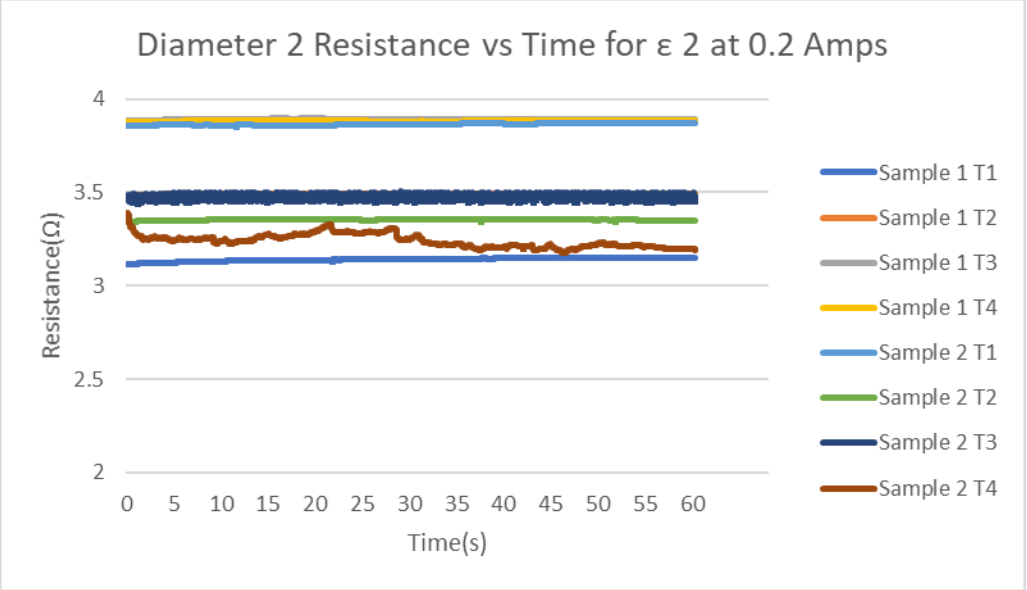
Diameter 2 Resistance vs Time for ε 2 at 0.2 Amps
Resistance(Ω)
Time(s)
2
2.5
3
3.5
4
0 5 10 15 20 25 30 35 40 45 50 55 60
Sample 1 T1
Sample 1 T2
Sample 1 T3
Sample 1 T4
Sample 2 T1
Sample 2 T2
Sample 2 T3
Sample 2 T4

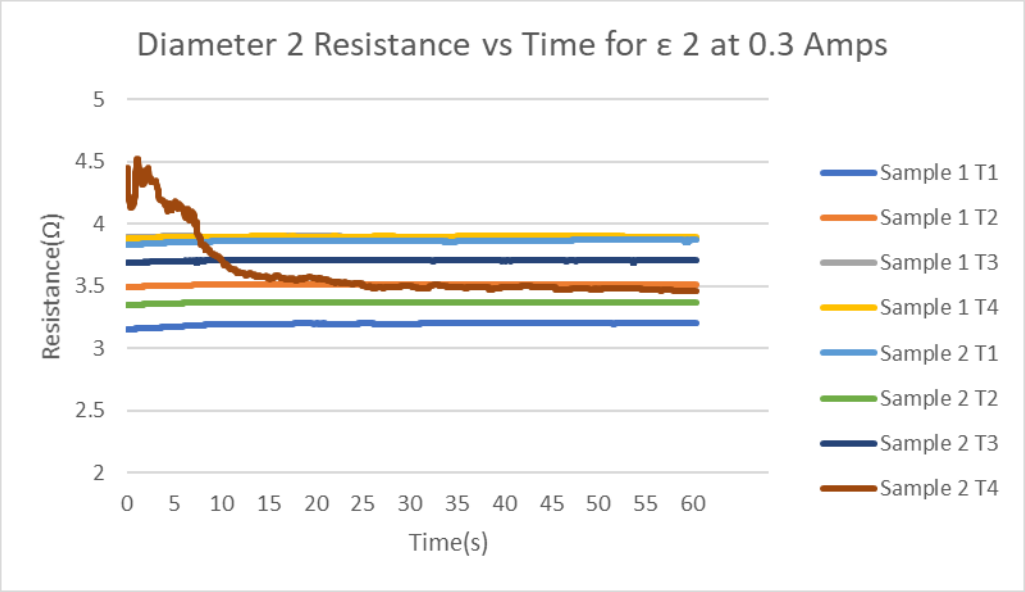
Diameter 2 Resistance vs Time for ε 2 at 0.3 Amps
Resistance(Ω)
5
4.5
4
3.5
3
2.5
2
0 5 10 15 20 25 30 35 40 45 50 55 60
Time(s)
Sample 1 T1
Sample 1 T2
Sample 1 T3
Sample 1 T4
Sample 2 T1
Sample 2 T2
Sample 2 T3
Sample 2 T4

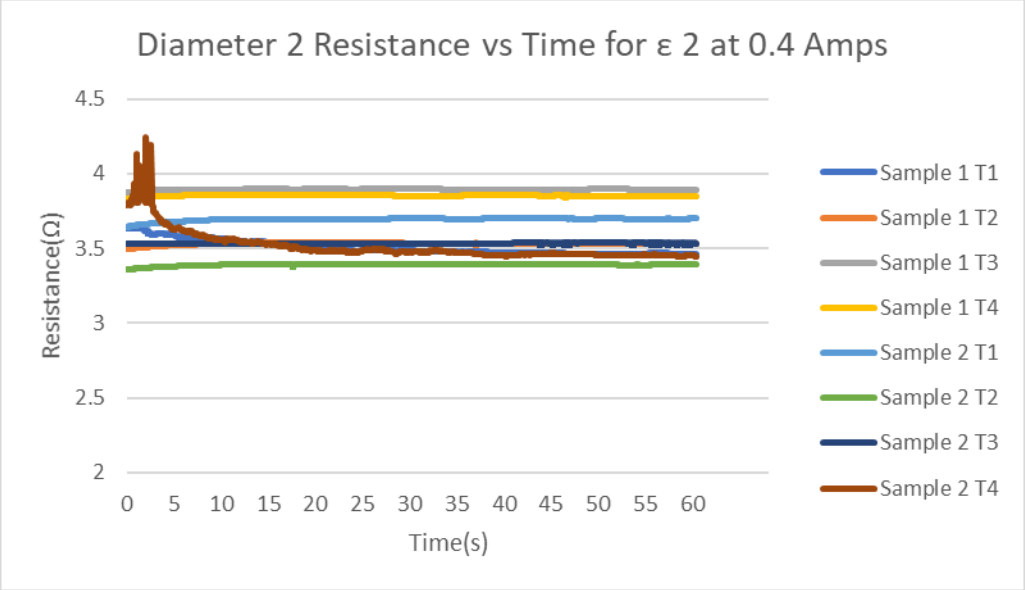
Diameter 2 Resistance vs Time for ε 2 at 0.4 Amps
Resistance(Ω)
4.5
4
3.5
3
2.5
2
0 5 10 15 20 25 30 35 40 45 50 55 60
Time(s)
Sample 1 T1
Sample 1 T2
Sample 1 T3
Sample 1 T4
Sample 2 T1
Sample 2 T2
Sample 2 T3
Sample 2 T4

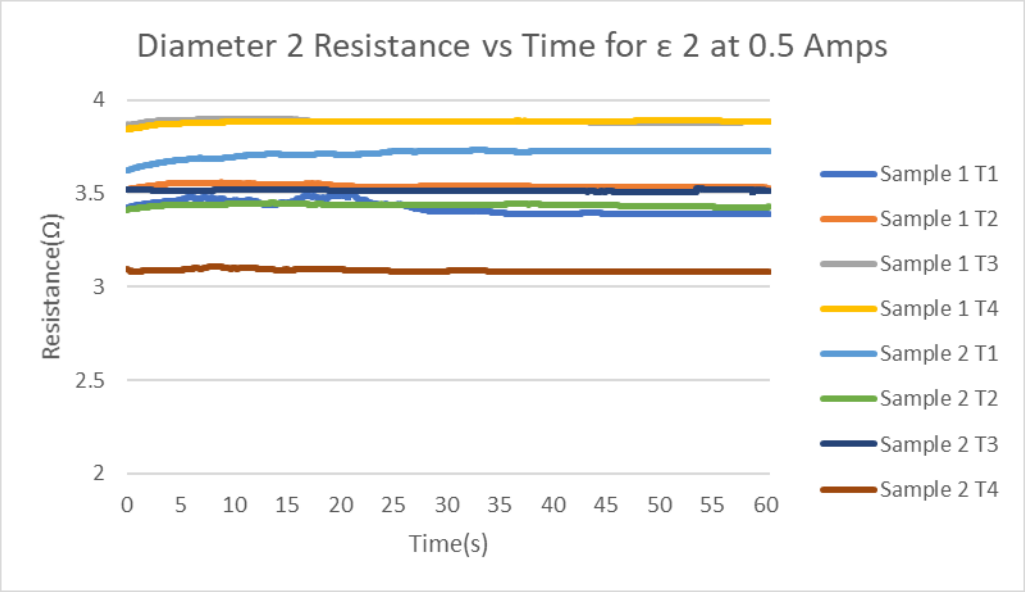
Diameter 2 Resistance vs Time for ε 2 at 0.5 Amps
Resistance(Ω)
4
3.5
3
2.5
2
0 5 10 15 20 25 30 35 40 45 50 55 60
Time(s)
Sample 1 T1
Sample 1 T2
Sample 1 T3
Sample 1 T4
Sample 2 T1
Sample 2 T2
Sample 2 T3
Sample 2 T4

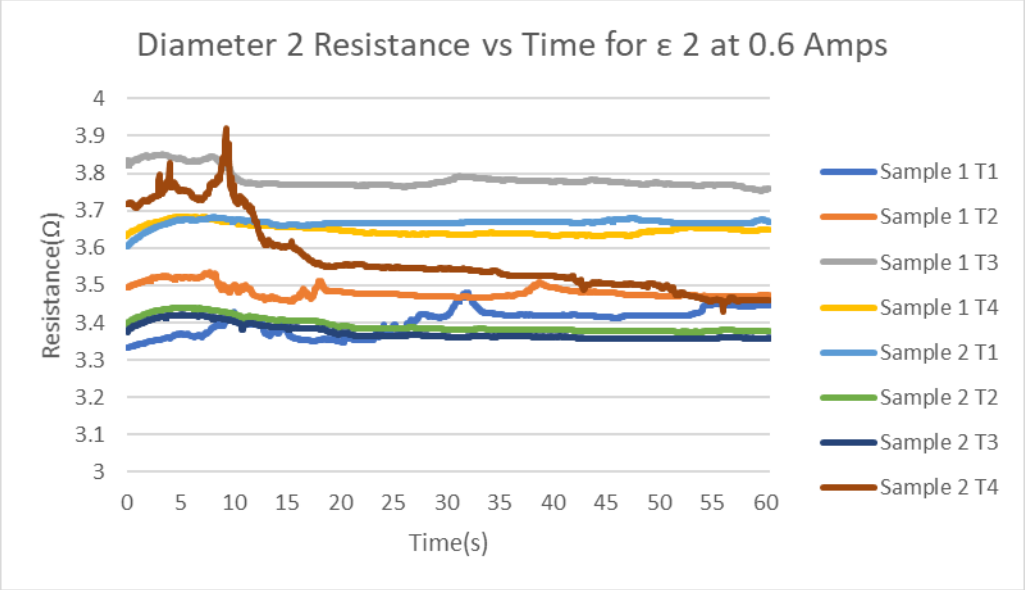
Diameter 2 Resistance vs Time for ε 2 at 0.6 Amps
Resistance(Ω)
4
3.9
3.8
3.7
3.6
3.5
3.4
3.3
3.2
3.1
3
0 5 10 15 20 25 30 35 40 45 50 55 60
Time(s)
Sample 1 T1
Sample 1 T2
Sample 1 T3
Sample 1 T4
Sample 2 T1
Sample 2 T2
Sample 2 T3
Sample 2 T4

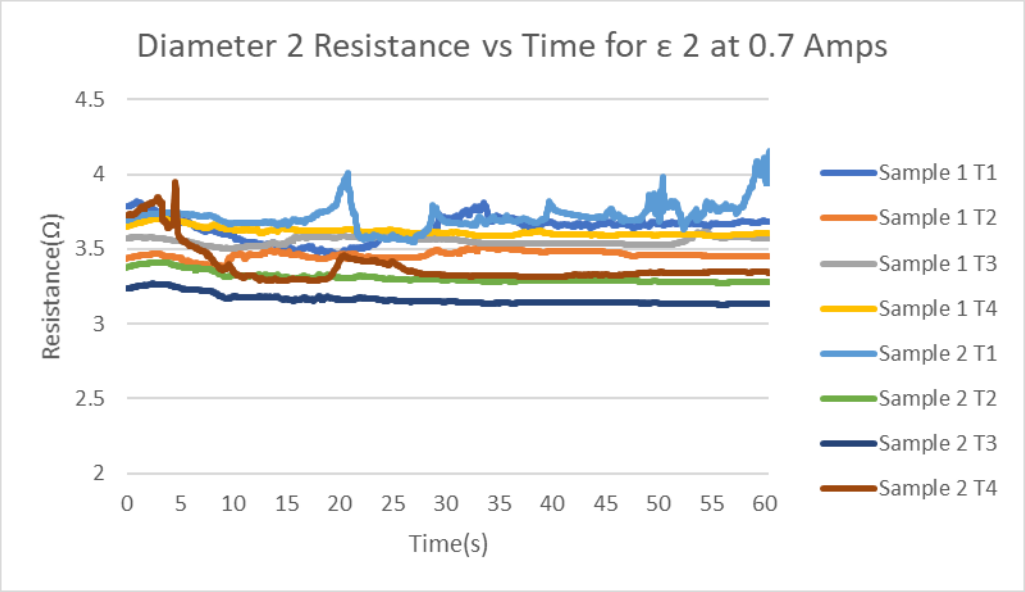
Diameter 2 Resistance vs Time for ε 2 at 0.7 Amps
Resistance(Ω)
4.5
4
3.5
3
2.5
2
0 5 10 15 20 25 30 35 40 45 50 55 60
Time(s)
Sample 1 T1
Sample 1 T2
Sample 1 T3
Sample 1 T4
Sample 2 T1
Sample 2 T2
Sample 2 T3
Sample 2 T4

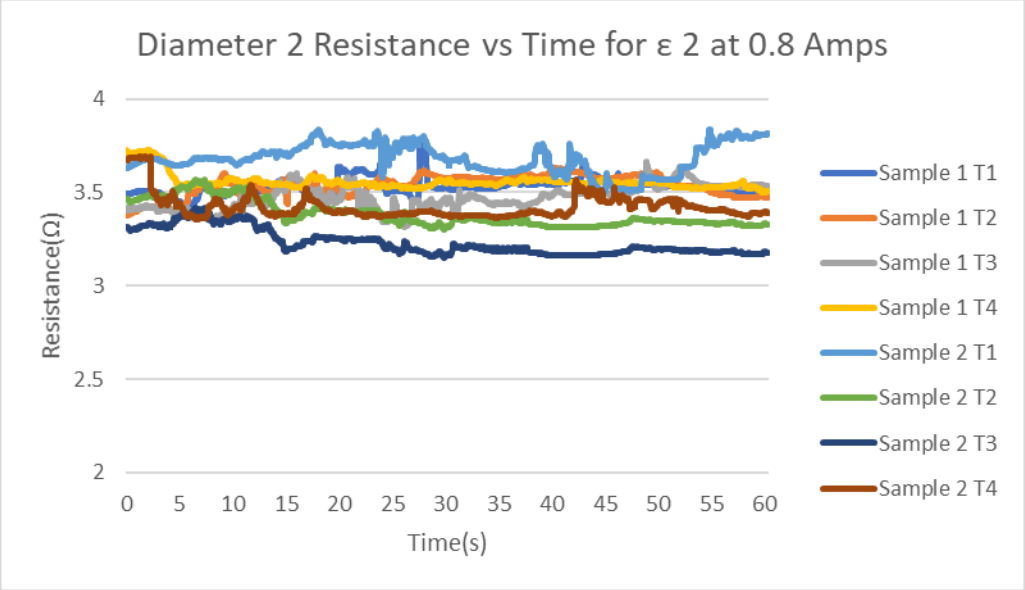
Diameter 2 Resistance vs Time for ε 2 at 0.8 Amps
Resistance(Ω)
4
3.5
3
2.5
2
0 5 10 15 20 25 30 35 40 45 50 55 60
Time(s)
Sample 1 T1
Sample 1 T2
Sample 1 T3
Sample 1 T4
Sample 2 T1
Sample 2 T2
Sample 2 T3
Sample 2 T4

Results of Diameter 1 (0.31 mm) Samples 1 and 2 included

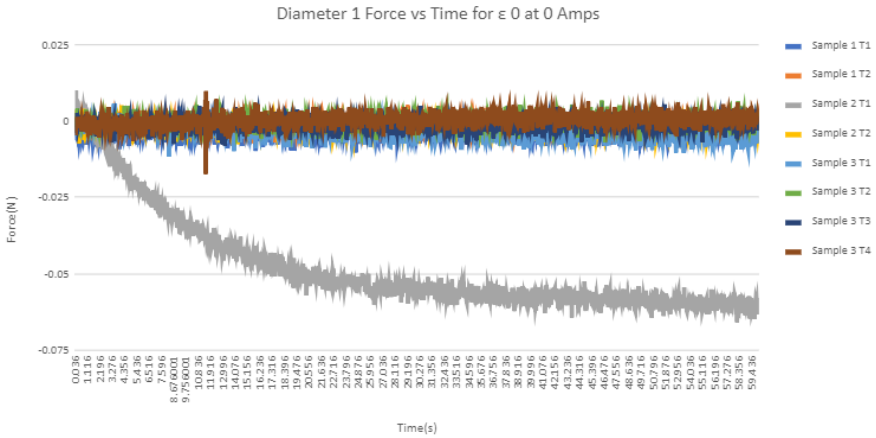

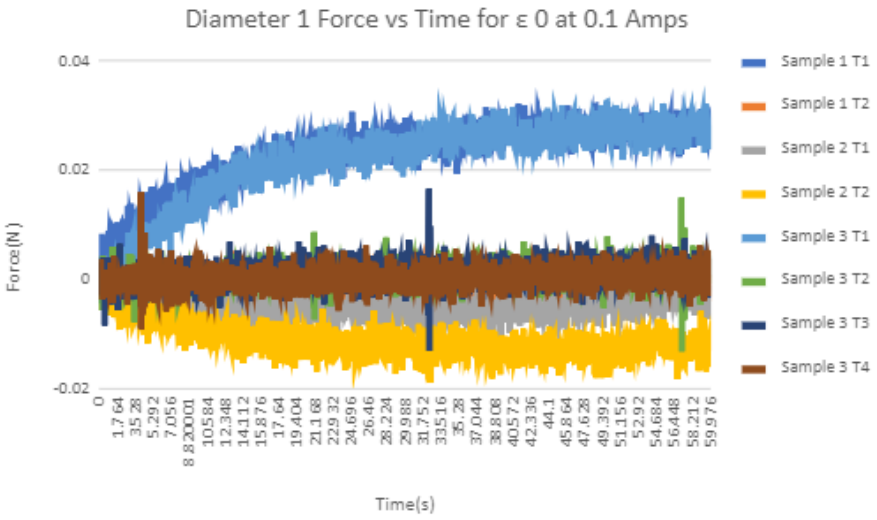

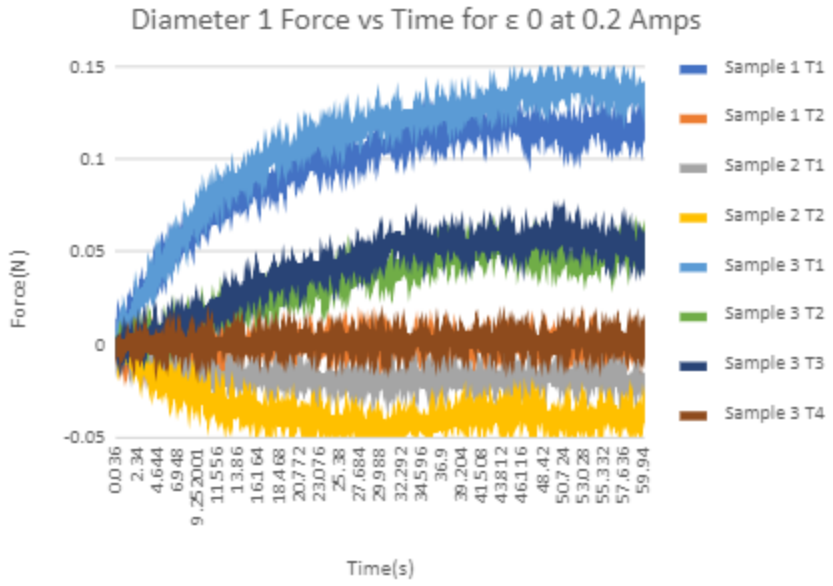
Diameter 1 Force vs Time for ε 0 at 0.2 Amps
Force(N)
0.15
0.1
0.05
0
-0.05
0.036
2.34
4.644
6.948
9.252001
11.556
13.86
16.164
18.468
20.772
23.076
25.38
27.684
29.988
32.292
34.596
36.9
39.204
41.508
43.812
46.116
48.42
50.724
53.028
55.332
57.636
59.94
Time(s)
Sample 1 T1
Sample 1 T2
Sample 2 T1
Sample 2 T2
Sample 3 T1
Sample 3 T2
Sample 3 T3
Sample 3 T4

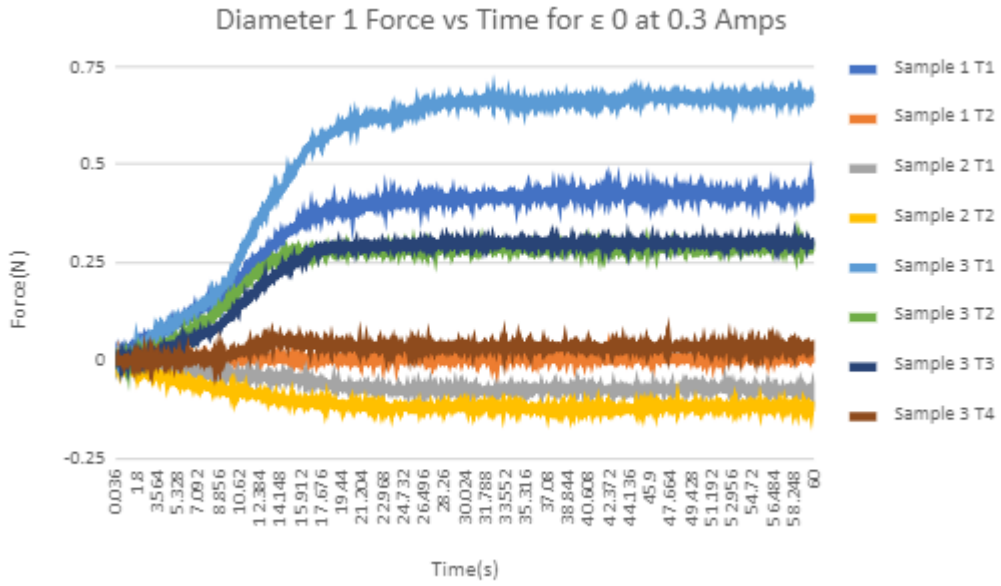
Diameter 1 Force vs Time for ε 0 at 0.3 Amps
Force(N)
0.75
0.5
0.25
0
-0.25
0.036
1.8
3.564
5.328
7.092
8.856
10.62
12.384
14.148
15.912
17.676
19.44
21.204
22.968
24.732
26.496
28.26
30.024
31.788
33.552
35.316
37.08
38.844
40.608
42.372
44.136
45.9
47.664
49.428
51.192
52.956
54.72
56.484
58.248
60
Time(s)
Sample 1 T1
Sample 1 T2
Sample 2 T1
Sample 2 T2
Sample 3 T1
Sample 3 T2
Sample 3 T3
Sample 3 T4

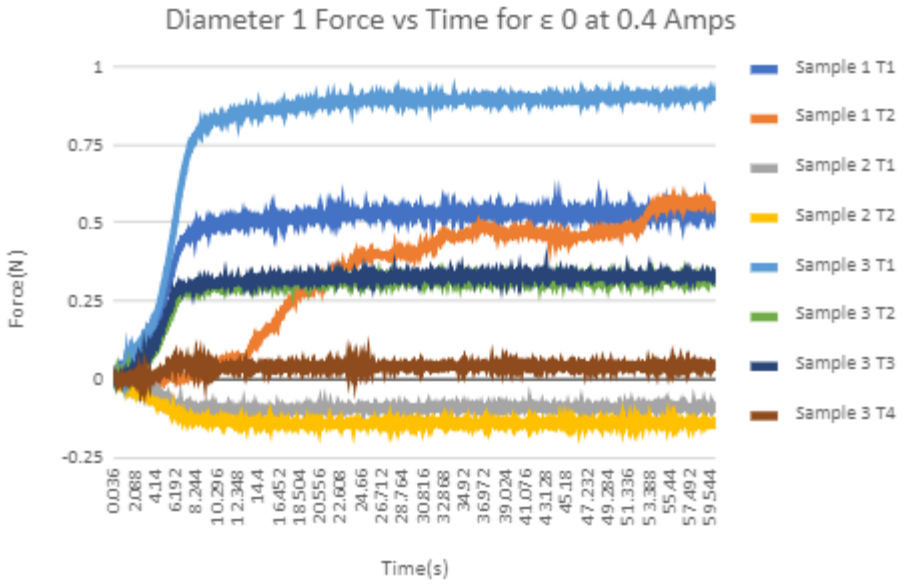
Diameter 1 Force vs Time for ε 0 at 0.4 Amps
Force(N)
Time(s)
Sample 1 T1
Sample 1 T2
Sample 2 T1
Sample 2 T2
Sample 3 T1
Sample 3 T2
Sample 3 T3
Sample 3 T4

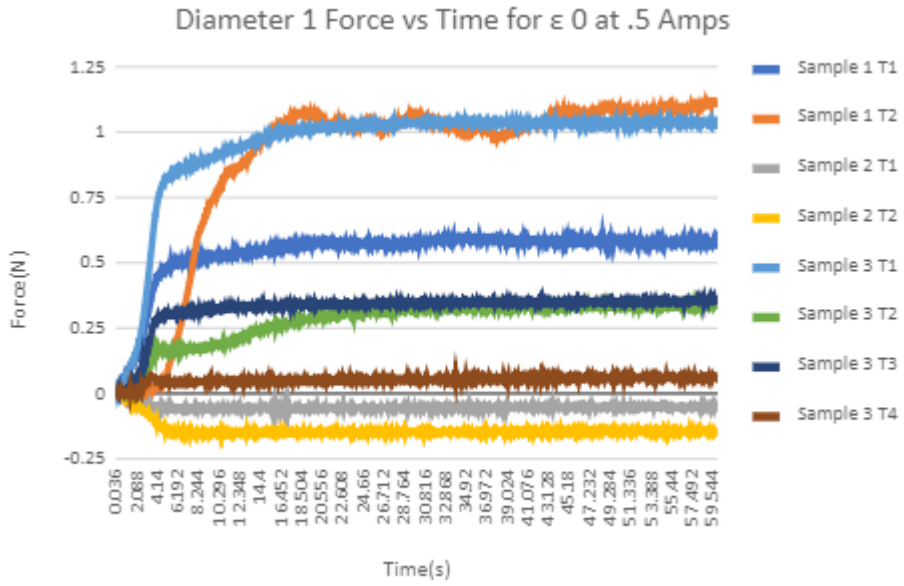
Diameter 1 Force vs Time for ε 0 at .5 Amps
Force(N)
Time(s)
Sample 1 T1
Sample 1 T2
Sample 2 T1
Sample 2 T2
Sample 3 T1
Sample 3 T2
Sample 3 T3
Sample 3 T4

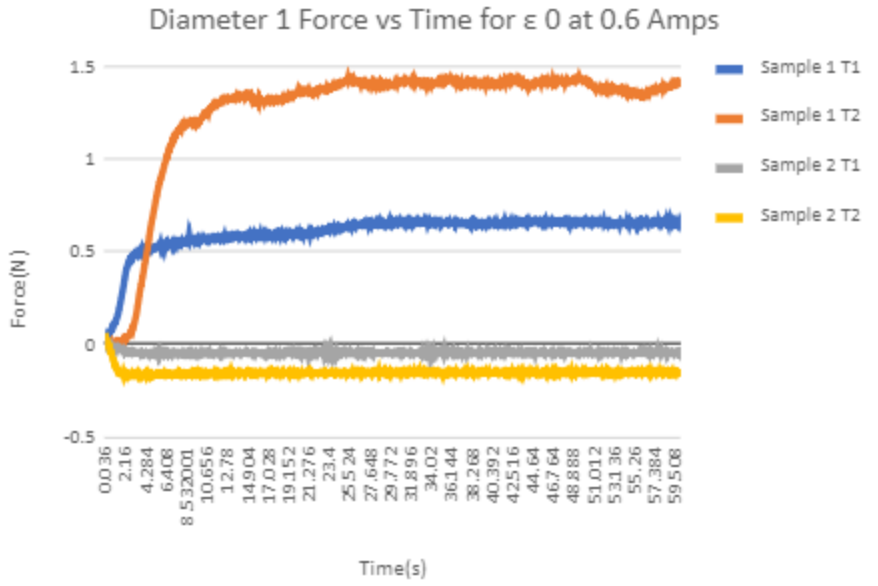
Diameter 1 Force vs Time for ε 0 at 0.6 Amps
Force(N)
Time(s)
Sample 1 T1
Sample 1 T2
Sample 2 T1
Sample 2 T2

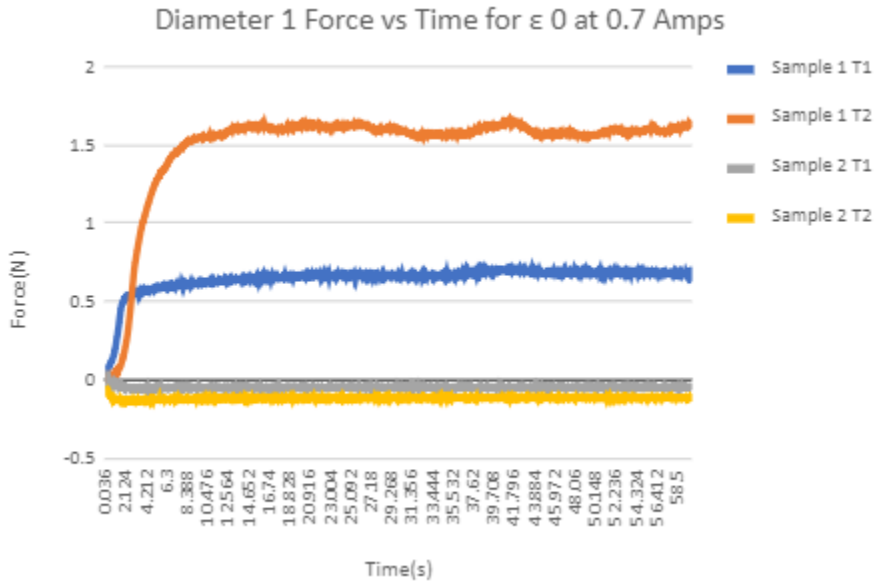
Diameter 1 Force vs Time for ε 0 at 0.7 Amps
Force(N)
Time(s)
Sample 1 T1
Sample 1 T2
Sample 2 T1
Sample 2 T2

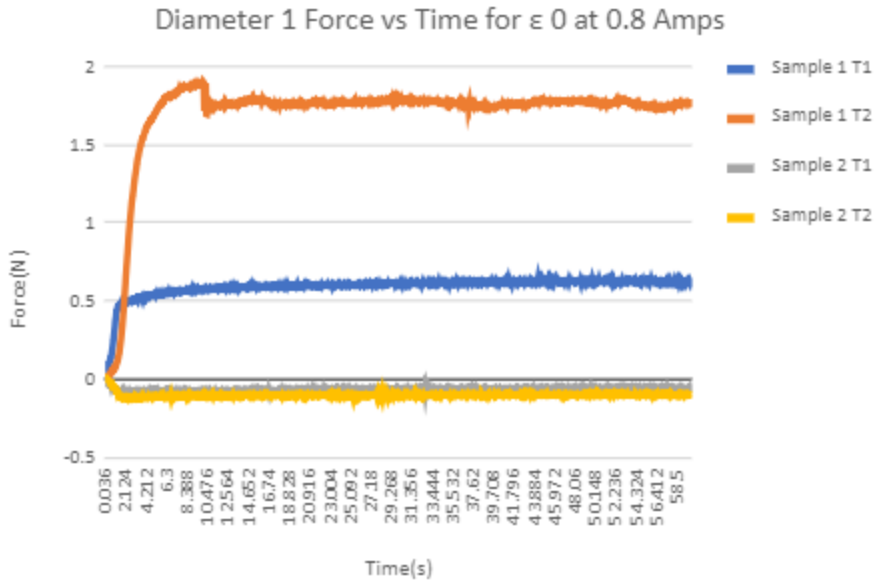
Diameter 1 Force vs Time for ε 0 at 0.8 Amps
Force(N)
2
1.5
1
0.5
0
-0.5
0.036
2.124
4.212
6.3
8.388
10.476
12.564
14.652
16.74
18.828
20.916
23.004
25.092
27.18
29.268
31.356
33.444
35.532
37.62
39.708
41.796
43.884
45.972
48.06
50.148
52.236
54.324
56.412
585
Time(s)
Sample 1 T1
Sample 1 T2
Sample 2 T1
Sample 2 T2

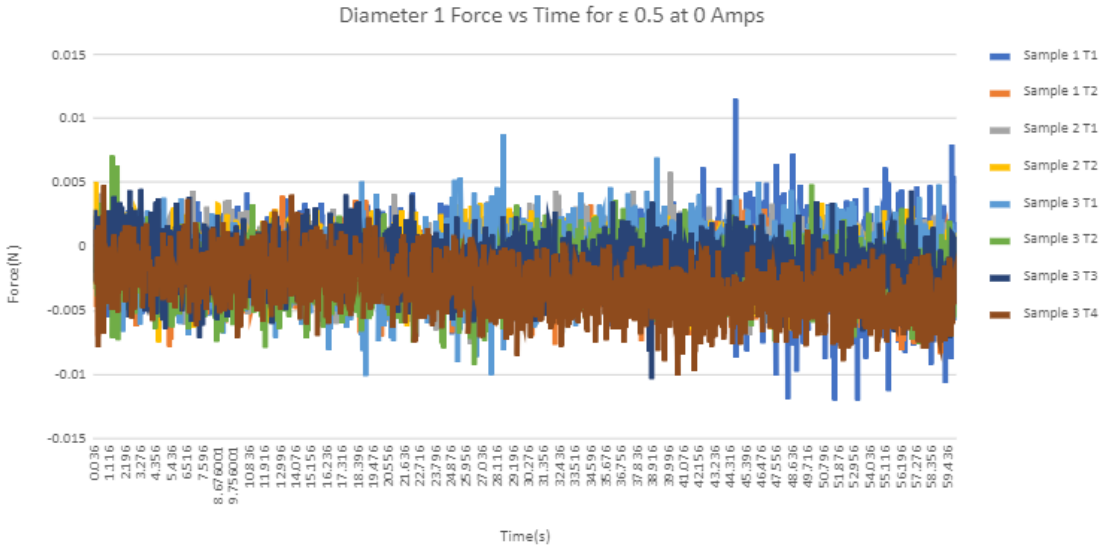
Diameter 1 Force vs Time for ε 0.5 at 0 Amps
Force (N)
Time(s)
Sample 1 T1
Sample 1 T2
Sample 2 T1
Sample 2 T2
Sample 3 T1
Sample 3 T2
Sample 3 T3
Sample 3 T4

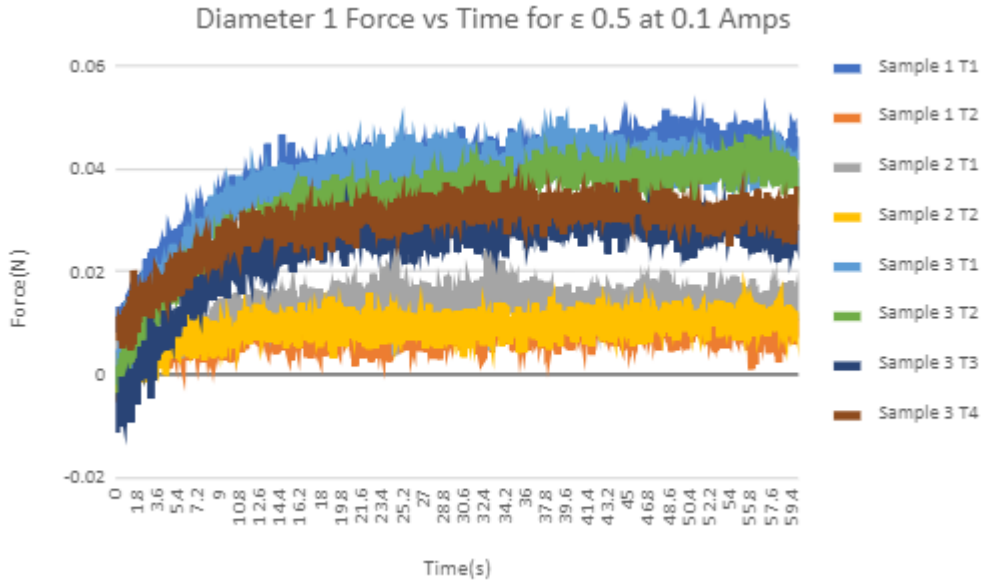
Diameter 1 Force vs Time for ε 0.5 at 0.1 Amps
Force (N)
Time(s)
Sample 1 T1
Sample 1 T2
Sample 2 T1
Sample 2 T2
Sample 3 T1
Sample 3 T2
Sample 3 T3
Sample 3 T4

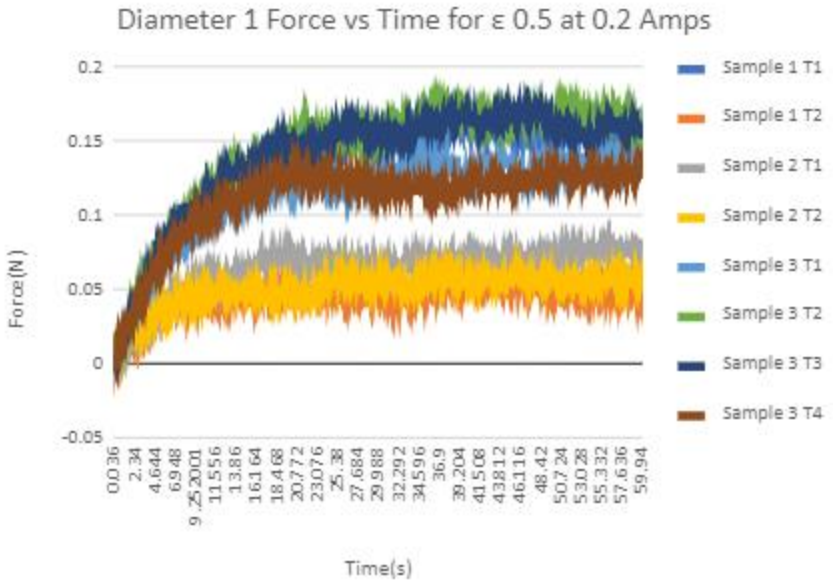
Diameter 1 Force vs Time for ε 0.5 at 0.2 Amps
Force(N)
Time(s)
Sample 1 T1
Sample 1 T2
Sample 2 T1
Sample 2 T2
Sample 3 T1
Sample 3 T2
Sample 3 T3
Sample 3 T4

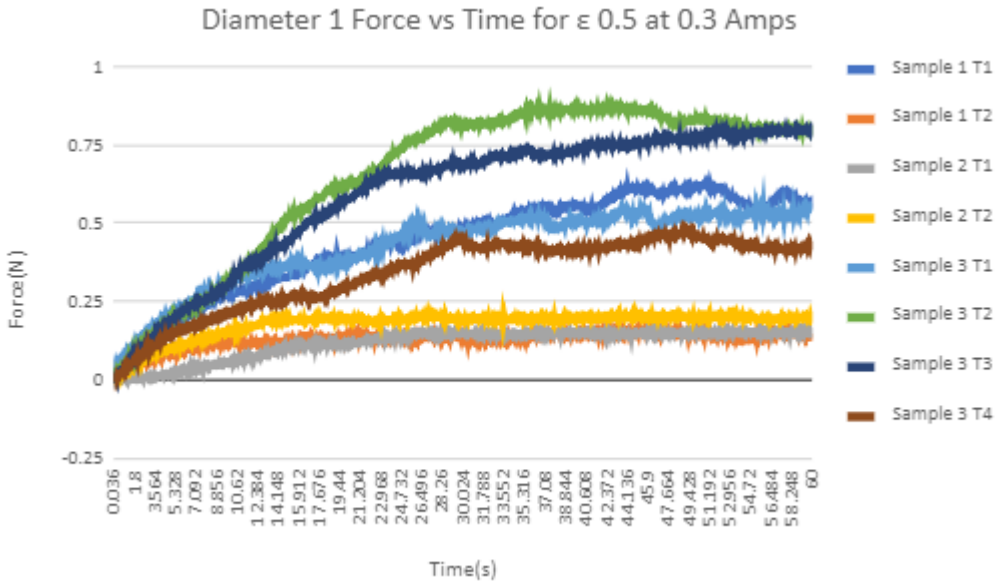
Diameter 1 Force vs Time for ε 0.5 at 0.3 Amps
Force(N)
Time(s)
Sample 1 T1
Sample 1 T2
Sample 2 T1
Sample 2 T2
Sample 3 T1
Sample 3 T2
Sample 3 T3
Sample 3 T4

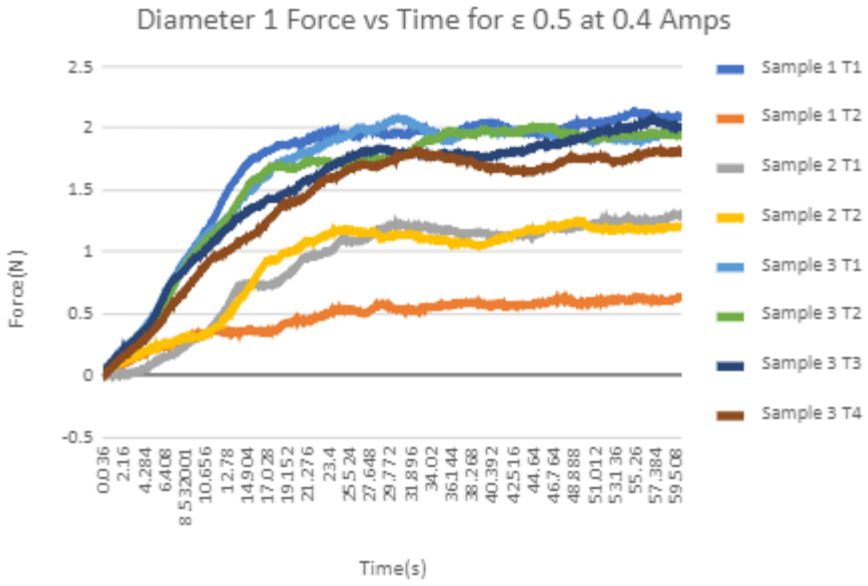
Diameter 1 Force vs Time for ε 0.5 at 0.4 Amps
Force(N)
Time(s)
Sample 1 T1
Sample 1 T2
Sample 2 T1
Sample 2 T2
Sample 3 T1
Sample 3 T2
Sample 3 T3
Sample 3 T4

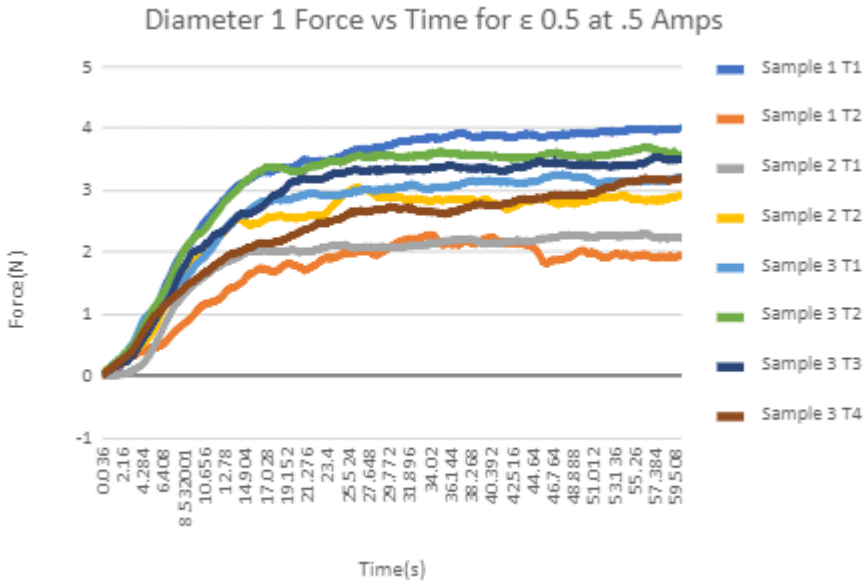
Diameter 1 Force vs Time for ε 0.5 at .5 Amps
Force(N)
Time(s)
Sample 1 T1
Sample 1 T2
Sample 2 T1
Sample 2 T2
Sample 3 T1
Sample 3 T2
Sample 3 T3
Sample 3 T4

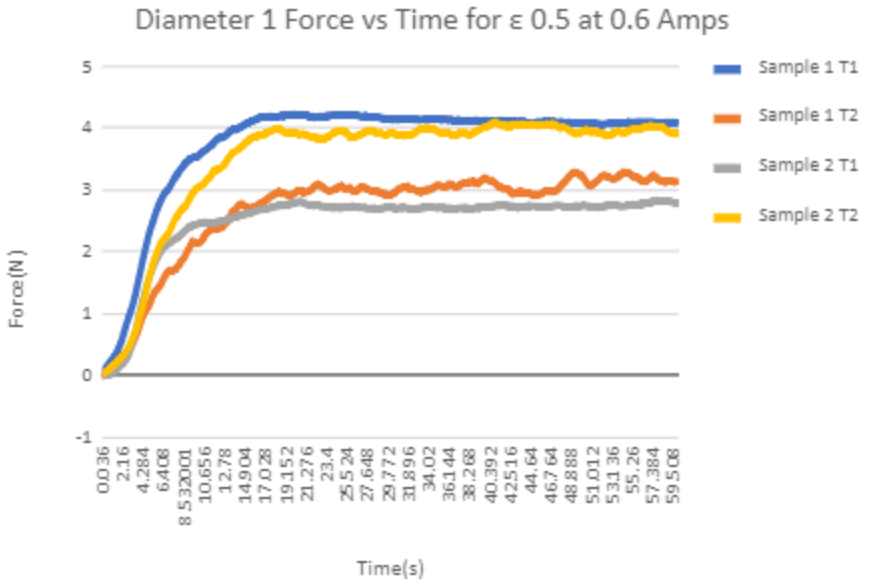
Diameter 1 Force vs Time for ε 0.5 at 0.6 Amps
Force(N)
Time(s)
Sample 1 T1
Sample 1 T2
Sample 2 T1
Sample 2 T2

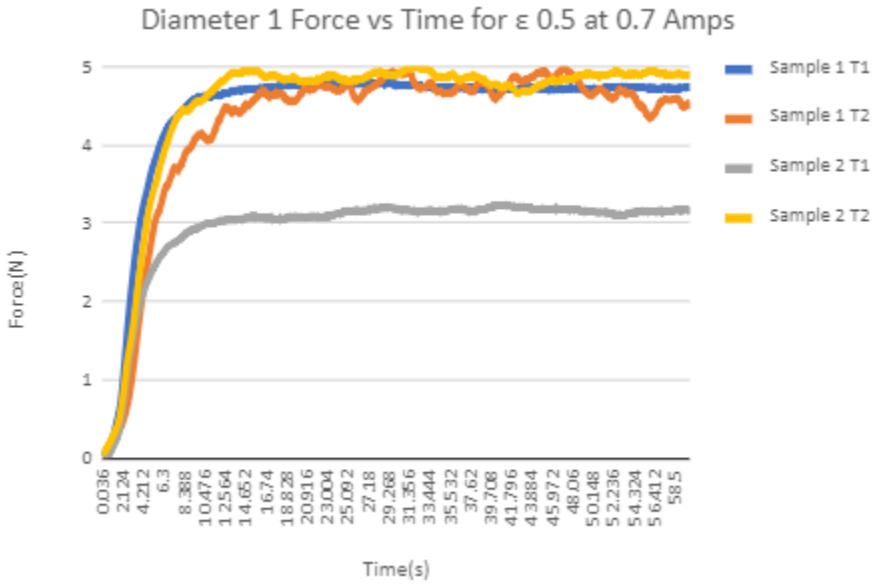
Diameter 1 Force vs Time for ε 0.5 at 0.7 Amps
Force(N)
Time(s)
Sample 1 T1
Sample 1 T2
Sample 2 T1
Sample 2 T2

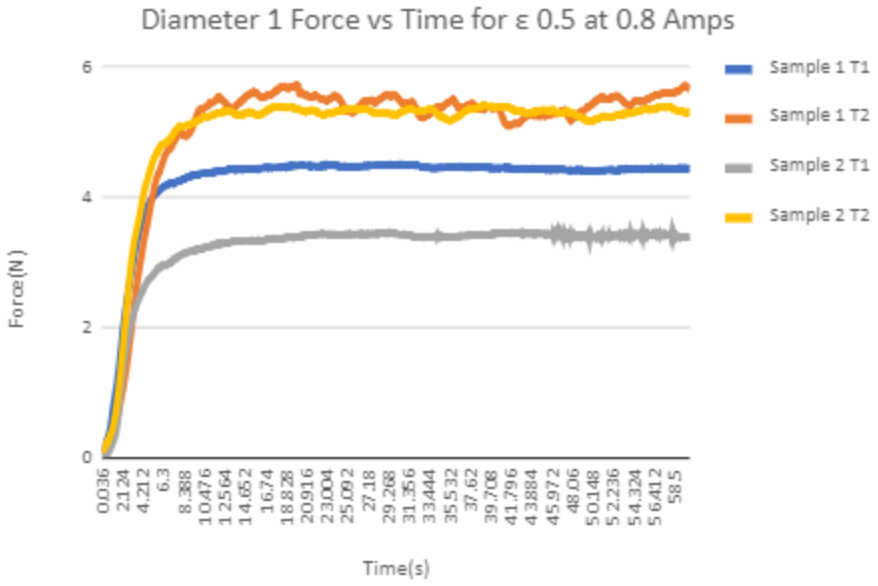
Diameter 1 Force vs Time for ε 0.5 at 0.8 Amps
Force(N)
Time(s)
Sample 1 T1
Sample 1 T2
Sample 2 T1
Sample 2 T2

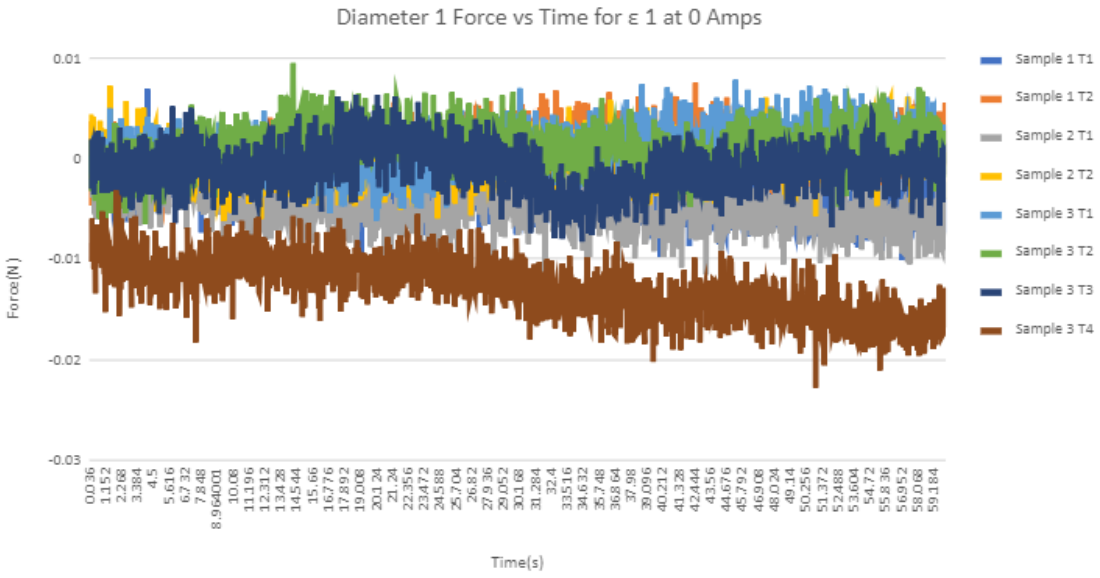
Diameter 1 Force vs Time for ε 1 at 0 Amps
Force(N)
Time(s)
Sample 1 T1
Sample 1 T2
Sample 2 T1
Sample 2 T2
Sample 3 T1
Sample 3 T2
Sample 3 T3
Sample 3 T4

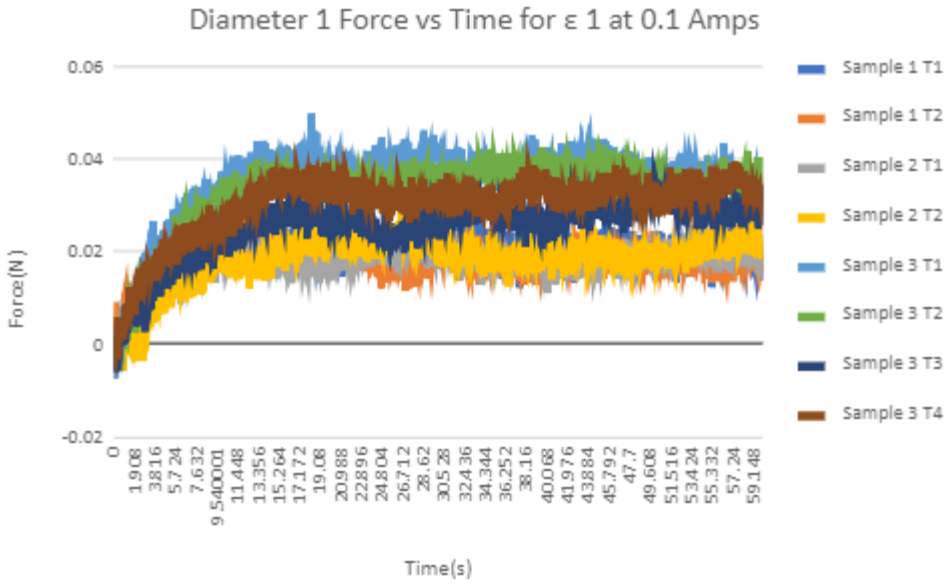
Diameter 1 Force vs Time for ε 1 at 0.1 Amps
Force(N)
Time(s)
Sample 1 T1
Sample 1 T2
Sample 2 T1
Sample 2 T2
Sample 3 T1
Sample 3 T2
Sample 3 T3
Sample 3 T4

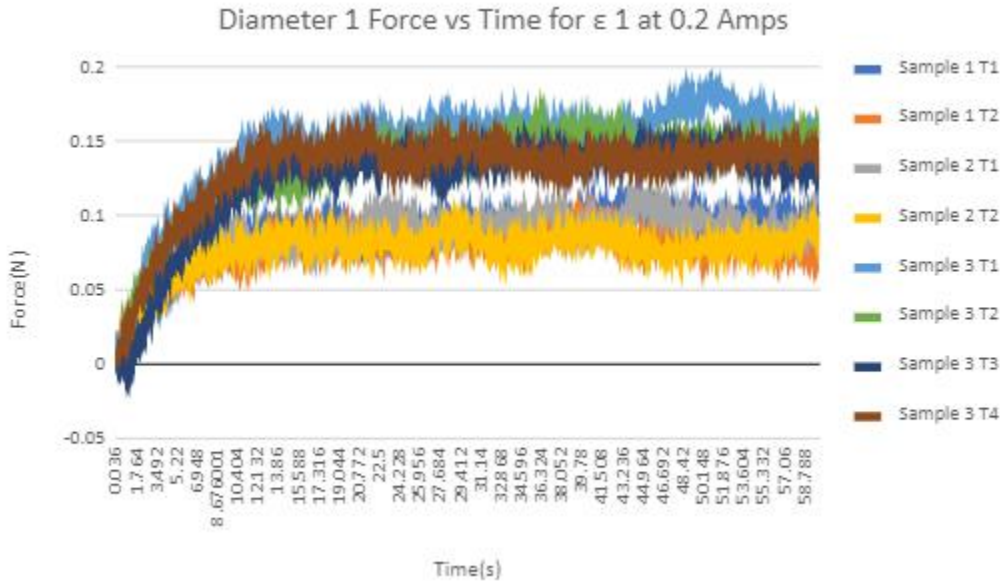
Diameter 1 Force vs Time for ε 1 at 0.2 Amps
Force(N)
Time(s)
Sample 1 T1
Sample 1 T2
Sample 2 T1
Sample 2 T2
Sample 3 T1
Sample 3 T2
Sample 3 T3
Sample 3 T4

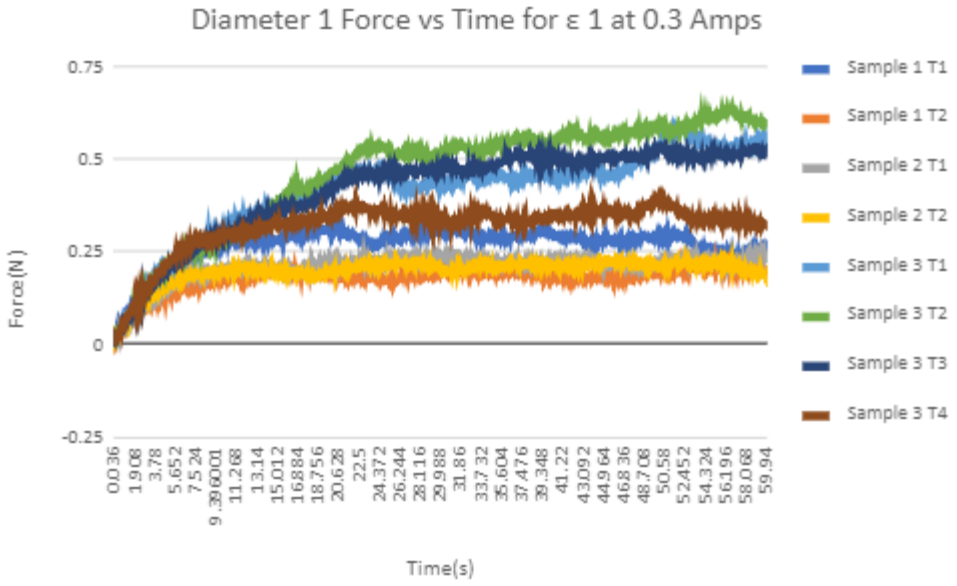
Diameter 1 Force vs Time for ε 1 at 0.3 Amps
Force(N)
Time(s)
Sample 1 T1
Sample 1 T2
Sample 2 T1
Sample 2 T2
Sample 3 T1
Sample 3 T2
Sample 3 T3
Sample 3 T4

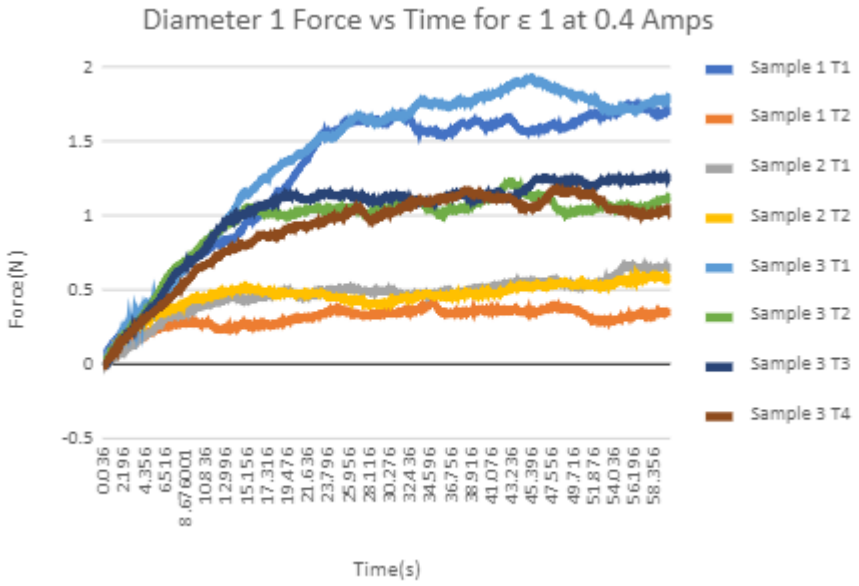
Diameter 1 Force vs Time for ε 1 at 0.4 Amps
Force(N)
Time(s)
Sample 1 T1
Sample 1 T2
Sample 2 T1
Sample 2 T2
Sample 3 T1
Sample 3 T2
Sample 3 T3
Sample 3 T4

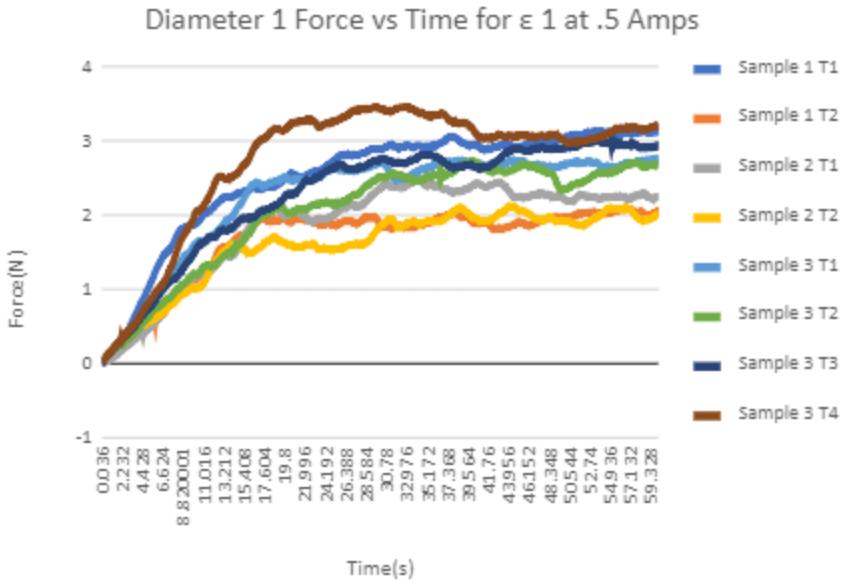
Diameter 1 Force vs Time for ε 1 at .5 Amps
Force(N)
4
3
2
1
0
-1
0.036
2.232
4.428
6.624
8.820001
11.016
13.212
15.408
17.604
19.8
21.996
24.192
26.388
28.584
30.78
32.976
35.172
37.368
39.564
41.76
43.956
46.152
48.348
50.544
52.74
54.936
57.132
59.328
Time(s)
Sample 1 T1
Sample 1 T2
Sample 2 T1
Sample 2 T2
Sample 3 T1
Sample 3 T2
Sample 3 T3
Sample 3 T4

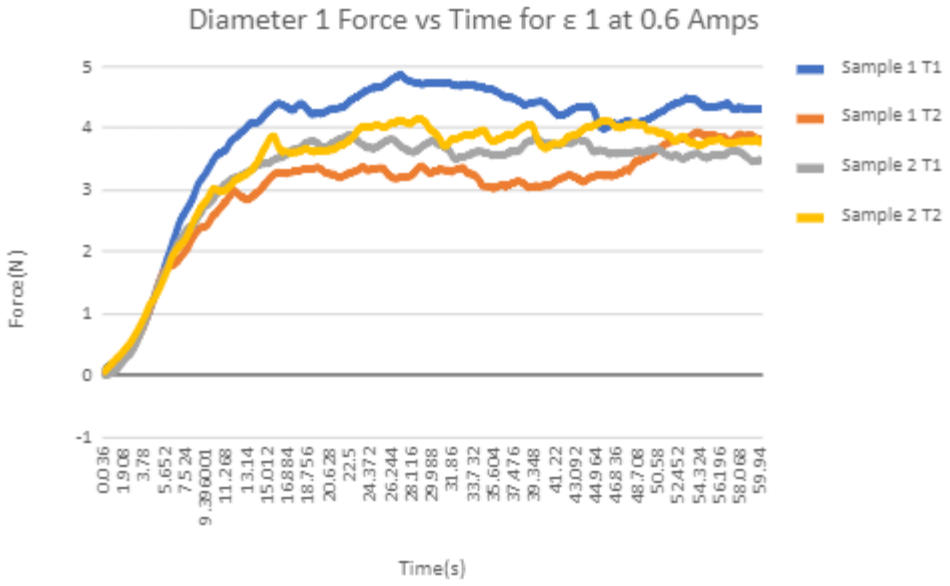
Diameter 1 Force vs Time for ε 1 at 0.6 Amps
Force(N)
Time(s)
Sample 1 T1
Sample 1 T2
Sample 2 T1
Sample 2 T2

,

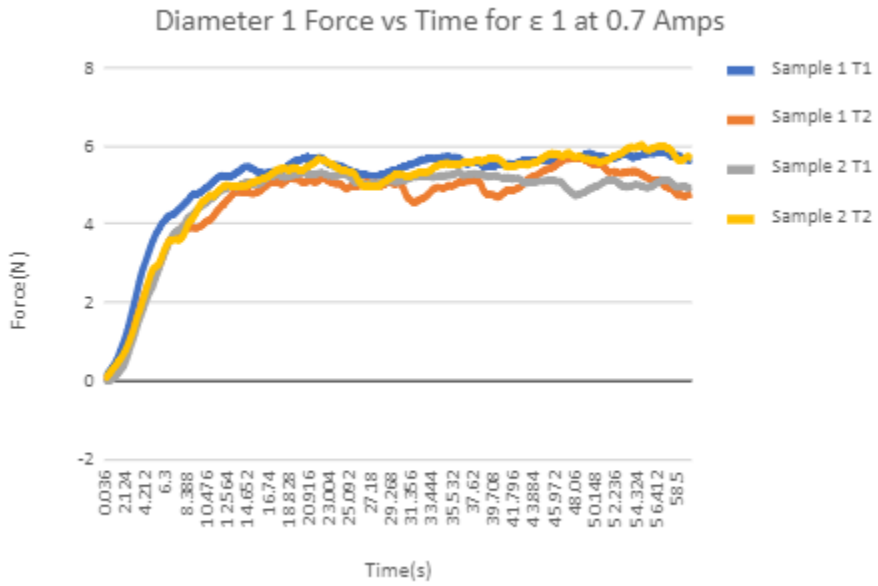
Diameter 1 Force vs Time for ε 1 at 0.7 Amps
Force(N)
Time(s)
Sample 1 T1
Sample 1 T2
Sample 2 T1
Sample 2 T2

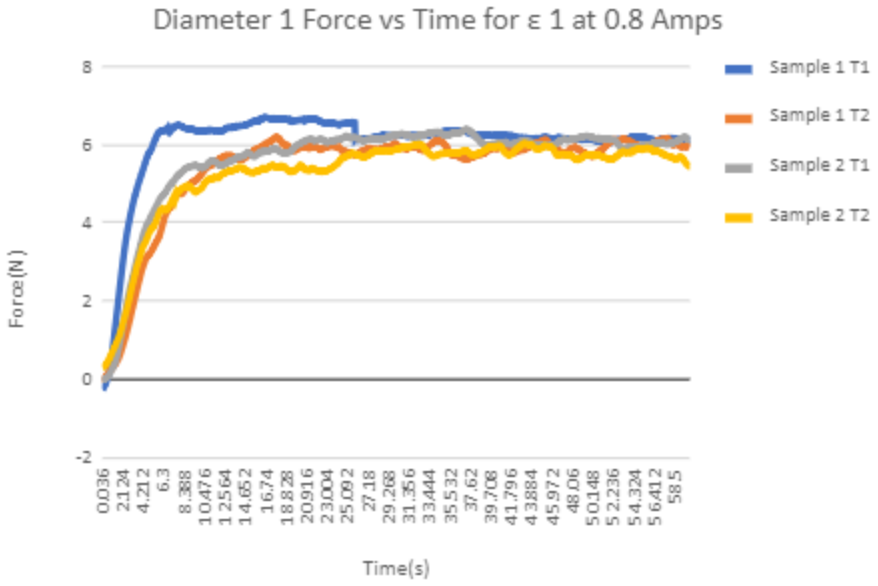
Diameter 1 Force vs Time for ε 1 at 0.8 Amps
Force(N)
Time(s)
Sample 1 T1
Sample 1 T2
Sample 2 T1
Sample 2 T2

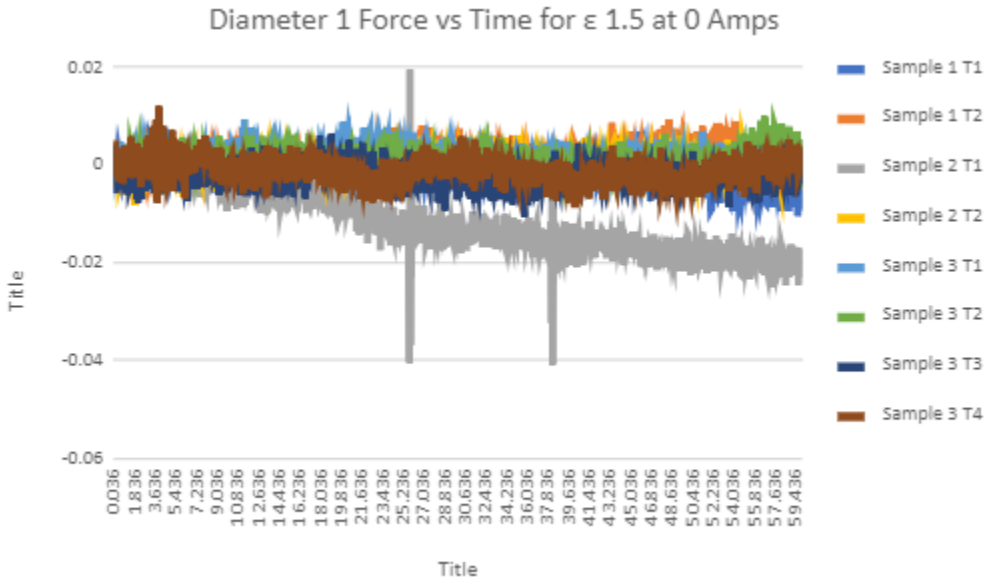
Diameter 1 Force vs Time for ε 1.5 at 0 Amps
Title
Title
Sample 1 T1
Sample 1 T2
Sample 2 T1
Sample 2 T2
Sample 3 T1
Sample 3 T2
Sample 3 T3
Sample 3 T4

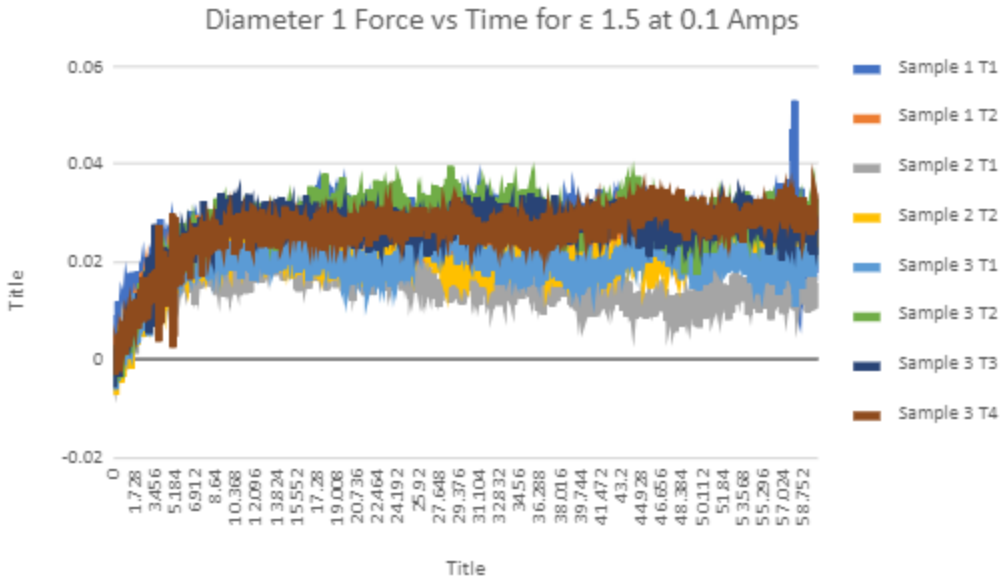
Diameter 1 Force vs Time for ε 1.5 at 0.1 Amps
0.06
0.04
0.02
0
-0.02
Title
0
1.728
3.456
5.184
6.912
8.64
10.368
12.096
13.824
15.552
17.28
19.008
20.736
22.464
24.192
25.92
27.648
29.376
31.104
32.832
34.56
36.288
38.016
39.744
41.472
43.2
44.928
46.656
48.384
50.112
51.84
53.568
55.296
57.024
58.752
Title
Sample 1 T1
Sample 1 T2
Sample 2 T1
Sample 2 T2
Sample 3 T1
Sample 3 T2
Sample 3 T3
Sample 3 T4

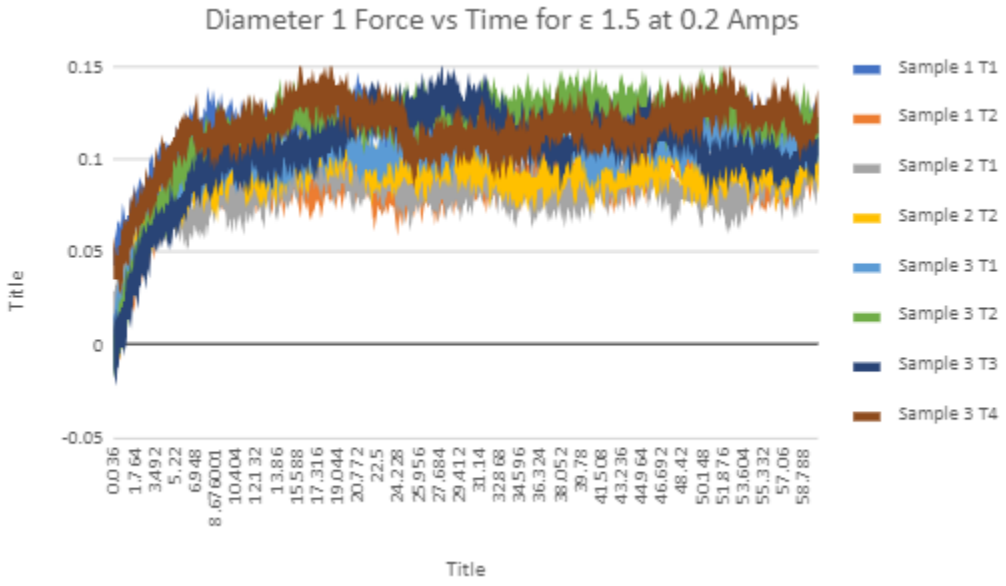
Diameter 1 Force vs Time for ε 1.5 at 0.2 Amps
0.15
0.1
0.05
0
-0.05
Title
0.036
1.764
3.492
5.22
6.948
8.676001
10.404
12.132
13.86
15.588
17.316
19.044
20.772
22.5
24.228
25.956
27.684
29.412
31.14
32.868
34.596
36.324
38.052
39.78
41.508
43.236
44.964
46.692
48.42
50.148
51.876
53.604
55.332
57.06
58.788
Title
Sample 1 T1
Sample 1 T2
Sample 2 T1
Sample 2 T2
Sample 3 T1
Sample 3 T2
Sample 3 T3
Sample 3 T4

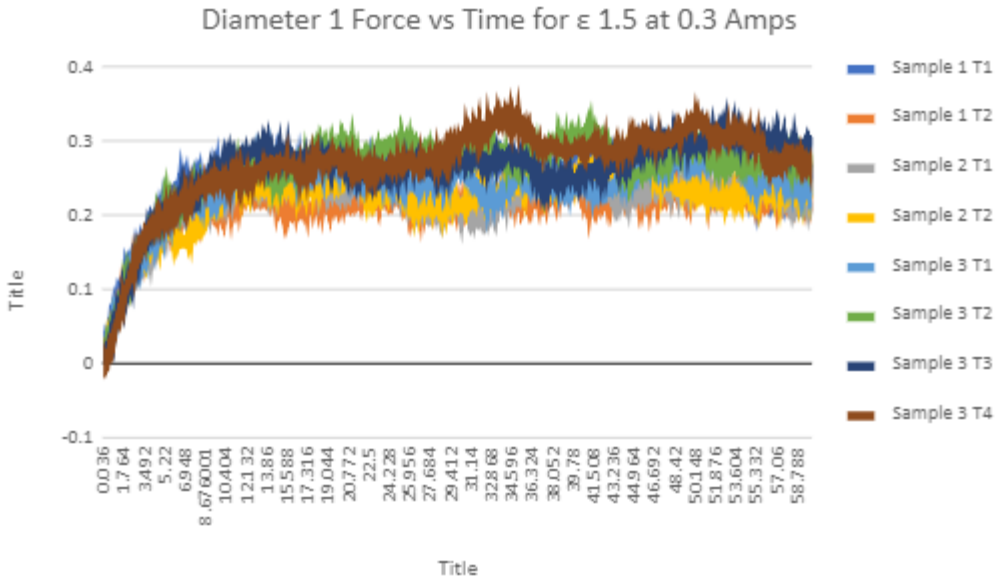
Diameter 1 Force vs Time for ε 1.5 at 0.3 Amps
Title
Title
Sample 1 T1
Sample 1 T2
Sample 2 T1
Sample 2 T2
Sample 3 T1
Sample 3 T2
Sample 3 T3
Sample 3 T4

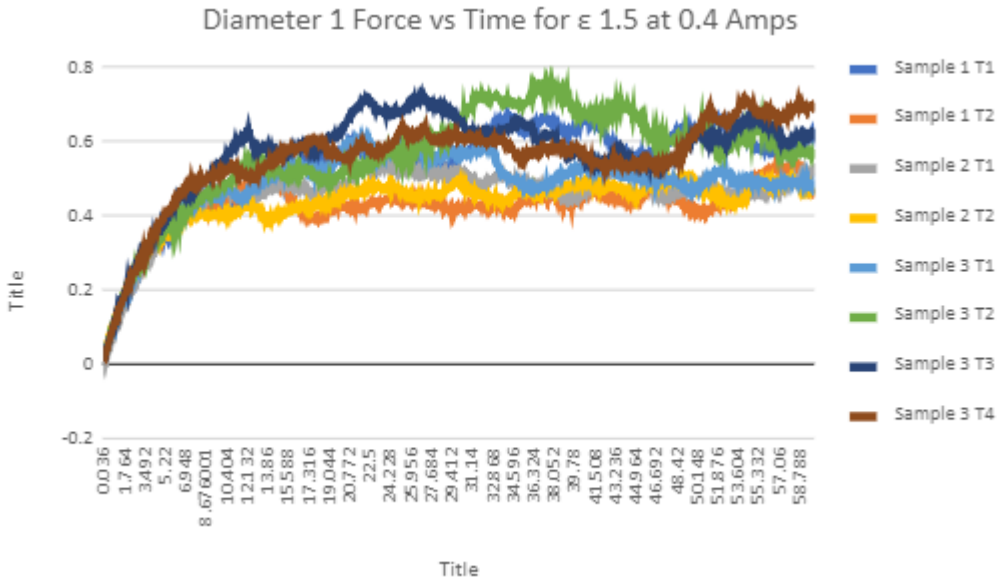
Diameter 1 Force vs Time for ε 1.5 at 0.4 Amps
Title
Title
Sample 1 T1
Sample 1 T2
Sample 2 T1
Sample 2 T2
Sample 3 T1
Sample 3 T2
Sample 3 T3
Sample 3 T4

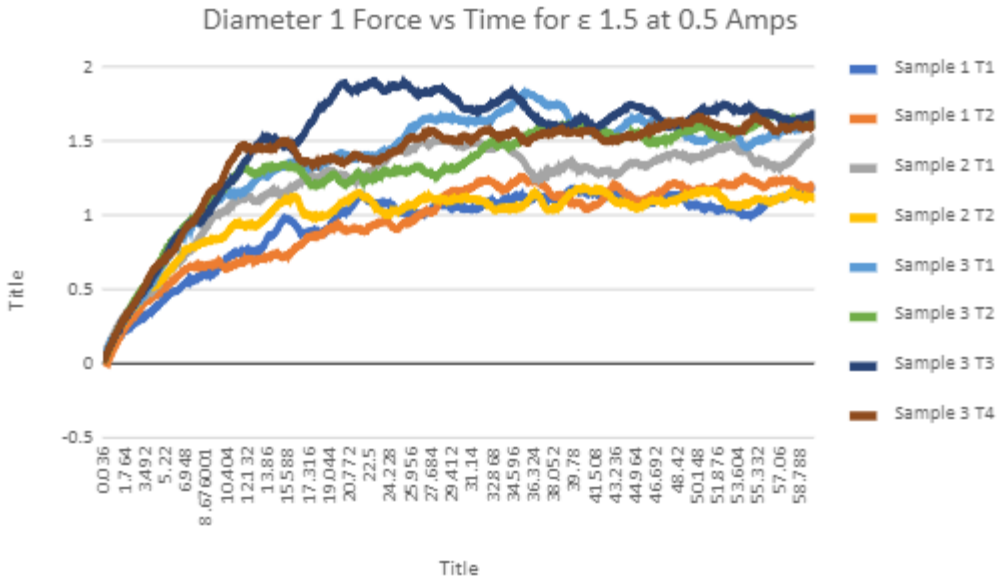
Diameter 1 Force vs Time for ε 1.5 at 0.5 Amps
Title
Sample 1 T1
Sample 1 T2
Sample 2 T1
Sample 2 T2
Sample 3 T1
Sample 3 T2
Sample 3 T3
Sample 3 T4

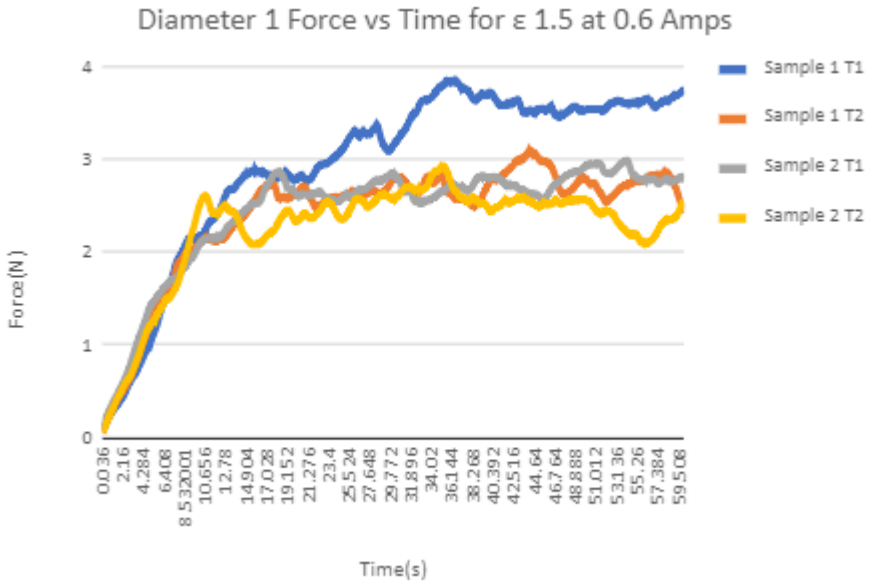
Diameter 1 Force vs Time for ε 1.5 at 0.6 Amps
Force(N)
Time(s)
Sample 1 T1
Sample 1 T2
Sample 2 T1
Sample 2 T2

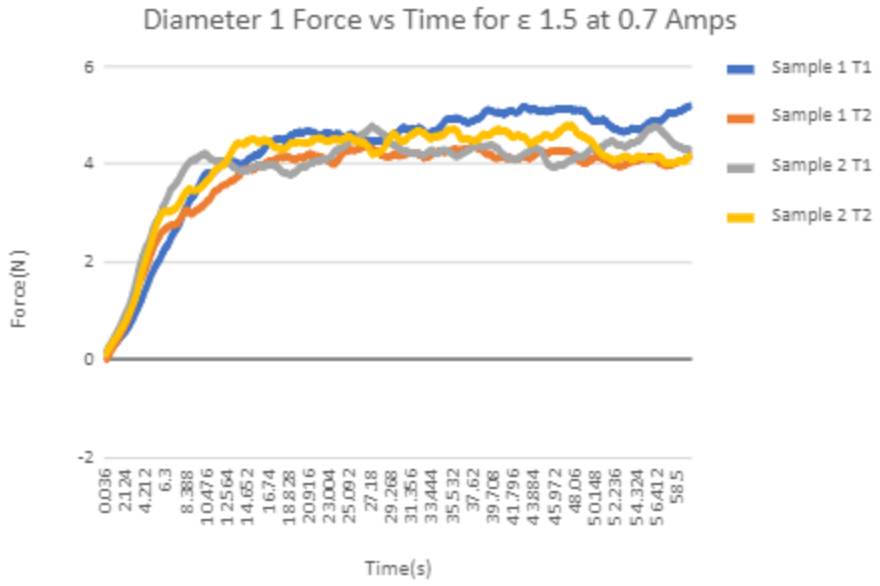
Diameter 1 Force vs Time for ε 1.5 at 0.7 Amps
Sample 1 T1
Sample 1 T2
Sample 2 T1
Sample 2 T2
Force(N)
Time(s)

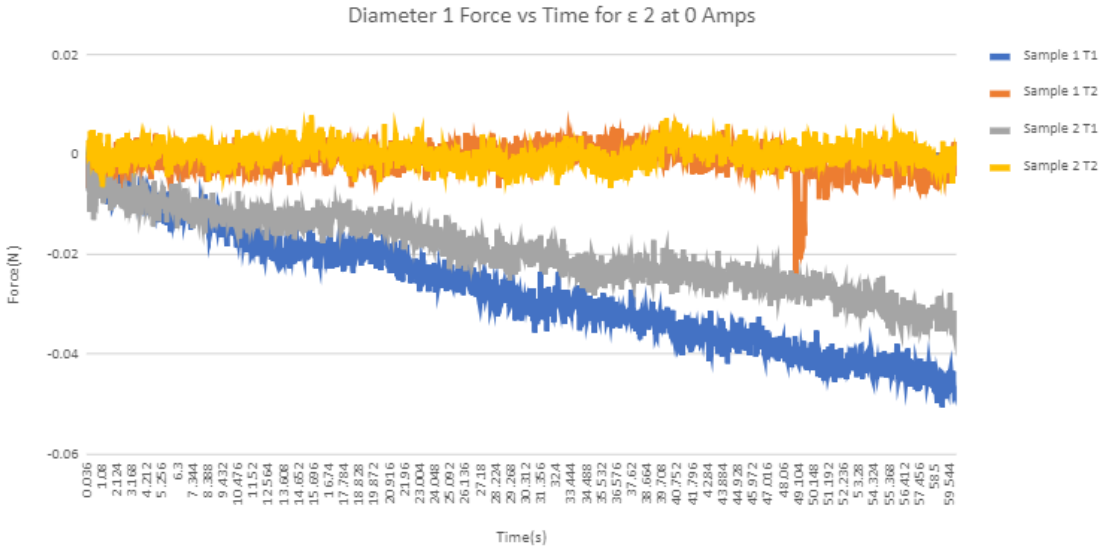
Diameter 1 Force vs Time for ε 2 at 0 Amps
Sample 1 T1
Sample 1 T2
Sample 2 T1
Sample 2 T2
Force(N)
Time(s)

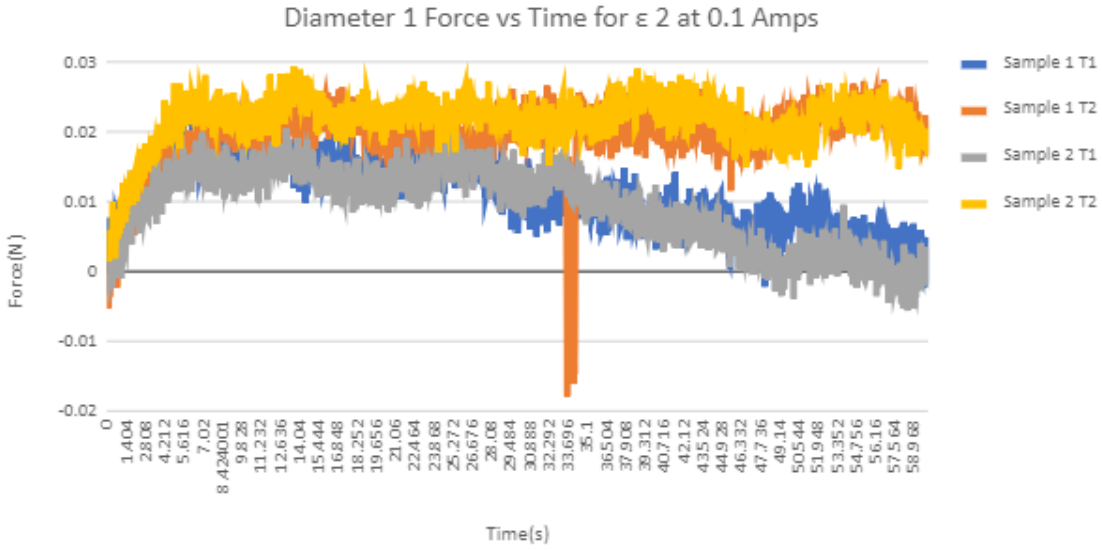
Diameter 1 Force vs Time for ε 2 at 0.1 Amps
Force(N)
Time(s)
Sample 1 T1
Sample 1 T2
Sample 2 T1
Sample 2 T2

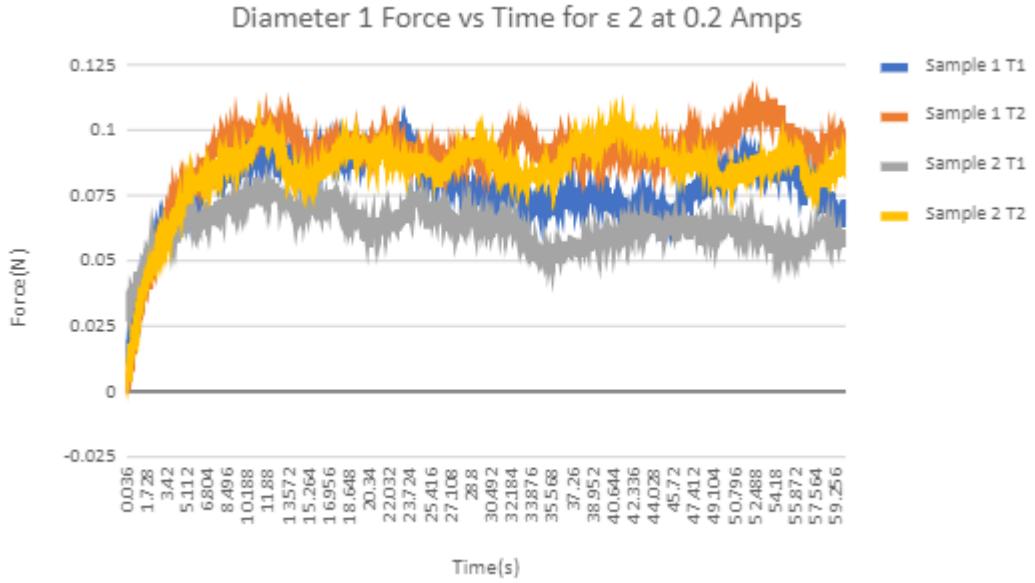
Diameter 1 Force vs Time for ε 2 at 0.2 Amps
Force(N)
Time(s)
Sample 1 T1
Sample 1 T2
Sample 2 T1
Sample 2 T2

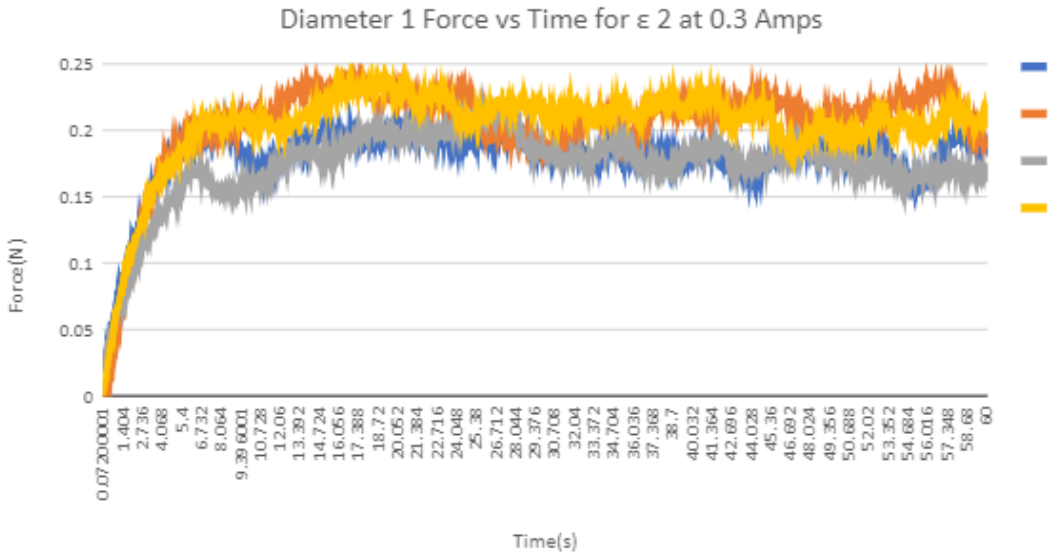
Diameter 1 Force vs Time for ε 2 at 0.3 Amps
Force(N)
Time(s)

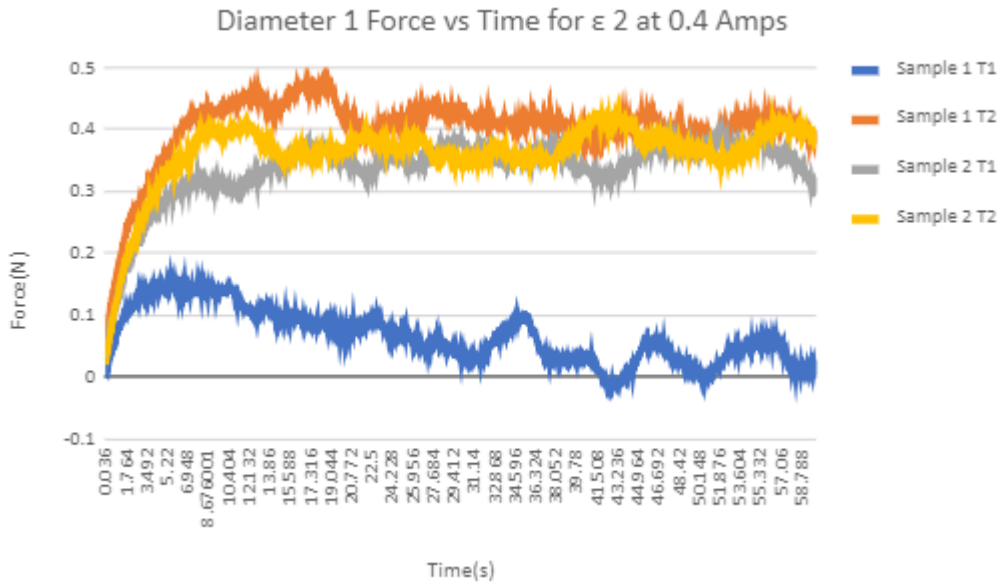
Diameter 1 Force vs Time for ε 2 at 0.4 Amps
Sample 1 T1
Sample 1 T2
Sample 2 T1
Sample 2 T2
Force(N)
Time(s)

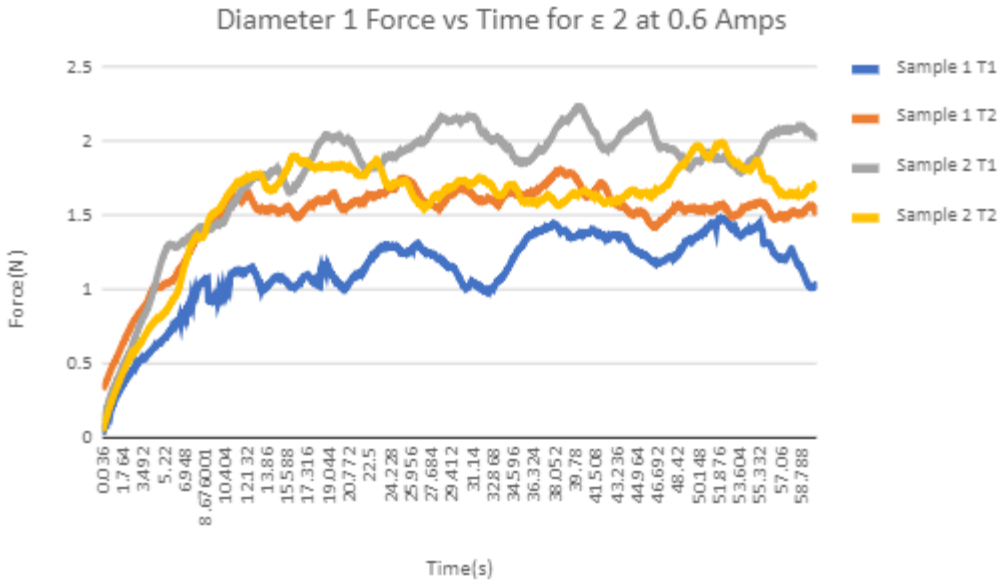
Diameter 1 Force vs Time for ε 2 at 0.6 Amps
Force(N)
Time(s)
Sample 1 T1
Sample 1 T2
Sample 2 T1
Sample 2 T2

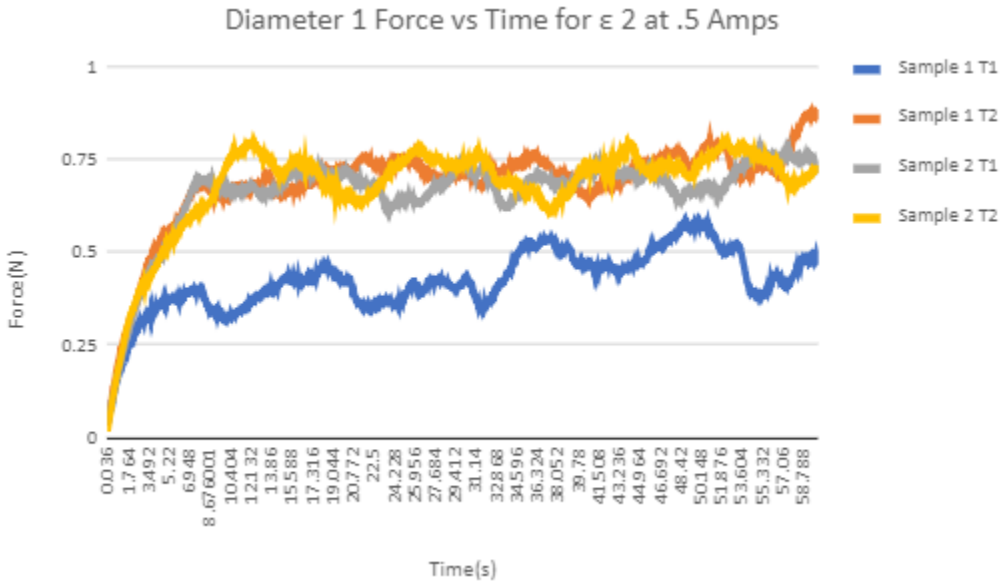
Diameter 1 Force vs Time for ε 2 at .5 Amps
Force(N)
Time(s)
Sample 1 T1
Sample 1 T2
Sample 2 T1
Sample 2 T2

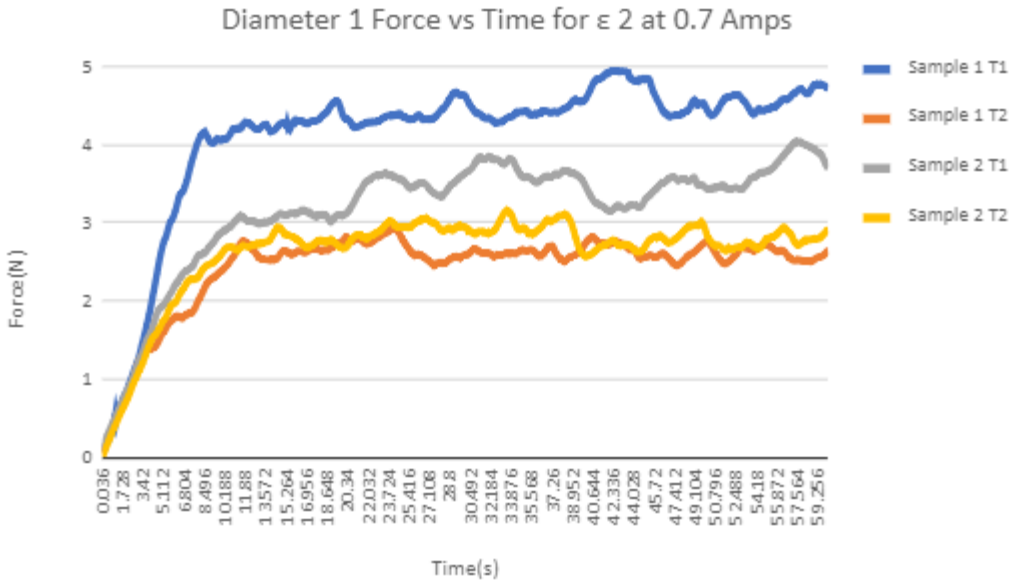
Diameter 1 Force vs Time for ε 2 at 0.7 Amps
Force(N)
Time(s)
Sample 1 T1
Sample 1 T2
Sample 2 T1
Sample 2 T2

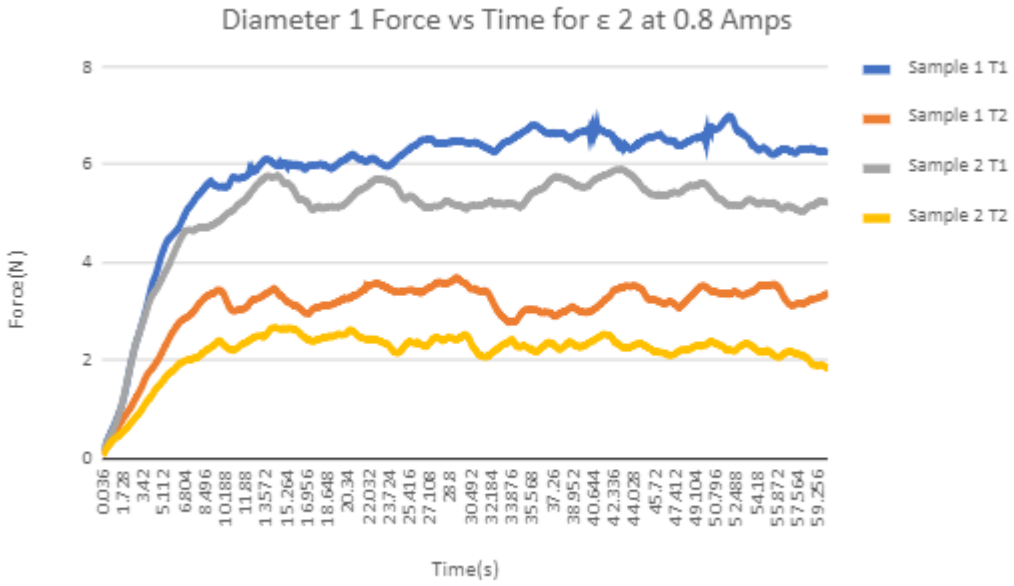
Diameter 1 Force vs Time for ε 2 at 0.8 Amps
Force(N)
Time(s)
Sample 1 T1
Sample 1 T2
Sample 2 T1
Sample 2 T2

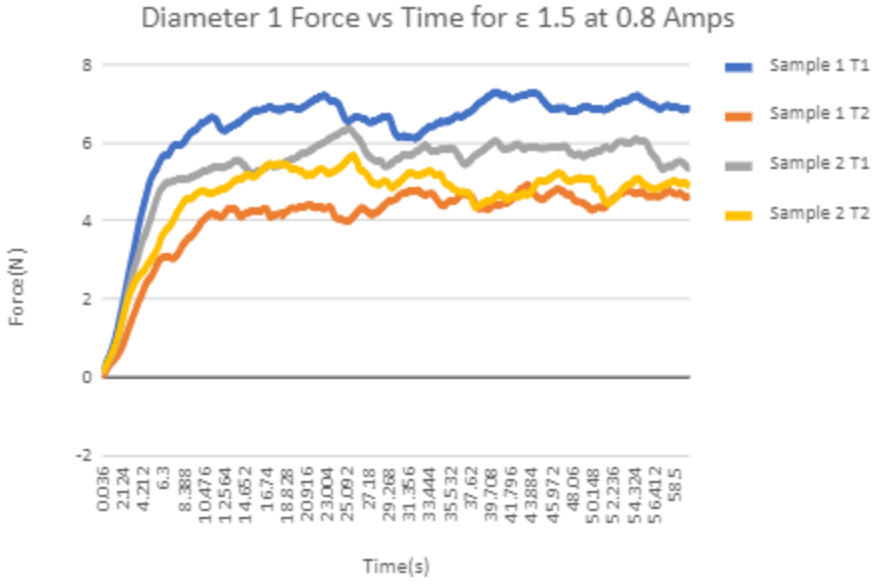
Diameter 1 Force vs Time for ε 1.5 at 0.8 Amps
Force(N)
8
6
4
2
0
-2
0.036
2.124
4.212
6.3
8.388
10.476
12.564
14.652
16.74
18.828
20.916
23.004
25.092
27.18
29.268
31.356
33.444
35.532
37.62
39.708
41.796
43.884
45.972
48.06
50.148
52.236
54.324
56.412
585
Time(s)
Sample 1 T1
Sample 1 T2
Sample 2 T1
Sample 2 T2

Force, Resistance, Power Tables Diameter 1

D1 E1 Force Max

A1 Trial	Force Max	Time	A2 Trial	Force Max	Time	A3 Trial	Force Max	Time	A4 Trial	Force Max	Time	A5 Trial	Force Max	Time
S3 T1	0.01	3.53	S3 T1	0.03	49.82	S3 T1	0.14	53.89	S3 T1	0.68	59.26	S3 T1	0.91	58.07
S3 T2	0.01	46.26	S3 T2	0.01	57.13	S3 T2	0.06	43.20	S3 T2	0.30	58.64	S3 T2	0.32	59.47
S3 T3	0.01	51.80	S3 T3	0.02	32.36	S3 T3	0.06	48.60	S3 T3	0.30	58.39	S3 T3	0.34	43.16
S3 T4	0.01	11.52	S3 T4	0.02	4.10	S3 T4	0.01	21.17	S3 T4	0.05	14.15	S3 T4	0.06	6.16
AVE	0.010	28.278	AVE	0.020	35.853	AVE	0.068	41.715	AVE	0.333	47.610	AVE	0.41	41.72
RANGE	0.000	48.270	RANGE	0.020	53.030	RANGE	0.130	32.720	RANGE	0.630	45.110	RANGE	0.85	53.31
SD	0.000	21.035	SD	0.007	20.422	SD	0.047	12.449	SD	0.225	19.321	SD	0.31	21.50

A6 Trial	Force Max	Time
S3 T1	1.04	34.85
S3 T2	0.34	59.40
S3 T3	0.36	59.47
S3 T4	0.06	3.60
AVE	0.45	39.33
RANGE	0.98	55.87

SD	0.36	22.94

D1 E1 Max power

A1 Sample	Power (W)	A2 Sample	Power (W)	A3 Sample	Power (W)	A4 Sample	Power (W)	A5 Sample	Power (W)	A6 Sample	Power (W)
S3 T1	0.00	S3 T1	0.06	S3 T1	0.26	S3 T1	0.56	S3 T1	1.09	S3 T1	1.67
S3 T2	0.00	S3 T2	0.07	S3 T2	0.27	S3 T2	0.58	S3 T2	1.01	S3 T2	1.57
S3 T3	0.00	S3 T3	0.07	S3 T3	0.30	S3 T3	0.61	S3 T3	1.05	S3 T3	1.57
S3 T4	0.00	S3 T4	0.08	S3 T4	0.29	S3 T4	0.61	S3 T4	1.07	S3 T4	1.67
AVE	0.00	AVE	0.070	AVE	0.016	AVE	0.105	AVE	0.446	AVE	1.317
RANGE	0.00	RANGE	0.020	RANGE	0.005	RANGE	0.019	RANGE	0.066	RANGE	0.161
SD	0.00	SD	0.007	SD	0.002	SD	0.008	SD	0.024	SD	0.078
A6		A7		A8		A9					

D1 E1 Resistance Min, Max, and Difference

Sample	Resist Min	Resist Max	Diff	Sample	Resist Min	Resist Max	Diff	Sample	Resist Min	Resist Max	Diff	Sample	Resist Min	Resist Max	Diff	Sample	Resist Min	Resist Max	Diff
S3 T1	0.063	0.064	0.001	S3 T1	0.243	0.256	0.013	S3 T1	0.463	0.562	0.099	S3 T1	0.899	1.089	0.190	S3 T1	1.372	1.673	0.301
S3 T2	0.066	0.066	0.000	S3 T2	0.258	0.272	0.013	S3 T2	0.472	0.578	0.105	S3 T2	0.842	1.010	0.168	S3 T2	1.321	1.575	0.254
S3 T3	0.066	0.066	0.000	S3 T3	0.279	0.298	0.019	S3 T3	0.509	0.610	0.101	S3 T3	0.856	1.052	0.196	S3 T3	1.327	1.574	0.247
S3 T4	0.074	0.079	0.005	S3 T4	0.273	0.289	0.016	S3 T4	0.535	0.615	0.079	S3 T4	0.925	1.072	0.147	S3 T4	1.406	1.668	0.263
AVE			0.002	AVE			0.016	AVE			0.096	AVE			0.175	AVE			0.266

RA	0.0	RA	0.0	RA	0.0	RA	0.0	RA	0.0	RA	0.0
NG	05	NG	06	NG	26	NG	49	NG	54		
E		E		E		E		E			
SD	0.0	SD	0.0	SD	0.0	SD	0.0	SD	0.0		
	02		03		10		19		21		

D1 E1 Max power											
0		0.1		0.2		0.3		0.4		0.5	
Sample	Power (W)	Sample	Power (W)	Sample	Power (W)	Sample	Power (W)	Sample	Power (W)	Sample	Power (W)
S3 T1	0	S3 T1	0.01	S3 T1	0.01	S3 T1	0.09	S3 T1	0.47	S3 T1	1.40
S3 T2	0	S3 T2	0.01	S3 T2	0.01	S3 T2	0.10	S3 T2	0.41	S3 T2	1.24
S3 T3	0	S3 T3	0.01	S3 T3	0.02	S3 T3	0.11	S3 T3	0.44	S3 T3	1.24
S3 T4	0	S3 T4	0.01	S3 T4	0.02	S3 T4	0.11	S3 T4	0.46	S3 T4	1.39
AVE	0	AVE	0.01	AVE	0.02	AVE	0.11	AVE	0.45	AVE	1.32
RANGE	0	RANGE	0.00	RANGE	0.00	RANGE	0.02	RANGE	0.07	RANGE	0.16
SD	0	SD	0.00	SD	0.00	SD	0.01	SD	0.02	SD	0.08

D1 E2 Force Max														
A1			A2			A3			A4			A5		
Trial	Force Max	Time	Trial	Force Max	Time	Trial	Force Max	Time	Trial	Force Max	Time	Trial	Force Max	Time
S2 T1	0.01	28.51	S2 T1	0.05	39.06	S2 T1	0.14	59.40	S2 T1	0.55	60.00	S2 T1	2.08	30.78
S2 T2	0.01	1.30	S2 T2	0.05	55.58	S2 T2	0.18	51.70	S2 T2	0.88	43.27	S2 T2	2.01	44.53
S2 T3	0.00	3.31	S2 T3	0.04	36.47	S2 T3	0.17	47.34	S2 T3	0.80	59.44	S2 T3	2.07	56.99
S2 T4	0.00	0.72	S2 T4	0.04	45.61	S2 T4	0.13	58.75	S2 T4	0.48	49.18	S2 T4	1.81	57.85
AVE	0.01	8.46	AVE	0.05	44.18	AVE	0.16	54.30	AVE	0.68	52.97	AVE	1.99	47.54

RANGE	0.01	27.79	RANGE	0.01	19.11	RANGE	0.05	12.06	RANGE	0.40	16.73	RANGE	0.27	27.07
SD	0.01	11.62	SD	0.01	7.38	SD	0.02	5.03	SD	0.17	7.07	SD	0.11	11.02
A6														
Trial	Force Max	Time												
S2 T1	3.25	47.74												
S2 T2	3.69	56.23												
S2 T3	3.54	57.53												
S2 T4	3.20	60.00												
AVE	3.42	55.38												
RANGE	0.49	12.26												
SD	0.20	4.61												

D1 E2 Resistance Min, Max, and Difference																			
A1				A2				A3				A4				A5			
Sample	Resist Min	Resist Max	Diff	Sample	Resist Min	Resist Max	Diff	Sample	Resist Min	Resist Max	Diff	Sample	Resist Min	Resist Max	Diff	Sample	Resist Min	Resist Max	Diff
S3 T1	8	8	0	S3 T1	0.07	0.07	0	S3 T1	0.25	0.26	0.01	S3 T1	1.73	1.86	0.13	S3 T1	2.27	2.52	0.25
S3 T2	8	8	0	S3 T2	0.07	0.07	0	S3 T2	0.27	0.28	0.01	S3 T2	1.73	1.99	0.26	S3 T2	2.16	2.54	0.38
S3 T3	8	8	0	S3 T3	0.06	0.06	0	S3 T3	0.25	0.26	0.01	S3 T3	1.7	1.95	0.25	S3 T3	2.14	2.47	0.34
S3 T4	8	8	0	S3 T4	0.07	0.07	0	S3 T4	0.27	0.28	0.01	S3 T4	1.79	1.97	0.18	S3 T4	2.28	2.63	0.36

AVE			0.00	AVE	0.07	0.07	0.00	AVE	0.26	0.27	0.01	AVE	1.74	1.94	0.21	AVE	2.21	2.54	0.33
RANGE			0.00	RANGE	0.01	0.01	0.00	RANGE	0.02	0.02	0.00	RANGE	0.09	0.13	0.13	RANGE	0.14	0.16	0.13
SD			0.00	SD	0.00	0.00	0.00	SD	0.01	0.01	0.00	SD	0.03	0.05	0.05	SD	0.06	0.06	0.05
A6																			
Sample	Resist Min	Resist Max	Diff																
S3 T1	2.71	3.01	0.3																
S3 T2	2.68	3.2	0.52																
S3 T3	2.62	2.99	0.37																
S3 T4	2.71	3.21	0.49																
AVE	2.68	3.10	0.42																
RANGE	0.09	0.22	0.22																
SD	0.04	0.10	0.09																
D1 E2 Max power																			
0		0.1		0.2		0.3		0.4		0.5									
Sample	Power (W)	Sample	Power (W)	Sample	Power (W)	Sample	Power (W)	Sample	Power (W)	Sample	Power (W)								
S3 T1	0	S3 T1	0.00	S3 T1	0.01	S3 T1	1.04	S3 T1	2.54	S3 T1	4.53								
S3 T2	0	S3 T2	0.00	S3 T2	0.02	S3 T2	1.19	S3 T2	2.58	S3 T2	5.12								
S3 T3	0	S3 T3	0.00	S3 T3	0.01	S3 T3	1.14	S3 T3	2.44	S3 T3	4.47								
S3 T4	0	S3 T4	0.00	S3 T4	0.02	S3 T4	1.16	S3 T4	2.77	S3 T4	5.15								

AVE	0	AVE	0.00	AVE	0.01	AVE	1.13	AVE	2.58	AVE	4.82							
RANGE	0	RANGE	0.00	RANGE	0.00	RANGE	0.15	RANGE	0.33	RANGE	0.68							
SD	0	SD	0.00	SD	0.00	SD	0.06	SD	0.12	SD	0.32							

D1 E3 Force Max													
		A2			A3			A4			A5		
Force Max	Time	Trial	Force Max	Time	Trial	Force Max	Time	Trial	Force Max	Time	Trial	Force Max	Time
0.01	3.53	S3 T1	0.03	49.8	S3 T1	0.14	53.9	S3 T1	0.68	59.3	S3 T1	0.91	58.1
0.01	46.3	S3 T2	0.01	57.1	S3 T2	0.06	43.2	S3 T2	0.3	58.6	S3 T2	0.32	59.5
0.01	51.8	S3 T3	0.02	32.4	S3 T3	0.06	48.6	S3 T3	0.3	58.4	S3 T3	0.34	43.2
0.01	11.5	S3 T4	0.02	4.1	S3 T4	0.01	21.2	S3 T4	0.05	14.2	S3 T4	0.06	6.16
0.01	28.28	AVE	0.02	35.85	AVE	0.07	41.72	AVE	0.33	47.61	AVE	0.41	41.72
0.00	48.27	RANGE	0.02	53.03	RANGE	0.13	32.72	RANGE	0.63	45.11	RANGE	0.85	53.31
0.00	21.04	SD	0.01	20.42	SD	0.05	12.45	SD	0.23	19.32	SD	0.31	21.50
Force Max	Time												
1.04	34.9												
0.34	59.4												
0.36	59.5												
0.06	3.6												
0.45	39.33												
0.98	55.87												
0.36	22.94												

D1 E3 Resistance Min, Max, and Difference																			
A1				A2				A3				A4				A5			
Sample	Resist Min	Resist Max	Diff	Sample	Resist Min	Resist Max	Diff	Sample	Resist Min	Resist Max	Diff	Sample	Resist Min	Resist Max	Diff	Sample	Resist Min	Resist Max	Diff
S3 T1	8	8	0	S3 T1	7.88	8.22	0.33	S3 T1	7.16	7.54	0.38	S3 T1	6.29	6.7	0.4	S3 T1	5.7	6.24	0.5
S3 T2	8	8	0	S3 T2	6.13	6.15	0.02	S3 T2	6.12	6.15	0.03	S3 T2	5.9	6.34	0.4	S3 T2	5.43	5.94	0.5
S3 T3	8	8	0	S3 T3	6.23	6.24	0.01	S3 T3	6.21	6.24	0.03	S3 T3	6.02	6.47	0.5	S3 T3	5.47	6.21	0.7
S3 T4	8	8	0	S3 T4	6.6	6.7	0.1	S3 T4	6.37	6.49	0.12	S3 T4	6.16	6.21	0.1	S3 T4	5.62	6.07	0.5
AVE			0.00	AVE			0.12	AVE			0.14	AVE			0.34	AVE			0.56
RANGE			0.00	RANGE			0.32	RANGE			0.35	RANGE			0.41	RANGE			0.29
SD			0.00	SD			0.13	SD			0.14	SD			0.17	SD			0.11
A6																			
Sample	Resist Min	Resist Max	Diff																
S3 T1	5.47	5.86	0.38																
S3 T2	5.48	5.9	0.42																
S3 T3	5.28	5.67	0.39																
S3 T4	5.4	6.18	0.78																
AVE			0.49																
RANGE			0.40																
SD			0.17																

D1 E3 Max power											
0		0.1		0.2		0.3		0.4		0.5	
Sample	Power (W)	Sample	Power (W)	Sample	Power (W)	Sample	Power (W)	Sample	Power (W)	Sample	Power (W)
S3 T1	0	S3 T1	6.76	S3 T1	11.37	S3 T1	13.47	S3 T1	15.58	S3 T1	17.17
S3 T2	0	S3 T2	3.78	S3 T2	7.56	S3 T2	12.06	S3 T2	14.11	S3 T2	17.41
S3 T3	0	S3 T3	3.89	S3 T3	7.79	S3 T3	12.56	S3 T3	15.43	S3 T3	16.07
S3 T4	0	S3 T4	4.49	S3 T4	8.42	S3 T4	11.57	S3 T4	14.74	S3 T4	19.10
AVE	0	AVE	4.73	AVE	8.79	AVE	12.41	AVE	14.96	AVE	17.44
RANGE	0	RANGE	2.97	RANGE	3.81	RANGE	1.90	RANGE	1.46	RANGE	3.02
SD	0	SD	1.20	SD	1.52	SD	0.70	SD	0.58	SD	1.08

D1 E4 Force Max													
		A2			A3			A4			A5		
Force Max	Time	Trial	Force Max	Time	Trial	Force Max	Time	Trial	Force Max	Time	Trial	Force Max	Time
0.01	56.7	S3 T1	0.03	45.76	S3 T1	0.12	30.31	S3 T1	0.28	14.9	S3 T1	0.6	22.36

0.01	4.39	S3 T2	0.04	28.69	S3 T2	0.14	51.26	S3 T2	0.32	41	S3 T2	0.75	37.22
0.01	45.68	S3 T3	0.03	35.5	S3 T3	0.14	28.12	S3 T3	0.32	52.2	S3 T3	0.72	26.78
0.01	3.92	S3 T4	0.04	45.86	S3 T4	0.14	18.76	S3 T4	0.33	33.95	S3 T4	0.71	54.18
0.01	27.67	AVE	0.04	40.71	AVE	0.14	32.11	AVE	0.31	35.51	AVE	0.70	35.14
0.00	52.78	RANGE	0.01	39.53	RANGE	0.02	32.50	RANGE	0.05	37.30	RANGE	0.15	31.82
0.00	23.84	SD	0.01	12.68	SD	0.01	11.88	SD	0.02	13.56	SD	0.06	12.25
Force Max	Time												
1.82	35.86												
1.68	56.34												
1.9	22.82												
1.66	55.04												
1.77	42.52												
0.24	33.52												
0.10	13.97												

D1 E4 Resistance Min, Max, and Difference																			
A1				A2				A3				A4				A5			
Sample	Resist Min	Resist Max	Diff	Sample	Resist Min	Resist Max	Diff	Sample	Resist Min	Resist Max	Diff	Sample	Resist Min	Resist Max	Diff	Sample	Resist Min	Resist Max	Diff
S3 T1	8	8	0	S3 T1	8	8	0	S3 T1	5.86	5.9	0.04	S3 T1	5.91	6	0.1	S3 T1	5.84	5.98	0.1
S3 T2	8	8	0	S3 T2	8	8	0	S3 T2	5.96	6.01	0.05	S3 T2	6.07	6.13	0.1	S3 T2	5.78	5.92	0.1
S3 T3	8	8	0	S3 T3	8	8	0	S3 T3	6.56	6.99	0.43	S3 T3	6.17	6.26	0.1	S3 T3	5.82	5.98	0.2
S3 T4	8	8	0	S3 T4	8	8	0	S3 T4	6.76	7.06	0.3	S3 T4	6.18	6.32	0.1	S3 T4	5.87	6.1	0.2
AVE			0.00	AVE			0.00	AVE			0.21	AVE			0.10	AVE			0.17
RANGE			0.00	RANGE			0.00	RANGE			0.39	RANGE			0.08	RANGE			0.08
SD			0.00	SD			0.00	SD			0.17	SD			0.03	SD			0.03
A6																			
Sample	Resist Min	Resist Max	Diff																
S3 T1	5.56	5.91	0.34																

S3 T2	5.6	5.8	0.2																
S3 T3	5.51	5.72	0.21																
S3 T4	5.6	5.91	0.31																
AVE			0.27																
RANGE			0.14																
SD			0.06																

D1 E4 Max power											
0		0.1		0.2		0.3		0.4		0.5	
Sample	Power (W)	Sample	Power (W)	Sample	Power (W)	Sample	Power (W)	Sample	Power (W)	Sample	Power (W)
S3 T1	0	S3 T1	6.40	S3 T1	6.96	S3 T1	10.80	S3 T1	14.30	S3 T1	17.46
S3 T2	0	S3 T2	6.40	S3 T2	7.22	S3 T2	11.27	S3 T2	14.02	S3 T2	16.82
S3 T3	0	S3 T3	6.40	S3 T3	9.77	S3 T3	11.76	S3 T3	14.30	S3 T3	16.36
S3 T4	0	S3 T4	6.40	S3 T4	9.97	S3 T4	11.98	S3 T4	14.88	S3 T4	17.46
AVE	0	AVE	6.40	AVE	8.48	AVE	11.45	AVE	14.38	AVE	17.03
RANGE	0	RANGE	0.00	RANGE	3.01	RANGE	1.18	RANGE	0.87	RANGE	1.10
SD	0	SD	0.00	SD	1.39	SD	0.46	SD	0.31	SD	0.47

Force, Resistance, and Power Diameter 2

D2 E1 Force Max																		A1
A1				A2				A3				A4				A5		

Trial	Force Max	Time		Trial	Force Max	Time		Trial	Force Max	Time		Trial	Force Max	Time		Trial	Force Max	Time
S1 T1	0.00	58.86		S1 T1	0.02	55.19		S1 T1	0.08	56.52		S1 T1	0.30	59.26		S1 T1	1.44	59.98
S1 T2	0.01	15.66		S1 T2	0.02	52.70		S1 T2	0.05	52.24		S1 T2	0.24	58.36		S1 T2	0.34	17.64
S1 T3	0.00	1.51		S1 T3	0.01	57.31		S1 T3	0.05	52.24		S1 T3	0.16	60.00		S1 T3	0.32	25.60
S1 T4	0.01	15.12		S1 T4	0.01	50.83		S1 T4	0.02	2.59		S1 T4	0.04	58.57		S1 T4	0.12	20.05
S2 T1	0.01	53.86		S2 T1	0.02	53.46		S2 T1	0.05	53.82		S2 T1	0.21	59.90		S2 T1	0.35	20.88
S2 T2	0.01	21.38		S2 T2	0.03	51.70		S2 T2	0.08	59.44		S2 T2	0.32	60.00		S2 T2	0.52	21.67
S2 T3	0.00	7.13		S2 T3	0.01	59.76		S2 T3	0.03	59.18		S2 T3	0.12	58.90		S2 T3	0.21	19.15
S2 T4	0.01	51.59		S2 T4	0.01	45.47		S2 T4	0.03	56.52		S2 T4	0.09	57.56		S2 T4	0.22	19.55
AVE	0.01	28.14		AVE	0.01	53.30		AVE	0.05	49.07		AVE	0.19	59.07		AVE	0.44	25.56

RANGE	0.01	57.35		RANGE	0.02	14.29		RANGE	0.07	56.84		RANGE	0.28	2.44		RANGE	1.32	42.34
SD	0.00	22.92		SD	0.01	4.34		SD	0.02	18.99		SD	0.10	0.89		SD	0.42	14.10
A6				A7				A8				A9						
Trial	Force Max	Time		Trial	Force Max	Time		Trial	Force Max	Time		Trial	Force Max	Time				
S1 T1	1.58	54.11		S1 T1	1.79	59.65		S1 T1	1.91	56.99		S1 T1	2.04	2.04				
S1 T2	0.35	10.76		S1 T2	0.37	6.34		S1 T2	0.36	4.00		S1 T2	0.38	2.00				
S1 T3	0.32	11.45		S1 T3	0.33	6.44		S1 T3	0.35	38.74		S1 T3	0.38	2.00				
S1 T4	0.14	9.97		S1 T4	0.17	6.05		S1 T4	0.17	4.32		S1 T4	0.19	1.29				
S2 T1	0.36	11.12		S2 T1	0.45	6.80		S2 T1	0.61	23.72		S2 T1	0.70	2.00				
S2 T2	0.54	11.92		S2 T2	0.58	59.69		S2 T2	0.62	58.79		S2 T2	0.65	2.00				
S2 T3	0.26	10.55		S2 T3	0.26	6.80		S2 T3	0.26	4.61		S2 T3	0.21	2.00				
S2 T4	0.23	9.94		S2 T4	0.24	6.16		S2 T4	0.24	4.43		S2 T4	0.24	1.31				
AVE	0.47	16.23		AVE	0.52	19.74		AVE	0.57	24.45		AVE	0.60	1.83				

RANGE	1.44	44.17		RANGE	1.62	53.64		RANGE	1.74	54.79		RANGE	1.86	0.76				
SD	0.46	15.32		SD	0.53	24.65		SD	0.57	24.08		SD	0.61	0.33				

D2 E1 Resistance Max, Min, and Diff																			
A1				A2				A3				A4				A5			
Sample	Resist Min	Resist Max	Diff	Sample	Resist Min	Resist Max	Diff	Sample	Resist Min	Resist Max	Diff	Sample	Resist Min	Resist Max	Diff	Sample	Resist Min	Resist Max	Diff
S1 T1	0.00	0.00	0.00	S1 T1	3.86	3.89	0.03	S1 T1	3.86	3.87	0.01	S1 T1	0.35	3.87	3.53	S1 T1	3.91	5.01	1.10
S1 T2	0.00	0.00	0.00	S1 T2	3.68	3.69	0.01	S1 T2	3.63	3.68	0.06	S1 T2	0.30	3.68	3.37	S1 T2	3.19	3.66	0.47
S1 T3	0.00	0.00	0.00	S1 T3	4.45	4.56	0.11	S1 T3	4.19	4.51	0.32	S1 T3	0.42	4.78	4.36	S1 T3	3.11	4.67	1.56
S1 T4	0.00	0.00	0.00	S1 T4	3.58	3.60	0.02	S1 T4	3.53	3.59	0.06	S1 T4	0.30	3.59	3.29	S1 T4	3.08	3.57	0.49
S2 T1	0.00	0.00	0.00	S2 T1	4.37	4.39	0.02	S2 T1	4.28	4.36	0.08	S2 T1	0.36	4.37	4.00	S2 T1	3.54	4.11	0.57
S2 T2	0.00	0.00	0.00	S2 T2	4.75	4.79	0.04	S2 T2	4.60	4.68	0.08	S2 T2	0.39	4.52	4.13	S2 T2	3.92	4.30	0.38
S2 T3	0.00	0.00	0.00	S2 T3	4.26	4.28	0.02	S2 T3	4.28	4.36	0.09	S2 T3	0.36	4.29	3.94	S2 T3	3.64	4.25	0.61
S2 T4	0.00	0.00	0.00	S2 T4	4.27	4.28	0.01	S2 T4	4.24	4.30	0.06	S2 T4	0.36	4.32	3.96	S2 T4	3.63	4.18	0.55

AVE			0.00	AVE			0.03	AVE			0.09	AVE			3.87	AVE			0.66
RANGE			0.00	RANGE			0.11	RANGE			0.31	RANGE			1.07	RANGE			1.18
SD			0.00	SD			0.03	SD			0.10	SD			0.39	SD			0.40
A6				A7				A8				A9							
Sample	Resist Min	Resist Max	Diff	Sample	Resist Min	Resist Max	Diff	Sample	Resist Min	Resist Max	Diff	Sample	Resist Min	Resist Max	Diff				
S1 T1	3.74	4.78	1.05	S1 T1	3.56	4.65	1.09	S1 T1	3.55	4.17	0.62	S1 T1	3.47	4.14	0.67				
S1 T2	3.16	3.66	0.50	S1 T2	3.12	3.63	0.50	S1 T2	3.07	3.58	0.51	S1 T2	3.05	3.55	0.50				
S1 T3	3.02	4.25	1.23	S1 T3	2.99	4.14	1.15	S1 T3	3.11	4.13	1.01	S1 T3	3.25	3.84	0.59				
S1 T4	3.05	3.58	0.52	S1 T4	3.04	3.54	0.50	S1 T4	3.04	3.57	0.53	S1 T4	3.02	3.54	0.51				
S2 T1	3.67	4.17	0.50	S2 T1	3.45	3.97	0.53	S2 T1	3.53	4.20	0.67	S2 T1	3.41	4.07	0.66				
S2 T2	3.71	4.12	0.41	S2 T2	3.45	4.07	0.62	S2 T2	3.35	3.81	0.45	S2 T2	3.41	4.01	0.60				
S2 T3	3.58	4.28	0.70	S2 T3	3.44	4.16	0.72	S2 T3	3.28	3.93	0.65	S2 T3	3.30	3.93	0.63				
S2 T4	3.54	4.18	0.64	S2 T4	3.47	4.10	0.63	S2 T4	3.40	4.05	0.66	S2 T4	3.31	3.97	0.66				
AVE			0.64	AVE			0.72	AVE			0.64	AVE			0.60				

RANGE			0.82	RANGE			0.65	RANGE			0.56	RANGE			0.17				
SD			0.28	SD			0.26	SD			0.17	SD			0.07				

D2 E1 Max Power Watts									
0		0.1		0.2		0.3		0.4	
Sample	Power (W)	Sample	Power (W)	Sample	Power (W)	Sample	Power (W)	Sample	Power (W)
S1 T1	0	S1 T1	1.51321	S1 T1	2.99538	S1 T1	4.49307	S1 T1	10.04004
S1 T2	0	S1 T2	1.36161	S1 T2	2.70848	S1 T2	4.06272	S1 T2	5.35824
S1 T3	0	S1 T3	2.07936	S1 T3	4.06802	S1 T3	6.85452	S1 T3	8.72356
S1 T4	0	S1 T4	1.296	S1 T4	2.57762	S1 T4	3.86643	S1 T4	5.09796
S2 T1	0	S2 T1	1.92721	S2 T1	3.80192	S2 T1	5.72907	S2 T1	6.75684
S2 T2	0	S2 T2	2.29441	S2 T2	4.38048	S2 T2	6.12912	S2 T2	7.396
S2 T3	0	S2 T3	1.83184	S2 T3	3.80192	S2 T3	5.52123	S2 T3	7.225
S2 T4	0	S2 T4	1.83184	S2 T4	3.698	S2 T4	5.59872	S2 T4	6.98896
AVE	0	AVE	1.766935	AVE	3.503978	AVE	5.28186	AVE	7.198325
RANGE	0	RANGE	0.99841	RANGE	1.80286	RANGE	2.98809	RANGE	4.94208

SD	0	SD	0.327948	SD	0.617577	SD	0.978566	SD	1.519772
0.5		0.6		0.7		0.8			
Sample	Power (W)	Sample	Power (W)	Sample	Power (W)	Sample	Power (W)		
S1 T1	11.4242	S1 T1	12.9735	S1 T1	12.17223	S1 T1	13.71168		
S1 T2	6.6978	S1 T2	7.90614	S1 T2	8.97148	S1 T2	10.082		
S1 T3	9.03125	S1 T3	10.28376	S1 T3	11.93983	S1 T3	11.79648		
S1 T4	6.4082	S1 T4	7.51896	S1 T4	8.92143	S1 T4	10.02528		
S2 T1	8.69445	S2 T1	9.45654	S2 T1	12.348	S2 T1	13.25192		
S2 T2	8.4872	S2 T2	9.93894	S2 T2	10.16127	S2 T2	12.86408		
S2 T3	9.1592	S2 T3	10.38336	S2 T3	10.81143	S2 T3	12.35592		
S2 T4	8.7362	S2 T4	10.086	S2 T4	11.48175	S2 T4	12.60872		
AVE	8.579813	AVE	9.8184	AVE	10.85093	AVE	12.08701		
RANGE	5.016	RANGE	5.45454	RANGE	3.42657	RANGE	3.6864		
SD	1.454909	SD	1.567308	SD	1.289534	SD	1.289385		

D2 E2 Force Max

A1				A2				A3				A4				A5		
Trial	Force Max	Time		Trial	Force Max	Time		Trial	Force Max	Time		Trial	Force Max	Time		Trial	Force Max	Time
S1 T1	0.02	57.49		S1 T1	0.05	48.10		S1 T1	0.20	52.63		S1 T1	0.54	52.24		S1 T1	1.91	52.60
S1 T2	0.01	4.61		S1 T2	0.04	53.82		S1 T2	0.17	52.74		S1 T2	0.38	49.97		S1 T2	1.40	59.58
S1 T3	0.01	42.41		S1 T3	0.04	58.28		S1 T3	0.15	59.47		S1 T3	0.39	59.58		S1 T3	0.95	59.94
S1 T4	0.00	52.60		S1 T4	0.03	59.65		S1 T4	0.13	54.25		S1 T4	0.31	49.10		S1 T4	0.95	55.73
S2 T1	0.00	3.78		S2 T1	0.05	28.44		S2 T1	0.21	60.00		S2 T1	0.55	59.54		S2 T1	1.57	60.00
S2 T2	0.00	0.50		S2 T2	0.05	55.48		S2 T2	0.18	51.23		S2 T2	0.47	42.80		S2 T2	1.39	52.09
S2 T3	0.00	6.19		S2 T3	0.02	54.86		S2 T3	0.12	32.76		S2 T3	0.33	58.86		S2 T3	1.16	58.18
S2 T4	-0.03	57.64		S2 T4	0.04	16.67		S2 T4	0.17	44.75		S2 T4	0.36	46.48		S2 T4	0.93	58.64
AVE	0.00	28.15		AVE	0.04	46.91		AVE	0.17	50.98		AVE	0.42	52.32		AVE	1.28	57.09
RANGE	0.05	57.13		RANGE	0.03	42.98		RANGE	0.09	27.24		RANGE	0.24	16.78		RANGE	0.98	7.91
SD	0.01	26.53		SD	0.01	15.74		SD	0.03	8.79		SD	0.09	6.42		SD	0.35	3.24
A6				A7				A8				A9						

Trial	Force Max	Time		Trial	Force Max	Time		Trial	Force Max	Time		Trial	Force Max	Time				
S1 T1	3.63	55.33		S1 T1	5.39	59.54		S1 T1	6.71	54.40		S1 T1	7.14	44.35				
S1 T2	2.87	56.81		S1 T2	3.94	60.00		S1 T2	4.33	54.97		S1 T2	4.81	35.89				
S1 T3	2.55	56.92		S1 T3	4.55	60.00		S1 T3	5.38	50.04		S1 T3	5.93	35.06				
S1 T4	2.53	59.08		S1 T4	4.31	57.06		S1 T4	5.49	31.10		S1 T4	6.35	44.82				
S2 T1	3.04	54.50		S2 T1	4.42	57.82		S2 T1	6.75	33.48		S2 T1	6.42	28.15				
S2 T2	2.98	53.64		S2 T2	4.47	59.36		S2 T2	6.04	38.38		S2 T2	6.69	52.99				
S2 T3	2.72	46.01		S2 T3	4.30	50.44		S2 T3	4.90	60.00		S2 T3	6.53	56.23				
S2 T4	2.83	59.29		S2 T4	4.41	55.44		S2 T4	5.68	57.60		S2 T4	6.49	60.00				
AVE	2.89	55.20		AVE	4.47	57.46		AVE	5.66	47.50		AVE	6.29	44.69				
RANGE	1.10	13.28		RANGE	1.45	9.56		RANGE	2.41	28.90		RANGE	2.33	31.85				
SD	0.35	4.22		SD	0.41	3.26		SD	0.83	11.44		SD	0.69	11.21				

D2 E2 Resistance Max, Min, and Diff

A1				A2				A3				A4				A5			
Sample	Resist Min	Resist Max	Diff	Sample	Resist Min	Resist Max	Diff	Sample	Resist Min	Resist Max	Diff	Sample	Resist Min	Resist Max	Diff	Sample	Resist Min	Resist Max	Diff
S1 T1	0.00	0.00	0.00	S1 T1	6.23	6.50	0.27	S1 T1	5.23	5.41	0.18	S1 T1	4.90	5.11	0.21	S1 T1	4.31	4.97	0.66
S1 T2	0.00	0.00	0.00	S1 T2	4.71	4.76	0.05	S1 T2	4.66	4.84	0.18	S1 T2	4.47	4.60	0.13	S1 T2	3.92	4.82	0.90
S2 T1	0.00	0.00	0.00	S2 T1	4.36	4.37	0.00	S2 T1	4.36	4.40	0.05	S2 T1	4.26	4.38	0.12	S2 T1	4.05	4.52	0.47
S2 T2	0.00	0.00	0.00	S2 T2	3.53	3.54	0.01	S2 T2	3.54	3.63	0.10	S2 T2	3.55	3.63	0.08	S2 T2	3.31	3.66	0.35
S3 T1	0.00	0.00	0.00	S3 T1	6.15	6.25	0.10	S3 T1	4.78	4.82	0.05	S3 T1	4.52	4.64	0.12	S3 T1	3.96	4.83	0.87
S3 T2	0.00	0.00	0.00	S3 T2	4.67	4.77	0.11	S3 T2	4.43	4.54	0.11	S3 T2	4.14	4.34	0.20	S3 T2	3.67	4.08	0.41
S3 T3	0.00	0.00	0.00	S3 T3	3.98	4.00	0.02	S3 T3	3.95	3.99	0.04	S3 T3	3.85	3.95	0.10	S3 T3	3.53	4.75	1.23
S3 T4	0.00	0.00	0.00	S3 T4	4.91	4.98	0.07	S3 T4	4.87	5.50	0.64	S3 T4	4.76	5.08	0.32	S3 T4	4.04	4.56	0.51
AVE			0.00	AVE			0.08	AVE			0.17	AVE			0.16	AVE			0.68
RANGE			0.00	RANGE			0.27	RANGE			0.60	RANGE			0.24	RANGE			0.88
SD			0.00	SD			0.09	SD			0.20	SD			0.08	SD			0.30
A6				A7				A8				A9							
Sample	Resist Min	Resist Max	Diff	Sample	Resist Min	Resist Max	Diff	Sample	Resist Min	Resist Max	Diff	Sample	Resist Min	Resist	Diff				

														Max					
S1 T1	4.08	5.08	1.00	S1 T1	3.54	4.42	0.87	S1 T1	3.50	4.32	0.82	S1 T1	3.38	4.26	0.88				
S1 T2	3.75	4.44	0.70	S1 T2	3.67	4.18	0.51	S1 T2	3.52	4.07	0.54	S1 T2	3.67	4.13	0.46				
S2 T1	3.45	4.21	0.76	S2 T1	3.31	3.93	0.62	S2 T1	3.33	4.11	0.78	S2 T1	3.17	3.90	0.73				
S2 T2	3.21	3.65	0.45	S2 T2	3.05	3.80	0.75	S2 T2	2.99	3.56	0.56	S2 T2	3.32	3.92	0.60				
S3 T1	3.56	4.27	0.71	S3 T1	3.23	4.12	0.90	S3 T1	3.54	4.53	0.99	S3 T1	3.06	3.78	0.72				
S3 T2	3.52	4.33	0.81	S3 T2	3.32	4.20	0.88	S3 T2	3.23	4.10	0.87	S3 T2	3.09	3.85	0.76				
S3 T3	3.74	4.50	0.77	S3 T3	3.39	4.51	1.12	S3 T3	3.30	4.00	0.71	S3 T3	3.36	3.86	0.50				
S3 T4	3.85	4.35	0.50	S3 T4	3.48	4.38	0.90	S3 T4	3.35	4.16	0.80	S3 T4	3.25	4.00	0.75				
AVE			0.71	AVE			0.82	AVE			0.76	AVE			0.68				
RANGE			0.56	RANGE			0.61	RANGE			0.44	RANGE			0.42				
SD			0.18	SD			0.19	SD			0.15	SD			0.14				

D2 E2 Max Power Watts									
0		0.1		0.2		0.3		0.4	
Sample	Power (W)	Sample	Power (W)	Sample	Power (W)	Sample	Power (W)	Sample	Power (W)

S1 T1	0	S1 T1	4.225	S1 T1	5.85362	S1 T1	7.83363	S1 T1	9.88036
S1 T2	0	S1 T2	2.26576	S1 T2	4.68512	S1 T2	6.348	S1 T2	9.29296
S1 T3	0	S1 T3	1.90969	S1 T3	3.872	S1 T3	5.75532	S1 T3	8.17216
S1 T4	0	S1 T4	1.25316	S1 T4	2.63538	S1 T4	3.95307	S1 T4	5.35824
S2 T1	0	S2 T1	3.90625	S2 T1	4.64648	S2 T1	6.45888	S2 T1	9.33156
S2 T2	0	S2 T2	2.27529	S2 T2	4.12232	S2 T2	5.65068	S2 T2	6.65856
S2 T3	0	S2 T3	1.6	S2 T3	3.18402	S2 T3	4.68075	S2 T3	9.025
S2 T4	0	S2 T4	2.48004	S2 T4	6.05	S2 T4	7.74192	S2 T4	8.31744
AVE	0	AVE	2.48939875	AVE	4.3811175	AVE	6.05278125	AVE	8.254535
RANGE	0	RANGE	2.97184	RANGE	3.41462	RANGE	3.88056	RANGE	4.52212
SD	0	SD	0.985590065	SD	1.113726055	SD	1.265805474	SD	1.432726255
0.5		0.6		0.7		0.8			
Sample	Power (W)	Sample	Power (W)	Sample	Power (W)	Sample	Power (W)		
S1 T1	12.9032	S1 T1	11.72184	S1 T1	13.06368	S1 T1	14.51808		
S1 T2	9.8568	S1 T2	10.48344	S1 T2	11.59543	S1 T2	13.64552		
S1 T3	8.86205	S1 T3	9.26694	S1 T3	11.82447	S1 T3	12.168		

S1 T4	6.66125	S1 T4	8.664	S1 T4	8.87152	S1 T4	12.29312		
S2 T1	9.11645	S2 T1	10.18464	S2 T1	14.36463	S2 T1	11.43072		
S2 T2	9.37445	S2 T2	10.584	S2 T2	11.767	S2 T2	11.858		
S2 T3	10.125	S2 T3	12.20406	S2 T3	11.2	S2 T3	11.91968		
S2 T4	9.46125	S2 T4	11.51064	S2 T4	12.11392	S2 T4	12.8		
AVE	9.54505625	AVE	10.577445	AVE	11.85008125	AVE	12.57914		
RANGE	6.24195	RANGE	3.54006	RANGE	5.49311	RANGE	3.08736		
SD	1.609088161	SD	1.138433133	SD	1.467660837	SD	0.966312333		

D2 E3 Force Max																	
A1				A2				A3				A4				A5		
Trial	Force Max	Time		Trial	Force Max	Time		Trial	Force Max	Time		Trial	Force Max	Time		Trial	Force Max	Time
S1 T1	0.01	0.76		S1 T1	0.05	54.68		S1 T1	0.16	48.28		S1 T1	0.36	51.91		S1 T1	0.77	52.60
S1 T2	0.01	0.04		S1 T2	0.04	35.03		S1 T2	0.16	56.66		S1 T2	0.39	56.59		S1 T2	0.93	58.57

S1 T3	0.00	5.40		S1 T3	0.04	30.24		S1 T3	0.13	40.72		S1 T3	0.34	47.99		S1 T3	0.67	42.95
S1 T4	0.01	3.78		S1 T4	0.04	48.24		S1 T4	0.18	18.90		S1 T4	0.35	55.66		S1 T4	0.73	42.12
S2 T1	0.00	0.50		S2 T1	0.05	57.53		S2 T1	0.39	45.32		S2 T1	0.86	55.33		S2 T1	0.42	57.35
S2 T2	0.00	45.68		S2 T2	0.05	57.20		S2 T2	0.20	59.62		S2 T2	0.40	51.59		S2 T2	0.76	32.33
S2 T3	0.01	23.90		S2 T3	0.04	15.30		S2 T3	0.16	45.79		S2 T3	0.38	56.23		S2 T3	0.77	56.20
S2 T4	-0.02	54.47		S2 T4	0.04	51.30		S2 T4	0.15	52.13		S2 T4	0.36	54.18		S2 T4	0.73	51.48
AVE	0.00	16.82		AVE	0.04	43.69		AVE	0.19	45.93		AVE	0.43	53.69		AVE	0.72	49.20
RANGE	0.03	54.43		RANGE	0.01	42.23		RANGE	0.25	40.72		RANGE	0.53	8.60		RANGE	0.51	26.24
SD	0.01	22.06		SD	0.00	15.29		SD	0.08	12.56		SD	0.18	2.97		SD	0.14	9.21
A6				A7				A8				A9						
Trial	Force Max	Time		Trial	Force Max	Time		Trial	Force Max	Time		Trial	Force Max	Time				
S1 T1	2.11	60.00		S1 T1	4.63	60.00		S1 T1	6.95	55.48		S1 T1	8.75	59.33				
S1 T2	2.70	52.96		S1 T2	4.21	57.56		S1 T2	6.63	44.42		S1 T2	8.88	50.62				
S1 T3	1.29	57.28		S1 T3	3.36	50.62		S1 T3	5.24	50.90		S1 T3	7.40	55.19				
S1 T4	1.90	57.60		S1 T4	3.91	59.62		S1 T4	5.73	38.23		S1 T4	7.93	45.00				

S2 T1	2.18	49.36		S2 T1	4.47	55.12		S2 T1	6.29	44.32		S2 T1	8.10	46.44				
S2 T2	1.72	45.68		S2 T2	4.01	51.66		S2 T2	6.23	57.74		S2 T2	8.40	38.63				
S2 T3	1.74	58.36		S2 T3	4.40	56.34		S2 T3	5.76	39.53		S2 T3	8.00	31.25				
S2 T4	1.65	60.00		S2 T4	3.84	56.95		S2 T4	6.29	48.10		S2 T4	8.57	32.62				
AVE	1.91	55.15		AVE	4.10	55.98		AVE	6.14	47.34		AVE	8.25	44.88				
RANGE	1.40	14.32		RANGE	1.27	9.38		RANGE	1.70	19.51		RANGE	1.48	28.08				
SD	0.42	5.29		SD	0.41	3.40		SD	0.54	7.06		SD	0.49	10.18				

D2 E3 Resistance Max, Min, and Diff																		
A1				A2				A3				A4				A5		
Sample	Resist Min	Resist Max	Diff	Sample	Resist Min	Resist Max	Diff	Sample	Resist Min	Resist Max	Diff	Sample	Resist Min	Resist Max	Diff	Sample	Resist Min	Resist Max	Diff
S1 T1	10.46	14.22	3.75	S1 T1	6.18	6.94	0.77	S1 T1	4.98	5.57	0.59	S1 T1	4.56	5.19	0.64	S1 T1	3.94	4.76	0.81
S1 T2	4.89	4.93	0.04	S1 T2	4.93	4.98	0.04	S1 T2	4.93	5.04	0.11	S1 T2	4.39	4.90	0.51	S1 T2	4.09	4.85	0.77
S1 T3	3.52	3.53	0.00	S1 T3	3.54	3.54	0.00	S1 T3	3.55	3.56	0.01	S1 T3	3.46	3.55	0.09	S1 T3	3.32	3.65	0.33
S1 T4	5.68	6.08	0.40	S1 T4	4.67	4.74	0.07	S1 T4	4.26	4.30	0.05	S1 T4	3.95	4.17	0.23	S1 T4	3.71	4.02	0.31
S2 T1	3.99	3.99	0.00	S2 T1	5.94	5.99	0.05	S2 T1	3.99	4.08	0.09	S2 T1	3.85	4.03	0.18	S2 T1	3.52	3.97	0.45

S2 T2	3.70	3.70	0.00	S2 T2	3.70	3.71	0.00	S2 T2	3.71	3.72	0.01	S2 T2	3.68	3.71	0.03	S2 T2	3.50	3.81	0.31
S2 T3	4.59	5.05	0.46	S2 T3	4.37	4.54	0.17	S2 T3	4.26	4.47	0.21	S2 T3	3.98	4.12	0.14	S2 T3	3.76	4.20	0.45
S2 T4	5.01	5.03	0.02	S2 T4	4.84	4.99	0.15	S2 T4	4.62	4.87	0.25	S2 T4	4.15	4.42	0.27	S2 T4	3.81	4.46	0.65
AVE	5.23	5.82	0.58	AVE	4.77	4.93	0.16	AVE	4.29	4.45	0.17	AVE	4.00	4.26	0.26	AVE	3.70	4.21	0.51
RANGE	6.94	10.69	3.75	RANGE	2.64	3.40	0.76	RANGE	1.43	2.01	0.58	RANGE	1.09	1.64	0.60	RANGE	0.77	1.21	0.50
SD	1.94	3.27	1.44	SD	1.02	1.04	0.28	SD	0.97	0.93	0.20	SD	0.92	0.92	0.20	SD	0.91	0.97	0.17
A6				A7				A8				A9							
Sample	Resist Min	Resist Max	Diff	Sample	Resist Min	Resist Max	Diff	Sample	Resist Min	Resist Max	Diff	Sample	Resist Min	Resist Max	Diff				
S1 T1	3.94	4.76	0.81	S1 T1	3.90	4.39	0.50	S1 T1	3.53	4.34	0.81	S1 T1	3.38	4.07	0.69				
S1 T2	4.09	4.85	0.77	S1 T2	3.90	4.44	0.55	S1 T2	3.76	4.20	0.44	S1 T2	3.43	4.06	0.63				
S1 T3	3.32	3.65	0.33	S1 T3	3.23	3.64	0.41	S1 T3	3.01	3.52	0.51	S1 T3	3.13	3.94	0.82				
S1 T4	3.71	4.02	0.31	S1 T4	3.51	4.01	0.50	S1 T4	3.29	3.86	0.57	S1 T4	2.99	3.40	0.41				
S2 T1	3.52	3.97	0.45	S2 T1	3.80	4.34	0.54	S2 T1	3.51	4.20	0.70	S2 T1	3.61	4.51	0.90				
S2 T2	3.50	3.81	0.31	S2 T2	3.38	3.62	0.24	S2 T2	3.09	3.86	0.77	S2 T2	3.10	3.88	0.78				
S2 T3	3.76	4.20	0.45	S2 T3	3.44	4.18	0.74	S2 T3	3.30	4.03	0.73	S2 T3	3.33	3.94	0.61				

S2 T4	3.81	4.46	0.65	S2 T4	3.56	4.11	0.55	S2 T4	3.28	4.09	0.81	S2 T4	3.19	3.87	0.68				
AVE	3.70	4.21	0.51	AVE	3.59	4.09	0.50	AVE	3.35	4.01	0.67	AVE	3.27	3.96	0.69				
RANGE	0.77	1.21	0.50	RANGE	0.67	0.82	0.50	RANGE	0.75	0.82	0.38	RANGE	0.62	1.11	0.49				
SD	0.91	0.97	0.17	SD	0.90	1.02	0.12	SD	0.81	0.98	0.15	SD	0.81	0.89	0.14				

D2 E3 Max Power Watts									
A1		A2		A3		A4		A5	
Sample	Power (W)	Sample	Power (W)	Sample	Power (W)	Sample	Power (W)	Sample	Power (W)
S1 T1	0.00	S1 T1	0.07	S1 T1	0.22	S1 T1	0.47	S1 T1	0.76
S1 T2	0.00	S1 T2	0.05	S1 T2	0.20	S1 T2	0.44	S1 T2	0.78
S1 T3	0.00	S1 T3	0.04	S1 T3	0.14	S1 T3	0.32	S1 T3	0.58
S1 T4	0.00	S1 T4	0.05	S1 T4	0.17	S1 T4	0.38	S1 T4	0.64
S2 T1	0.00	S2 T1	0.06	S2 T1	0.16	S2 T1	0.36	S2 T1	0.64
S2 T2	0.00	S2 T2	0.04	S2 T2	0.15	S2 T2	0.33	S2 T2	0.61
S2 T3	0.00	S2 T3	0.05	S2 T3	0.18	S2 T3	0.37	S2 T3	0.67
S2 T4	0.00	S2 T4	0.05	S2 T4	0.19	S2 T4	0.40	S2 T4	0.71
AVE	0.00	AVE	0.05	AVE	0.18	AVE	0.38	AVE	0.67
RANGE	0.00	RANGE	0.03	RANGE	0.08	RANGE	0.15	RANGE	0.19
SD	0.00	SD	0.01	SD	0.03	SD	0.05	SD	0.07
A6		A7		A8		A9			
Sample	Power (W)	Sample	Power (W)	Sample	Power (W)	Sample	Power (W)		
S1 T1	1.19	S1 T1	1.58	S1 T1	2.13	S1 T1	2.61		

S1 T2	1.21	S1 T2	1.60	S1 T2	2.06	S1 T2	2.60		
S1 T3	0.91	S1 T3	1.31	S1 T3	1.73	S1 T3	2.52		
S1 T4	1.00	S1 T4	1.44	S1 T4	1.89	S1 T4	2.17		
S2 T1	0.99	S2 T1	1.56	S2 T1	2.06	S2 T1	2.89		
S2 T2	0.95	S2 T2	1.30	S2 T2	1.89	S2 T2	2.48		
S2 T3	1.05	S2 T3	1.50	S2 T3	1.97	S2 T3	2.52		
S2 T4	1.11	S2 T4	1.48	S2 T4	2.00	S2 T4	2.48		
AVE	1.05		1.47		1.97		2.53		
RANGE	0.30		0.30		0.40		0.71		
SD	0.11		0.11		0.13		0.20		

D2 E4 Force Max																	
A1				A2				A3				A4				A5	
Trial	Force Max	Time		Trial	Force Max	Time		Trial	Force Max	Time		Trial	Force Max	Time		Trial	Force Max
S1 T1	0.00	1.48		S1 T1	0.05	27.43		S1 T1	0.13	26.71		S1 T1	0.34	24.37		S1 T1	0.6
S1 T2	0.00	1.84		S1 T2	0.04	35.53		S1 T2	0.14	42.55		S1 T2	0.35	42.44		S1 T2	0.6
S1 T3	0.01	51.23		S1 T3	0.04	32.40		S1 T3	0.13	21.96		S1 T3	0.31	30.96		S1 T3	0.5
S1 T4	0.01	7.38		S1 T4	0.03	40.79		S1 T4	0.12	22.36		S1 T4	0.28	43.24		S1 T4	0.5
S2 T1	0.03	36.11		S2 T1	0.04	57.06		S2 T1	0.15	59.44		S2 T1	0.34	47.20		S2 T1	0.6
S2 T2	0.01	2.02		S2 T2	0.05	17.50		S2 T2	0.15	37.30		S2 T2	0.35	49.68		S2 T2	0.6
S2 T3	0.00	1.26		S2 T3	0.04	27.22		S2 T3	0.13	26.50		S2 T3	0.25	24.16		S2 T3	0.6
S2 T4	0.00	9.68		S2 T4	0.03	58.28		S2 T4	0.12	57.06		S2 T4	0.32	29.30		S2 T4	0.5
AVE	0.01	13.87		AVE	0.04	37.03		AVE	0.14	36.73		AVE	0.32	36.42		AVE	0.6
RANGE	0.03	49.97		RANGE	0.02	40.79		RANGE	0.03	37.48		RANGE	0.10	25.52		RANGE	0.1
SD	0.01	19.08		SD	0.01	14.45		SD	0.01	15.09		SD	0.04	10.36		SD	0.0
A6				A7				A8				A9					

Trial	Force Max	Time		Trial	Force Max	Time		Trial	Force Max	Time		Trial	Force Max	Time			
S1 T1	1.17	60.00		S1 T1	2.22	39.46		S1 T1	4.76	52.92		S1 T1	7.40	47.05			
S1 T2	1.39	53.17		S1 T2	3.96	44.10		S1 T2	5.98	48.53		S1 T2	6.69	51.62			
S1 T3	1.06	46.44		S1 T3	2.27	56.30		S1 T3	3.92	32.69		S1 T3	5.73	47.09			
S1 T4	1.06	56.05		S1 T4	1.89	51.73		S1 T4	3.51	45.36		S1 T4	5.82	57.53			
S2 T1	1.25	44.28		S2 T1	2.62	40.93		S2 T1	4.52	33.52		S2 T1	7.61	53.39			
S2 T2	1.32	43.70		S2 T2	2.35	45.68		S2 T2	3.76	59.94		S2 T2	5.86	51.84			
S2 T3	1.20	59.80		S2 T3	2.59	39.24		S2 T3	4.23	52.70		S2 T3	6.06	46.84			
S2 T4	1.08	59.98		S2 T4	2.26	34.99		S2 T4	3.54	58.75		S2 T4	6.33	25.06			
AVE	1.19	52.93		AVE	2.52	44.06		AVE	4.28	48.05		AVE	6.44	47.55			
RANGE	0.34	16.30		RANGE	2.07	21.31		RANGE	2.47	27.25		RANGE	1.89	32.47			
SD	0.12	7.16		SD	0.63	7.05		SD	0.82	10.39		SD	0.73	9.82			

D2 E4 Resistance Max, Min, and Diff																	
A1				A2				A3				A4				A5	
Sample	Resist Min	Resist Max	Diff	Sample	Resist Min	Resist Max	Diff	Sample	Resist Min	Resist Max	Diff	Sample	Resist Min	Resist Max	Diff	Sample	Resi Min
S1 T1	0.00	0.00	0.00	S1 T1	4.06	4.07	0.01	S1 T1	4.05	4.05	0.01	S1 T1	4.06	4.07	0.01	S1 T1	4.0
S1 T2	0.00	0.00	0.00	S1 T2	4.06	4.07	0.01	S1 T2	4.05	4.05	0.01	S1 T2	4.06	4.07	0.01	S1 T2	4.0
S1 T3	0.00	0.00	0.00	S1 T3	3.84	3.84	0.00	S1 T3	3.84	3.85	0.01	S2 T1	3.87	3.89	0.01	S2 T1	3.8
S1 T4	0.00	0.00	0.00	S1 T4	3.82	3.84	0.02	S1 T4	3.80	3.82	0.03	S2 T2	3.76	3.80	0.04	S2 T2	3.6
S2 T1	0.00	0.00	0.00	S2 T1	4.05	4.06	0.01	S2 T1	4.04	4.07	0.03	S3 T1	3.99	4.17	0.18	S3 T1	3.8
S2 T2	0.00	0.00	0.00	S2 T2	4.14	4.19	0.05	S2 T2	4.10	4.16	0.06	S3 T2	4.09	4.13	0.05	S3 T2	3.9
S2 T3	0.00	0.00	0.00	S2 T3	3.92	4.22	0.30	S2 T3	4.10	4.32	0.22	S3 T3	4.30	4.32	0.03	S3 T3	4.0
S2 T4	0.00	0.00	0.00	S2 T4	3.91	3.93	0.02	S2 T4	3.89	3.91	0.03	S3 T4	3.88	3.91	0.03	S3 T4	3.9
AVE			0.00	AVE			0.05	AVE			0.05	AVE			0.04	AVE	
RANGE			0.00	RANGE			0.30	RANGE			0.21	RANGE			0.17	RANGE	

SD			0.00	SD			0.10	SD			0.07	SD			0.06	SD	
A6				A7				A8				A9					
Sample	Resist Min	Resist Max	Diff	Sample	Resist Min	Resist Max	Diff	Sample	Resist Min	Resist Max	Diff	Sample	Resist Min	Resist Max	Diff		
S1 T1	3.82	4.00	0.18	S1 T1	3.55	3.92	0.37	S1 T1	3.16	3.62	0.46	S1 T1	3.56	3.91	0.35		
S1 T2	3.82	4.00	0.18	S1 T2	3.55	3.92	0.37	S1 T2	3.16	3.62	0.46	S1 T2	3.56	3.91	0.35		
S1 T3	3.88	3.94	0.06	S1 T3	3.62	3.90	0.28	S1 T3	2.98	3.24	0.26	S1 T3	3.04	3.54	0.49		
S1 T4	3.65	3.74	0.09	S1 T4	3.52	3.96	0.44	S1 T4	2.89	3.28	0.39	S1 T4	3.17	3.70	0.52		
S2 T1	3.81	3.89	0.07	S2 T1	3.76	3.93	0.18	S2 T1	3.18	3.53	0.35	S2 T1	3.59	4.03	0.44		
S2 T2	3.79	4.05	0.25	S2 T2	3.55	3.83	0.28	S2 T2	3.02	3.25	0.22	S2 T2	3.19	3.65	0.46		
S2 T3	4.01	4.16	0.15	S2 T3	3.61	3.94	0.33	S2 T3	3.02	3.34	0.32	S2 T3	3.37	3.72	0.36		
S2 T4	3.81	3.98	0.17	S2 T4	3.70	4.01	0.31	S2 T4	3.02	3.43	0.41	S2 T4	3.20	3.82	0.61		
AVE			0.14	AVE			0.32	AVE			0.36	AVE			0.45		
RANGE			0.20	RANGE			0.27	RANGE			0.24	RANGE			0.26		
SD			0.07	SD			0.08	SD			0.09	SD			0.10		

D2 E4 Max Power Watts									
0		0.1		0.2		0.3		0.4	
Sample	Power (W)	Sample	Power (W)	Sample	Power (W)	Sample	Power (W)	Sample	Power (W)
S1 T1	0	S1 T1	1.65649	S1 T1	3.2805	S1 T1	4.96947	S1 T1	6.75684
S1 T2	0	S1 T2	1.65649	S1 T2	3.2805	S1 T2	4.96947	S1 T2	6.75684
S1 T3	0	S1 T3	1.47456	S1 T3	2.9645	S1 T3	4.53963	S1 T3	6.14656
S1 T4	0	S1 T4	1.47456	S1 T4	2.91848	S1 T4	4.332	S1 T4	5.50564
S2 T1	0	S2 T1	1.64836	S2 T1	3.31298	S2 T1	5.21667	S2 T1	6.05284
S2 T2	0	S2 T2	1.75561	S2 T2	3.46112	S2 T2	5.11707	S2 T2	6.724
S2 T3	0	S2 T3	1.78084	S2 T3	3.73248	S2 T3	5.59872	S2 T3	6.82276
S2 T4	0	S2 T4	1.54449	S2 T4	3.05762	S2 T4	4.58643	S2 T4	6.49636
AVE	0	AVE	1.623925	AVE	3.2510225	AVE	4.9161825	AVE	6.40773

RANGE	0	RANGE	0.30628	RANGE	0.814	RANGE	1.26672	RANGE	1.31712
SD	0	SD	0.10932235	SD	0.252884125	SD	0.386326088	SD	0.437580068
0.5		0.6		0.7		0.8			
Sample	Power (W)	Sample	Power (W)	Sample	Power (W)	Sample	Power (W)		
S1 T1	8	S1 T1	9.21984	S1 T1	9.17308	S1 T1	12.23048		
S1 T2	8	S1 T2	9.21984	S1 T2	9.17308	S1 T2	12.23048		
S1 T3	7.7618	S1 T3	9.126	S1 T3	7.34832	S1 T3	10.02528		
S1 T4	6.9938	S1 T4	9.40896	S1 T4	7.53088	S1 T4	10.952		
S2 T1	7.56605	S2 T1	9.26694	S2 T1	8.72263	S2 T1	12.99272		
S2 T2	8.20125	S2 T2	8.80134	S2 T2	7.39375	S2 T2	10.658		
S2 T3	8.6528	S2 T3	9.31416	S2 T3	7.80892	S2 T3	11.07072		
S2 T4	7.9202	S2 T4	9.64806	S2 T4	8.23543	S2 T4	11.67392		
AVE	7.8869875	AVE	9.2506425	AVE	8.17326125	AVE	11.4792		
RANGE	1.659	RANGE	0.84672	RANGE	1.82476	RANGE	2.96744		
SD	0.451155894	SD	0.225447128	SD	0.719245274	SD	0.914504682		

D2 E5 Force Max																		
A1				A2				A3				A4				A5		
Trial	Force Max	Time		Trial	Force Max	Time		Trial	Force Max	Time		Trial	Force Max	Time		Trial	Force Max	Time
S1 T1	0.00	0.40		S1 T1	0.04	53.32		S1 T1	0.13	45.76		S1 T1	0.30	41.83		S1 T1	0.54	30.10
S1 T2	0.01	25.81		S1 T2	0.04	55.66		S1 T2	0.14	43.20		S1 T2	0.31	24.77		S1 T2	0.56	27.36
S1 T3	0.03	31.39		S1 T3	0.03	13.03		S1 T3	0.13	18.97		S1 T3	0.30	29.30		S1 T3	0.51	49.00

S1 T4	0.01	8.10		S1 T4	0.04	45.50		S1 T4	0.13	48.82		S1 T4	0.28	44.10		S1 T4	0.50	39.49
S2 T1	0.00	13.36		S2 T1	0.03	25.09		S2 T1	0.12	23.33		S2 T1	0.27	55.84		S2 T1	0.52	40.54
S2 T2	0.01	54.58		S2 T2	0.03	28.40		S2 T2	0.12	29.48		S2 T2	0.31	26.53		S2 T2	0.54	43.45
S2 T3	0.02	57.46		S2 T3	0.04	42.66		S2 T3	0.14	20.63		S2 T3	0.27	19.58		S2 T3	0.50	46.76
S2 T4	-0.01	0.32		S2 T4	0.03	9.07		S2 T4	0.11	57.82		S2 T4	0.26	29.95		S2 T4	0.46	32.36
AVE	0.01	23.93		AVE	0.04	34.09		AVE	0.13	36.00		AVE	0.29	33.99		AVE	0.52	38.63
RANGE	0.04	57.13		RANGE	0.01	46.58		RANGE	0.03	38.84		RANGE	0.05	36.25		RANGE	0.10	21.64
SD	0.01	22.66		SD	0.00	17.81		SD	0.01	14.72		SD	0.02	12.12		SD	0.03	7.93
A6				A7				A8				A9						
Trial	Force Max	Time		Trial	Force Max	Time		Trial	Force Max	Time		Trial	Force Max	Time				
S1 T1	0.98	32.44		S1 T1	1.71	31.86		S1 T1	3.13	59.90		S1 T1	5.61	46.19				
S1 T2	1.01	59.94		S1 T2	1.86	39.31		S1 T2	3.34	34.96		S1 T2	5.35	50.40				
S1 T3	0.80	40.50		S1 T3	1.50	59.94		S1 T3	2.90	53.75		S1 T3	3.35	51.30				
S1 T4	0.83	36.47		S1 T4	1.43	60.00		S1 T4	2.69	58.57		S1 T4	4.54	58.46				
S2 T1	0.87	32.69		S2 T1	1.58	58.86		S2 T1	3.13	59.90		S2 T1	4.90	57.53				

S2 T2	0.92	43.60		S2 T2	1.39	20.41		S2 T2	3.21	22.64		S2 T2	3.49	30.38				
S2 T3	0.81	42.01		S2 T3	1.64	59.44		S2 T3	2.77	36.14		S2 T3	4.49	53.86				
S2 T4	0.90	59.29		S2 T4	1.67	56.84		S2 T4	2.93	48.92		S2 T4	4.61	43.56				
AVE	0.89	43.37		AVE	1.60	48.33		AVE	3.01	46.85		AVE	4.54	48.96				
RANGE	0.21	27.50		RANGE	0.48	39.59		RANGE	0.65	37.26		RANGE	2.26	28.08				
SD	0.08	10.82		SD	0.16	15.63		SD	0.23	14.00		SD	0.80	9.08				

D2 E5 Resistance Max, Min, and Diff																			
A1				A2				A3				A4				A5			
Sample	Resist Min	Resist Max	Diff	Sample	Resist Min	Resist Max	Diff	Sample	Resist Min	Resist Max	Diff	Sample	Resist Min	Resist Max	Diff	Sample	Resist Min	Resist Max	Diff
S1 T1	3.08	3.11	0.03	S1 T1	3.12	3.15	0.04	S1 T1	3.15	3.20	0.05	S1 T1	3.46	3.64	0.17	S1 T1	3.39	3.50	0.11
S1 T2	3.48	3.48	0.00	S1 T2	3.48	3.50	0.01	S1 T2	3.49	3.51	0.03	S1 T2	3.49	3.54	0.05	S1 T2	3.52	3.56	0.04
S1 T3	3.90	3.91	0.01	S1 T3	3.88	3.90	0.01	S1 T3	3.88	3.91	0.03	S1 T3	3.87	3.90	0.03	S1 T3	3.87	3.90	0.04
S1 T4	3.89	3.90	0.01	S1 T4	3.87	3.88	0.01	S1 T4	3.88	3.90	0.02	S1 T4	3.83	3.86	0.03	S1 T4	3.84	3.89	0.05
S2 T1	5.34	5.51	0.17	S2 T1	3.86	3.87	0.02	S2 T1	3.83	3.87	0.04	S2 T1	3.64	3.70	0.06	S2 T1	3.62	3.73	0.11

S2 T2	3.36	3.37	0.01	S2 T2	3.34	3.35	0.01	S2 T2	3.35	3.37	0.03	S2 T2	3.36	3.40	0.04	S2 T2	3.41	3.45	0.04
S2 T3	4.92	5.09	0.17	S2 T3	3.44	3.50	0.06	S2 T3	3.68	3.71	0.03	S2 T3	3.53	3.54	0.01	S2 T3	3.50	3.53	0.02
S2 T4	3.79	4.46	0.67	S2 T4	3.18	3.39	0.21	S2 T4	3.46	4.52	1.06	S2 T4	3.45	4.24	0.79	S2 T4	3.08	3.11	0.03
AVE	3.97	4.10	0.13	AVE	3.52	3.57	0.05	AVE	3.59	3.75	0.16	AVE	3.58	3.73	0.15	AVE	3.53	3.58	0.05
RANGE	2.26	2.40	0.66	RANGE	0.77	0.74	0.20	RANGE	0.73	1.32	1.04	RANGE	0.51	0.84	0.78	RANGE	0.79	0.79	0.09
SD	0.78	0.85	0.23	SD	0.31	0.28	0.07	SD	0.27	0.41	0.36	SD	0.19	0.27	0.27	SD	0.26	0.26	0.04
A6				A7				A8				A9							
Sample	Resist Min	Resist Max	Diff	Sample	Resist Min	Resist Max	Diff	Sample	Resist Min	Resist Max	Diff	Sample	Resist Min	Resist Max	Diff				
S1 T1	3.39	3.50	0.11	S1 T1	3.33	3.48	0.15	S1 T1	3.45	3.82	0.36	S1 T1	3.40	3.77	0.37				
S1 T2	3.52	3.56	0.04	S1 T2	3.46	3.54	0.08	S1 T2	3.38	3.51	0.13	S1 T2	3.37	3.63	0.26				
S1 T3	3.87	3.90	0.04	S1 T3	3.75	3.85	0.10	S1 T3	3.50	3.62	0.11	S1 T3	3.32	3.67	0.35				
S1 T4	3.84	3.89	0.05	S1 T4	3.63	3.68	0.05	S1 T4	3.59	3.70	0.11	S1 T4	3.50	3.72	0.22				
S2 T1	3.62	3.73	0.11	S2 T1	3.60	3.68	0.08	S2 T1	3.55	4.15	0.61	S2 T1	3.50	3.84	0.33				
S2 T2	3.41	3.45	0.04	S2 T2	3.38	3.44	0.06	S2 T2	3.27	3.41	0.14	S2 T2	3.30	3.57	0.27				
S2 T3	3.50	3.53	0.02	S2 T3	3.36	3.42	0.07	S2 T3	3.13	3.27	0.14	S2 T3	3.15	3.42	0.27				

S2 T4	3.08	3.11	0.03	S2 T4	3.43	3.92	0.49	S2 T4	3.29	3.95	0.66	S2 T4	3.36	3.69	0.33				
AVE	3.53	3.58	0.05	AVE	3.49	3.63	0.13	AVE	3.39	3.68	0.28	AVE	3.36	3.66	0.30				
RANGE	0.79	0.79	0.09	RANGE	0.42	0.50	0.44	RANGE	0.46	0.89	0.55	RANGE	0.35	0.42	0.14				
SD	0.26	0.26	0.04	SD	0.15	0.19	0.15	SD	0.16	0.29	0.23	SD	0.11	0.13	0.05				

D2 E5 Max Power Watts									
0		0.1		0.2		0.3		0.4	
Sample	Power (W)	Sample	Power (W)	Sample	Power (W)	Sample	Power (W)	Sample	Power (W)
S1 T1	0	S1 T1	0.99225	S1 T1	2.048	S1 T1	3.97488	S1 T1	4.9
S1 T2	0	S1 T2	1.225	S1 T2	2.46402	S1 T2	3.75948	S1 T2	5.06944
S1 T3	0	S1 T3	1.521	S1 T3	3.05762	S1 T3	4.563	S1 T3	6.084
S1 T4	0	S1 T4	1.50544	S1 T4	3.042	S1 T4	4.46988	S1 T4	6.05284
S2 T1	0	S2 T1	1.49769	S2 T1	2.99538	S2 T1	4.107	S2 T1	5.56516
S2 T2	0	S2 T2	1.12225	S2 T2	2.27138	S2 T2	3.468	S2 T2	4.761
S2 T3	0	S2 T3	1.225	S2 T3	2.75282	S2 T3	3.75948	S2 T3	4.98436
S2 T4	0	S2 T4	1.14921	S2 T4	4.08608	S2 T4	5.39328	S2 T4	3.86884

AVE	0	AVE	1.27973	AVE	2.8396625	AVE	4.186875	AVE	5.160705
RANGE	0	RANGE	0.52875	RANGE	2.03808	RANGE	1.92528	RANGE	2.21516
SD	0	SD	0.189451081	SD	0.587853498	SD	0.571227954	SD	0.684473848
0.5		0.6		0.7		0.8			
Sample	Power (W)	Sample	Power (W)	Sample	Power (W)	Sample	Power (W)		
S1 T1	6.125	S1 T1	7.26624	S1 T1	10.21468	S1 T1	11.37032		
S1 T2	6.3368	S1 T2	7.51896	S1 T2	8.62407	S1 T2	10.54152		
S1 T3	7.605	S1 T3	8.8935	S1 T3	9.17308	S1 T3	10.77512		
S1 T4	7.56605	S1 T4	8.12544	S1 T4	9.583	S1 T4	11.07072		
S2 T1	6.95645	S2 T1	8.12544	S2 T1	12.05575	S2 T1	11.79648		
S2 T2	5.95125	S2 T2	7.10016	S2 T2	8.13967	S2 T2	10.19592		
S2 T3	6.23045	S2 T3	7.01784	S2 T3	7.48503	S2 T3	9.35712		
S2 T4	4.83605	S2 T4	9.21984	S2 T4	10.92175	S2 T4	10.89288		
AVE	6.45088125	AVE	7.9084275	AVE	9.52462875	AVE	10.75001		
RANGE	2.76895	RANGE	2.202	RANGE	4.57072	RANGE	2.43936		
SD	0.855592309	SD	0.774184377	SD	1.407602877	SD	0.69771122		

Average max force, time to max force, and resistance for Diameter 1 (0.31 mm) Samples 1 and 2

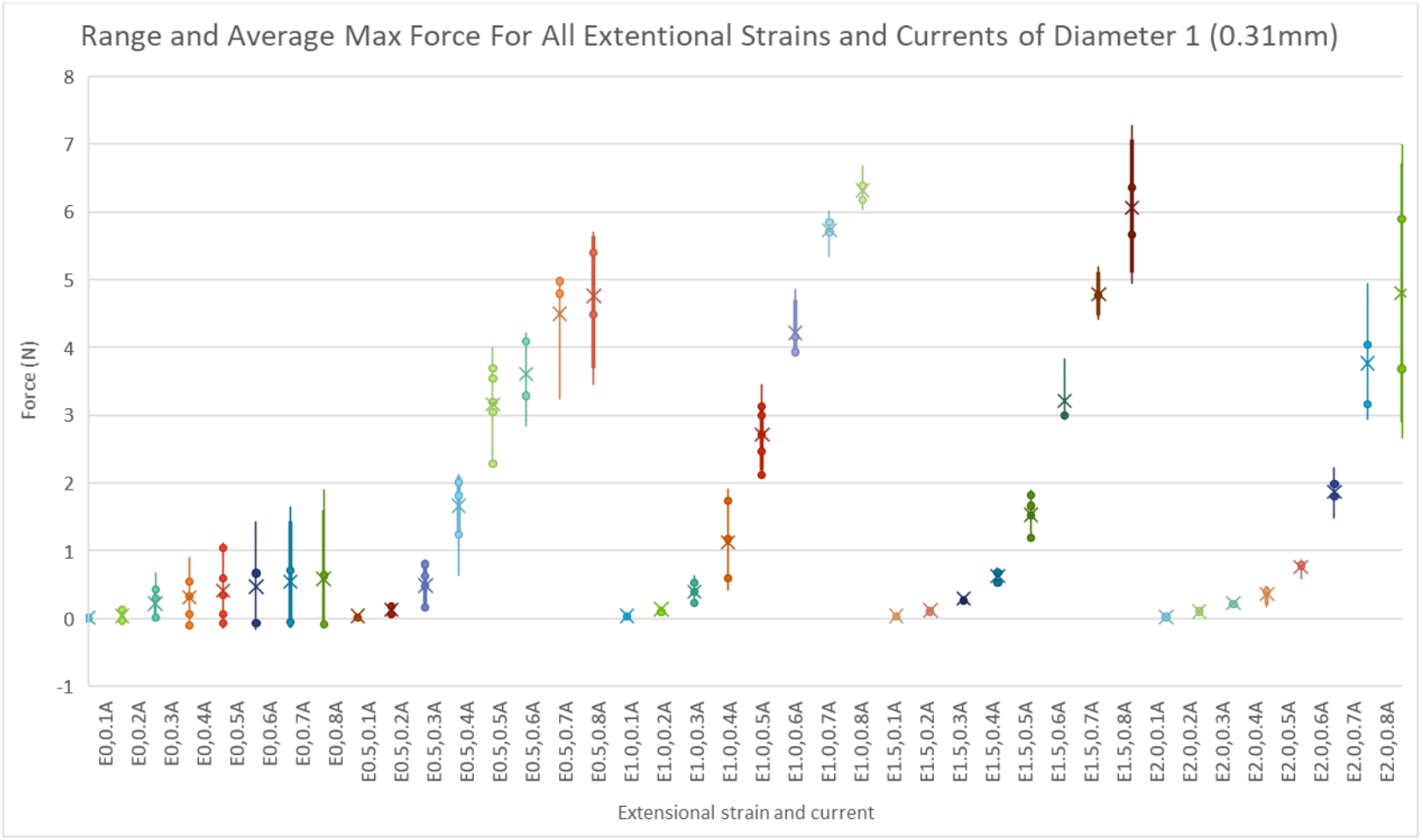

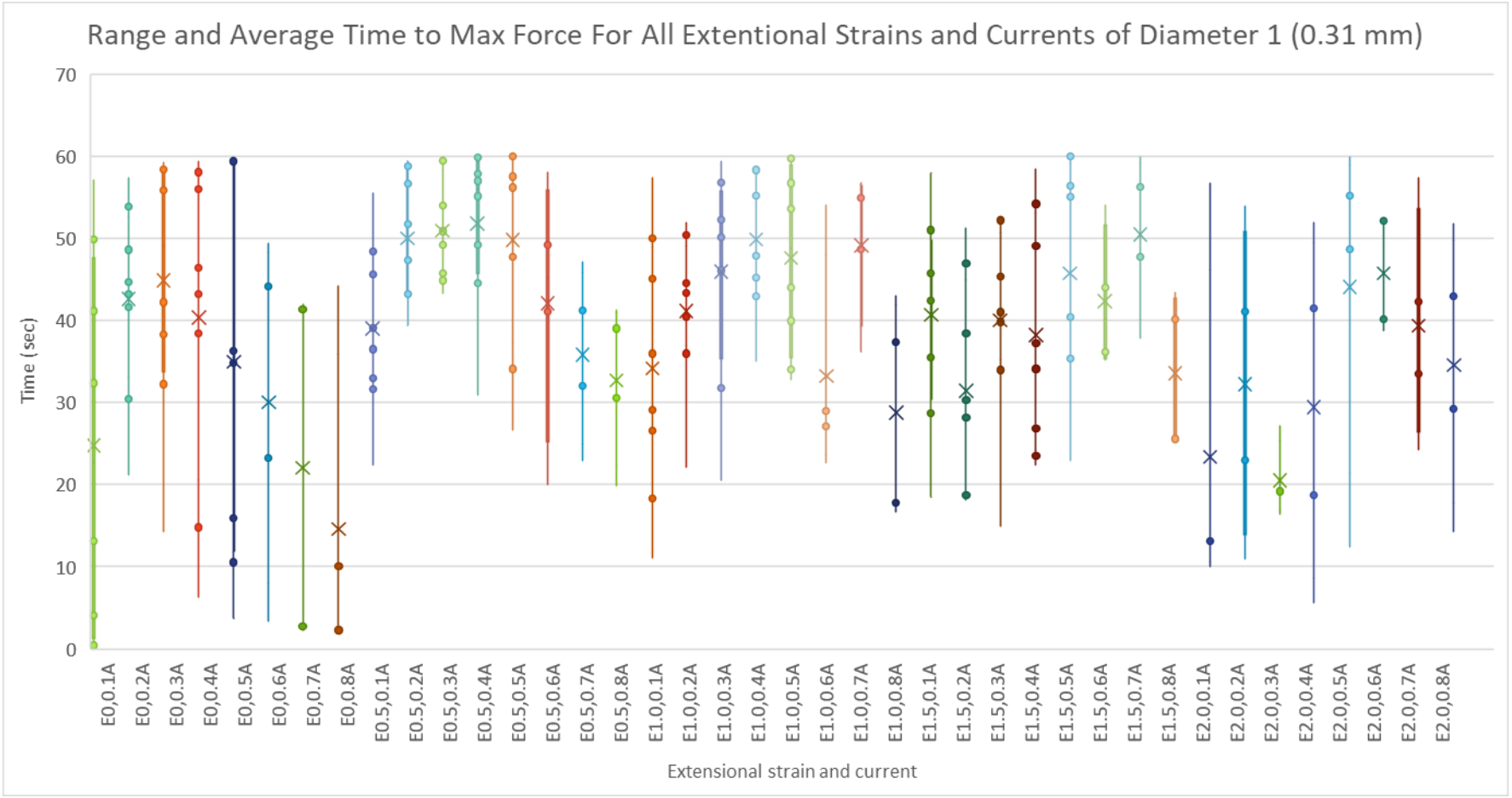
Range and Average Time to Max Force For All Extentional Strains and Currents of Diameter 1 (0.31 mm)
Time (sec)
70
60
50
40
30
20
10
0
E0,0.1A
E0,0.2A
E0,0.3A
E0,0.4A
E0,0.5A
E0,0.6A
E0,0.7A
E0,0.8A
E0.5,0.1A
E0.5,0.2A
E0.5,0.3A
E0.5,0.4A
E0.5,0.5A
E0.5,0.6A
E0.5,0.7A
E0.5,0.8A
E1.0,0.1A
E1.0,0.2A
E1.0,0.3A
E1.0,0.4A
E1.0,0.5A
E1.0,0.6A
E1.0,0.7A
E1.0,0.8A
E1.5,0.1A
E1.5,0.2A
E1.5,0.3A
E1.5,0.4A
E1.5,0.5A
E1.5,0.6A
E1.5,0.7A
E1.5,0.8A
E2.0,0.1A
E2.0,0.2A
E2.0,0.3A
E2.0,0.4A
E2.0,0.5A
E2.0,0.6A
E2.0,0.7A
E2.0,0.8A
Extensional strain and current

Appendix B

Diameter 1 (0.31 mm) Sample 1 Test 1	Diameter 1 (0.31 mm) Sample 1 Test 2	Diameter 1 (0.31 mm) Sample 2 Test 1	Diameter 1 (0.31 mm) Sample 2 Test 2	Diameter 1 (0.31 mm) Sample 3 Test 1	Diameter 1 (0.31 mm) Sample 3 Test 2	Diameter 1 (0.31 mm) Sample 3 Test 3	Diameter 1 (0.31 mm) Sample 3 Test 4
E0A0	E2.0A0.8	E2.0A0	E0A0.8	E0A0	E2.0A0.8	E0A0.8	E2.0A0
E0A0.1	E2.0A0.7	E2.0A0.1	E0A0.7	E0A0.1	E2.0A0.7	E0A0.7	E2.0A0.1
E0A0.2	E2.0A0.6	E2.0A0.2	E0A0.6	E0A0.2	E2.0A0.6	E0A0.6	E2.0A0.2
E0A0.3	E2.0A0.5	E2.0A0.3	E0A0.5	E0A0.3	E2.0A0.5	E0A0.5	E2.0A0.3
E0A0.4	E2.0A0.4	E2.0A0.4	E0A0.4	E0A0.4	E2.0A0.4	E0A0.4	E2.0A0.4
E0A0.5	E2.0A0.3	E2.0A0.5	E0A0.3	E0A0.5	E2.0A0.3	E0A0.3	E2.0A0.5
E0A0.6	E2.0A0.2	E2.0A0.6	E0A0.2	E0A0.6	E2.0A0.2	E0A0.2	E2.0A0.6
E0A0.7	E2.0A0.1	E2.0A0.7	E0A0.1	E0A0.7	E2.0A0.1	E0A0.1	E2.0A0.7
E0A0.8	E2.0A0	E2.0A0.8	E0A0	E0A0.8	E2.0A0	E0A0	E2.0A0.8
E0.5A0	E1.5A0.8	E1.5A0	E0.5A0.8	E0.5A0	E1.5A0.8	E0.5A0.8	E1.5A0
E0.5A0.1	E1.5A0.7	E1.5A0.1	E0.5A0.7	E0.5A0.1	E1.5A0.7	E0.5A0.7	E1.5A0.1
E0.5A0.2	E1.5A0.6	E1.5A0.2	E0.5A0.6	E0.5A0.2	E1.5A0.6	E0.5A0.6	E1.5A0.2
E0.5A0.3	E1.5A0.5	E1.5A0.3	E0.5A0.5	E0.5A0.3	E1.5A0.5	E0.5A0.5	E1.5A0.3
E0.5A0.4	E1.5A0.4	E1.5A0.4	E0.5A0.4	E0.5A0.4	E1.5A0.4	E0.5A0.4	E1.5A0.4
E0.5A0.5	E1.5A0.3	E1.5A0.5	E0.5A0.3	E0.5A0.5	E1.5A0.3	E0.5A0.3	E1.5A0.5
E0.5A0.6	E1.5A0.2	E1.5A0.6	E0.5A0.2	E0.5A0.6	E1.5A0.2	E0.5A0.2	E1.5A0.6
E0.5A0.7	E1.5A0.1	E1.5A0.7	E0.5A0.1	E0.5A0.7	E1.5A0.1	E0.5A0.1	E1.5A0.7
E0.5A0.8	E1.5A0	E1.5A0.8	E0.5A0	E0.5A0.8	E1.5A0	E0.5A0	E1.5A0.8
E1.0A0	E1.0A0.8	E1.0A0	E1.0A0.8	E1.0A0	E1.0A0.8	E1.0A0.8	E1.0A0
E1.0A0.1	E1.0A0.7	E1.0A0.1	E1.0A0.7	E1.0A0.1	E1.0A0.7	E1.0A0.7	E1.0A0.1
E1.0A0.2	E1.0A0.6	E1.0A0.2	E1.0A0.6	E1.0A0.2	E1.0A0.6	E1.0A0.6	E1.0A0.2
E1.0A0.3	E1.0A0.5	E1.0A0.3	E1.0A0.5	E1.0A0.3	E1.0A0.5	E1.0A0.5	E1.0A0.3
E1.0A0.4	E1.0A0.4	E1.0A0.4	E1.0A0.4	E1.0A0.4	E1.0A0.4	E1.0A0.4	E1.0A0.4
E1.0A0.5	E1.0A0.3	E1.0A0.5	E1.0A0.3	E1.0A0.5	E1.0A0.3	E1.0A0.3	E1.0A0.5
E1.0A0.6	E1.0A0.2	E1.0A0.6	E1.0A0.2	E1.0A0.6	E1.0A0.2	E1.0A0.2	E1.0A0.6
E1.0A0.7	E1.0A0.1	E1.0A0.7	E1.0A0.1	E1.0A0.7	E1.0A0.1	E1.0A0.1	E1.0A0.7
E1.0A0.8	E1.0A0	E1.0A0.8	E1.0A0	E1.0A0.8	E1.0A0	E1.0A0	E1.0A0.8

E1.5A0	E0.5A0.8	E0.5A0	E1.5A0.8	E1.5A0	E0.5A0.8	E1.5A0.8	E0.5A0
E1.5A0.1	E0.5A0.7	E0.5A0.1	E1.5A0.7	E1.5A0.1	E0.5A0.7	E1.5A0.7	E0.5A0.1
E1.5A0.2	E0.5A0.6	E0.5A0.2	E1.5A0.6	E1.5A0.2	E0.5A0.6	E1.5A0.6	E0.5A0.2
E1.5A0.3	E0.5A0.5	E0.5A0.3	E1.5A0.5	E1.5A0.3	E0.5A0.5	E1.5A0.5	E0.5A0.3
E1.5A0.4	E0.5A0.4	E0.5A0.4	E1.5A0.4	E1.5A0.4	E0.5A0.4	E1.5A0.4	E0.5A0.4
E1.5A0.5	E0.5A0.3	E0.5A0.5	E1.5A0.3	E1.5A0.5	E0.5A0.3	E1.5A0.3	E0.5A0.5
E1.5A0.6	E0.5A0.2	E0.5A0.6	E1.5A0.2	E1.5A0.6	E0.5A0.2	E1.5A0.2	E0.5A0.6
E1.5A0.7	E0.5A0.1	E0.5A0.7	E1.5A0.1	E1.5A0.7	E0.5A0.1	E1.5A0.1	E0.5A0.7
E1.5A0.8	E0.5A0	E0.5A0.8	E1.5A0	E1.5A0.8	E0.5A0	E1.5A0	E0.5A0.8
E2.0A0	E0A0.8	E0A0	E2.0A0.8	E2.0A0	E0A0.8	E2.0A0.8	E0A0
E2.0A0.1	E0A0.7	E0A0.1	E2.0A0.7	E2.0A0.1	E0A0.7	E2.0A0.7	E0A0.1
E2.0A0.2	E0A0.6	E0A0.2	E2.0A0.6	E2.0A0.2	E0A0.6	E2.0A0.6	E0A0.2
E2.0A0.3	E0A0.5	E0A0.3	E2.0A0.5	E2.0A0.3	E0A0.5	E2.0A0.5	E0A0.3
E2.0A0.4	E0A0.4	E0A0.4	E2.0A0.4	E2.0A0.4	E0A0.4	E2.0A0.4	E0A0.4
E2.0A0.5	E0A0.3	E0A0.5	E2.0A0.3	E2.0A0.5	E0A0.3	E2.0A0.3	E0A0.5
E2.0A0.6	E0A0.2	E0A0.6	E2.0A0.2	E2.0A0.6	E0A0.2	E2.0A0.2	E0A0.6
E2.0A0.7	E0A0.1	E0A0.7	E2.0A0.1	E2.0A0.7	E0A0.1	E2.0A0.1	E0A0.7
E2.0A0.8	E0A0	E0A0.8	E2.0A0	E2.0A0.8	E0A0	E2.0A0	E0A0.8

Diameter 2 (0.38 mm)	Diameter 2 (0.38 mm)	Diameter 2 (0.38 mm)	Diameter 2 (0.38 mm)	Diameter 2 (0.38 mm) Sample 2	Diameter 2 (0.38 mm) Sample 2	Diameter 2 (0.38 mm) Sample 2	Diameter 2 (0.38 mm) Sample 2

Sample 1 Test 1	Sample 1 Test 2	Sample 1 Test 3	Sample 1 Test 4	Test 1	Test 2	Test 3	Test 4
E0A0	E2.0A0.8	E0A0.8	E2.0A0	E2.0A0	E0A0.8	E2.0A0.8	E0A0
E0A0.1	E2.0A0.7	E0A0.7	E2.0A0.1	E2.0A0.1	E0A0.7	E2.0A0.7	E0A0.1
E0A0.2	E2.0A0.6	E0A0.6	E2.0A0.2	E2.0A0.2	E0A0.6	E2.0A0.6	E0A0.2
E0A0.3	E2.0A0.5	E0A0.5	E2.0A0.3	E2.0A0.3	E0A0.5	E2.0A0.5	E0A0.3
E0A0.4	E2.0A0.4	E0A0.4	E2.0A0.4	E2.0A0.4	E0A0.4	E2.0A0.4	E0A0.4
E0A0.5	E2.0A0.3	E0A0.3	E2.0A0.5	E2.0A0.5	E0A0.3	E2.0A0.3	E0A0.5
E0A0.6	E2.0A0.2	E0A0.2	E2.0A0.6	E2.0A0.6	E0A0.2	E2.0A0.2	E0A0.6
E0A0.7	E2.0A0.1	E0A0.1	E2.0A0.7	E2.0A0.7	E0A0.1	E2.0A0.1	E0A0.7
E0A0.8	E2.0A0	E0A0	E2.0A0.8	E2.0A0.8	E0A0	E2.0A0	E0A0.8
E0.5A0	E1.5A0.8	E0.5A0.8	E1.5A0	E1.5A0	E0.5A0.8	E1.5A0.8	E0.5A0
E0.5A0.1	E1.5A0.7	E0.5A0.7	E1.5A0.1	E1.5A0.1	E0.5A0.7	E1.5A0.7	E0.5A0.1
E0.5A0.2	E1.5A0.6	E0.5A0.6	E1.5A0.2	E1.5A0.2	E0.5A0.6	E1.5A0.6	E0.5A0.2
E0.5A0.3	E1.5A0.5	E0.5A0.5	E1.5A0.3	E1.5A0.3	E0.5A0.5	E1.5A0.5	E0.5A0.3
E0.5A0.4	E1.5A0.4	E0.5A0.4	E1.5A0.4	E1.5A0.4	E0.5A0.4	E1.5A0.4	E0.5A0.4
E0.5A0.5	E1.5A0.3	E0.5A0.3	E1.5A0.5	E1.5A0.5	E0.5A0.3	E1.5A0.3	E0.5A0.5
E0.5A0.6	E1.5A0.2	E0.5A0.2	E1.5A0.6	E1.5A0.6	E0.5A0.2	E1.5A0.2	E0.5A0.6
E0.5A0.7	E1.5A0.1	E0.5A0.1	E1.5A0.7	E1.5A0.7	E0.5A0.1	E1.5A0.1	E0.5A0.7
E0.5A0.8	E1.5A0	E0.5A0	E1.5A0.8	E1.5A0.8	E0.5A0	E1.5A0	E0.5A0.8
E1.0A0	E1.0A0.8	E1.0A0.8	E1.0A0	E1.0A0	E1.0A0.8	E1.0A0.8	E1.0A0
E1.0A0.1	E1.0A0.7	E1.0A0.7	E1.0A0.1	E1.0A0.1	E1.0A0.7	E1.0A0.7	E1.0A0.1
E1.0A0.2	E1.0A0.6	E1.0A0.6	E1.0A0.2	E1.0A0.2	E1.0A0.6	E1.0A0.6	E1.0A0.2
E1.0A0.3	E1.0A0.5	E1.0A0.5	E1.0A0.3	E1.0A0.3	E1.0A0.5	E1.0A0.5	E1.0A0.3
E1.0A0.4	E1.0A0.4	E1.0A0.4	E1.0A0.4	E1.0A0.4	E1.0A0.4	E1.0A0.4	E1.0A0.4
E1.0A0.5	E1.0A0.3	E1.0A0.3	E1.0A0.5	E1.0A0.5	E1.0A0.3	E1.0A0.3	E1.0A0.5
E1.0A0.6	E1.0A0.2	E1.0A0.2	E1.0A0.6	E1.0A0.6	E1.0A0.2	E1.0A0.2	E1.0A0.6
E1.0A0.7	E1.0A0.1	E1.0A0.1	E1.0A0.7	E1.0A0.7	E1.0A0.1	E1.0A0.1	E1.0A0.7
E1.0A0.8	E1.0A0	E1.0A0	E1.0A0.8	E1.0A0.8	E1.0A0	E1.0A0	E1.0A0.8
E1.5A0	E0.5A0.8	E1.5A0.8	E0.5A0	E0.5A0	E1.5A0.8	E0.5A0.8	E1.5A0
E1.5A0.1	E0.5A0.7	E1.5A0.7	E0.5A0.1	E0.5A0.1	E1.5A0.7	E0.5A0.7	E1.5A0.1

E1.5A0.2	E0.5A0.6	E1.5A0.6	E0.5A0.2	E0.5A0.2	E1.5A0.6	E0.5A0.6	E1.5A0.2
E1.5A0.3	E0.5A0.5	E1.5A0.5	E0.5A0.3	E0.5A0.3	E1.5A0.5	E0.5A0.5	E1.5A0.3
E1.5A0.4	E0.5A0.4	E1.5A0.4	E0.5A0.4	E0.5A0.4	E1.5A0.4	E0.5A0.4	E1.5A0.4
E1.5A0.5	E0.5A0.3	E1.5A0.3	E0.5A0.5	E0.5A0.5	E1.5A0.3	E0.5A0.3	E1.5A0.5
E1.5A0.6	E0.5A0.2	E1.5A0.2	E0.5A0.6	E0.5A0.6	E1.5A0.2	E0.5A0.2	E1.5A0.6
E1.5A0.7	E0.5A0.1	E1.5A0.1	E0.5A0.7	E0.5A0.7	E1.5A0.1	E0.5A0.1	E1.5A0.7
E1.5A0.8	E0.5A0	E1.5A0	E0.5A0.8	E0.5A0.8	E1.5A0	E0.5A0	E1.5A0.8
E2.0A0	E0A0.8	E2.0A0.8	E0A0	E0A0	E2.0A0.8	E0A0.8	E2.0A0
E2.0A0.1	E0A0.7	E2.0A0.7	E0A0.1	E0A0.1	E2.0A0.7	E0A0.7	E2.0A0.1
E2.0A0.2	E0A0.6	E2.0A0.6	E0A0.2	E0A0.2	E2.0A0.6	E0A0.6	E2.0A0.2
E2.0A0.3	E0A0.5	E2.0A0.5	E0A0.3	E0A0.3	E2.0A0.5	E0A0.5	E2.0A0.3
E2.0A0.4	E0A0.4	E2.0A0.4	E0A0.4	E0A0.4	E2.0A0.4	E0A0.4	E2.0A0.4
E2.0A0.5	E0A0.3	E2.0A0.3	E0A0.5	E0A0.5	E2.0A0.3	E0A0.3	E2.0A0.5
E2.0A0.6	E0A0.2	E2.0A0.2	E0A0.6	E0A0.6	E2.0A0.2	E0A0.2	E2.0A0.6
E2.0A0.7	E0A0.1	E2.0A0.1	E0A0.7	E0A0.7	E2.0A0.1	E0A0.1	E2.0A0.7
E2.0A0.8	E0A0	E2.0A0	E0A0.8	E0A0.8	E2.0A0	E0A0	E2.0A0.8

Arduino Code

Encoder and load cell code

```
//The purpose of this code is to save a file with the timestamp, the force applied by the SMA
(measured with a load cell) and the distance moved. It takes a measurement every 0.2 seconds.
#include "HX711.h" //include library for load cell amplifier
#define calibration factor -213200.00 //This value is obtained by using the SparkFun_HX711_Calibration
sketch
#define DOUT  A0 // connect to DAT on the HX711 board
#define CLK  10 // connect to the CLK on the HX711 board
//VDD & VCC on HX711 connected to 5V Arduino
//GND on HX711 connected to GND Arduino
// Other end HX711 connect to load cell (according to color)
#define encoderI 2 // One input from the photogate
#define encoderQ 3 // The other input from the photogate // Only use one interrupt in this example
```

```
HX711 scale(DOUT, CLK);

volatile int count; //To avoid the compiler from optimizing count

void setup() {
  Serial.begin(115200); // High rate

  scale.set_scale(calibration_factor); //This value is obtained by using the
SparkFun_HX711_Calibration sketch
  scale.tare(); //Assuming there is no weight on the scale at start up, reset the scale to 0

  count=0; //Assume lineair encoder is at 0
  pinMode(encoderI, INPUT); //Configures the specified pin to behave as an input
  pinMode(encoderQ, INPUT); //Configures the specified pin to behave as an input

  attachInterrupt(0, handleEncoder, CHANGE); //First number (0) directs to use digital pin 2 as
interrupt number
  //handeEncoder = ISR, CHANGE=mode (more info at:
https://www.arduino.cc/reference/en/language/functions/external-interrupts/attachinterrupt/)
}


void loop() {
  Serial.print(millis()); //to keep track of time
  Serial.print(", Load Cell, ");

  Serial.print(scale.get_units(), 3); //scale.get_units() returns a float, 3 decimal places // output
in kg

  Serial.print(", Encoder, ");
  Serial.println(count); //prints the current posistion
  delay(200);//delay with 200ms

}

void handleEncoder()//makes the encoder count up and down depending on the direction of the movement
```

```
{
  if(digitalRead(encoderI) == digitalRead(encoderQ))
  {
    count++; //count up
  }
  else
  {
    count--; // count down
  }

}
```

Relay code

```
//This Code Controlled the relays that would cycle power to the SMA's. This is required to do the
automated cycle testing
#define RELAY1 6//define to which pins the relays are connected to (this will control power to the
SMA)
#define RELAY2 7//this relay turn on/off the fan
void setup()
{
  Serial.begin(115200);//start serial communication
  pinMode(RELAY1, OUTPUT);//set the relay pins as output
  pinMode(RELAY2, OUTPUT);
  pinMode(RELAY4, OUTPUT);
  }
void loop()
{
  digitalWrite(RELAY1, HIGH);//Turn on the power to the SMA's
  digitalWrite(RELAY2, LOW);//Turn the fan off
  delay (22000);//wait during 22 seconds while the SMA is getting power and will perform its actuation
  digitalWrite(RELAY1, LOW);//turn off the power to the SMA
  digitalWrite(RELAY2, HIGH);//Turn the fan on
  delay(30000);//wait 30 seconds to start the cycle again. During this time the SMA will stretch again
and return to its original elongated state.}
```